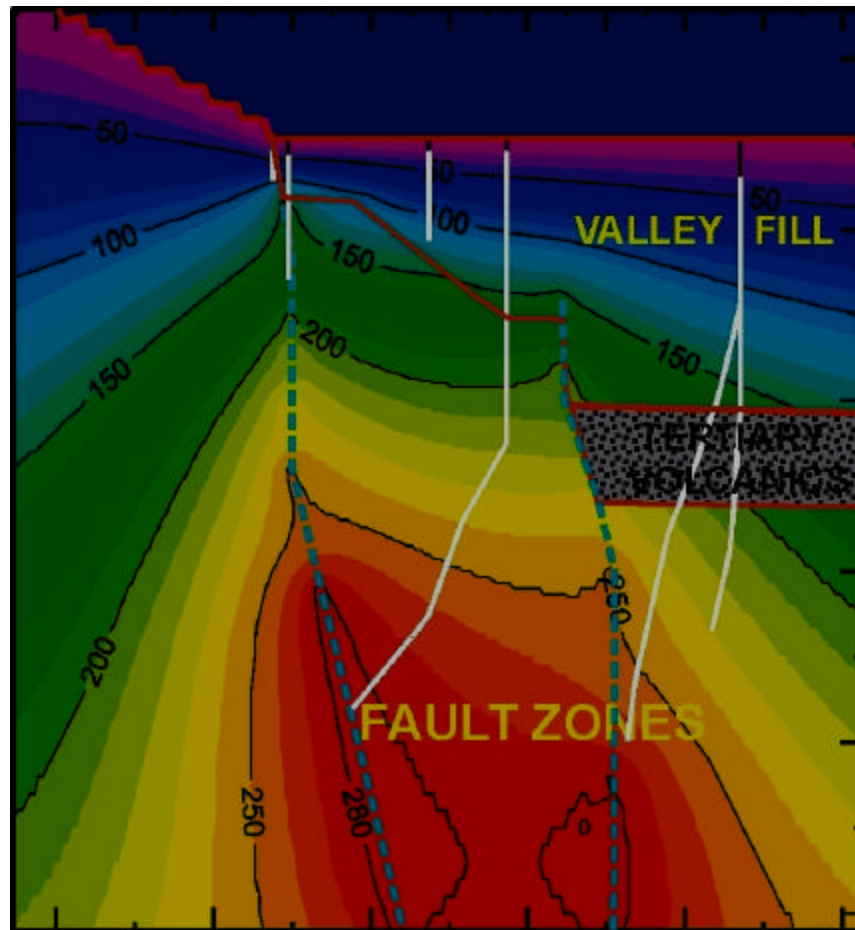


*Geothermal Technologies Program
Geoscience and Supporting Technologies*

2001 University Research Summaries



Blackwell et al., 2001



Prepared by: Idaho National Engineering
and Environmental Laboratory

U.S. DOE Office of Wind and
Geothermal Technologies



On the cover: A two fault, finite difference, numerical thermal model of the Dixie Valley Geothermal Field from Blackwell et al.

United States Department of Energy University Geothermal Research
Summaries of Recent Research

Foreword

Bob Creed
U. S. Department of Energy
Idaho Operations Office

The U. S. Department of Energy Office of Wind and Geothermal Technologies (DOE) is funding advanced geothermal research through University Geothermal Research solicitations. These solicitations are intended to generate research proposals in the areas of fracture permeability location and characterization, reservoir management and geochemistry. The work funded through these solicitations should stimulate the development of new geothermal electrical generating capacity through increasing scientific knowledge of high-temperature geothermal systems. In order to meet this objective researchers are encouraged to collaborate with the geothermal industry. These objectives and strategies are consistent with DOE Geothermal Energy Program strategic objectives.

The solicitations have resulted in proposal submissions, selections and awards being made through a competitive merit review process managed by the Idaho Operations Office (ID) with assistance from the Idaho National Engineering and Environmental Laboratory (INEEL). Award selection and subsequent management is an ID responsibility. Funding for these solicitations has ranged from over \$ 3 million in FY-99 to \$1.2 million in FY-02. Additional geothermal research summaries, software and geothermal related web-sites can be found at: <http://id.inel.gov/geothermal>.

The solicitations and subsequent awards have resulted in productive communications and collaborations between academia and the geothermal community. The exchange of ideas between award recipients, DOE laboratories and the geothermal industry has led to significant improvements in our understanding of how geothermal systems can be found, characterized and produced in a sustainable manner. Another important result of these collaborations has been the release, by industry, of large, valuable, and formerly proprietary resource databases into the public domain. The donation and release of this data reflects the importance that industry places on these collaborations and adds tremendous value to other activities where previously proprietary data can be used to generate and test ideas leading to the efficient identification, characterization, and sustainable development of geothermal resources.

Peer reviewers ranked 86% of the recently funded research above average at the 2001 external peer review of DOE geothermal geoscience research. University research received nine of the eleven highest scores (including the two highest). This rate of success indicates that we have been successful in providing high quality research in the context of addressing industry supported scientific objectives.

Another significant component of this program has been the training, development and support of intellectual infrastructure. Many graduate students and post-doctoral researchers have been supported with DOE funded geothermal research grants.

Continuity and scientific expertise in the merit review, award and management process are important in maintaining quality and responsiveness in this program. Significant technical management capabilities and commitment at ID and the INEEL ensure that awards are made and managed consistent with programmatic and scientific objectives with the least cost to the taxpayer. Success in using these strategies has been demonstrated through the addition of significant geothermal electrical generating capacity.

There are many high quality and significant papers in this compendium and bringing attention to some does not mean that others are less worthy of special notice. The paper by Hulen et al. provides some concise discussions on the relationship between scientific efforts and industry participation. The Blackwell et al. paper is an excellent example of how proprietary data has reached the public domain through useful research. These papers also effectively illustrate the development and use of conceptual models that will have wide use in the geothermal community. The silica scaling research by Heaney and Brantley is another good example of the responsiveness of DOE geothermal research to specific needs of the geothermal industry.

Research done in a vacuum is not useful. In each of the papers you will see that the researchers have made significant efforts to disseminate their results to the geothermal community through presentations at meetings and the peer reviewed literature. The work done by Moller and Weare is a good example of research that has resulted in high quality publications and technology transfer (<http://geotherm.ucsd.edu>) in the area of chemical behavior under geothermal conditions.

Several research projects (see Moller and Weare, Ghassemi, Wannamaker et al., and Rial for example) involve the development and use of computer codes to speed the applicability of research results. These codes typically have been designed with user-friendly, graphical user-interfaces and will be freely available to the geothermal community. In order to fully maximize the Government's investment in these projects, workshops should be held to demonstrate the use and utility of these codes. Also noteworthy is the web-site described in the Nash paper (<http://www.egi-geothermal.org>). This web-site is a concise compendium of geothermal data and imagery that should prove to be very helpful to the geothermal community.

The projects summarized in this volume demonstrate the practical and scientific value of DOE-sponsored geothermal research. In order to fully leverage research results, case studies should be compiled. This effort would involve teams of industry, academia, and DOE national laboratory personnel. Multiple research products would be used and tested to support geothermal development. The process and results of this scientific and technical effort would be coordinated to ensure focus on geothermal development while establishing the utility of DOE funded geothermal research and technology. Feedback in this process would be used to more effectively focus new research. Such a coordinated effort would also encourage multi-disciplinary communications in a setting where hypotheses are generated and tested in the real world. A similar exercise was conducted at Dixie Valley with positive results. The results of this exercise will be discussed at a June 2002 workshop in Reno, Nevada. More coordination efforts along these lines should be conducted in the future.

TABLE OF CONTENTS

GEOLOGY

Characterization and Conceptual Modeling of Magmatically-Heated and Deep-Circulation, High-Temperature Hydrothermal Systems in the Basin and Range and Cordilleran USA, University of Utah, Jeffrey B. Hulen	1
Geothermal Resource Analysis and Structure of Basin and Range Systems, Especially Dixie Valley Geothermal Field, Nevada, Southern Methodist University, David Blackwell, Maria Richards, and Kenneth W. Wisian.....	10
Improved Technologies for Geothermal Resource Evaluation Western U.S. Geothermal System, University of Utah, Gregory D. Nash.....	20
Improving Exploration Models of Andesite-Hosted Geothermal Systems, University of Utah, Joseph N. Moore	27
Geothermal Reservoirs: Products of Cooling Plutons, School of Thought, Stanley, ID, Denis L. Norton.....	32

GEOPHYSICS

Enhanced Data Acquisition and Inversion for Electrical Resistivity Structure in Geothermal Exploration and Reservoir Assessment, University of Utah, Philip E. Wannamaker, John A. Stodt, Jeffrey B. Hulen.....	37
Characterization of Fracture Patterns in The Geysers and Coso Geothermal Reservoirs by Shear-Wave Splitting, University of North Carolina, J. A. Rial	43
Imaging Tools for Electrical Resistivity in Geothermal Exploration and Reservoir Assessment, University of Utah, A. C. Tripp.....	50
Numerical Analysis of Three-Component Induction Logging in Geothermal Reservoirs, University of Wisconsin-Madison, Dr. David L. Alumbaugh	54
Core Analysis for the Development and Constraint of Physical Models of Geothermal Reservoirs, New England Research Inc., Vermont, G. N. Boitnott	60

RESERVOIR MANAGEMENT

A Thermoelastic Hydraulic Fracture Design Tool for Geothermal Reservoir Development, University of North Dakota, A. Ghassemi.....	68
Modeling Production/Injection Strategies in Fracture-Dominated Geothermal Reservoirs, Kansas State University, Dr. Daniel Swenson.....	77
Fundamentals of Steam-Water Flow in Porous Media, Stanford University, Roland N. Horne and Kewen Li	83

GEOCHEMISTRY

A Geochemical and Microanalytical Study of Silica Scale Deposition in Geothermal Brines, The Pennsylvania State University, Peter J. Heaney and Susan L. Brantley	88
Tracing Geothermal Fluids: Two-Phase Tracer Development, University of Utah, Michael C. Adams	94
Technology for Increasing Geothermal Energy Productivity, University of California, Nancy Møller; John H. Weare	101
The Development of Tracers for Use in Geothermal Reservoirs, University of Utah, Peter E. Rose, Joel M. Harris, Phaedra Kilbourn, and Christian Kasteler	107
Gas Analysis of Geothermal Fluid Inclusions: A New Technology for Geothermal Exploration, New Mexico Tech, David I. Norman	113
Key Word Index.....	122
Author Index.....	125

CHARACTERIZATION AND CONCEPTUAL MODELING OF MAGMATICALLY-HEATED AND DEEP-CIRCULATION, HIGH-TEMPERATURE HYDROTHERMAL SYSTEMS IN THE BASIN AND RANGE AND CORDILLERAN USA

Principal Investigator – Jeffrey B. Hulen
Energy & Geoscience Institute, University of Utah
423 Wakara Way, Suite 300, Salt Lake City, UT 84108
801-581-8497 jhulen@egi.utah.edu

Collaborating Investigators – Joseph N. Moore, Michael C. Adams, Susan J. Lutz (all at the Energy & Geoscience Institute) and Denis L. Norton, School of Thought, P.O. Box 310, Stanley, ID 83278

Key Words – The Geysers; Dixie Valley; Glass Mountain; Salton Sea; hydrothermal system; conceptual model; igneous intrusion; granitoid; granite; rhyolite; faults; fractures; analysis, breccias; permeability; porosity; mineralization; hydrothermal alteration

Project Background and Status

The western USA is one of the world's richest geothermal provinces. This tectonically and thermally active region has an installed geothermal electric-power production capacity of ~2500 MWe, with the solid promise of several times that amount still to be developed.

Examples of this great potential can be found throughout the West. The Salton Sea geothermal system, in California's Imperial Valley (a part of the Basin and Range), has a current capacity of 335 MWe, but can likely support seven times that value. In other words, just this one system may one day supply enough electricity for ~9,000,000 people. The Glass Mountain system, at Medicine Lake volcano in the southern Cascade Range of northern California, is the biggest known, wholly undeveloped, high-temperature geothermal system in the contiguous 48 states. Nevada's current 260 MWe capacity scarcely hints at the hidden systems surely yet to be found in the state.

The West's geothermal wealth and the nation's ever-expanding need for clean, renewable energy sources underpin the Department of Energy's stated aim for geothermal energy to provide 10% of the region's electric power by the year 2020. Achieving this ambitious goal requires continuing support for mission-oriented geothermal research at National Laboratories, the U.S. Geological Survey and other agencies, and geoscience-oriented Universities.

Not only are geothermal reservoirs exceptionally complex natural phenomena, they are also concealed from direct observation. Transforming them from raw prospects into profitable, long-lived

producers of electrical energy is therefore arduous, risky, and expensive. We can help geothermal companies ease this process, while reducing costs and improving the odds for success, by maintaining a robust national geothermal research program. The more that we know about these systems, the more readily and cost-effectively they can be found, developed, and managed.

Governed by the foregoing philosophy, we have undertaken to obtain greater insight into the intricate and interlinked geological, geochemical, thermal, and mechanical controls on the inception, evolution, and 3-D geometry of the two types of high-temperature hydrothermal system found in the western United States. The first type is distinguished by having an obvious igneous heat source. Examples include systems at The Geysers, the Salton Sea, and Glass Mountain. The second type is ostensibly heated entirely in response to circulation along deeply-penetrating faults and fractures in regions of thinned crust and elevated heat flow. This is the dominant type of system in Nevada, and the prime example is the Dixie Valley field in Churchill County

At the close of FY 2001, we were well underway in constructing conceptual geological and geochemical models for the study systems noted above. The Geysers field has received most of our attention to date. We have modeled the northern Geysers, with emphasis on a transect through Geysers Coring Project corehole SB-15-D (Hulen, 2001; Norton and Hulen, 2001), and on the high-temperature Aidlin sub-reservoir in the extreme northwestern part of the field (Hulen *et al.*, 2001). The Salton Sea system modeling effort began in earnest only in late FY 2001, when a full suite of subsurface data and borehole samples was finally made available. Even

so, we have already made an exciting volcanological discovery that has changed concepts about geothermal heat sources and hydrology throughout the Salton Trough (*Hulen and Pulka, 2001*). We have completed several interesting ancillary studies at Dixie Valley, but have really just begun our field-wide modeling work there. Redoubled efforts on this exemplary deep-circulation system are planned for FY 2002. The Glass Mountain modeling study has been temporarily deferred because of DOE funding limitations.

Project Objectives

- (1) Working closely with our counterparts in the U.S. geothermal industry, refine and develop new conceptual, geological, and geochemical models for western U.S. high-temperature hydrothermal systems, including new ones certain to be found in the Cascades and adjoining Basin and Range.
- (2) Assist domestic geothermal companies in application of the new models for risk-reduced and more cost-effective exploration, development, expansion, and maintenance of these systems. Better resource knowledge through conceptual modeling will mean fewer million-dollar “dry holes” and more successful high-temperature wells.
- (3) Maintain and augment the EGI Geothermal Sample Laboratory as a unique western U.S. and international research collection of geothermal cores, cuttings, and resource information.

Approach

There are several ways to stimulate development of known U.S. geothermal systems, and to enhance the likelihood of locating and producing the new ones that remain to be found in the region: (1) increasing access to public lands for responsible resource development; (2) extending production-tax credits to geothermal energy as well as wind and other renewables; (3) refining drilling and production technologies; and (4) simply improving basic knowledge of the resource itself.

Of these four approaches, the first two are political concerns beyond the scope of this report. The second two are both germane, but (4) is fundamental. Even the most sophisticated drilling

system can cleanly miss, at enormous expense, an incompletely understood resource target.

Accordingly, we are in the midst of formulating the next generation of conceptual, geological, and geochemical models for high-temperature western U.S. geothermal resources. The models will help provide answers to the following key questions not only about these systems, but by extension their analogues abroad.

- What are the characteristics and 3-D configurations of the large-fracture networks that control most high-temperature fluid flow? . . . of the small-fracture stockworks and primary pore volumes that are not major flow channels but are important for thermal-fluid storage? Improving knowledge of these features will be important not only for more efficient extraction of indigenous reservoir fluids, but for planning and executing long-term injection strategies.
- In what ways do primary lithologic variables influence the creation of fracture permeability by tectonic and hydrothermal disruption? . . . of other types of porosity and permeability (e.g., dissolution)?
- How do igneous intrusions interact with the rock and fluid regimes they intrude to create, enhance, or occlude porosity and permeability? Can the relevant processes be modeled to predict permeability “sweet spots” in hydrothermal systems, or, conversely, to identify and avoid nonproductive reservoir sectors?
- How can broad-scale and local alteration mineralogy and zoning be used to help deduce a system’s hydrothermal history, and to provide vectors toward productive thermal-fluid channels and reservoir volumes?
- How can the compositions and crosscutting relationships of hydrothermal veins and breccias be better utilized to (1) decipher a system’s thermal and chemical evolution; and (2) to narrow the search for fluid conduits?
- How do “blind” hydrothermal systems differ from their superficially expressed counterparts? Are there subtle surface clues, not yet recognized, that point to these systems’ subsurface presence?

Meeting these goals requires a mix of traditional and innovative research techniques judiciously applied by a research group with a balanced blend of skills, talents, backgrounds, and viewpoints.

Our research program for the full five-year performance period of this grant has been organized into the following tasks:

- Generation of refined conceptual, exploration, and production models for The Geysers geothermal system (industry partner Calpine Corporation), with emphasis on the northern, high-temperature part of the field. Among research methods applied to this Task are (1) field-wide, four-dimensional (three spatial plus temporal), geological and geochemical mapping and reservoir characterization; (2) petrologic studies of cuttings and cores, with emphasis on tracing fluid sources and evolutionary histories, and on characterization of alteration mineralogy and zoning as these features relate to a field's overall geologic framework; (3) organic-geochemical studies, principally to define independent paleotemperature measurements for reservoir rocks; (4) radiometric age-dating; and (5) numerical hydrothermal-history modeling.
- Generation of refined conceptual and geological/geochemical models for the Salton Sea geothermal field (industry partner CalEnergy Operating Company; CEOC), where a major expansion is underway. Same approach as for The Geysers, but tailored to the unique geologic setting and tectonomagmatic history of the Salton Trough.
- Generation of refined exploration and production models for the Glass Mountain geothermal system (industry partner Calpine Corporation). Same approach as above, but modified to fit a southern Cascade Range composite volcano. Knowledge gained from this study will help narrow the search for similar such systems concealed beneath cool-water "rain curtains" along the full length of the Cascade arc and its eastern flank.
- Generation of refined exploration and conceptual models for western Great Basin "deep-circulation" geothermal systems (various corporate partners, but principally Caithness Energy). Limited work focused to date on the Dixie Valley geothermal system.

Methods for implementing each of these tasks are as follows:

- Lithologic, stratigraphic, structural, alteration, and mineralization mapping at each system, at various levels of detail depending upon the resource. Where data density permits, 3-D maps and block diagrams are prepared, as these can be superior to 2-D sections for understanding the true character of a subsurface resource.
- Petrologic studies, including standard petrographic characterization, whole-rock geochemical analysis, microchemical analysis of selected secondary phases, fluid-inclusion microthermometry and gas analysis.
- Organic geochemistry, for mapping fluid-flow paths and monitoring both natural and production-induced reservoir processes.
- $^{40}\text{Ar}/^{39}\text{Ar}$ age-spectrum dating and thermal-history modeling.
- Numerical pluton-cooling and hydrothermal-history modeling by D.L. Norton, who is separately funded but working closely with the PI on this project.

Results to Date

A partial list of major accomplishments through FY 2001 for this project (Grant DE-FG07-00ID13891, Task I) is as follows:

- Determined the sealing mechanism and mineralogy inhibiting thermal-fluid escape and groundwater incursion at the Glass Mountain system (*Hulen and Lutz, 1999*).
- Worked closely with D.L. Norton to complete numerical igneous-intrusion and thermal-history models for the north-central Geysers steam field, California, with emphasis on a transect through Geysers Coring Project corehole SB-15-D (*Hulen, 2001; Norton and Hulen, 2001*).
- Examined the role of strike-slip fault tectonics in guiding intrusion of the Geysers felsite (*Hulen and Norton, 2000*). Determined that the pluton likely was emplaced sequentially in pull-aparts developed between right-stepping, right-lateral wrench-fault zones.

- Completed preliminary work on the use of indigenous bitumens as thermal-history indicators in The Geysers and other high-temperature hydrothermal systems.
- With CEOC, characterized scaling mechanisms and scale compositions for selected production and injection wells at the Salton Sea geothermal field (*Lutz et al., 2000, 2001*).
- Also with CEOC, discovered and characterized an ancient (~0.65 Ma), buried, rhyolite dome complex at the Salton Sea field (**Figs. 1 and 2; *Hulen and Pulka, 2001*). Developed a working model incorporating the influence of this igneous body and implied granitic plutons on past, present, and future hydrothermal fluid flow at the Salton Sea and elsewhere in the Salton Trough (Fig. 3).
- Investigated, with Pat Dobson and Tim Kneafsy of LBL, the nature of porosity and permeability at shallow levels in a portion of the Yellowstone hydrothermal system (*Dobson et al., 2000, 2001*).
- Completed a detailed study of the Aidlin sector of The Geysers (*Hulen et al., 2001*), and determined the following: (a) Unlike the rest of the field, Aidlin produces exclusively from a “high-temperature” reservoir (Fig. 4); (b) the reservoir has cooled ~100°C from its thermal maximum; (c) atypically for The Geysers, the reservoir is hosted principally by “normal” reservoir rocks, that is, non-hornfelsic lithologies containing only small amounts of hydrothermal or metamorphic biotite; (d) like the rest of The Geysers, the top of the Aidlin reservoir closely coincides with the upper limit of pervasive hydrothermal epidote (Fig. 4).

Plans

At the close of FY 2001, 40% of our five-year project has been completed, and most of the project’s stated interim goals to this point have been met. Work on the important Geysers system will continue into year 3, with a focus on the high-temperature reservoir slated for deep injection.

The Salton Sea geologic model is still in the early stages of preparation, and we anticipate that its completion will involve a large effort each year for the remaining duration of the grant.

**Figures follow references

Because of DOE budget cuts for FY 2002, we have reluctantly sidelined work on the Glass Mountain geothermal system pending restoration of funding for this project.

Thus far in our research program, we have emphasized magmatically-heated western U.S. geothermal systems. During ensuing years of the grant, we will transfer some of that emphasis to the deep-circulation systems, a type which will account for many new discoveries in the Great Basin. We have completed alteration mapping, lithologic logging of cuttings, and the study of hot-spring deposits at the Dixie Valley field, but will strive during the coming year to place disparate data from these investigations into a coherent 3-D geologic context.

Technology Transfer; References

The following publications through FY 2001 have been supported, wholly or in part, by this grant. Citations for the present document are highlighted in bold text.

1. Adams, M.C., Moore, J.N., Bjornstad, S., and Norman, D.I., 2000, Geologic history of the Coso geothermal system: Japan, World Geothermal Congress, Proceedings.
2. Allis, R.G., Johnson, S., Nash, G.D., and Benoit, R., 2000, Mapping changes in surface thermal activity at Dixie Valley geothermal field, Nevada: *Geoth. Resourc. Counc.*, Trans., v. 23, p. 499-504.
3. **Dobson, P., Hulen, J., Kneafsy, T.J., and Simmons, A., 2000, The role of lithology and alteration on permeability and fluid flow at the Yellowstone geothermal system, Wyoming: *Stanford University, 25th Wkshp. on Geoth. Res. Eng., Proc.***
4. **Dobson, P., Hulen, J., Kneafsy, T.J., and Simmons, A., 2001, Permeability at Yellowstone – A natural analogue for Yucca Mountain processes: Las Vegas, Nevada, 9th International High-Level Radioactive Waste Management Conference (April 29-May 1, 2001.**
5. Gruszkiewicz, M.S., Horita, J., Simonson, J.M., Mesmer, R.E., and Hulen, J.B., 2001, Water adsorption at high temperature on core samples from The Geysers geothermal field, California: *Geothermics*, v. 30, p. 269-302.

6. Hulen, J.B. (Guest Editor), 2001, **The Geysers Coring Project and the Geysers-Clear Lake igneous-geothermal domain (special issue):** *Geothermics*, v. 30, p. 165-394.
7. Hulen, J.B., and Wright, P.M., 2001, Geothermal energy – Clean, sustainable energy for the benefit of humanity and the environment: *U.S. Department of Energy Brochure* (May 2001), 8 p.
8. Hulen, J.B., and Collister, J.W., 1999 (issued February 2000), The oil-bearing, Carlin-type gold deposits of Yankee basin, Alligator Ridge district, Nevada: *Econ. Geol.*, v. 94, p. 1029-1051.
9. Hulen, J.B., and Langton, D., 2001, The EGI Geothermal Sample Laboratory – A western U.S. and international geothermal research collection and study center: *Univ. of Utah, Energy & Geosci. Inst. Rpt.*, 202 p.
10. Hulen, J.B., and Lutz, S.J., 1999 (October), **Altered volcanic rocks as hydrologic seals on the geothermal system of Med. Lake volcano, Calif.:** *Geoth. Resourc. Counc. Bull.*, v. 28, p. 217-222.
11. Hulen, J.B., and Norton, D.L., 2000, **Wrench-fault tectonics and emplacement of The Geysers felsite:** *Geoth. Resourc. Counc., Trans.*, v. 24, p. 289-298.
12. Hulen, J.B., and Pulka, F.S., 2000, **Deeply concealed rhyolite and associated phreatomagmatic tuff in the southeastern Salton Sea geothermal field, California:** *Stanford Univ., 26th Wkshp. on Geoth. Res. Eng., Proc.*
13. Hulen, J.B., Norton, D.L., Moore, J.N., Beall, J.J., and Walters, M.A., 2001, **Initial insights into the origin, configuration, and thermal-chemical evolution of the Aidlin steam reservoir, northwest Geysers geothermal system, California:** *Geoth. Resourc. Counc., Trans.*, v. 25, 10 p.
14. Lutz, S.J., and Hulen, J.B., 2000, Depositional setting for nickel mineralization in the Jurassic Boyer Ranch Formation and the Humboldt igneous complex, Bolivia area, northern Stillwater Range, Nevada (abstract): *GSA, 2000 Ann. Mtng. (Reno, Nevada), Progr. with Abstr.*
15. Lutz, S.J., Hulen, J.B., and Osborn, W., 2000, **Production-well scales from the Salton Sea geothermal field, California:** *Stanford Univ., 25th Wkshp. on Geoth. Res. Engineering, Proc.*
16. Lutz, S.J., Hulen, J.B., and Osborn, W.L., 2001, **Chemical, mineralogical, and textural characterization of production-well scales from Salton Sea geothermal wells:** *Stanford Univ., 26th Wkshp. on Geoth. Res. Eng., Proc.*
17. Lutz, S.J., Hulen, J.B., and Schriener, A., Jr., 2000, Alteration, geothermometry, and granitoid intrusions in well 31-17, Medicine Lake volcano geothermal system, California: *Stanford Univ., 25th Wkshp on Geoth. Res. Eng., Proc.*, p. 289-295.
18. Klusman, R.W., Moore, J.N., and LeRoy, M.P., 2000, Potential for surface gas-flux measurements in exploration and surface evaluation of geothermal resources: *Geothermics*, v. 29, p. 637-670.
19. Moore, J.N., Adams, M.C., Sperry, T.L., Bloomfield, K.K., and Kunzman, R., 2000, Preliminary results of geochemical monitoring and tracer tests at the Cove Fort-Sulphurdale geothermal system, Utah: *Stanford Univ., 25th Wkshp. on Geoth. Res. Eng., Proc.*
20. Norton, D.L., and Hulen, J.B., 2001, **Preliminary numerical analysis of the magma-hydrothermal history of The Geysers geothermal system, California, USA:** *Geothermics*, v. 30, p. 211-234.
21. Persoff, P., and Hulen, J.B., 2001, Hydrologic characterization of reservoir metagraywacke from shallow and deep levels of The Geysers vapor-dominated geothermal system, California, USA: *Geothermics*, v. 30, p.169-192.
22. Wannamaker, P.E., Hulen, J.B., and Heizler, M.T., 2000, Early Miocene lamproite from the Colorado Plateau tectonic province, Utah: *J. Volc. Geoth. Res.*, v. 24, p. 637-640.

**Figures follow references

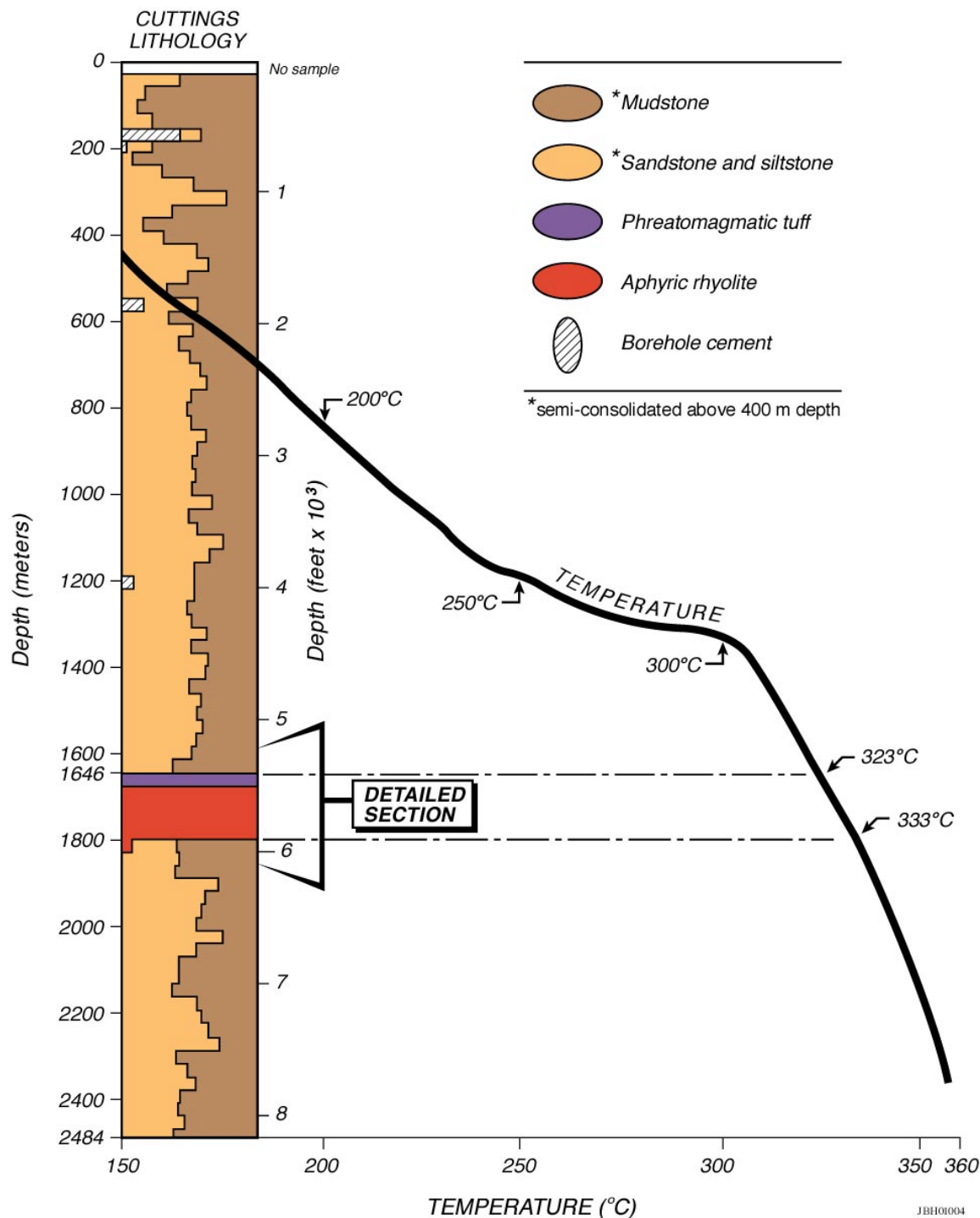


Figure 1. Generalized lithologic and temperature log for well Smith IW-2, in the Salton Sea geothermal field, showing position of rhyolite flow/dome and tuff interval. Depths shown are as drilled, but close to true vertical depths. The well is inclined generally northeastward at 6-11°; total drilled depth at 2484 m = true vertical depth of 2464 m. Data from Epoch Well Logging (1998) and this study.

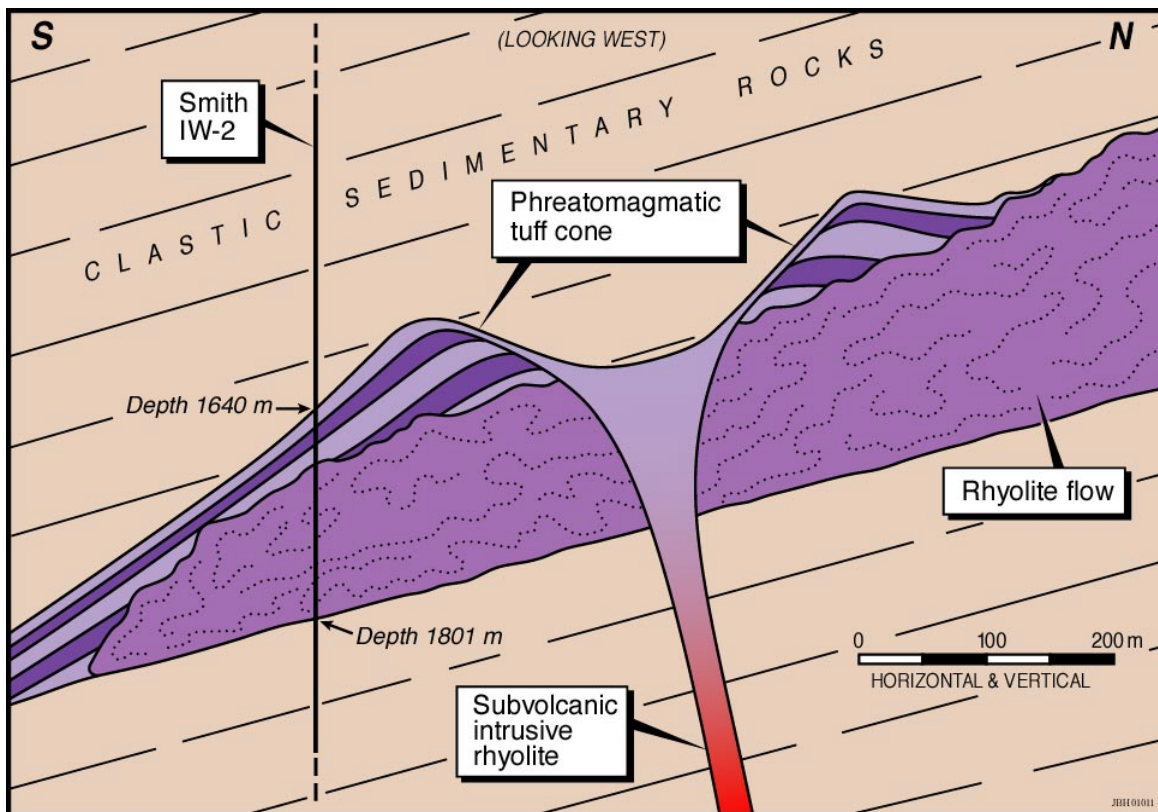


Figure 2. Geologic interpretation of the Smith IW-2 rhyolite and tuff interval.

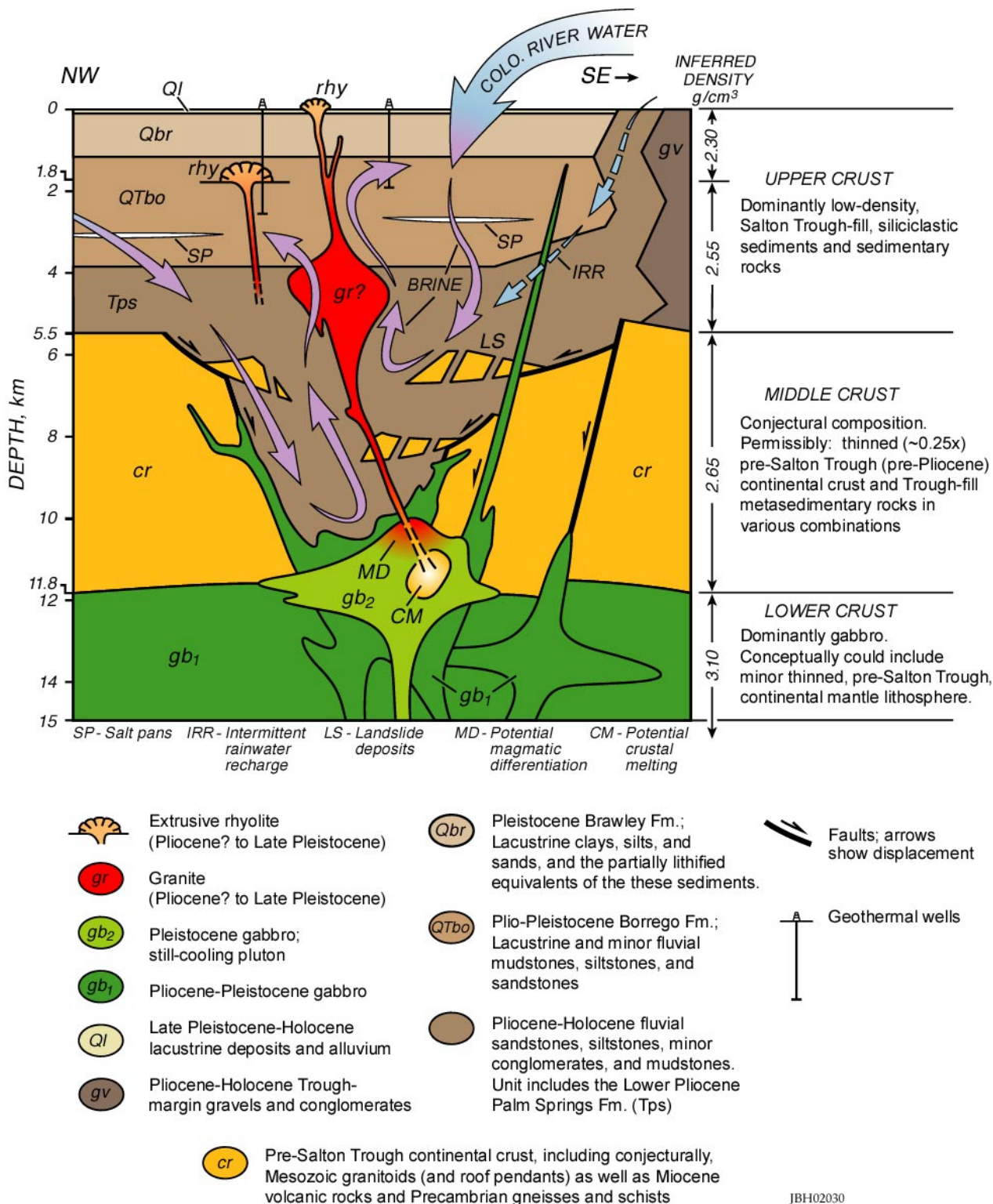


Figure 3. Conceptual lithostratigraphic section through the western Salton Trough and the Salton Sea pull-apart zone. Based on the landmark studies of Wilfred Elders, Arthur Lachenbruch, Michael McKibben, and others, and modified on the basis of new deep-drilling information from the Salton Sea geothermal field. Synthesis by J. Hulen and D. Norton.

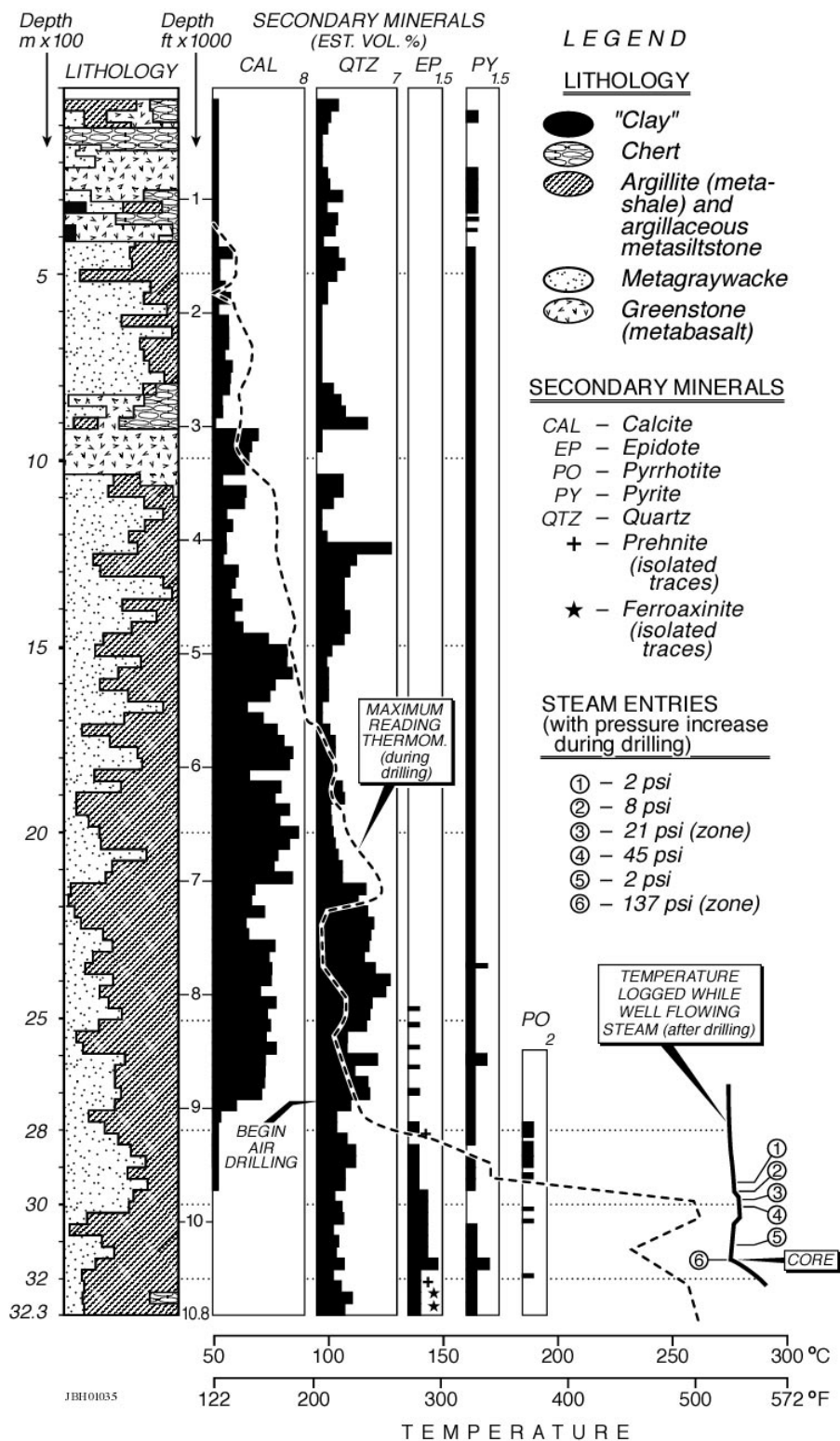


Figure 4. Generalized lithologic, temperature, and secondary-mineral log for geothermal well Aidlin-8, in the northeastern Geysers steam field, California.

GEOHERMAL RESOURCE ANALYSIS AND STRUCTURE OF BASIN AND RANGE SYSTEMS, ESPECIALLY DIXIE VALLEY GEOHERMAL FIELD, NEVADA

Principal Investigator - David Blackwell

Department of Geological Sciences, Southern Methodist University,
Dallas, Texas 75275-0395

Collaborating Investigators – Maria Richards, and Kenneth W. Wisian

Department of Geological Sciences, Southern Methodist University,
Dallas, Texas 75275-0395

blackwel@passion.isem.smu.edu

Key Words - Basin & Range, Extension, Geothermal System, Temperature

Project Background and Status

This project is in the final year of a three calendar year study. The project was devised to bring into the public domain, and to the attention of geothermal developers, valuable thermal gradient and heat flow data collected during the extensive industry exploration episode in the 1970's and early 80's. In addition Caithness Corp. agreed to allow publication and interpretation of important exploration results in Dixie Valley obtained in 1993 and 1994. Obtaining, making public, and interpreting a significant and valuable block of previously proprietary data has been a key aspect of the project. Although industry has a keen interest in this project as evidenced by the commitment of proprietary data, the economic climate has not allowed them to perform this type of a study.

Project Objective

This project has had two main thrusts. The first is to develop a better understanding of the geology of Basin and Range extensional geothermal systems. This objective has been met by developing a detailed geologic model of a major Basin and Range geothermal system, to aid in the development of geothermal systems throughout the province. Dixie Valley, Nevada is the example for the model.

The second thrust is to use thermal techniques to better characterize the thermal resources of the Western United States. The second objective has been met by development and frequent updating of a data base of regional geothermal gradient/heat flow data for exploration use in the development of new geothermal resources using the world wide web as the publication medium (see www.smu.edu/geothermal). We have used this database to develop evaluation and resource estimation techniques for extensional geothermal systems.

Approach

The first project, characterizing extensional geothermal systems in the Basin and Range involves the following steps. First a detailed model of the Oxbow and DVPP sections of Dixie Valley, Nevada geothermal system, based on extensive thermal, seismic, drilling, geologic and potential field data, much of which was previously proprietary or was collected for this study, has been constructed (see Figures 1, 2, and 3). The extension of the characterization to other Basin and Range systems is a task in progress.

The second project is to assess the geothermal resource in place in the western US. A site specific heat flow/gradient/well database has been developed with over 5,000 wells included. These data are available via interactive pages on the Internet. The American Association of Petroleum Geologists (AAPG) as part of this project will publish a revised Geothermal Map of North America. These compilations/maps are a basic starting point for any work involving geothermal resources and are also a primary input to other areas such as tectonics/earthquake hazard assessment and petroleum generation. Distribution through the AAPG should greatly enhance awareness of geothermal resources in the economic geology community.

Research Results

Dixie Valley Model

The Dixie Valley, Nevada, geothermal field (Figure 1) has a rated output of approximately 62 MW and has been producing electrical power since 1988. This field represents the largest, hottest Basin and Range fault hosted, extensional, geothermal system. The thermal source is deep circulation along a part of the

normal fault zone between the Stillwater Range and Dixie Valley. The last major event along this segment of the Dixie Valley fault was about 3,000 ya. North and south of this area are sections of the fault zone that have been historically active and produced major earthquakes (in 1954 a Ms 6.8 earthquake occurred on the fault zone about 30 km to the south, Bell and Katzner, 1987). The seismic interpretation was that the fault responsible for the earthquake dipped about 75° and the epicenter was at about 15 km (Doser, 1989). Fluid-entry temperatures in the producing geothermal wells range are 220 to 248°C (Benoit, 1992).

The Oxbow field has been described by Benoit (1992, 1999). It consists of two groups of production wells in sections 33 and 7 (Figure 1), with injection wells in between (section 5) and to the south (section 18). Two hot wells located several km to the southwest, 66-21 (218 °C) and 45-14, (195 °C) have a few lpm of artesian flow. The northern most well, 76-28 (Tmax of 162 °C at 2350 m) and the 62-21 well in the middle of the valley (Tmax of 184 °C at 3318 m) appear to approach background conditions. The producing zones in the Oxbow field are all at about the same depth and the wells are all about the same distance from the range front so that a reservoir model with a single, range bounding, normal fault dipping at about 54° satisfies the observations (Benoit, 1992).

In 1993 and 1994 Caithness Corp. (later joined with ESI to form Dixie Valley Power Partners, DVPP) drilled two deep exploration wells (62A-23 and 36-14) south of the Oxbow field. The temperature in 62A-23 (265°C) was higher than the production temperatures in the Oxbow field but the well had no flow capacity. More detailed results of the exploration have been described by Blackwell et al. (2000a, 2000b) and are briefly summarized. The initial exploration model of the geothermal system in the DVPP area (shaded area in Figure 1) was of a single range-bounding fault with a dip of about 54°. The drilling of the 62-23 and 62A-23 wells demonstrated that “the range bounding fault” at that location had to dip at an angle of 65° or steeper. However both legs of this well were completely tight with no evidence for a major fault in either leg. The 36-14 well was then drilled closer to the range front, but intersected basement at only 1 km, much too shallow for a single fault model. Consequently the well was deviated toward the range below about 1500 m. At 3,050 TVD the well intersected a permeable zone with over-pressured fluid at a temperature of 280°C.

Thus the wells have temperatures higher than in the producing field and the temperatures increase to the total depth of the wells. The wells are separated by over 1 km at a depth of 3 km. Hot water circulating along a single, range bounding, steeply dipping normal fault can not explain this thermal data. Thus the deep well data in the DVPP lease area require at least two major distinct thermal fluid structures to be present.

A two fault, finite difference, numerical thermal model was developed based on the temperature and geological constraints from the wells. The geometry inferred for the numerical model to fit the observed temperatures in the wells is shown in Figure 2. The boundary conditions included a surface temperature of 15°C and an assumed background heat flow of 80 mW/m². Two thermal conductivity values were assumed, one for the Cenozoic units (1.25 W/m/K) and one for pre Cenozoic rocks (2.5 W/m/K). The heat flow and thermal conductivity values are consistent with the thermal regime in the deep wells away from the geothermal system.

Heat transfer was assumed to be conductive except along the fault zones. The circulation of geothermal fluid along the fault controls the assumed temperature at a particular depth. The calculation shown was done for a period of existence of the system of 70,000 y. That time is long enough to reach near thermal equilibrium over an area on the order of the size of Figure 2. The temperature-depth curves from the deep wells suggest that major transient effects are not generally present.

Both the positions of the faults and the temperature distribution on the faults were varied to give a best match for the observed temperatures in the deep wells. The calculated temperatures along positions corresponding to the tracks of the wells were compared to the observed temperature-depth curves for 36-14 and 62A-23 until a close fit was obtained.

The thermal model and results of a gravity survey described by Blackwell et al. (1999) give a framework for understanding the structure of the geothermal system in the Dixie Valley area. The general model of the geothermal system is of deep meteoric water circulation and heating in the fractured Basin and Range basement rocks. The fluid flows upward along a complex, active, normal fault zone that bounds the Stillwater Range and Dixie Valley. Above 4,500 m the fault zone includes more than one strand having active geothermal fluid circulation along it. The data suggest that there are

complex variations of fault structure along the strike of the range/valley contact, and require that the boundary be a series of faults rather than only one structure. For example there are piedmont faults along most of the contact that take up much of the displacement between the range-valley topographic contact and the valley. However, most of the topographic relief is due to a series of faults at the range/valley contact that in general have relatively little displacement of the valley fill. Finally the extension process is evident in the ubiquitous occurrence of antithetic faults forming grabens on the hanging wall (down thrown side) of the major faults, a detail not shown on Figure 2 but illustrated in the generalized model shown in Figure 3. The structure of the fault zone deduced here is similar to the structure of the fault zone in the area of the 1954 earthquake about 30 km to the south. The 1954 vicinity has a range bounding fault zone, a piedmont fault zone, and an antithetic graben system (see Bell and Katzner, 1987).

General Characteristics of Basin and Range Geothermal Systems

Some implications of the geometry of the normal fault system for geothermal exploration are clear from examination of Figures 2 and 3. For example the fault system along the range front has several targets for drilling, not just one range-front fault. Any thermal manifestations along the range front are not directly connected to the production zones in piedmont faults. Flow on the piedmont faults would be discharged into the valley fill considerably away from the range valley conflict. As an example discharge into the valley fill must have transpired before production allowing for the natural through flow along the fault zone that feeds the wells today in section 7, (Figure 1).

Deep drilling, temperature gradient exploration, and thermal manifestations together indicate most of the strands have some high temperature fluid flow in some places in the greater Dixie Valley geothermal system. The complexity offers challenges to the exploration and drilling, but it also offers reservoir opportunities and sizes that were not expected based on the single fault model.

In general the results from Dixie Valley show how complicated and indirect the thermal manifestations of Basin and Range systems can be. The low water tables and the multiple strands lead to these complicated patterns. Three scenarios for the surface manifestations associated with Basin and Range geothermal systems are shown in Figure 4. In turn the

complicated patterns lead to complicated geochemical evolution of the shallow geothermal fluids. Often the samples of geothermal fluid come from these evolved waters and do not simply relate to the deeper geothermal fluids. Therefore the chemical geothermometers that have been used to evaluate deeper reservoir temperatures may not be valid in many cases. We believe the evidence suggests that a system with a spring temperature or a shallow well temperature of near boiling must be assumed to be much hotter at depth unless precluded by intermediate/deep drilling or deep geochemical sampling. Certainly temperatures in the range of 150 °C, suitable for binary power production, are possible. We compiled a first-cut list of such systems (Table 1) as a guide for thinking about the location of future Basin and Range resource development. There are 23 undeveloped systems on the list. Most of these systems are candidates for additional detailed resource evaluation.

Resource Evaluation of Basin and Range Systems

In developing geothermal resources, determining how much energy can be commercially extracted is always a major factor. The uncertainty in this factor has significant impact on the economics of development. What is needed is an indicator of production capacity that is available at an early stage - after a system has been defined, but before development. The variables involved are numerous and have large uncertainty: producible temperatures, finding producible permeability or fractures, drilling difficulties, long term temperature and pressure drawdowns, etc.

The need for an early stage resource assessment has been obvious since the industry began. The work has been along several lines: volume calculations, planar fracture flows, heat budgets, and surface heat fluxes. Volume calculations have been the most widely employed. They involve estimating the temperature, volume and recovery factor for a geothermal system. The idea is straight forward, but volume and recovery factors are subject to large uncertainty. A fundamental problem with this method is that it treats a geothermal system as a static entity and most geothermal systems are obviously dynamic systems. In these systems, there is no reservoir in the conventional meaning of the term (implying a defined body with negligible flux). Volume calculations are the source of most of the published assessments such as the USGS assessments for the United States (Muffler, 1979). The other volume

techniques have been summarized elsewhere (Wisian et al., 2001).

The surface heat flux method has obvious attractions - heat flux is a major system parameter and relates directly to the strength of the geothermal system. Previously, the surface flux has been used as a starting point in calculating the total heat stored underground to which a recovery factor is then applied (as in the volume method) to determine the producible energy (Muffler and Cataldi, 1978). While this method is theoretically sound it has large uncertainties, similar to the other methods.

The study of Wisian et al. (2001) based on substantially more development experiences since the 1970's, shows that the surface heat flux approach (treating heat loss as the sum of the convective and conductive components) has substantial utility in estimating development potential of geothermal areas. Instead of establishing a direct calculation of heat in the system and then producible energy, an empirical correlation is sought between the two end points: heat loss and production capacity. Data summarizing the electric and thermal production from geothermal systems around the world are readily available (Lund, 2000). The site specific database of thermal wells (www.smu.edu/geothermal) has been used to generate heat flow maps for geothermal systems in the western US with enough data.

In addition values for selected systems worldwide were derived from published sources. Bibby et al. (1995) compiled heat loss values for the geothermal systems in the Taupo Volcanic Zone, New Zealand. Ndolo (2000) summarized the heat losses in the Northern Kenya Rift systems, but only one system, Olkaria, produces power, and thus provides a data point.

Conductive loss at the surface is only one component of the total heat loss. Heat is also lost by radiation (usually negligible) and by fluid/steam discharge. Discharge, particularly in visibly active systems, can be a significant percentage of the total heat loss, but appears to be less than 20% in most cases. Extensive tabulations of heat loss through spring discharge are available (i.e. Garside and Shilling, 1979, Renner et al., 1975) and where possible, these values are included in the total heat loss calculations.

The energy production and total heat loss values for geothermal systems in the US are shown in Figure 5. Total heat loss values are generally minimum values. In most cases the values are probably within a half

order of magnitude of actual. Though the potential errors may seem large, they do not effect conclusions. Errors in generating capacity are negligible, although there is variation in reporting standards.

If only the high quality (1 or 2 rating) data are plotted as shown in Figure 5, no systems are found to produce more than 10 times the natural output. The worldwide data are consistent with this conclusion. The data points cover three orders of magnitude in generating capacity and almost two in total heat loss. Several systems produce at almost ten times their natural heat loss (Los Azufres, Mexico, Coso, and The Geysers in California). The majority of systems produce power at less than the natural heat loss rate.

Based on limited data, early studies suggested that heat could be withdrawn at a ratio of 4 to 100 times the natural rate (White, 1965; Suyama et al., 1975). With this expanded data set, a factor of 10 appears to be a well-defined, empirical limit to power production from a geothermal system. Implicit in this relation is a planned production life of 20-30 years. Higher production can be sustained for shorter periods.

The relationship can be used to predict the capacity of unexploited systems. In Figure 6 the possible generating capacity of a number of Basin and Range systems with heat loss estimates is plotted at an assumed value of 5 times the natural heat loss. These are currently undeveloped areas that have geothermal potential. One of the difficulties in determining a heat loss for areas with few wells is estimating the surface size of the system for the heat flow portion of the calculation. Some areas have more than one listing to represent diverse forecasts in size.

The above discussion assumes that the geothermal system is produced "as is", with no stimulation beyond the usual reinjection. Enhanced Geothermal System (EGS) techniques offer the potential to push production above the "normal" limit (Robertson-Tait and Lovekin, 2000).

This relationship has potential as a predictive tool early in the exploration or development phase of a geothermal project. Shallow temperature gradient surveys are relatively inexpensive, and are a direct measure of the target (heat). The ability to set at least an upper limit on production early in development can reduce the uncertainty and risk in an inherently risky business.

Technology Transfer/Collaborations

The results were presented at the GRC annual meeting, other national and international meetings and are being prepared for submission to other professional journals. The geothermal gradient/heat flow regional database can be downloaded from the web site www.smu.edu/geothermal. A total of almost 6,000 sites are in the geothermal database. Over 2,500 sites are contained in the regional thermal database.

The research phases so far have involved close industry collaboration. Initially interaction was with both Oxbow and Caithness Corp., who funded the geophysical studies that were the foundation for the early phases of this project. Close collaboration continues with Caithness Corp., now the sole owner of the larger Dixie Valley producing area.

During the past couple of years additional exploration has occurred in geothermal systems at Rye Patch, Nevada and Animas, New Mexico. Both these areas appear to structurally resemble Dixie Valley in unexpectedly close ways. Thus the Basin and Range model development described in this report has been extremely important in the success of activities associated with those projects.

Conclusions

There are reasons to be optimistic about the resource potential of the remaining geothermal areas to be explored in the western US, in spite of the lack of exploration and evaluation activity in the last 10+ years:

1. The "fault" reservoirs in Basin and Range systems are more complicated, i.e. larger than anticipated;
2. There is potential for higher temperatures than realized and the geochemical temperatures for many systems, if they are even available, are minimums;
3. There are many systems with shallow temperatures of > 80 °C but no intermediate or deep drilling;
4. The Basin and Range systems are hard to find because of the confusing surface and shallow subsurface evidence (illustrated in Figure 4) so there probably remain many undiscovered/underevaluated systems at this time.

5. The discovery of the close correlation between heat loss in a geothermal system and the electrical power produced from it could be used as a better way to evaluate the geothermal potential of Basin and Range systems. The USGS Circular 790 approach using estimates of geochemical temperature, reservoir volume and the recovery factor has not proved very accurate and useful for exploration or resource planning and needs to be updated after 20 years.

References

- Bell, J. W., and T. Katzner, Surficial geology, hydrology, and late Quaternary tectonics of the IXL Canyon area, NV, *Nev. Bur. Mines and Geol. Bull.* 102, 52 pp, 1987.
- Benoit, D., A case history of injection through 1991 at Dixie Valley, Nevada, *Geothermal Res. Council Trans.*, 16, 611-620, 1992.
- Benoit, W.R., Conceptual models of the Dixie Valley, Nevada geothermal field, *Trans. Geothermal Resources Council*, 23, 505-511, 1999.
- Bibby, H.M., T.G. Caldwell, F.J. Davey, and T.H. Webb, Geophysical evidence on the structure of the Taupo Volcanic Zone and its hydrothermal circulation, *J. Volcanol. Geotherm. Res.*, 68, 29-58, 1995.
- Blackwell, D. D., B. Gollan, and D. Benoit, Temperatures in the Dixie Valley, Nevada geothermal system, *Trans. Geothermal Resources Council*, v. 24, p. 223-228, 2000.
- Blackwell, D. D., B. Gollan, and D. Benoit, Thermal Regime in the Dixie Valley, Nevada geothermal system, ed. E. Iglesias, D. Blackwell, T. Hunt, J. Lund, S. Tamanyu, and K. Kimbara, *Trans. World Geothermal Congress 2000*, 991-996, 2000.
- Blackwell, D. D., K. W. Wisian, D. Benoit, and B. Gollan, Structure of the Dixie Valley geothermal system, a "typical Basin and Range geothermal system, from thermal and gravity data, *Geothermal Resources Council Trans.*, 23, 525-531, 1999.
- Doser, Diane I., 1986, Earthquake processes in the Rainbow Mountain-Fairview Peak-Dixie Valley, Nevada, Region 1954-1959, *Journal of*

- Geophysical Research*, Vol. 91, No. B12, p. 12,572 -12,586.
- Garside, L.J., and J.H. Shilling, Thermal Waters of Nevada, *Nevada Bureau of Mines and Geology Bull. 91*, 163p., 1979.
- Lund, J.W., World Status of Geothermal Energy Use Overview 1995-1999, *Geothermal Resources Council Transactions, 24*, 383-388, 2000.
- Muffler, P., and R. Cataldi, Methods for Regional Assessment of Geothermal Resources, *Geothermics*, 7, 53-89, 1978.
- Muffler, L.J.P., ed, 1979, Assessment of Geothermal Resources of the United States--1978, *U. S. Geol. Surv. Circ. 790*, 163 pp.
- Ndolo, J., Evaluation of Heat Loss in the Northern Kenya Rift Valley, *Proceedings, World Geothermal Congress 2000, Kyushu-Tohoku, Japan, May 28 – June 10, 2000*, 1497-1502, 2000.
- Renner, J.L., D.E. White, and D.L. Williams, Hydrothermal Convection Systems, in White, D.F., and D.L. Williams eds., Assessment of Geothermal Resources of the United States – 1975, *USGS Circular 726*, 5-57, 1975.
- Robertson-Tait, A, and J.W. Lovekin, Potential Sites and Experiments for Enhanced Geothermal Systems in the Western United States, *Geothermal Res. Council Trans.*, 24, 169-174, 2000.
- Sanyal, S.K., Forty Years of Production History at The Geysers Geothermal Field, California – The Lessons Learned, *Geothermal Resources Council Trans.*, 24, 317-323, 2000.
- Suyama, J., K. Sumi, K. Baba, I. Takashima, and K. Yuhara, Assessment of Geothermal Resources of Japan, Proceedings, United States – Japan Geological Surveys Panel Discussion on the Assessment of Geothermal Resources, Tokyo, Japan,, *Geol. Surv. Japan*, 63-119, 1975.
- White, D.E., Geothermal Energy, *USGS Bulletin 1450-A*, 5p., 1965.
- Wisian, K. W., D. D. Blackwell, and M. Richards, Correlation of Surface heat loss and total energy production for geothermal systems, *Trans. Geothermal Resources Council*, 25, 2001.
- Wisian, K. W., D. D. Blackwell, and M. Richards, Heat flow in the western U. S. and extensional geothermal systems, *Proceedings, 24th Workshop on Geothermal Reservoir Engineering, Stanford University, Stanford, CA.*, pp. 219-226. 1999.

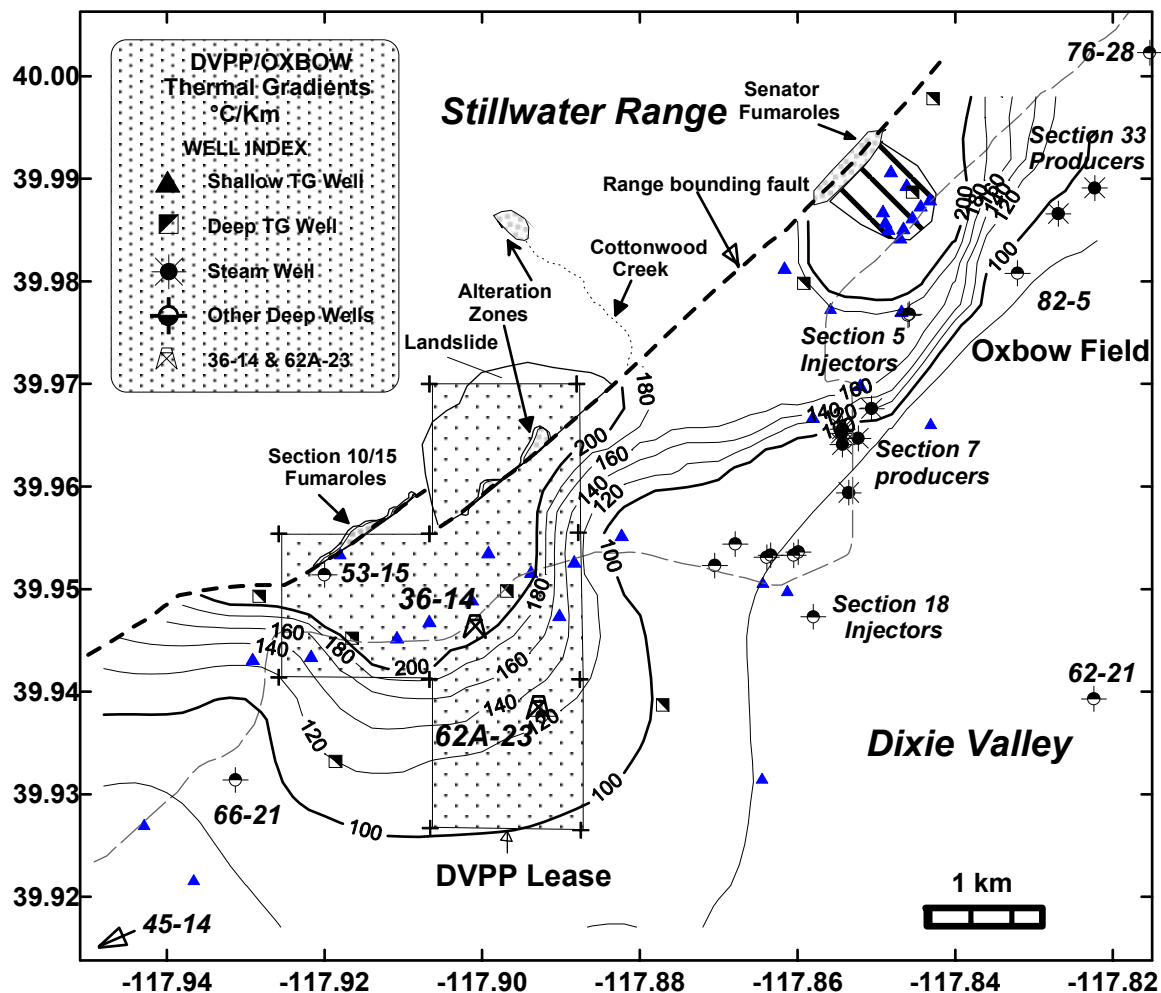


Figure 1. Index map of the Dixie Valley geothermal field. The shaded area represents the Dixie Valley Power Partners lease. The light dashed line is the county road.

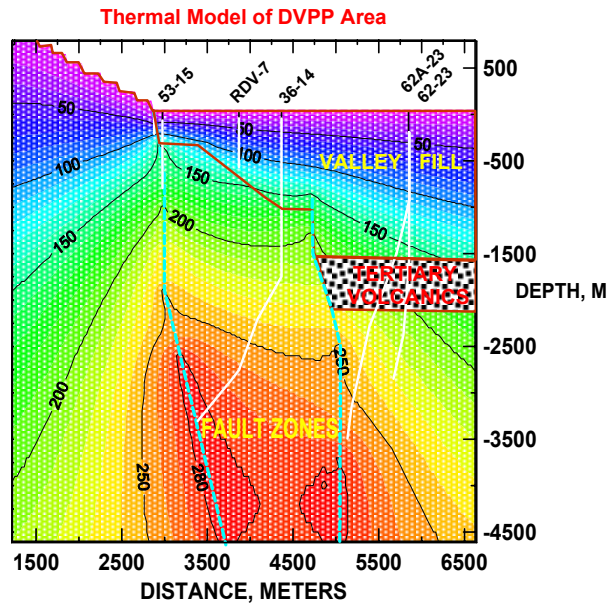


Figure 2. Thermal model resulting from Caithness exploration in Dixie Valley in 1993-1994 (Blackwell et al., 2000a, 2000b).

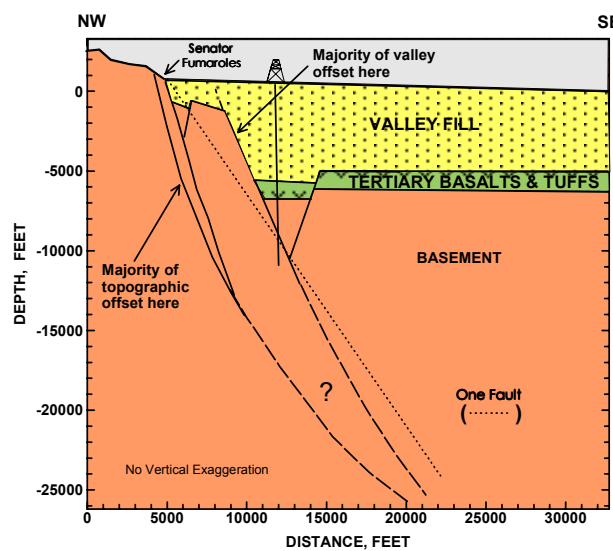


Figure 3. Idealized Dixie Valley structure model based on gravity, seismic and well data (Blackwell et al., 1999, 2000a, 2000b). The general existence of piedmont faulting (major faults outboard of the topographic scarps) and graben fractures result in larger and more complicated reservoirs than expected based on a single fault model (the dotted line).

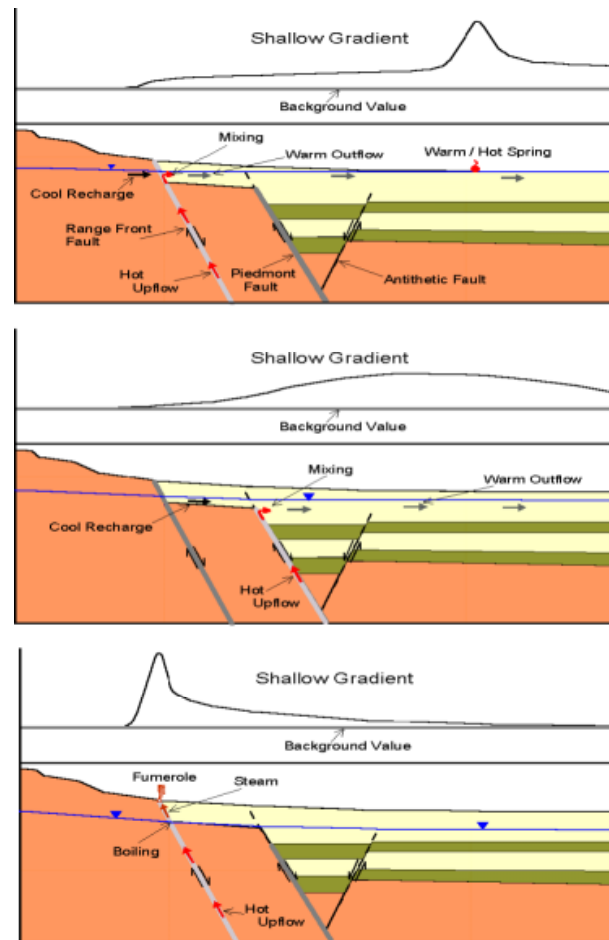


Figure 4. Characteristics of shallow thermal anomalies associated with Basin and Range geothermal systems.

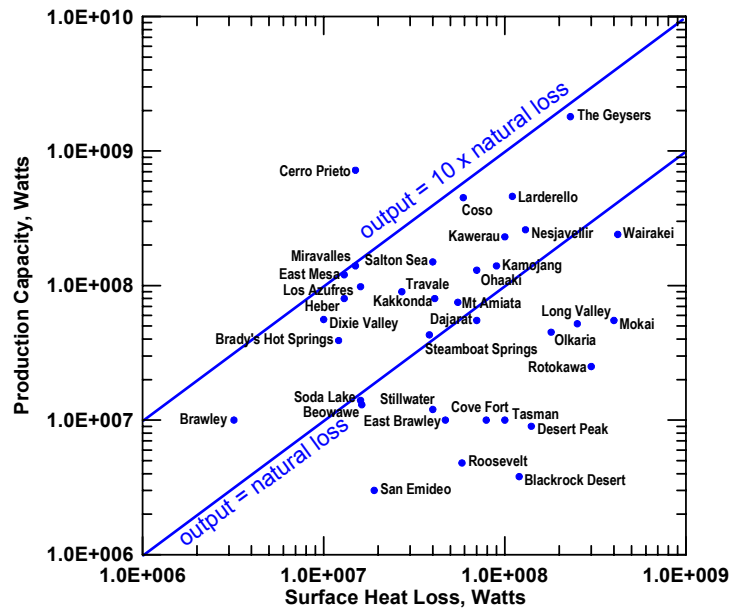


Figure 5. Comparison of heat loss and electrical power production. Cerro Prieto, Mexico is the only system above the 10X line.

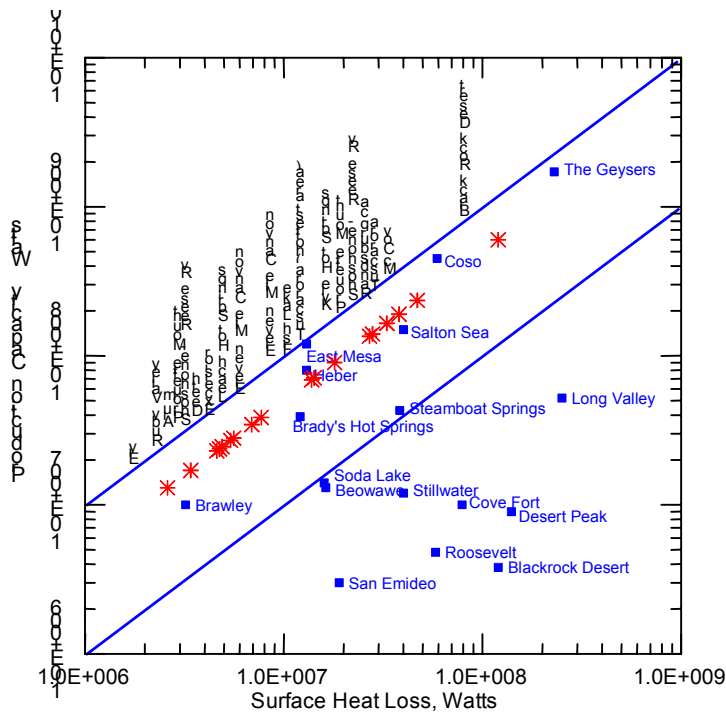


Figure 6. Predicted power production for some Basin and Range geothermal systems with heat loss numbers. A hypothetical 5X ratio is assumed. Black Rock Desert is actually a composite figure for several systems. Multiple listings of areas are from choosing different surface areas for the heat flow portion of the calculation.

Table 1. Systems in Regional Thermal Data Base with maximum temperature over 80°C. Based on the drilling results and the complicated surface manifestations in Basin and Range systems, all of the unexplored systems in the list, regardless of their geochemistry, merit additional exploration. Areas actually producing power at this time are in red.

AREA	STATE	MAX TEMP (C)	AREA	STATE	MAX TEMP (C)
Medicine Lake	CA	107	Humboldt House	NV	194
Geysers	CA	360	Leach Hot Spr.	NV	132
Salton Sea	CA	355	McCoy	NV	102
Bear RV	ID	111	Moana	NV	97
Driggs (AMS)	ID	210	Pirouette Mtn.	NV	87
Hailey (AMS)	ID	189	San Emidio Desert	NV	138
Pocatello (AMS)	ID	117	Shellbourne	NV	198
Preston (AMS)	ID	188	Soda Lake	NV	216
Raft RV	ID	150	Steamboat Spr.	NV	179
Texton	MT	90	Stillwater	NV	177
Marysville	MT	106	Tuscarora	NV	93
Albuquerque (AMS)	NM	343	Wells (AMS)	NV	115
Animas	NM	210	Breitenbush	OR	141
Alum	NV	91	Boise (AMS)	OR	110
Bacon Flat	NV	153	Borax Lake	OR	100
Baltazor	NV	128	Glass Butte	OR	94
Beowawe	NV	216	Klamath Falls (AMS)	OR	130
Black Rock Desert	NV	131	Lakeview	OR	103
Blue Mtn.	NV	81	Newberry Volcano	OR	344
Brady	NV	212	Vale	OR	136
Colado	NV	139	Vancouver (AMS)	OR	82
Desert Peak	NV	204	Best	UT	95
Dixie Valley	NV	251	Cove Fort	UT	178
Eleven Mile Canyon	NV	82	Crystal Hot Spr.	UT	83
Ruby Mtns.	NV	136	Newcastle	UT	127
Fallon	NV	191	Roosevelt Hot Spr.	UT	268
Fish Lake	NV	179	Thermex	UT	96
Hawthorne	NV	83			

IMPROVED TECHNOLOGIES FOR GEOTHERMAL RESOURCE EVALUATION FY 2001 RESEARCH SUMMARY

Principal Investigator - Gregory D. Nash
Energy & Geoscience Institute
University of Utah
423 Wakara Way, Suite 300
Salt Lake City, UT 84108
gnash@egi.utah.edu

Key Words - Remote Sensing; GIS; Hyperspectral; Mineralogy; Cove Fort-Sulphurdale, Utah; Dixie Valley, Nevada.

Project Background and Status

Background

This project explores the use of geomatics technologies, including remote sensing and geographic information systems, to solve specific problems in geothermal exploration and technology transfer. This includes a primary focus on the testing and use of new remote sensing data types and data processing techniques that facilitate the interpretation of features on the surface of the Earth that can indicate hidden faults and areas of permeability, and that may lead to the discovery of hidden hydrothermal convection systems.

This work directly addresses *DOE Program Objectives* related to “Economic Competitiveness – Reducing Geothermal Power Development Costs”, as these new techniques can provide important geologic information leading to greater success in drilling to find and develop vitally needed new geothermal resources. This research also specifically addresses the “Geoscience and Supporting Technologies, University

Research – Active Faulting Areas” area of the DOE Geothermal Strategy which will be discussed below.

Status

Excellent progress has been made on this project during FY 2001 with an emphasis on two geographic areas: Cove Fort-Sulphurdale, Utah and Dixie Valley, Nevada.

Work for the Cove Fort-Sulphurdale area has focused on using hyperspectral data, acquired using a field spectroradiometer, to determine if geobotanical anomalies, related to the hydrothermal convection

system and geologic structures, could be detected. This work has been completed and a final paper, “Vegetation Anomalies at Cove Fort-Sulphurdale Area, Utah: Implications for Use in Geothermal Exploration,” has been completed.

Work for Dixie Valley has also progressed very well. Several hyperspectral data preprocessing and processing techniques were tested leading to two cost-effective methods of detecting and mapping soil-mineralogy anomalies that are related to buried structures and hydrothermal convection. A paper describing this work has been completed and is listed below.

Remote sensing data analysis for geologic structure mapping has also been done in support of the Andesitic Hosted Geothermal Systems subtask. A paper describing this work has been completed and is listed below.

Project Objectives

The principal objective of this project is to determine if remote sensing data can be used in novel ways for geothermal exploration. This includes testing different data types and data processing methodologies that can facilitate interpretation leading to the detection of hidden faults, zones of permeability, and hidden hydrothermal convection systems. This includes geobotanical analyses, soil-mineralogy analysis, and geologic structure mapping.

A secondary objective is to improve the delivery of technology transfer using the Internet to augment the classical approach of paper publication and presentation.

Research Results

Cove Fort-Sulphurdale, Utah

It was hypothesized that geobotanical anomalies, related to geologic structure, might exist over this hydrothermal convection system. Reservoir pressure decreases in the past, resulting from production, may have increased boiling and the possibility of gasses reaching the surface through permeable structures. This would allow toxic gasses, such as H₂S, to penetrate the soil and directly affect vegetation. Deleterious soil acidification could also occur from this process. To test this hypothesis, big sagebrush spectra were acquired using a field spectroradiometer with a 10 nm sampling interval over the 400 – 1000 nm (visible and near-infrared) spectral region. Specific parameters of the resultant spectral curves were used to classify the vegetation as anomalous or non-anomalous. These included: (1) the 699 nm/765 nm ratio described by Carter and Miller, 1994, (2) the red-edge point-of-inflection to determine if blue-shifting was occurring (Miller et al., 1985), and (3) the position, in nanometers, of the visible green maximum reflection, which was observed during this project as being a potentially useful parameter. Upon inspection and statistical analysis of the stated parameters, four classes were determined to describe the big sagebrush that were analyzed including: Healthy, Probably Healthy, Probably Stressed, and Stressed.

Figure 1 shows the results of the spectral analysis for the area adjacent to and surrounding the Utah Municipal Power Agency power plant (south study area). It can be seen that a clearly defined major anomaly lies in the area marked as “A”. This anomaly was spatially correlative with the range-front fault of the Tusher Range and suggests that geothermal gasses were escaping along this structure. It also suggests that synthetic faults were present to the west and also acting as conduits for upwardly migrating reservoir gasses. Geophysical work, done by Ross and Mackelprang (2001), also shows evidence that unmapped synthetic faults exist to the west of the range-front fault corroborating this postulation.

The area marked “B” shows several anomalous samples that are sporadically intermixed with healthy vegetation. The random nature of these anomalies may indicate that gas leakage, along the several associated faults that cross the area, was present, but not consistent. This is the only area in the study where this pattern exists. Area “C” shows a single shrub anomaly directly on a fault.

Figure 2 shows the results of the spectral analysis of big sagebrush in the north study area, which was located approximately 5 km north of the power plant. The most significant anomaly in this area is marked “A”. This anomaly was located around and adjacent to an old sulfur mine where host rocks were hydrothermally altered. Several NNE trending faults, that could be acting as conduits for geothermal system gasses, cut through this anomaly. The area marked “B” had three anomalous samples, which may indicate buried permeable structures that are allowing gasses to escape into the soil. The sample station marked “C” may be either a spurious result or an anomaly that was related to the WNW trending fault that passes just to its south. The sample station marked “D” had two anomalous samples that were relatively close to an old sulfur mine where active fumaroles are found. Both of these anomalies are on a known fault.

The results of this study indicate that mapping geobotanical anomalies, using high spatial resolution hyperspectral data, can be useful for geothermal exploration and for siting new wells in areas proximal to producing steam fields. This technique can directly aid industry for field expansion by facilitating the detection of buried faults and zones of permeability. Portable field spectroradiometers, which provide spatial resolution at the sub-shrub level, can provide a cost-effective method of data collection at the local level and would be useful in areas with moderate to heavy vegetation cover. High spatial resolution airborne hyperspectral data could provide data over larger areas and would be particularly useful where vegetation cover is relatively dense.

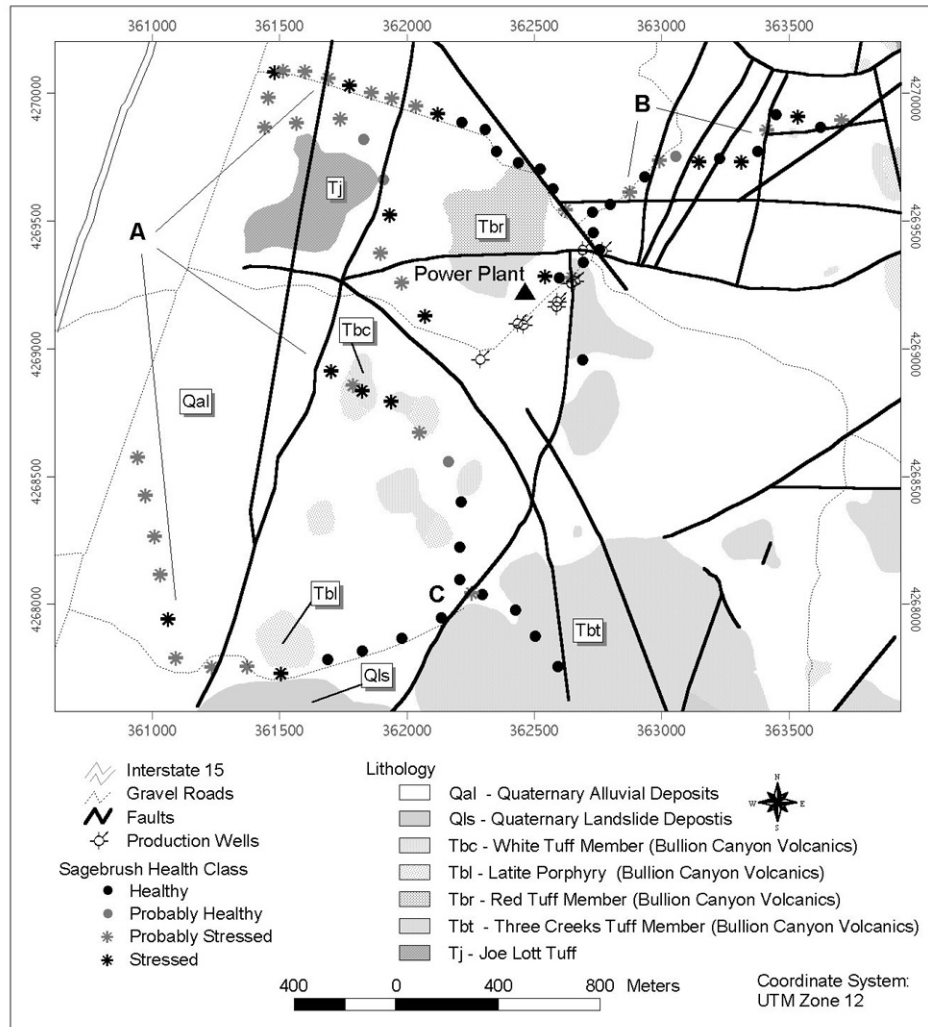


Figure 1. South study area. A major vegetation anomaly, marked "A" is spatially correlative with the Tusher Mountains range-front fault (shown on map) and synthetic faults to the west (not shown). Sporadic anomalies are associated with the faults near "B" and a single shrub anomaly can be seen at site "C", which is located directly over a fault.

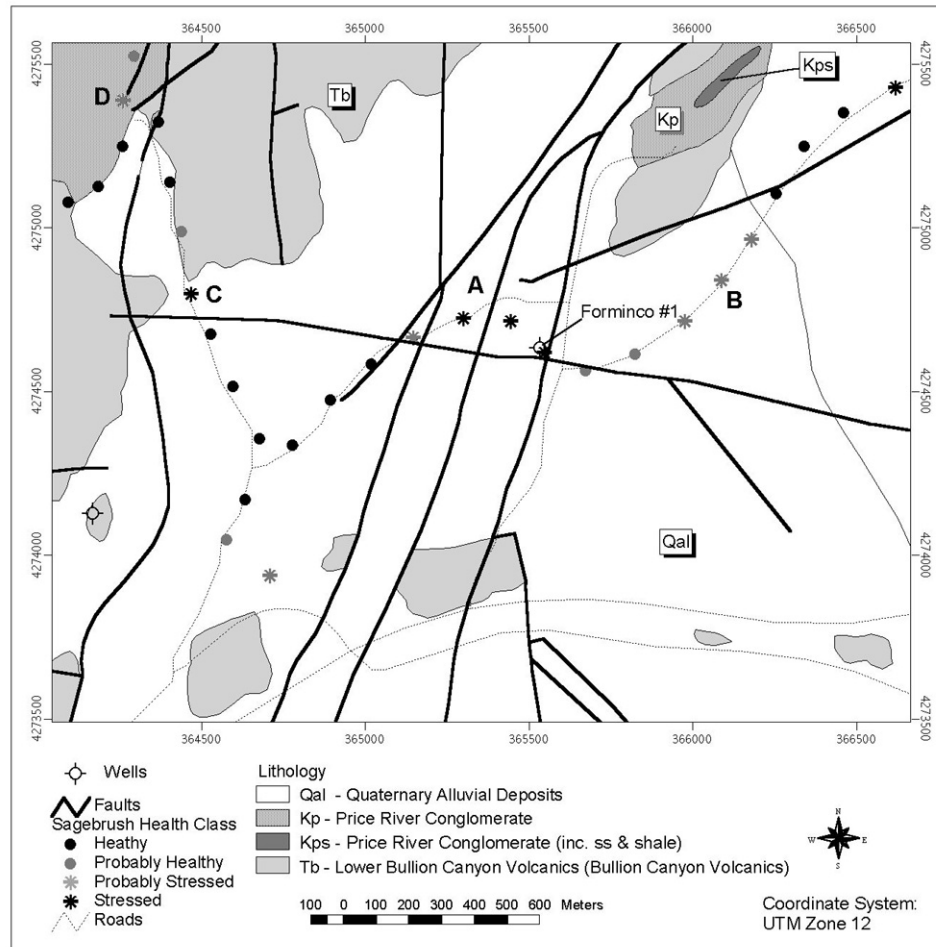


Figure 2. North study area. The area marked "A" is the strongest anomaly. The center of this anomaly is hydrothermally altered, faulted, and has been mined for sulfur. Area "B" has no apparent hydrothermal alteration at the surface or mapped faults, but may be underlain by permeable structures. Area "C" may be a spurious anomaly or may be related to the WNW trending fault nearby. Area "D" shows two anomalies from shrubs that were on a fault and in relatively close proximity to active fumaroles and hydrothermally altered rock exposed in an old sulfur mine.

Dixie Valley, Nevada

This study was undertaken to determine if any hydrothermal convection system related soil-mineralogy anomalies could be detected using hyperspectral data. The dataset used was NASA Jet Propulsion Lab's (JPL) Airborne Visible/Infrared Imaging Spectrometer (AVIRIS), which was acquired on May 20, 1995. This data had 224 channels, with a sampling interval of approximately 10 nm, ranging from 383 nm to 2508 nm. The spatial resolution of the dataset (pixel

footprint size) was 20 m and the image is 614 x 512 pixels.

Before analysis, this dataset was first preprocessed to correct for atmospheric effects and to convert from radiance to apparent reflectance. This was necessary to allow proper data interpretation.

The preprocessed data were then processed to accomplish spectral unmixing. This was necessitated as each pixel generally contains a mix of materials. Unsupervised and supervised methods were tested. The unsupervised method, Polytopic

Vector Analysis (Johnson et al., 2001), was tested as a cost-effective method that could eventually be applied by industry using personnel with minimal training. This analysis resulted in the extraction of five spectral end-members including kaolinite, chlorite, muscovite, olivine (from an outcrop), and a mixture of what was probably calcite and chlorite. Tests are now being run to resolve the pure fifth end-member from the image.

The more conceptually complicated supervised methodology included the following processing steps:

1. Minimum noise fraction (MNF) transformation;
2. Pixel purity index (PPI) generation;
3. Selection of mineral spectra end-members from the PPI;
4. Mixture tuned matched filtering (MTMF) using end-members; and
5. Color enhancement (optional).

This processing was done using RSI ENVI software. Five spectral end-members including kaolinite, chlorite, muscovite, calcite, and olivine (from an outcrop) were derived. An example end-member can be seen in Figure 3. It is anticipated that additional end-members will be found through refined interpretation using mineral spectra from field samples.

This work has resulted in the identification of a significant linear calcium carbonate soil anomaly that is clearly associated with the hydrothermal convection system (Figure 4). This anomaly falls in line with recent fumarole activity, along a buried fault, that was first noticed shortly after the image was taken. The fumaroles were the result of pressure reductions, related to production, which led to reservoir boiling.

Initial results also indicate that there may be elevated levels of kaolinite associated with this anomaly. If this is the case, the kaolinite may be the result of previous hydrothermal alteration along buried structures. Additional statistical analysis will be done to determine if the kaolinite is truly anomalous. The calcium carbonate anomaly was likely the result of previous fumarole or hot spring mineralization that could not be visually detected due to burial.

Soil-mineralogy anomaly detection, which can be facilitated using hyperspectral data analysis, can be

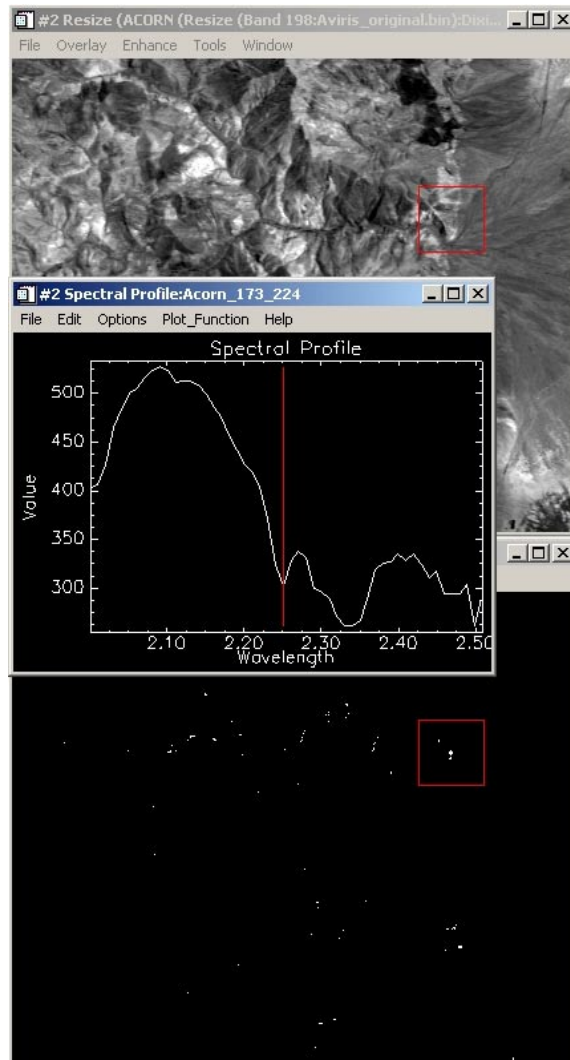


Figure 3. An example of the interactive extraction of a spectral end-member from the Dixie Valley apparent reflectance image (top). The PPI image (bottom) guides the analyst to pixels that are the most likely to have unique spectra. This example shows a good chlorite spectral end-member (center).

an important exploration tool both in close proximity to producing steam fields and for new targets. It will be useful for detecting buried hydrothermally altered faults, within reasonable proximity of the surface, and buried fumarole and hot spring deposits, which can indicate potentially permeable structures and possibly lead to the discovery of new hidden systems.

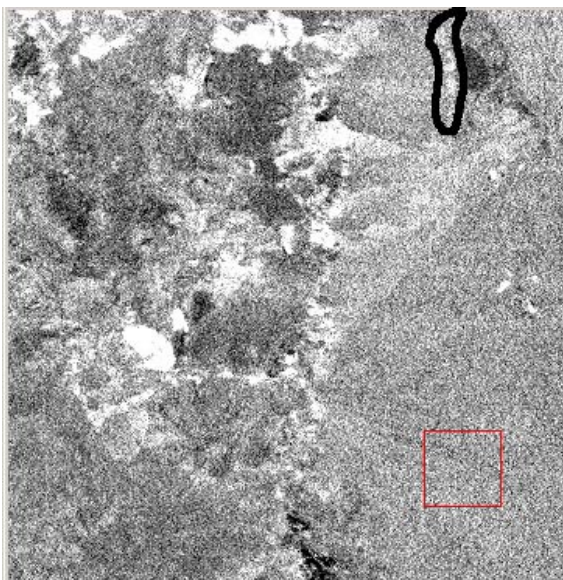


Figure 4. A soil calcium carbonate anomaly, bounded by a dark black outline, was mapped using the supervised hyperspectral unmixing methodology.

This cost of this type of a hyperspectral soil-mineralogy survey would vary depending on the data type used and its acquisition cost. It is estimated that there would be a range from about \$60.00 - \$250.00 per km² for data and processing/interpretation costs. Fieldwork would be additional and may be necessary to verify the interpretation.

Future Plans

The initial success of the Dixie Valley soil-mineralogy anomaly study suggests expanding the geographic area beyond the rather restricted limits of the current study. Therefore, we will work closely with Caithness Energy to choose new data, in adjacent or nearby areas, that will enhance this research and also benefit them in their drilling program. Remote sensing studies of the very promising Salton Sea area, California, will also be done during FY 2002.

In addition, we plan on working closely with Lawrence Livermore National Laboratory and their geothermal remote sensing program. This will allow us maximize data acquisition, reduce costs through cooperation, and allow better cross-fertilization of ideas.

Collaborations, Papers Published, and Technology Transfer

The work described in the document has been done in cooperation with the Utah Municipal Power Agency (Cove Fort-Sulphurdale) and Caithness Energy (Dixie Valley).

Papers resulting from FY 2001 research include:

Nash, G. D. and M. W. Hernandez (2001), "Cost-effective Vegetation Anomaly Mapping for Geothermal Exploration," *Twenty-Sixth Workshop on Geothermal Reservoir Engineering Stanford University*, Stanford, California, January 28-30, 2001.

Nemcok, M, J. McCulloch, G. Nash, and J. Moore (2001), "Fault Kinematics in the Karaha-Telaga Bodas, Indonesia, Geothermal Field: An Interpretation Tool for Remote Sensing Data," *Geothermal Resources Council Transactions*, 25, 411 - 415.

Nash G. D. (2002), "Soil Mineralogy Anomaly Detection in Dixie Valley, Nevada using Hyperspectral Data," *Twenty-Seventh Workshop on Geothermal Reservoir Engineering Stanford University*, Stanford, California, January 28-30, 2002.

In addition to the presentation and publication of research results, a web site, <http://www.egi-geothermal.org>, has been established to aid in this endeavor. Numerous papers generated by the *Western U.S. Geothermal Systems Grant* have been linked both by subtask and geographically using ArcIMS Internet mapping technology. This gives ready access to research results to interested parties through multiple spatial and standard queries. Data resulting from this project is also being added to a readily accessible archive in the most widely used GIS format.

References

- Carter, G. A. (1994), "Early Detection of Plant Stress by Digital Imaging Within Narrow Stress-Sensitive Wavebands," *Remote Sensing of Environment*, 50, 295-302.
- Chang, S. H. and W. Collins (1983), "Confirmation of the Airborne Biogeophysical Mineral Exploration Technique Using Laboratory Methods," *Economic Geology*, 78, 723-736.

Collins, W., S. H. Chang, G. Rains, F. Canny, and R. Ashley (1983), "Airborne Biogeophysical Mapping of Hidden Mineral Deposits," *Economic Geology*, 78, 737-749.

Johnson, G.W., Ehrlich, R., and Full, W. (2002), "Principal Components Analysis And Receptor Models In Environmental Forensics", in *An Introduction to Environmental Forensics* (Murphy and Morrison, Editors), Academic Press, San Diego, 461-515.

Miller, J. R., E. W. Hare, R. A. Neville, R. P. Gauthier, W. D. McColl, and S. M. Till, 1985, Correlations of metal concentration with anomalies in narrow band multispectral imagery of the vegetation red reflectance edge, *Proceedings of the Fourth Thematic Conference, Remote Sensing for Exploration Geology*, San Francisco, CA: Environmental Research Institute of Michigan, 143-153.

Ross, H. P. and C.E. Mackelprang (2001), "Ground Magnetic and electrical Resistivity Surveys Cove Fort-Sulphurdale Geothermal Area, Utah," Utah Municipal Power Agency Report, 29.

IMPROVING EXPLORATION MODELS OF ANDESITE-HOSTED GEOTHERMAL SYSTEMS

Principal Investigator - Joseph N. Moore

Energy & Geoscience Institute, 423 Wakara Way, Suite 300, Salt Lake City, UT 84108

e-mail: jmoore@egi.utah.edu

Key Words - volcanic-hosted geothermal systems, vapor-dominated regimes

Project Background and Status

Conceptual models provide the framework for essentially all geothermal exploration and development. These models are used to locate and prioritize geothermal systems, site drill holes and predict the characteristics of the reservoir before extensive drilling has occurred. Most of the world's producing geothermal systems are associated with andesite volcanoes. Similar geothermal systems are likely within the Cascades of the western U.S., but this province is still largely untapped and poorly understood.

U. S. geothermal companies specifically requested the investigations being conducted under this five-year program. Our study of Karaha-Telaga Bodas (Indonesia) is a joint effort between the Karaha Bodas Co. LLC (an affiliate of Caithness Energy LLC) while work on Bulalo (Philippines) is a cooperative program with Philippine Geothermal Inc. (a subsidiary of Unocal). Karaha-Bodas Co. LLC has provided more than 4 km of core from 4 coreholes, cuttings from production wells drilled to depths of 3 km, MT and gravity data, downhole pressures and temperatures, gamma-ray surveys, electric image logs, chemical and isotopic analyses of water and gas samples, well-test results and existing petrographic and geologic information. This is the most comprehensive data set currently available from any andesite-hosted system.

Project Objectives

The objective of this project is to develop better exploration models of volcanic-hosted systems through an improved understanding of reservoir geometries, permeabilities, fluid chemistries and evolutions. Meeting this goal will have three important results. First, it will lead to improved exploration strategies within the high Cascades, which holds great potential for geothermal development in the U.S. Second, it will reduce the cost of exploration and development by minimizing the number of wells needed and by improving drilling targets in volcanic-hosted systems. Third, this information will help the U.S. industry remain leaders in geothermal exploration and development.

Approach

The basic premise behind this investigation is that there are common geologic factors that favor the formation and growth of geothermal systems in specific geologic environments. The geologic factors that are most important will become evident through a comparison of detailed studies of individual systems. Downhole temperature, pressure, production and geochemical data are allowing us to characterize the present-day structures of the geothermal reservoirs. Mineralogic and fluid inclusion studies are providing information on their evolutions. Modeling of the geophysical data is yielding insight into their geometries and heat sources. Satellite images of surface structural trends and alteration zones, thin sections of core and cuttings samples, fracture logging of core holes and electric image logs are being used to characterize permeabilities at different scales. Information on the age of the systems and major hydrothermal events is being obtained from $^{40}\text{Ar}/^{39}\text{Ar}$ and ^{14}C dating.

The results of these investigations are being critically examined in light of concepts generated from studies of other geothermal systems. In this regard, recently completed investigations of Tiwi, Philippines (Moore et al., 2000a) and The Geysers, U.S. (Moore et al., 2000b, 2001a) are particularly relevant. For example, Karaha-Telaga Bodas and Tiwi are associated with young andesitic volcanoes; both display evidence of a magmatic influence, both have wells that discharge highly acidic fluids and both appear to be relatively large systems. However, Karaha-Telaga Bodas has a large vapor-dominated regime, whereas Tiwi does not. Thus fundamental differences exist between the two systems, despite their apparent similarities. In contrast, the presence of vapor-dominated regimes at both The Geysers and Karaha-Telaga Bodas suggests that there may be some similarities in their reservoir properties and evolutions, despite differences in their geologic settings. A generalized conceptual model that can be applied to the exploration and development of andesite-hosted volcanic systems will be developed from these investigations.

Results

Prior to our investigations of Karaha-Telaga Bodas, little was known about this potentially significant resource or about the evolution of vapor-dominated geothermal systems in volcanic terrains. Although vapor-dominated systems are widely sought after because of their high productivities, few are known (e.g. Darajat, Indonesia; The Geysers, California; Larderello, Italy). Thus, our studies of Karaha-Telaga Bodas represent a unique opportunity to evaluate the evolution and characteristics of vapor-dominated systems. Furthermore, few time-temperature-composition histories of geothermal systems have been developed. This information is used to develop natural state models and predict how a system will behave during production.

The Karaha-Telaga Bodas Geothermal System

Exploration at Karaha-Telaga Bodas has focused on a portion of the volcanic ridge extending from Kawah Galunggung to the north (Fig. 1). The fumarole field at Kawah Saat, a shallow acidic lake (Telaga Bodas) and chloride-sulfate-bicarbonate springs occur at the southern end of the prospect. A smaller fumarole field, Kawah Karaha, occurs at the northern end of the prospect. Figure 2 is a north-south cross section of the field based on our interpretation of the downhole measurements and gravity data (Allis et al., 2000; Tripp et al., 2002). The pressure-temperature data indicate that the resource is partially vapor-dominated and that these conditions extend laterally for more than 10 km and vertically to depths below sea level. A liquid-dominated resource with measured temperatures of at least 350°C and low salinities (1-2 weight percent TDS; Powell et al. 2001) lies beneath the vapor-dominated regime.

Mineral parageneses, fluid inclusion systematics and ^{14}C dating indicate that the vapor-dominated regime developed very recently (Moore et al., 2002a). The ^{14}C dating indicates that lakebeds encountered at a depth of 988.8 m were deposited 5910 +/- 76 years BP. The age of the lakebeds is younger than expected. It implies that significant volcano building, high-temperature hydrothermal alteration (>300°C) related to an extensive liquid-dominated system and the development of the modern vapor-dominated regime occurred since the lakebeds were buried. This liquid system appears to have formed in response to the intrusion of quartz diorite emplaced at a depth of <3 km near the Telaga Bodas thermal area.

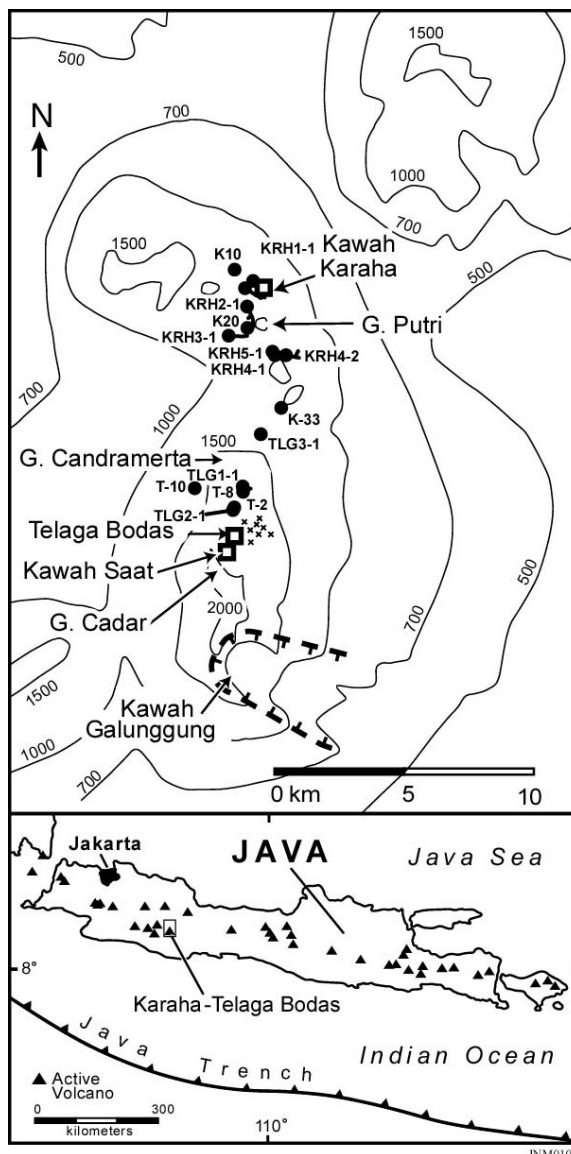


Figure 1. Map illustrating the distribution of volcanic features, thermal manifestations (Kawah Saat, Telaga Bodas, thermal springs (x's) and Kawah Karaha), and geothermal wells (filled circles) at Karaha-Telaga Bodas. Contour lines show surface elevations in meters above sea level.

The transition from a high-temperature liquid-dominated system to vapor-dominated conditions is represented by the widespread deposition of chalcedony and quartz. Fluid inclusions in quartz indicate that the, chalcedony was deposited at temperatures in excess of 250°C. At these temperatures, extreme supersaturation of silica with respect to quartz is required. Continued boiling and

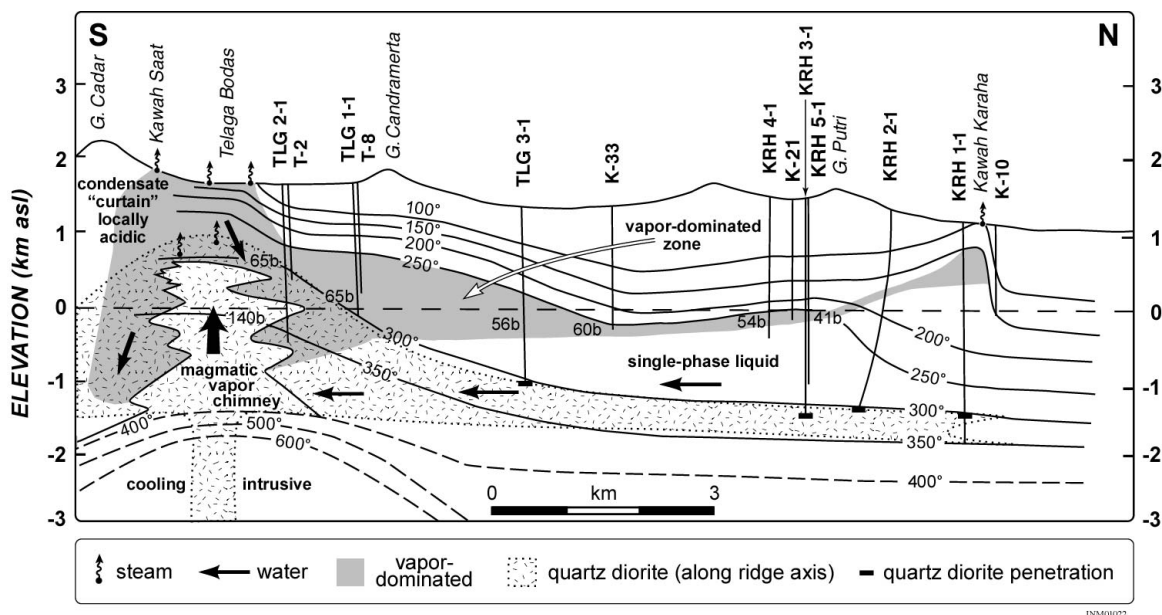


Figure 2. North-south cross section through the Karaha-Telaga Bodas geothermal system. Modified from Allis et al. (2000) and Tripp et al. (2002).

escape of the steam resulted in a progressive increase in the salinities of the residual fluids. Fluids with salinities up to 24 weight percent NaCl-CaCl₂ equivalent were trapped in the quartz crystals. Catastrophic depressurization and boiling is required to produce chalcedony at temperatures >250°C. Depressurization of the liquid-dominated system could have been triggered by massive slope failure of Galunggung Volcano ~4200 years ago (Katili and Sudradjat, 1984).

As the liquid levels and pressures within the reservoir declined, steam condensate percolated downward. Interactions between the condensate and wall rocks produced advanced argillic alteration assemblages and veins dominated by the successive appearance of anhydrite, pyrite, calcite and fluorite (Moore et al., 2002b). Fluid inclusions trapped in anhydrite and calcite suggest that temperatures increased again after deposition of the quartz due to renewed magmatic heating. Boiling off of the descending condensate resulted in a progressive increase in its salinity with depth and eventually the deposition of chemical precipitates consisting of NaCl, KCl, FeCl_x and Ti-Si-Fe. The presence of these precipitates demonstrates that the rocks had dried out prior to drilling. Hypersaline fluids trapped in anhydrite at 300°C may record conditions shortly before complete dry out occurred.

The waters encountered in the reservoir rocks underlying the vapor-dominated region could not represent residual liquids remaining after deposition of the chalcedony and quartz. These fluids would have had salinities much greater than the 1-2 weight percent of the produced waters. The low salinity waters most likely represent mixtures of meteoric recharge and descending condensate.

The importance of these investigations is perhaps most clearly demonstrated by the willingness of the geothermal industry to initiate and actively participate in studies with EGI, provide access to data and samples that are not in the public domain and to encourage publication of the results.

Future Plans

During the remainder of the award period, our investigations will focus on:

- 1) Deciphering the evolutions of individual systems through detailed mineral paragenetic and fluid inclusion investigations;
- 2) The distribution and evolution of reservoir permeability through fracture logging of core holes and interpretation of electric image logs;
- 3) Determination of fluid sources and reservoir processes (e.g. boiling and mixing) through measurement of fluid inclusion gases (H₂O, CO₂, CH₄, H₂S, H₂, N₂, Ar, and C₂₋₇);

- 4) The absolute ages of geothermal activity ($^{40}\text{Ar}/^{39}\text{Ar}$ and ^{14}C dating); and
 5) Developing conceptual models of andesite-hosted systems. The model presented by Allis and Moore (2000) will be refined and tested.

Collaborations

Our studies represent collaborative efforts with the geothermal industry and other organizations. The associations we have developed bring a broad range of demonstrated expertise to the project. Key collaborators include: M. Adams (EGI; geochemistry), R. Allis (Utah Geological Survey; temperature-pressure data), P. Browne (University of Auckland; geology and geochemistry), B. Christenson (Institute of Geological and Nuclear Sciences New Zealand; geochemistry), T. DeRocher (Caithness Energy), M. Heizler (New Mexico Bureau of Mines, $^{40}\text{Ar}/^{39}\text{Ar}$ spectrum dating), S. Lutz (EGI, mineralogy), J. McCulloch (Caithness Energy), D. Mindenhall (Institute of Geological and Nuclear Sciences, New Zealand; palaeontology and radiocarbon dating), G. Nash (EGI; remote sensing), M. Nemcok (EGI, structural geology), D. Norman (New Mexico Tech; fluid inclusion gas analyses), S. Petty (Caithness Energy), T. Powell (Thermochem, Inc.; geochemistry), I. Raharjo (University of Utah; geophysics) J. Renner (INEEL; mineralogy), J. Stimac (Unocal), A. Tripp (EGI; gravity data) and P. Wannamaker (MT data).

Sixteen technical papers have resulted from the research conducted under this grant. Four were delivered at the 2002 Stanford Reservoir Engineering Conference; one will be presented at the 2002 Geothermal Resources Council meeting. Two (Moore et al., 2001a and Nemcok et al., 2001a) were invited presentations at international conferences. The full citations of these papers are given below.

References

*Allis, R. and Moore, J. (2000), "Evolution of volcano-hosted vapor-dominated geothermal systems," *Geothermal Resources Council Transactions*, 24, 211-216.

*Allis, R., Moore, J., McCulloch, J., Petty, S. and DeRocher, T. (2000), "Karah-Telaga Bodas, Indonesia: a partially vapor-dominated geothermal system," *Geothermal Resources Council Transactions*, 24, 217-222.

*Hulen, J.B. and Lutz, S.J. (2000), "Evolution of the uppermost Awibengkok (Indonesia) geothermal system: Evidence from I/S geothermometry and

natural hydraulic fractures," *Geothermal Resources Council Transactions*, 24, 239-245.

Katili, J. A. and Sudradjat, A. (1984), "Galunggung: the 1982-83 eruption", *Volcanological Survey of Indonesia*, Bandung, 102 p.

Moore, J.N., Adams, M.C. and Anderson, A. J. (2000b), "The fluid-inclusion and mineralogic record of the transition from liquid- to vapor-dominated conditions in The Geysers geothermal system, California," *Economic Geology*, 95, 1719-1737.

*Moore, J., Lutz, S., Renner, J., McCulloch, J. and Petty, S. (2000), "Evolution of a volcanic-hosted vapor-dominated system: petrologic and geochemical data from corehole T-8, Karaha-Telaga Bodas, Indonesia," *Geothermal Resources Council Transactions*, 24, 259-263.

Moore, J.N., Powell, T.S., Heizler, MT. and Norman, D.I. (2000a), "Mineralization and hydrothermal history of the Tiwi geothermal system, Philippines," *Economic Geology*, 95, 1001-1023.

*Moore, J.N, Allis, R.G. and McCulloch, J.E. (2001b), "The origin and development of vapor-dominated geothermal systems," invited presentation, *11th Annual V.M. Goldschmidt Conference*, May 20-24, 2001, Hot Springs, Virginia.

Moore, J.N., Norman, D.I. and Kennedy, B.M. (2001a), "Fluid inclusion gas compositions from an active magmatic-hydrothermal system: A case study of The Geysers geothermal field, U.S.A.," *Chemical Geology*, 173, 3-30.

**Moore, J. N., Allis, R., Renner, J. L., Mindenhall, D. and McCulloch, J. (2002a), "Petrologic evidence for boiling to dryness in the Karaha-Telaga Bodas geothermal system, Indonesia," *27th Workshop on Geothermal Reservoir Engineering*, Stanford University, in press.

**Moore, J. N., Christensen, B., Browne, P. R. L. and Lutz, S. J. (2002b), "The mineralogic consequences and behavior of descending acid-sulfate waters: an example from the Karaha-Telaga Bodas geothermal system, Indonesia," *27th Workshop on Geothermal Reservoir Engineering*, Stanford University, in press.

*Nemcok, M., McCulloch, J. and Moore, J. (2001), "Stress control of a fractured reservoir: analysis of electrical images and core from the Karaha-Telaga

Bodas geothermal system, Indonesia,” *Geothermal Resources Council Transactions*, 25, 417-421.

*Nemcok, M., McCulloch, J., Nash, G. and Moore, J. (2001), “Fault kinematics in the Karaha-Telaga Bodas, Indonesia, geothermal field: an interpretation tool for remote sensing data,” *Geothermal Resources Council Transactions*, 25, 411-416.

*Nemcok, M., Moore, J.N., Allis, R. and McCulloch, J. (2001a), “Fracture development within a stratovolcano: the Karaha-Telaga Bodas geothermal field, Java volcanic arc,” invited presentation, *Symposium on Mechanics of Jointing in the Crust*, Aug. 1-4, 2001, England.

**Nemcok, M., Moore, J.N., Allis, R. and McCulloch, J. (2002), “Fracture development within the Karaha-Telaga Bodas geothermal field, Indonesia,” *Geothermal Resources Council Transactions*, in press.

*Norman, D.I., Blamey, N. and Moore, J.N. (2001), “Overabundance of gaseous species and the source of organic compounds in geothermal fluids,” *Twenty-sixth Workshop on Geothermal Reservoir Engineering*, Stanford University.

**Norman, D.I., Blamey, N. and Moore, J.N. (2002), Interpreting geothermal processes and fluid sources from fluid inclusion organic compounds and CO₂/N₂ ratios: *Twenty-seventh Workshop on Geothermal Reservoir Engineering*, Stanford University.

*Powell, T., Moore, J., DeRocher, T. and McCulloch, J. (2001), “Reservoir geochemistry of the Karaha - Telaga Bodas prospect, Indonesia,” *Geothermal Resources Council Transactions*, 25, 363-367.

*Tripp, A., Cherkaev, E. and Moore, J. (2001), “Representation and inductive response of fractal resistivity distributions,” *Twenty-sixth Workshop on Geothermal Reservoir Engineering*, Stanford University.

**Tripp, A., Moore, J., Usher, G. and McCulloch, J. (2002), “Gravity modeling of the Karaha-Telaga Bodas geothermal system, Indonesia,” *27th Workshop on Geothermal Reservoir Engineering*, Stanford University, in press.

*Paper resulting from research under current grant.
**2002 deliverable.

GEOTHERMAL RESERVOIRS: PRODUCTS OF COOLING PLUTON

Principal Investigator – Denis L. Norton, Consultant
 Box 310
 Stanley, Idaho 83278
denis@ruralnetwork.net

Key Words – Reservoirs, dynamics, evolution, supercritical fluids, prospecting criteria

Project Purpose

Assessing the potential of a region to form and sustain a viable geothermal reservoir requires thorough understanding of how reservoirs form and the characteristics of the system that sustains them. Improvements in prospecting methods requires revisiting the process systematics that form reservoirs with this goal in mind and evaluating what parameters should be measured to optimize detection and guide intersection of the reservoirs. This goal can be achieved by a procedure that generates an ensemble of numerical/geological models depicting how source regions for reservoirs in a magma-hydrothermal system evolve.

Project Objectives

Three major targets are: 1) Synthesis of a generic models of geothermal reservoirs within the context of the regional magma-hydrothermal activity, 2) Produce a realistic set of dynamical models of the history of magma-hydrothermal activity typical of geothermal environments, and 3) Derive new and novel prospecting guides based on patterns derived from (1) and (2).

The project set out to characterize the space and time variations of fracture formation driven by progressive fluid pressure fronts as they propagate outward from a cooling pluton and to analyze the system dynamics as they occur at supercritical conditions, determine the properties of these zones that could be detected remotely. The studies focused on situations where magma-hydrothermal processes would develop conditions conducive to the formation of geothermal resources. The study drew primarily on Geysers Resource that appeared to contain evidence of how processes evolve through the near critical region of the H_2O -System.

Methods

Methods that quantitatively describe magma-hydrothermal activity have advanced to a stage that they can be used to effectively *interpret*

chronological and geometric relationships amongst mineral alternation, fractures and veins, and igneous event, *map* time-space variations of transport events, and *predict* the stage of evolutionary behavior of observed activity. A similar set of interacting processes determines the character of all systems; variability perceived amongst systems is a consequence of differences in process behavior. Consequently the theory of magma-hydrothermal activity is extensible to understanding how geothermal reservoirs form.

Behavior in magma-hydrothermal systems is studied with the aid of transport equations that represent the time dependency of any system property, here taken to be either mechanical, thermal or chemical energy, G among minerals and a fluid whose volume fraction (ϕ_f) and physical form of the pore space it occupies depends on space and time. The conservation of this property in a rock that contains \hat{I} mineral phases plus a single fluid can be written:

$$\frac{\partial(\phi_f G_f)}{\partial t} + \sum_i \frac{\partial(\phi_i G_i)}{\partial t} + \nabla \cdot (\phi_f \mathbf{v}_f G_f) = 0 \quad (1)$$

where t is time, ∇ , the gradient operator, l^{-1} ; subscripts f , fluid, and i , i^{th} mineral, \mathbf{v}_f is the fluid velocity and ϕ the volume fraction of the respective i^{th} phase. The first term in Equation 1 represents local change in any system property G of the fluid phase with time. The second term is the local change in the level of G in mineral phases summed over the all phases; it is linked to the first term through kinetic and equilibrium statements. The third term on left of equation 1, advective rate of change, exerts strong control over process behavior because it depends on the local rates of change in the quantities, G , and advection gradients, $\mathbf{v}_f G_f$. Integration of equation like 1 in the context of robust material equations of state and geologic observations constitute the study methods.

Results

The 305 km^3 of magma that crystallized into the Geysers Felsite cooled to present-day conditions in about 750 kyr . Following emplacement of the magma a broad zone of temperature increase moved toward the surface for about 125 kyr ; temperatures were first, perturbed at the surface

somewhere between 10 and 25 kyr following magma emplacement. The region that straddles the contact between Geysers Felsite and its lithocap rocks resided at supercritical state conditions near the critical point for the hydrothermal fluid for about 50 kyr , cf. Figure 1, trajectory 1 and 2.

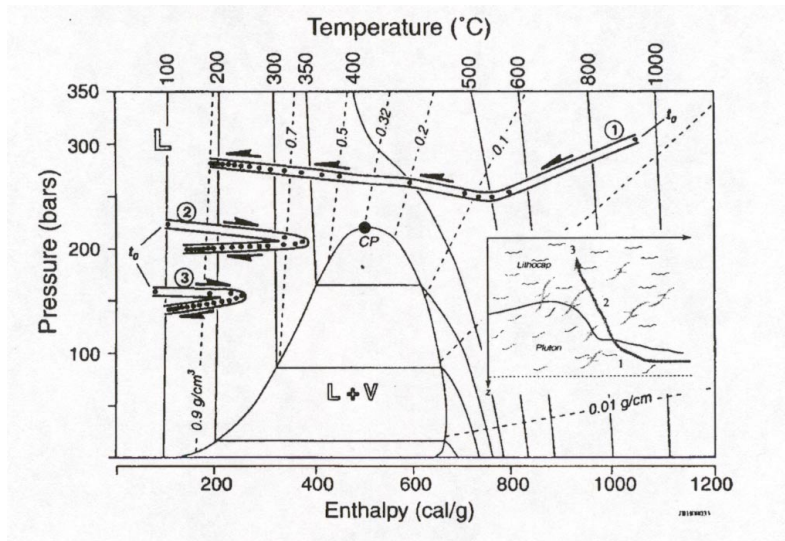


Figure 1. Enthalpy-Pressure project of the H_2O -System, showing the 2-phase “dome”, L+V, liquid, L and vapor, V regions. Above critical end point, CP, the phase is a supercritical fluid. Isotherms, $^\circ\text{C}$ and isochores, g/cm^3 are depicted respect phases. The hydrothermal history of rocks typical of locations shown within insert of generic section through Felsite are shown from initial intrusion of the felsite, t_0 , for 1 My in $50,000 \text{ yr}$ increments. Based on an ensemble of detailed numerical models, Norton and Hulen, 2001.

The thermal, mechanical and chemical processes that combined to dissipate the energy from the felsite interacted in an oscillatory manner. Such behavior is partially attributed to their interconnectedness through feedback relations, and because each feedback depends on hydrothermal fluid properties. The properties are demonstrably non-linear near critical points of the fluid. The tendency for lithocap rocks to be shifted in state conditions from t_0 toward the 2-phase dome is well know, but the shift to near critical conditions, cf trajectory 2 has previously unexplored consequences as does the decay of state conditions from within the pluton, cf trajectory 1. In all other magma-hydrothermal systems in the upper crust studied to date, vigorously flowing fluids are similarly attracted to extrema in transport, thermodynamic, and solvation properties of the fluid. The consequences of this process evolution

are reflected in geothermometric, mineral and fracture data, from the Geysers rocks.

Geothermometric Data (Fluid Inclusions)

The distribution of fluid inclusion filling temperatures from locations adjacent to the felsite-lithocap contact from Moore and Gunderson, 1995, are correlated with the theoretical trajectories of similar locations in the numerical models, Figure 2. The abundance of inclusions are mapped onto the pressure-enthalpy section with state trajectories of rock from the sample locations. The values from quartz in the felsite, left-hand figure, formed late in the cooling history, circa $300\text{--}400 \text{ kyr}$, whereas those in the lithocap, right-hand figure, formed early, circa $10\text{--}30 \text{ kyr}$, as required by progressive thermal states in the lithocap.

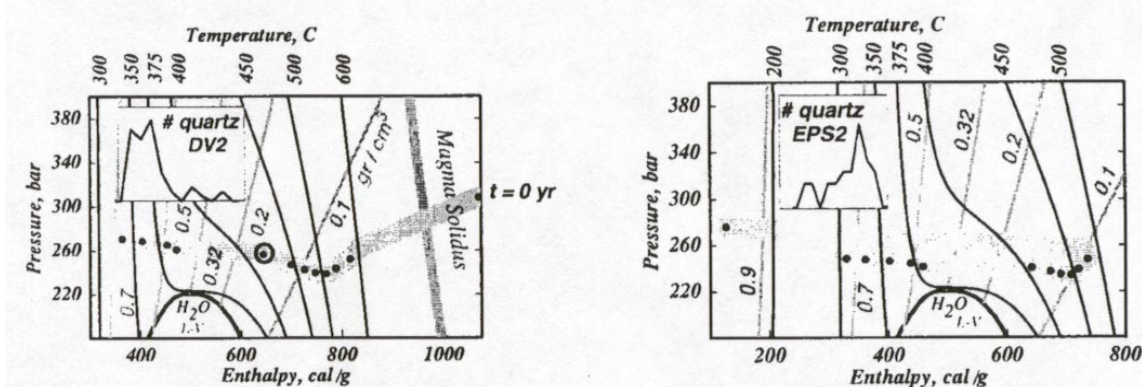


Figure 2. Time trajectory of rocks in numerical approximation of Geysers Felsite correlated with geothermometric data from within felsite, left-hand, and lithocap, right-hand. Dots at 50 kyr increment on trajectory, see Figure 1.

The time of formation of fluid inclusions relative to the time zero of magma emplacement is useful in understanding the relative ages of hydrothermal rock units. Compilation of system wide geothermometric data in the context of numerical representations of the thermal history of the heat source is recommended to help establish system age for all geothermal prospects. This method is new also to the field of fluid inclusion studies.

Mineral Records of Dynamical Behavior

The Geysers is renowned for enormous concentrations of tourmaline veins. The delicate zoning within some of these crystals reflects oscillations in chemical state associated typical of expectations from numerical models at near-critical conditions, Figure 3.

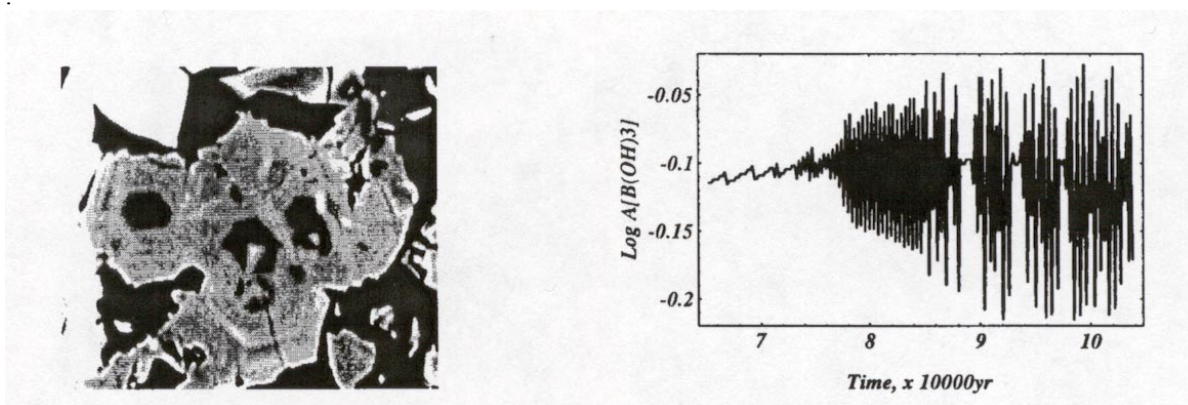
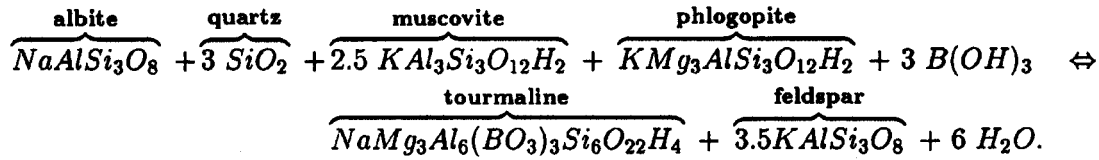


Figure 3. Left: Backscattered electron image of vein tourmalines from the carapace of the Geysers Felsite displaying oscillating chemical zones. The light gray core is dravite-like composition, $(\text{Na}, \text{Mg})\text{-rich}$, $\text{NaMg}_3\text{Al}_6\text{Si}_6\text{O}_{18}(\text{BO}_3)_3(\text{O}, \text{OH})_4$, and the rim is foitite, $(\square \text{Fe}^{2+} \text{Al}) \text{Al}_6\text{Si}_6\text{O}_{18}(\text{BO}_3)_3(\text{O}, \text{OH})_4$, is a x -site vacant tourmaline, \square with almost one-half of the x -site is vacant and the octahedral site is Al and Fe-rich. Field of view $\sim 100 \mu\text{m}$. Right: $\text{Log } a[\text{B}(\text{OH})_3]$ vs. time in equilibrium with: K-feldspar, quartz, albite, dravite, phlogopite, muscovite and unit activity of H_2O .

This particular tourmaline is the product of hydrothermal conditions near the magmalithocap contact during the early stages of energy dissipation from the magma, these compositional data help constrain the conditions between fluid and rock

several hundred thousands of years ago. An equilibrium reaction among minerals typical of this assemblage serves to discuss the significance of aqueous boron:



The equilibrium constant for this reaction is sensitive to conditions near the critical-region because of the control exerted by the stability of the aqueous ions at those state conditions. Mapping this equilibrium constant for state conditions encountered along trajectory 2, in Figure 1 displays the correlation of observed zoning in tourmaline, left hand Figure 3, with oscillatory concentrations of aqueous B(OH)_3 .

This relationship is typical of situations noted in other studies where always one finds that the patterns of hydrothermal alteration have geometries indicative of the temporal behavior of processes that caused them. Prospecting for resources could use this information to develop functional relationships of form and process that provide the basis for new interpretations. Similar relations undoubtedly exist in epidote compositions, which could refine criteria for detection of the reservoir top surface.

Fracture Propagation

The alteration of pore space caused by dispersion of energy from the felsite is evident in drill core of lithocap rock, Figure 4. Typical patterns noted in unaltered lithocap rock are contorted discontinuous blebs of calcite, ct, left panel. During the prograde hydrothermal event calcite is dissolved and these blebs are redistributed into elongate, narrow aperture vuggy, v, quartz, q, veins oriented roughly normal to the pluton-lithocap contact, right panel. Calcite dissolution, reformation of the pore form into an elongate percolation path, and partial filling with quartz sequentially occurred following temperature increases early, 10–50,000 yr, in the felsite cooling history.

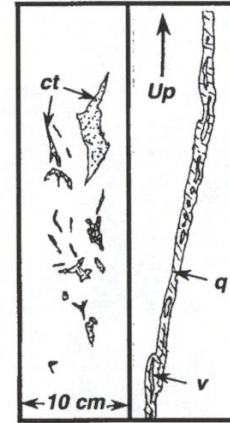


Figure 4.

The mechanical portion of the process is considered a quasi-static deformation of an isolated irregular pore into elliptical form, then extension during heating, when mechanical energy, J , levels in the fluid filled pore space exceeds a threshold value, J^* , the effective fracture resistance of the rock.

$$\frac{dl}{dt} = \begin{cases} \frac{\alpha(T)l}{2-\beta(T)P_f} \left(\frac{dT}{dt} \right) & J \geq J^* \\ 0 & J < J^* \end{cases} \quad (2)$$

$$\frac{dP_f}{dt} = \begin{cases} \frac{-\alpha(T)P_f}{2-\beta(T)P_f} \left(\frac{dT}{dt} \right) & J \geq J^* \\ \frac{\alpha(T)P_f}{1+\beta(T)P_f} \left(\frac{dT}{dt} \right) & J < J^* \end{cases} \quad (3)$$

$$J = \left(\frac{4(1-\sigma^2)}{3\pi E} \right) P_f^2 l \quad (4)$$

Conservation of fluid mass and energy relationships for fracture length, l , and internal fluid pressure, P_f are derived as functions of fluid properties, fluid pressure, P_f , and rate of temperature change. Where E is Youngs modulus and σ is Poisons Ratio. The competition among expansivity, $\alpha(T,P)$, of the fluid filling the pore and its compressibility, $\beta(T,P)$, determines the behavior of this process. Both parameters are strongly nonlinear in the super-critical region and continuously increase to $+\infty$ at the critical point the evolution of fracture pore space, Figure 5 is sensitive to small variations in temperature and hence pressure.

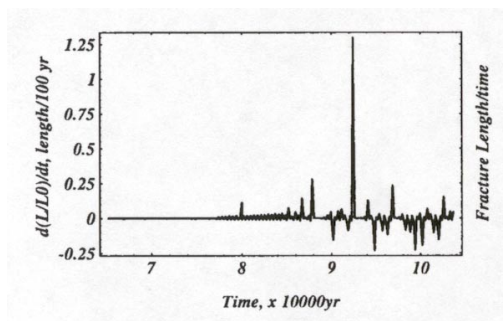


Figure 5. Change in fracture length versus time implied for convecting hydrothermal activity at location 2, inset Figure 1, near pluton-lithocap contact as derived from equations 2-4 for extension of fracture length by fluid pressure changes. Oscillatory growth is consequence of tiny pressure and temperature changes caused by fluctuating buoyancy.

Conclusions

As fluid flows tranverse from a single-phase supercritical fluid state toward a two-phase liquid-steam state their paths are determined by the dynamical behavior of process interactions “upstream”. Fracture propagation deflects the flow path to low pressure-high enthalpy (vapor dominate), while mineral sealing decreases advective cooling rates and deflects the path toward low enthalpy-low temperature (liquid dominate) regions. Geometric parameters of alteration features in the Geysers rocks suggest chaotic behavior.

Interest in these patterns and constraints placed on the timing events should be of profound interest to business, the Interior Department and academics whose project goals are to audit geothermal energy resources, should they so choose.

Completion

This new perspective in geothermal resource characterization is being applied to define the parameters needed to identify the most prospective regions of a potential reservoir for development. During the final few months of this project these considerations are being summarized for geothermalists. Specific guidelines are being developed on how to apply the dynamical patterns and time constraints on the evaluation of prospective regions. Perhaps the biggest impact will come to situations where

regions with potentially young magmas are being prospected.

Assessment of the potential geothermal resources in the United States completed some 20 years ago did not utilize concepts and understanding of processes associated with thermal anomalies in the shallow crust. Advances in the theoretical geochemistry of rocks, minerals and fluids, dynamical analyses of process evolution, as well as improved quantitative tools that permit mapping of alteration patterns in rocks in space (relative to causative thermal anomalies) and time (relative to causative thermal anomalies) coordinates were realized. This new body of information and theory offers new perspectives and opportunities, and is necessary for all future assessments. The critical concept is affording for the processes associated with the time-space dissipation of energy from thermal anomalies. The concluding work for this project outlines new methods that could greatly improve the auditing of thermal resources.

Published Results

Norton, D., 2000. Systematics of Magma-Hydrothermal Processes: Geothermal Resources Near Cooling Plutons. Geothermal Res. Council Annual Meeting.

Hulen, J.B., Norton, D.L., Moore, J.N., Beall, J.J., and Walters, M.A., 2001, Initial insights into origin, configuration, and thermal-chemical evolution of the Aidlin Steam Reservoir, Northwest Geysers steam field, Ca. GRC-Annual meeting.

Norton, D. and Hulen, Jeffrey B. 2001. Preliminary numerical analysis of the magma-hydrothermal history of the Geysers Geothermal System, California. Geothermics special issue. 30, 211-234.

Norton, D.L. and Dutrow, B.L. (2001). Complex Behavior of Magma-Hydrothermal Processes: Role of Supercritical Fluids. *Geochemica et Cosmochimica Acta*, v.65, pp. 4009-4017.

ENHANCED DATA ACQUISITION AND INVERSION FOR ELECTRICAL RESISTIVITY STRUCTURE IN GEOTHERMAL EXPLORATION AND RESERVOIR ASSESSMENT

Principal Investigators - Philip E. Wannamaker
University of Utah, Energy & Geoscience Institute
423 Wakara Way, Suite 300
Salt Lake City, UT 84108
pewanna@egi.utah.edu

Collaborating Investigators -John A. Stodt, Jeffrey B. Hulen
University of Utah, Energy & Geoscience Institute
423 Wakara Way, Suite 300
Salt Lake City, UT 84108

Key Words - Exploration, fluid properties, instrumentation, numerical simulation

Project Background

Predictive capability for subsurface resource location is one of the most desirable aspects of a geothermal exploration tool. Electrical resistivity is a primary physical property of the Earth which can be strongly affected by geothermal processes. Since an increased fluid content due to fracturing, and the development of more conductive alteration minerals (clays, etc.), can give rise to an electrical resistivity contrast, electromagnetic (EM) methods of probing have been investigated and applied for many years. The reliable mapping of electrical resistivity should increase chances of discovering blind geothermal resources, in defining the extent of geothermal reservoirs, in imaging controlling structures for geothermal systems, and in resolving permeable fracture zones (DOE/OGT Strategic Plan, 1998). Our research group at the University of Utah has provided solutions of global import in this field with respect to numerical simulation capability, interpretation philosophy, instrumentation, and field studies as detailed below.

Project Objectives

Our efforts are aimed at reduced drilling costs and increased reservoir base through more reliable technology for exploration and enhanced geothermal systems. Progress requires improvements in density and quality of field EM data, developing refined electrical models and EM modeling algorithms for the geothermal environment, and incorporating independent geological data in cooperative interpretations for EM data. For imaging subsurface resistivity structure, several modes of EM propagation have been used ranging from man-made sources in the time-domain to natural and artificial sources in the frequency domain. Due to the depth of exploration potential and the likelihood of substantial advances in

data quality and imaging capability as proposed herein, we are emphasizing the magnetotelluric (MT), CSAMT, and galvanic (DC) resistivity/IP methods. This approach also exploits emergence of new-generation array collection instrumentation for simultaneous MT-DC surveying.

Plans and Approach

One way to improve resistivity structural resolution is by developments in non-linear 2-D inversion of magnetotelluric (MT/CSAMT) and DC resistivity/IP responses. The standard approach is to minimize an objective function $W_{\lambda}(m)$ which is a weighted sum of data misfit and departure from *a priori* information:

$$W_{\lambda}(m) = \{(d-F[m])^T C_d^{-1} (d-F[m])\} + \lambda \{(m-m_0)^T C_m^{-1} (m-m_0)\}$$

The inversion of diffusive EM data must be stabilized, and the particular approach is embodied in the choice of the form of C_m . Our novel method is model-adaptive and exploits basic resolution principles of electrical methods such as similitude and fundamental correlations (e.g., conductivity-dimension) to avoid model artifacts, instead of using brute-force smoothing by damping slope or curvature.

Geothermal systems and other earth structure of course can be 3-D so we pursue this modeling capability as well. For adapting our own techniques and allowing efficient technology transfer, we require a straightforward, freely available source code. We have been cooperating with Y. Sasaki of Kyushu University who has provided such a program, implementing the 2nd-order, E-field staggered grid formulation (Smith, 1996; Alumbaugh et al., 1996; Sasaki, 1999, 2001). Accuracy, versatility and run time

tests were done against the integral equations platform of Wannamaker (1997), and the finite difference H-field code of Mackie et al. (1994). Currently, we are modifying and applying this algorithm to temporal changes in resistivity structure of geothermal fields with production over time, as described below. Prototype finite EM source and inversion capability have been tested also, and we will be improving upon those.

As a complement to commercial surveying capability, we are completing a multi-station field MT system with unique modes of acquisition and processing which is aimed particularly at eliminating man-made EM interference in already-producing geothermal systems. Increases in productivity and data accuracy are sought through simultaneous band acquisition with multi-site control via digital radio telemetry. The principal difficulty with the standard MT response model is the assumption that all noise on the system output (electric field) is uncorrelated with noises on the system inputs (magnetic field), whereas in the case of cultural interference the noises on the inputs and output are correlated. This is not met by the standard remote-reference method and we have been formulating a more complete MT noise model for this problem.

Research Results

Inversion tests for the 2-D MT case have been run on several sample data sets from Nevada, Utah and New Zealand. An example appears in Figure 1 for contracted data taken by Quantech Geoscience over

the Carlin gold trend of north-central Nevada in a contiguous profiling array. There are 57 100-m bipoles oriented in cross-strike orientation (TM mode) which is the more robust mode for 2-D interpretation (Wannamaker, 1999). Electrical structures have been confirmed by excavation or drilling. A prototype 2-D inversion program for the pole-dipole resistivity/IP problem utilizing analogous regularization principles has recently been completed and tested using synthetic data. Program structuring is underway for joint MT/DC inversion, desirable since the two methods have differing resolving capability when it comes to conductive versus resistive structures. Quantech has recently fielded a system acquiring array MT and DC measurements simultaneously, and we are proposing to apply this new-generation system and our inversion capability to basic structural and resource problems at the Dixie Valley thermal area.

An example calculation using our 3-D modeling algorithm is given for the Oguni system, in cooperation with John Pritchett of SAIC using the STAR P-T-X reservoir simulator (Figure 2). Input to the simulator includes ambient ($t = 0$) P-T-fluid composition-permeability conditions from available drilling and sampling, together with laboratory data on electrical properties of fluids and bulk mixtures versus P-T-X. After 50 years of production, dry steam zones are predicted to form near-surface close to and east of Hagenoyu-Matsuya hot springs (Figure 2a). The primary steam (higher resistivity) zone is predicted at a depth ~ 500 m also under the main southern production area, especially under well GH-19. Higher resistivities at ~ 750 m depth under the

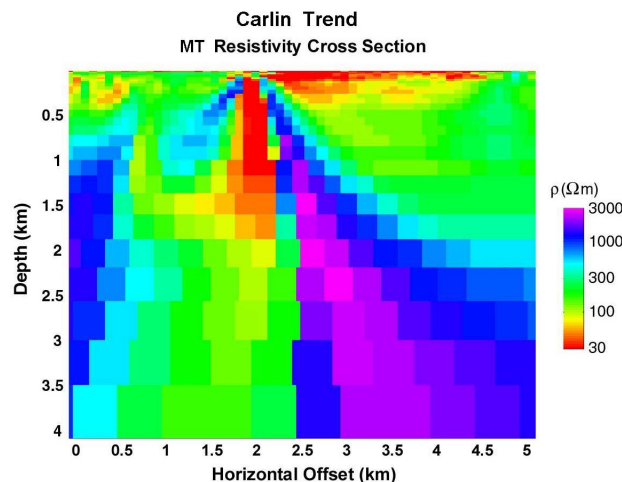


Figure 1. Electrical resistivity model cross-section derived from inversion of 57 MT sites taken as contiguous, 100 m bipoles across major gold prospect of the Carlin trend or north-central Nevada. Data courtesy of Quantech Geoscience Ltd.

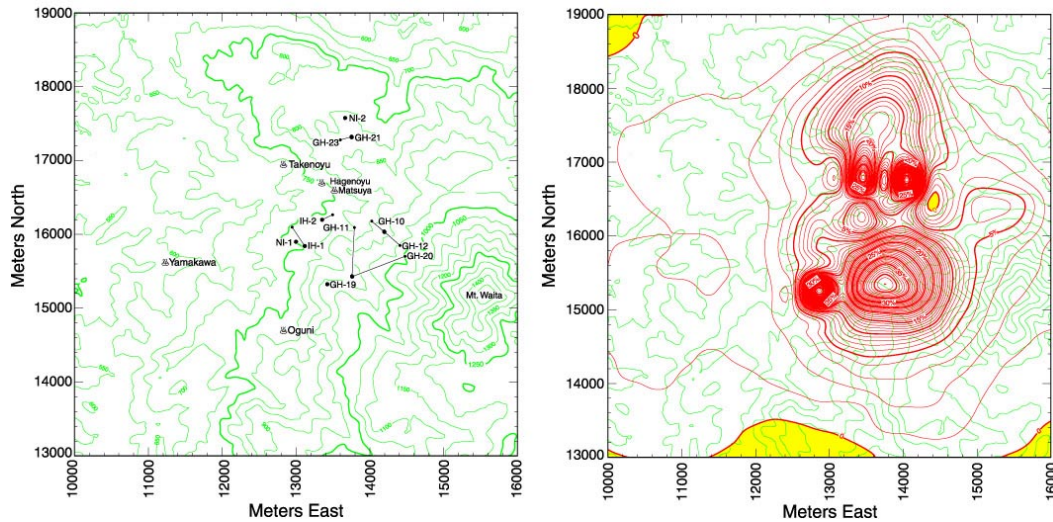


Figure 2a (left). Topography and locations of wells used for electrical power production in 50-year performance forecast for model Oguni geothermal field. Figure 2b (right). Relative 1 Hz apparent resistivity increase (in %) after 50 years of production/injection at Oguni.

NI-2 and GH-21 injection well areas occur due to injection of cooler fluids. Simulated increases in apparent resistivity due to steam formation and cooler water reinjection reach 40% beyond the initial ($t = 0$) response, and should be readily detectable in careful repeat MT surveys.

The overall design of the U. Utah/EGI MT system is essentially finished and we are dealing currently with the engineering details to implement the system (Figure 3a). The power supply units, interface boards to integrate E-field pre-amplifiers, channel cards, and E-field junction cases for low-impedance measurements are built. Firmware development is advanced in the areas of A/D control, timing control, custom high-speed synchronous serial data links, and paged memory communications protocols. A set of 900 MHz low-power digital spread-spectrum radios was acquired and tested to provide a low-power data telemetry option for system operations. Capability has been developed to measure accurately in ultra-high impedance environments (e.g., recent volcanics). We have developed a complete noise model for such systems which allows separation of non-plane wave noise transfer functions from the MT plane-wave function of primary interest (Figure 3b). As part of our improved robust processing developments to apply this model, we have implemented three-stage, combined coherence-sorting/jackknife outlier removal.

Technology Transfer/Collaborations/Education and Outreach

Quantech Geoscience Inc., which is emerging as the leading private contractor for array MT/resistivity data acquisition at prospect scales, has been using our prototype MT inversion code on newly acquired data sets in Nevada and report that it is the preferred imaging algorithm of all available. It has been incorporated into the industry-standard Geotools® and developed models are being linked to the GOCAD® geological object interpretation package. Quantec has contracted privately to modify the matrix solvers for use on new-generation, Intel-based computer clusters for parallel processing (Hargrove et al., 2001). The Utah 2-D finite element forward problem and derivatives is a founding component of the popular Occam-II inverse code used in many applications including new marine MT surveying for oil prospecting (Key et al., 2001). The generalized Green's functions relating EM fields of diverse sources and receivers derived by Wannamaker are at the heart of the 3-D finite difference algorithm of Alumbaugh et al (1996). A modified version of our 3-D MT modeling code is implemented by SAIC Corp. (J. Pritchett, project leader) for geothermal field production monitoring. This builds upon their previous reservoir simulations using DC resistivity and anticipates the need for CSAMT source modeling in real-world applications to noisy fields.

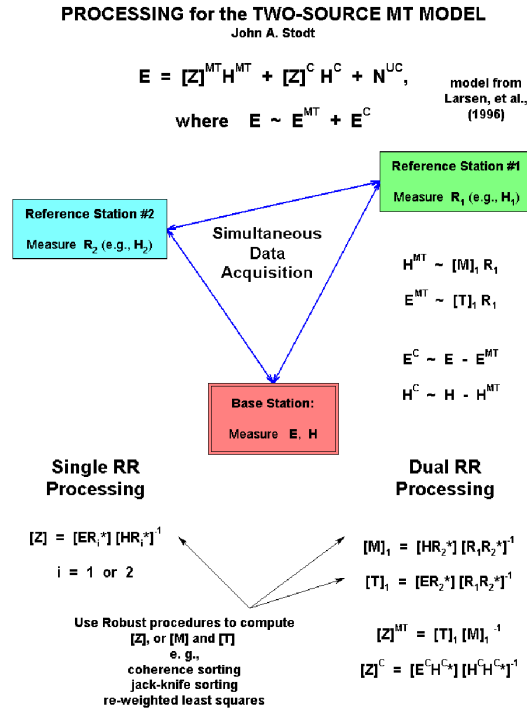
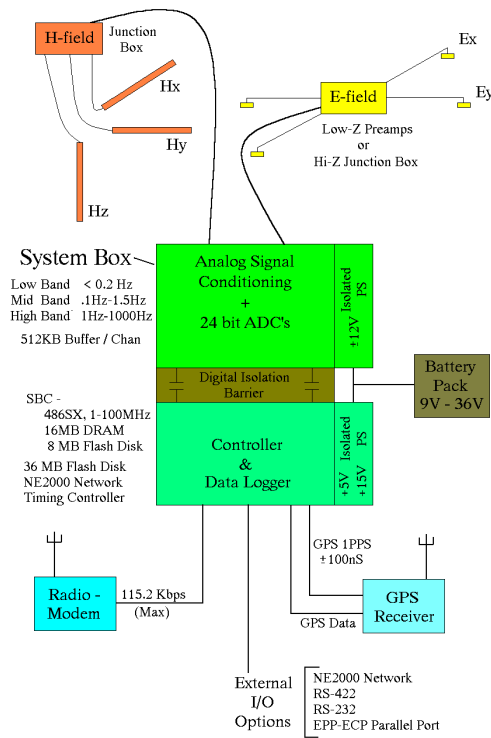


Figure 3a (left). Schematic of Utah MT system currently being completed under DOE support. Design combines simultaneous multi-band collection with high-speed, longer distance telemetry for effective productivity and noise suppression. Novel processing approaches (3b, right) consider two-source transfer functions (plane-wave plus cultural), to be applied at the Dixie Valley system.

The University of Utah MT system is a principal component of the EMSOC MT instrument facility, with companion support by the U.S. National Science Foundation. Complementary NSF support has clarified physical conditions of fluid existence in the deep crust and contrasted modes of occurrence of non-fluid conductivity causes (Wannamaker, 2000; Wannamaker et al., 2000). Convincing ties between fluid generation/movement, deformational regime and resistivity structure are demonstrated for the active New Zealand South Island, and for the U.S. Great Basin, using MT data from the Utah system (Wannamaker et al., 2001, 2002a; Wannamaker and Doerner, 2002). A full draft manuscript on our unique regularized inversion has been constructed for journal submission (Wannamaker et al., 2002b). Wannamaker was general co-chair of the 2nd G. W. Hohmann 3DEM symposium yielding 80 short papers (Wannamaker and Zhdanov, 1999) and over 20 full reviewed papers in a special Elsevier volume (Zhdanov and Wannamaker, 2002).

Our group has advanced EM methods for geothermal and other purposes with support from the DOE, NSF, USGS and private sources. The University environment is optimal for recognizing and combining technologies developed in diverse fields for application in geothermal exploration needs, and for educating our future personnel in problem-solving methods. Wannamaker has been a graduate advisor to numerous students at the University of Utah and elsewhere. These include Kim Kariya, Jeff Johnston, Louise Pellerin, Randall Mackie, Patricia Lugao, William Doerner, Fang Sheng, Carl Nettleton, Darrell Hall, Todd Ehlers, Efthimos Tartaras, Gabor Hursan, Victor Gonzalez, Weidong Li, Tim Sodergren, Derrick Hasterok, and Imam Raharjo. He has served as associate editor in electromagnetics for the journals Geophysics, Pure and Applied Geophysics, and Journal of Geophysical Research, and has been a reviewer of several books. He is Trustee and Treasurer of the Gerald W. Hohmann Memorial Trust for Teaching and Research in EM geophysics, which has created two student scholarships and a career achievement award from the SEG (see article in Leading Edge, Oct. 1998, pg. 1368).

Future Plans

Current two-dimensional inversion technology will be generalized to joint MT/DC applications. These represent the two dominant techniques in electrical methods of geothermal exploration and they are complementary in their resolution of subsurface structures. Application of the algorithms is to be for arbitrary data distributions, but will also be tailored to include the contiguous bipole array setups common to the contracting industry. We will be modifying the prototype finite source 3-D code by incorporating the accurate and versatile Green's functions from our long-standing integral equations algorithm. The first modules to be implemented will be for CSAMT and for the DC/IP method. Initial tests with topographic models show that reasonably accurate results are possible with this code. Our inversion approach will be able to accommodate the results of focused electrical array research by A. Tripp, also supported by DOE/OWGT, such that optimal data acquisition will be combined with appropriate inverse model construction for both surface and downhole EM arrays. It is our intention to provide a compact, easy-to-use 3-D platform which is completely in the public domain for both private and academic use.

We are proposing to address important structural and resource problems in a classic Basin and Range geothermal system by application of dense array EM measurements and improved inversion and instrumentation technology. The system selected is Dixie Valley, Nevada, the hottest extensional system in the province (Benoit, 1999; Blackwell et al., 2000). Basic goals of such a survey are 1), resolve a fundamental structural ambiguity at the Dixie Valley thermal area (single rangefront fault versus shallower, stepped pediment; 2), delineate fault zones which have experienced fluid flux as indicated by low resistivity (thereby contrasting permeable and impermeable areas); 3), image the disposition of the igneous (resistive) formations in the subsurface, which are interpreted to comprise good reservoir rock due to brittle rheology; and 4), from a generic standpoint, demonstrate the maximal resolving capability of complementary, fully sampled electrical data for subsurface structure. This is a large MT data set to manipulate so there is a substantial processing effort in the two-source method here. University of Utah instrumentation will be applied in acquiring data components not covered by the array, to define the resulting compromise in information content.

References

- Alumbaugh, D. L., G. A. Newman, L. Prevost, and J. N. Shadid, 1996, Three-dimensional wideband electromagnetic modeling on massively parallel computers, *Radio Sci.*, 31, 1-23.
- Benoit, D., 1999, A review of various conceptual models of the Dixie Valley, Nevada, geothermal field, *Geotherm. Resour. Counc. Trans.* 23, 505-511.
- Blackwell, D. D., B. Gollan, and D. Benoit, 2000, Structure of the Dixie Valley geothermal system, *Proc. World Geotherm. Congr.*, Kyushu-Tohoku, Japan, 991-996.
- Hargrove, W. W., F. M. Hoffman, and T. Sterling, 2001, The do-it-yourself supercomputer, *Scientific American*, August, 72-79.
- Key, K. W., S. C. Constable, A. S. Orange, 2001, New results using the marine magnetotelluric method over a 3-D structure, *EOS Trans. AGU*, 82(47), p. F321.
- Larsen J. C., R. L. Mackie, A. Manzella, A. Fiordelisi, and S. Rieven, 1996, Robust smooth magnetotelluric transfer functions, *Geophys. J. Int.*, 124, 801-819.
- Mackie, R. L., J. T. Smith, and T. R. Madden, 1994, Three-dimensional electromagnetic modeling using finite difference equations, *Radio Sci.*, 29, 923-935.
- Sasaki, Y., 1999, 3-D inversion of electrical and electromagnetic data on PC's, in Wannamaker, P. E., and M. S. Zhdanov, eds., *Three-dimensional electromagnetics*, *Proc. Second Internat. Symp. in mem. Gerald W. Hohmann*, University of Utah, Salt Lake City, 128-131.
- Sasaki, Y., 2001, Full 3-D inversion of electromagnetic data on PC, *J. Appl. Geoph.*, 46, 45-54.
- Smith, J. T., 1996, Conservative modeling of 3-D electromagnetic fields, Part II: biconjugate gradient solution and an accelerator, *Geophysics*, 61, 1319-1324.
- Wannamaker, P. E., 1997, Tensor CSAMT survey of the Sulphur Springs thermal area, Valles Caldera, New Mexico, Parts I&II: implications for structure of the western caldera and for CSAMT methodology: *Geophysics*, 62, 451-476.

- Wannamaker, P. E., 1999, Affordable magnetotellurics: interpretation in natural environments, in Three-dimensional electromagnetics, ed. by M. Oristaglio and B. Spies, Soc. Explor. Geophys., Invest. Geophys., Tulsa, 349-374.
- Wannamaker, P. E., 2000, Comment on "The petrologic case for a dry lower crust", by B. D. Yardley and J. W. Valley, *J. Geophys. Res.*, 105, 6057-6064.
- Wannamaker, P. E., 2000, Overview and testing of computer algorithms for three-dimensional EM simulation of resistivity changes induced by production from geothermal reservoirs: Maxwell Technologies report MSD-DTR-00-16, 22 pp.
- Wannamaker, P. E., and W. M. Doerner, 2002, Crustal structure of the Ruby Mountains and southern Carlin trend region, northeastern Nevada, from magnetotelluric data, *Ore Geology Reviews*, in revision.
- Wannamaker, P. E., and M. S. Zhdanov, eds., 1999, Three-dimensional electromagnetics, Proc. Second Internat. Symp. in mem. Gerald W. Hohmann, University of Utah, Salt Lake City, 342 pp.
- Wannamaker, P. E., J. B. Hulen, and M. T. Heizler, 2000, Early Miocene lamproite from the Colorado Plateau tectonic province, Utah, *J. Volc. Geotherm. Res.*, 96, 176-191.
- Wannamaker, P. E., J. M. Bartley, A. F. Sheehan, C. H. Jones, A. R. Lowry, Trevor A. Dumitru, Todd A. Ehlers, W. S. Holbrook, G. L. Farmer, M. J. Unsworth, D. B. Hall, D. S. Chapman, D. A. Okaya, B. E. John, and J. A. Wolfe, 2001, Great Basin-Colorado Plateau transition in central Utah: An interface between active extension and stable interior, in *The Geological Transition: Colorado Plateau to Basin and Range*, Proc. J. Hoover Mackin Symposium, ed. by M. C. Erskine, J. E. Faulds, J. M. Bartley and P. Rowley, Utah Geol. Assoc./Amer. Assoc. Petr. Geol. Guideb. 30/GB78, Cedar City, Utah, September 20-23, 1-38.
- Wannamaker, P. E., G. R. Jiracek, J. A. Stodt, T. G. Caldwell, A. D. Porter, V. M. Gonzalez, and J. D. McKnight, 2002a, Fluid generation and movement beneath an active compressional orogen, the New Zealand Southern Alps, inferred from magnetotelluric (MT) data, *J. Geophys. Res.*, in press.
- Wannamaker, P. E., P. P. DeLugao, and J. A. Stodt, 2002b, Two-dimensional inversion of magnetotelluric data using a-priori models and resolution principles of diffusive electromagnetics, *Geophys. J. Int.*, in prep.
- Zhdanov, M. S., and P. E. Wannamaker, 2002, Three-dimensional electromagnetics, Proc. Second Int'l Symp. in mem. Gerald W. Hohmann, *Methods in Geochemistry and Geophysics*, Vol. 35, Elsevier, Amsterdam, in press.

CHARACTERIZATION OF FRACTURE PATTERNS IN THE GEYSERS AND COSO GEOTHERMAL RESERVOIRS BY SHEAR-WAVE SPLITTING

Principal Investigator - J.A. Rial
University of North Carolina at Chapel Hill
Mitchell Hall, Dept of Geological Sciences CB#3315

Key Words – 3D maps, crack distribution, crack density, COSO, The Geysers, shear-wave splitting

Project Objectives

On the basis of shear wave splitting data recorded and processed from the Geysers and Coso geothermal fields this project aims at developing a computer-based methodology to produce 3D maps of crack distribution and crack density in fractured reservoirs. The raw data for the project consists of seismographic recordings of microearthquakes (MEQ) detected over many years by arrays of sensors in both The Geysers and Coso reservoirs. With the experience acquired in the processing and interpretation of these data we are developing a novel computer-based technology for the exploration of fractured geothermal and hydrocarbon reservoirs that, in its completed form, will include the following software packages (written in Matlab-compatible language):

- (1) Data analyzing package.
- (2) Forward modeling package
- (3) Inversion package.

Approach/Background

A shear-wave propagating through rocks with stress-aligned cracks will split into two waves, a fast one polarized parallel to the predominant crack direction, and a slow one, polarized perpendicular to it. In fact, the polarization direction ϕ of the fast split shear wave parallels the strike of the predominant cracks regardless of its initial polarization at the source, while the time delay δt between the fast and the slow waves is proportional

to crack density, or number of cracks per unit volume. The analysis of split shear waves is thus a valuable technique to detect and map the main orientation and intensity of fracturing in the subsurface, which, when fully developed as a computer application, could become a highly desirable technical and industrial resource to explore fracture-controlled geothermal and hydrocarbon reservoirs.

For the last few years we have studied and processed shear-wave splitting data in two seismically active, fracture-controlled environments, The Geysers and Coso geothermal fields in California, using 14- and 16-station seismic arrays of 3-component, mostly down-hole instruments running up to 480 samples/sec (Lou and Rial, 1994; 1995; 1997; Erten and Rial, 1998; Erten et al., 2001). From the careful analyses and processing of over 30,000 local microearthquakes we have to date collected what is arguably the world's largest and most complete set of high resolution, high quality shear-wave splitting observations. This constitutes one of the main contributions of this project to the geothermal community.

Status/Accomplishments

All phases of the proposed research are on schedule. Surface mapping of fast shear-wave polarizations and delay times in The Geysers and Coso has been completed and the results described in the previous peer reviewed report (San Diego, August 2001). Preliminary results have been published (see below).

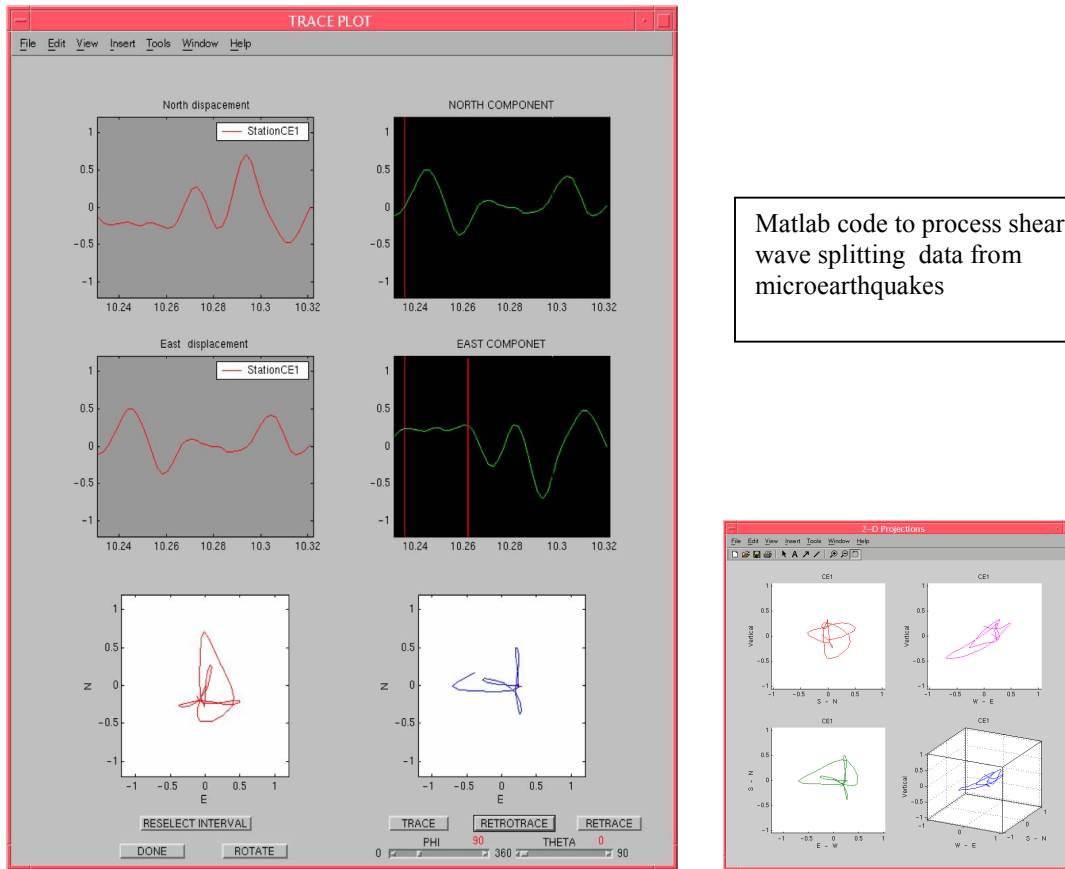


Figure 1. Matlab GUI (Graphic User Interface) from the data analyzing package. The purpose of this package is to provide the user with a complete set of interactive routines to read, display, frequency analyze, filter, window and process shear-wave splitting from seismographic data. The current input format is derived from the UW (University of Washington). The above example shows the part of the code (left) where the operator, after windowing and filtering the data, can determine the fast wave polarization direction ϕ and the time delay between the split shear waves δt . For illustration the figure shows shear wave seismograms (in red, left) from station CE1 (Coso) and the corresponding particle motion diagram (bottom left) for the selected window. When necessary, the instrument components are rotated interactively using the sliders and the tracer/retracer commands on the bottom right of the window. All these operations are automatic and can be restarted at any time. In routine work, the rotation of the seismographic components (right) is done to align the polarization of the fast shear wave with one of the coordinate axis. This gives the polarization angle ϕ in a geographic frame, and makes the seismographic components split, as shown. The time delay δt can then be measured (vertical red lines). Both parameters are automatically archived along with the identification of the station and the event. Vertical plane projections and three-dimensional plots of the particle motions can also be constructed and displayed, as shown in the inset on the lower right.

The data analyzing package (1) is now completed. The program consists in Matlab-based fully interactive GUIs (Graphic user interface) that allow display, windowing, spectral analysis and polarization analyses of three-component seismograms (Figure 1). The code also allows the operator to plot the ground particle motion in 2D

and 3D diagrams, rotate the components to determine the polarization ϕ , time delay δt and automatically store them for later use in the modeling and inversion procedures. This code has been successfully tested and used in the analyses and processing of the Geysers and Coso shear-wave splitting database.

Matlab code to compute synthetic shear-wave splitting data

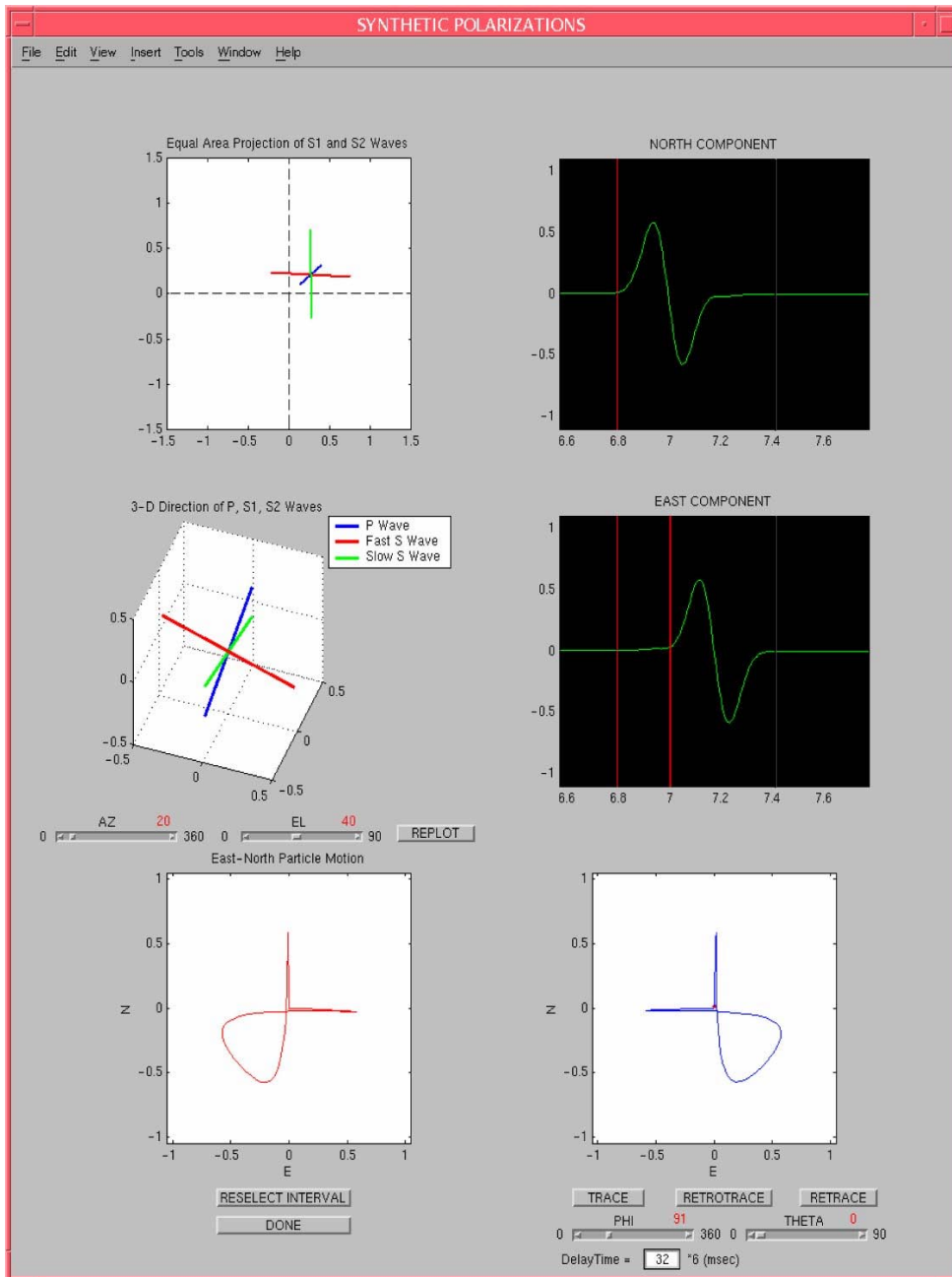


Figure 2. Example of Matlab GUI from the forward modeling package. Here synthetic polarizations and synthetic seismograms are computed for prescribed models of the anisotropy-producing medium. In the example above the medium is modeled using a HTI (hexagonal transverse isotropic) that represents saturated cracks. The operator can change orientation and dip of the cracks by using the sliders (left, middle) and re-plot the result, which shows the map and 3D orientation of the P-wave and the fast and slow shear waves (middle left) in the station's reference frame. The diagrams on the right are similar to those in Figure 1 and are used to simulate the rotation and measuring process of the real data. The results are automatically archived. The computed changes in polarization direction and time delay with azimuth, dip and strike of the cracks are used in the inversion process that follows.

The forward modeling package (2) is now near completion. This package has two important uses: a) it allows the operator to map polarization ϕ and delay δt on the area of interest, which helps determine data consistency, data anomalies and general azimuthal distribution of the data prior to interpretation, and b) the operator can interactively construct synthetic seismograms that reproduce the polarizations of the P, fast S1 and slow S2 split waves traveling through a standard Horizontal Transverse Isotropic (HTI) model that can fully simulate the anisotropy induced by a crack system (Figure 2). The operator can change the dip of the crack system and the crack density, as well as specify whether cracks are empty or fluid-saturated. As shown in Figure 2, the operator can construct two and three-dimensional graphs depicting the predicted synthetic polarizations for the P, S1 and S2 waves. The code computes synthetic seismograms and synthetic particle motions from which the predicted values of ϕ and δt are compared with actual ones in a station-by-station basis. The purpose of this package is to produce a first trial-and-error inversion of the data to use as fundamental constraints in the next step. The synthetic seismogram computations have been

successfully tested against published results of ϕ and δt for a number of transversely isotropic (TI) models.

This project has so far fully supported two graduate students and partially supported a post-doctoral associate.

Planned FY 2002 Milestones

- A) Completion of the forward modeling package (2). This includes the incorporation of an automatic code to detect and store the differences between synthetic and observed seismograms.
- B) Completion of two research papers that describe the results obtained in The Geysers and Coso regarding crack distribution. A research paper with a comprehensive study of the space-time variation of ϕ and δt at Coso and its implications to monitoring local tectonics and production has been submitted to the Journal of Volcanology and Geothermal Research. Completion of the seismographic analysis. The latest results for crack directions in SE Geysers and Coso are shown in Figures 3 and 4.

SE GEYSERS 99: AB events

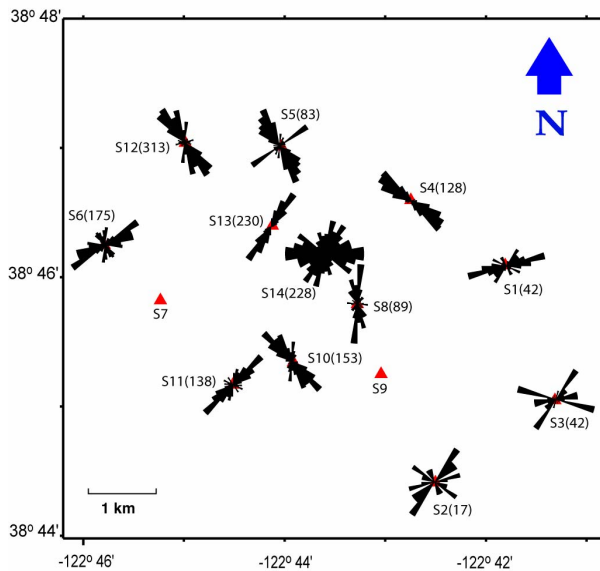


Figure 3. Rose diagrams for the SE Geysers area for events of quality A and B (best quality recordings), recorded in 1999. Numbers in parenthesis are the number of events used in each station. Though most stations show strong consistency in the measurements, stations 14 and 3 require a detail study to determine the source of the strong variability in detected orientations. These could be due to the presence of multiple crack planes, non-vertical dipping or strong scattering produced by geological structure. The data in stations 14 and 3 present an interesting challenge, and thus will be subject to careful study before tomographic inversion.

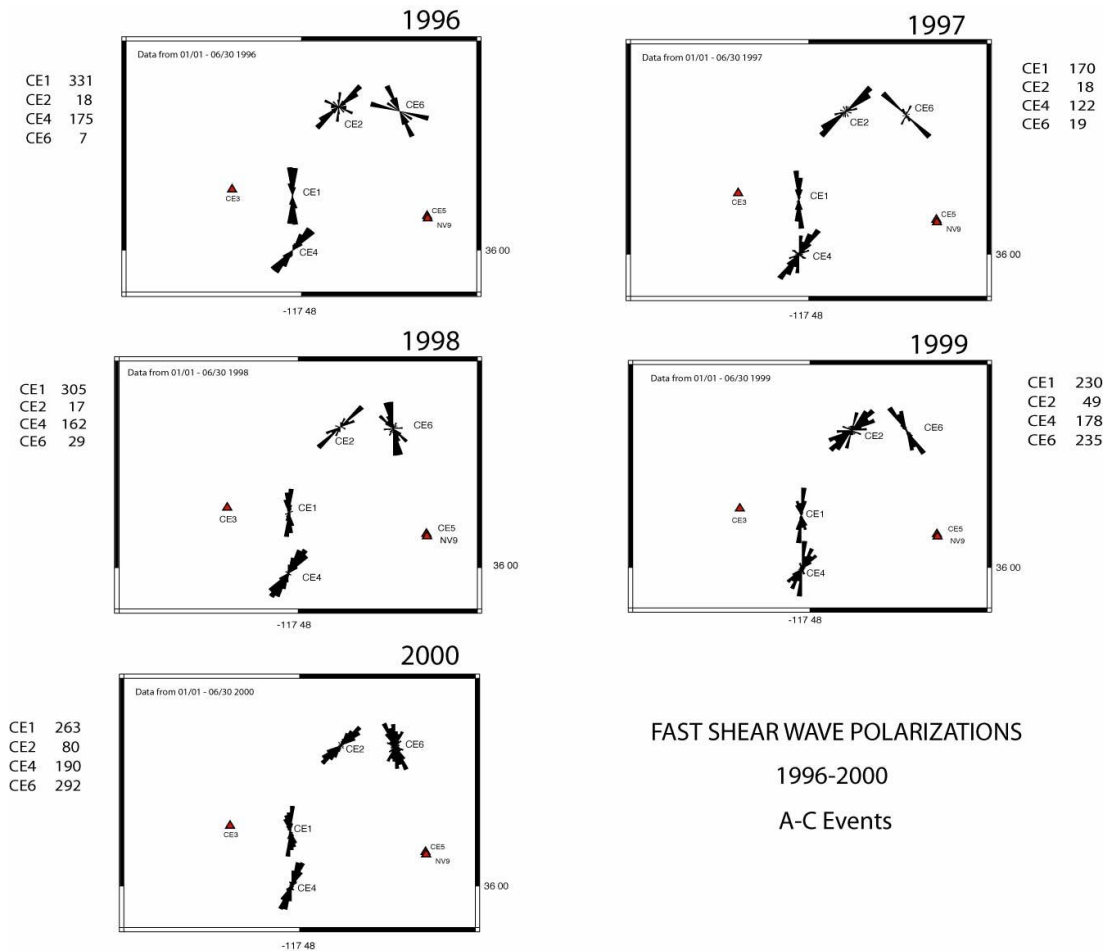


Figure 4. Rose diagrams for over 2,800 (quality A-C) events in the Coso reservoir from 1996-2000. The data are highly consistent and with the exception of the year 1999 (when changes due possibly to nearby production occurred), the rose diagrams are stable and the measurements consistent throughout.

C) Development and validation of the inversion package (3). This package consists of two parts:

a) Station-by-station inversion of the δt data to determine crack dip. The results will reflect local structure because accurate measurements of δt are limited to rays arriving at the station within the 35 degree vertical angle that constitutes the shear-wave window. Since at any given station ϕ and δt vary with azimuth in a predictable manner, the objective of this first inversion approach is to use the observed azimuthal variations of ϕ and δt to refine the crack direction determined before and accurately determine its dip.

b) Inversion of the crack density. The δt measurements corrected for crack dip will then be used to invert for crack density using groups of near stations and, if possible, the entire array. Because of the shear window limitation we anticipate that the density of ray crossings will be optimal only for some groups of nearby stations. The technique is however to be implemented for any distribution of sensors. The data for the inversion is first depicted in the form of maps showing the orientation of the fast shear wave with the corresponding time delay plotted at the epicenter of the event used to determine them (Figure 5).

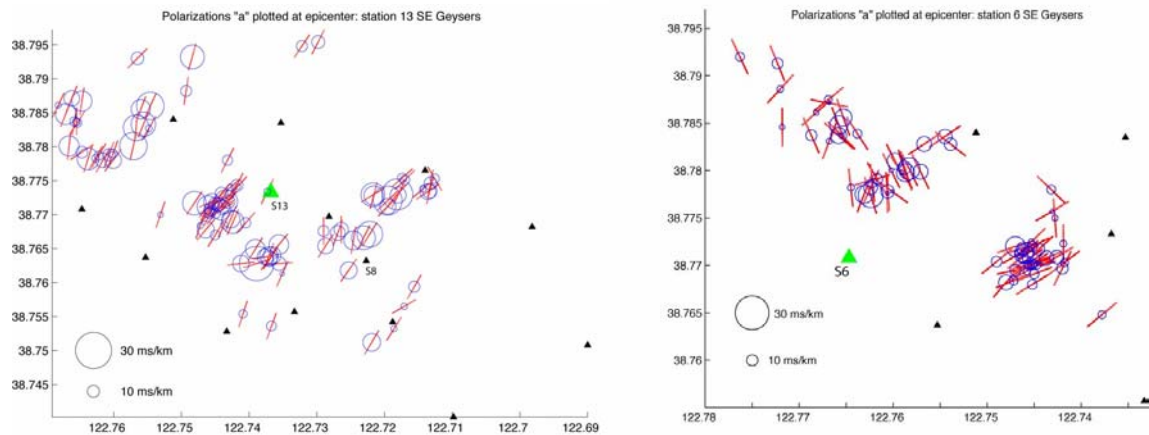


Figure 5. An example of mapping the polarization (short red bars) and delay times (circles) recorded at stations 13 and 6 (large green triangles) in SE Geysers. Any crack direction is plotted on the epicenter of the event from which it was determined, not on its actual location, which is of course, unknown. The small black triangles mark the locations of the rest of the stations in the array. Most data from station 13 are consistent with a fracture orientation N40-45E. To the southeast of the station a few polarizations are inconsistent with that direction. The distribution of time delays is not inconsistent with cracks dipping vertically or nearly so. The data set for station 6 (right) is more complex, showing strong azimuthal variation of polarization angle, which may be an indication of shallow dip of the crack system (60 degrees or less), or the presence of biplanar (more than one dominant direction) vertical cracks. The simultaneous inversion of these data will help resolve among these possibilities, as these maps provide strong constraints and useful hints.

Using both ϕ and delay δt for tomographic inversion of cracked reservoirs is a novel approach. With the high quality of data available we are in a unique position to produce a first-time result that will not only provide a close look at the 3D crack distribution in The Geysers and Coso, but may stimulate new research into seismic imaging of anisotropic/fractured media using observed space and time variations of ϕ and δt .

For instance, if understood correctly, spatial variations in ϕ and δt can be used to detect hidden or buried faults in seismically active zones, while understanding their time variations would make it possible to monitor production in crack-controlled reservoirs, understand the local stress field and monitor fluid migration. It would also be possible to use accurately detected time variations in ϕ and δt to better understand the focal mechanics of impending earthquakes, or even help forecast volcanic eruptions.

Major Reports published in FY 2001

Erten, D., M. Elkibbi and J.A. Rial (2001): Shear wave splitting and fracture patterns at The

Geysers (California) geothermal field., Geothermal Res. Eng. Proceedings, 26th Workshop, p139-147.

Erten, M. Elkibbi and J.A. Rial (2001) Shear wave Splitting and Fracture patterns at The Geysers, Spring Meeting, EOS AGU, Boston.

Vlahovic, G., Elkibbi, M., and J. A. Rial (2002). Temporal Variations of Fracture Directions and Fracture Densities in the Coso Geothermal Field from Analyses of Shear-wave Splitting, Geothermal Reservoir Engineering Proceedings, Twenty-seventh Workshop, Stanford University. SGP-TR-171 (In press).

Major Articles Published in FY 2001

Finished in 2001, to be published in 2002: Vlahovic, G., Elkibbi, M., and J. A. Rial (2002). Shear Wave Splitting and Reservoir Crack Characterization: Coso Geothermal Field. Submitted to *Jour. of Volcanology and Geothermal Research*.

References

- Erten, D., Rial, J. A., 1998. Extended studies of crack distribution and crack densities at NW Geysers, Spring Meeting, EOS AGU, 80, p.225
- Erten, D., Elkibbi, M., Rial, J.A., 2001. Shear wave Splitting and Fracture patterns at the Geysers (California) Geothermal Field, Proc. Workshop Geothermal Res. Eng, 26, p139-147.
- Lou, M., Rial, J. A., 1995. Modeling Elastic Wave Propagation in Inhomogeneous Anisotropic Media by the Pseudospectral Method, Geophys. Jour. Int., 120, 60-72.
- Lou, M., Rial, J.A., 1997. Characterization of geothermal reservoir crack patterns using shear-wave splitting, Geophysics, 62, 2, p487-495.
- Lou, M, Rial, J. A., 1994. Characterization of the crack geometry at the Coso, California geothermal reservoir by analyzing shear-wave splitting from microearthquakes, Proceedings of the 19th Workshop on Geothermal Reservoir Engineering, Stanford, SGP-TR-147, 15-20,1994.

IMAGING TOOLS FOR ELECTRICAL RESISTIVITY IN GEOTHERMAL EXPLORATION AND RESERVOIR ASSESSMENT

Principal Investigator - A.C. Tripp
University of Utah
1476 Federal Way, Salt Lake City, Utah 84103
actripp@mines.utah.edu

Key Words - Electromagnetics; Knowledge adaptive interpretation

Project Background and Status

Because reservoir production is primarily in fractured rock, a great deal of effort has been spent devising means of remotely sensing fractures and fracture zones using geophysics. Since increased fluid content or alteration of fractures can give rise to an electrical conductivity contrast, electromagnetic (EM) means of probing have been investigated extensively over the years. Although direct and indirect fracture responses have been noted in many field situations, a fracture response can be subtle and progress has been sporadic. The purpose of this project is to facilitate inductive fracture detection by providing the interpretation tools and knowledge-theoretic framework for innovative high resolution fracture detection and delineation.

Project Objectives

We seek to facilitate increased resolution of fractures by:

- 1) Identifying more realistic electrical models for fractures, further defining the geophysical target for cooperative interpretation in fracture environments;
- 2) Developing suitable software for calculating the EM response of realistic electrical fracture models including anisotropy, borehole metallic casing, and innovative basis functions;
- 3) Investigating cooperative knowledge adaptive EM experiment design and interpretation for fracture detection and delineation;
- 4) Providing modeling support for triaxial induction tool development by EMI, Inc.

Approach

Our research has been multi-disciplinary, drawing from mathematics, electrical engineering, biomedical imaging, geology, and reservoir

engineering. We attempt to identify realistic fracture and reservoir models, and eschew idealized models. We then attempt to calculate the EM response of these realistic models drawing from the geophysical, mathematical, electrical engineering, and biomedical imaging communities. Again in collaboration with geologists we develop cooperative interpretation schemes for fracture description from EM and other complementary data.

As the next section demonstrates, we have made reasonable progress in our program. The next year will be spent consolidating our present work and advancing the theory of cooperative fracture delineation from a complete suite of geophysical and geological data.

Research Results

Triaxial Device Modeling Support

The transmitter-receiver geometry used in traditional uniaxial induction logging was not accidental - a conductive smooth borehole gives a null response for axial magnetic field sources and sensors. However this nulling is not necessarily true for triaxial devices, which are designed to resolve features such as formation anisotropy or vertical fractures which are invisible to traditional tools.

Triaxial devices may be fabricated in the time or frequency domain. In the frequency domain, where the transmitter and receiver are separated, as in the EMI, Inc. device, borehole effects for conductive bore-fluids will be present and can overwhelm the response of formation features unless corrective means are taken, such as a focusing of the source fields. Borehole irregularities, such as breakouts, washouts, and key seats will also give responses which might mask formation properties. Time domain devices with separated transmitters and receivers will have a time window over which the borehole response is minimized. Time domain

devices with coincident sources and receivers, will have an appreciable borehole response. In the case of both frequency and time domain methods, numerical modeling of the borehole response is essential for full understanding and remediation of deleterious borehole effects.

Modeling borehole responses can be done using analytic modal responses, integral equations methods, or difference methods. Estimates of differential measurement sensitivities to borehole irregularities are approximated by a simple perturbation formula. Numerical modeling using integral equations for separated source-receiver geometries establishes bounds on the resolution of formation features in the presence of borehole fluid and borehole irregularities.

We have calculated borehole responses for the triaxial geometry in support of the EMI, Inc. development of a frequency domain triaxial induction tool. Resolution analyses for a conductive fracture and conductive boreholes using uniaxial and triaxial inductive logging are discussed in Bertete-Aguirre et al. (2000). These analyses, which use analytic sensitivity formulae, demonstrate that for magnetic dipole sources perpendicular to the borehole axis, conductive boreholes and their irregularities do mask the effects of conductive features at depth. Eccentering is also troublesome in this environment. Adaptively focusing an inductive source array to utilize the irregularities as elements of the source array optimizes the resolution of conductivity features away from the borehole (Cherkaev and Tripp, 2000; Bertete-Aguirre et al., 2001a)

Although a triaxial tool is extremely useful it is not a panacea. Cherkaev et al. (2000) and Bertete-Aguirre et al (2001b) demonstrate that full utilization of a triaxial tool in investigating the petrophysics of anisotropic material requires complementary sources of information. In the absence of this information, an interpretation of triaxial tool data often does not have a distinct advantage over an interpretation of traditional induction tool data.

EM Response of Fractal Conductivity Distributions

A long standing approximation in EM logging for fractures has been to assume that a fracture is an extended thin sheet, perhaps a half-plane. This approximation can be useful and is theoretically and numerically convenient. Convenience notwithstanding, examination of core, FMS logs,

and outcrop reveals that fracture zones can be geometrically self-similar over dimensional scales of less than millimeters to kilometers. In such a case, a strict geophysical model would have to account for such a fractal structure to truly represent the resistivity structure of the earth.

One method espoused in the electrical engineering literature models fractal structures with almost-periodic functions, such as band-limited Weierstrass functions. This representation gives a facile means of scaling small alternating sequences of open fracture and matrix rock, as observed in a borehole, to uniaxial anisotropic fracture packets. Parallel and transverse resistivities as functions of averaging window are easily calculated from such a distribution assuming that dip of the bedding with respect to the borehole is known - as would be the case with the auxiliary use of a FMS log, for example. The averaging windows are adjusted to the resolving length of the EM logging device under consideration and the EM frequency or time domain response of the subsequent averaged anisotropic layers or units are calculated using codes incorporating anisotropic conductivities.

The EM response of fractal conductivity variations, such as might be measured in a fracture envelope, have been presented in Tripp et al. (2001).

The time domain method of electromagnetic exploration has several distinct advantages over the frequency domain method, although instrumentation difficulties have apparently limited its use in inductive logging. One of its advantages is that the nature of the response is nicely visualized as a temporally diffusing field. For this reason, and to provide support for possible future work in a time-domain instrument for geothermal investigations, we have inverse Laplace transformed Moran and Gianzero's frequency domain expression for the response of an anisotropic earth. The expressions for the temporal vector and scalar potentials of an anisotropic earth are contained in Tripp et al. (2001).

Mapping Pumping Test Fluid Flow with Electromagnetics

The development of a triaxial induction tool facilitates new approaches to EM reservoir examination. Fracture detection as usually envisaged uses EM fields to detect conductivity contrasts originally present in the rock. This approach can be fine, but suffers from the fact that the detectible parameter is a secondary

characteristic of the reservoir properties of interest. However, if the fracture system is accessible, a fluid of enhanced electrical conductivity or magnetic susceptibility can be introduced which is traceable through its inductive signature on a triaxial induction tool. In this case fluid movement is being monitored, which is of direct interest in reservoir studies. The following idea has been discussed by Tripp and Cherkaev (2001).

Since high resolution of fluid movement is essential, all EM monitoring of the injected fluid will use adaptive array theory (Cherkaev and Tripp, 2000), which optimizes the resolution of a conductivity or magnetic susceptibility perturbation on an a-priori parameter distribution. Approximate real time inversion permit a source array which is adaptive during the course of the fluid injection.

The design of the chemical and physical properties of the injection fluid is a matter of some moment. The conductivity can be controlled by the ionic content, but the ionic content must not have deleterious effects on the physico-chemical properties of the formation. The EM response is also enhanced by the addition of fine ferromagnetic particles. These might be useful as a proppant in hydrofrac experiments.

The EM response can be interpreted in two ways. First it can be inverted to electric currents, which will approximate the hydrologic fluid flow lines. This is a linear inversion problem. The second method is to invert the EM data to anomalous electrical conductivity and magnetic susceptibility distributions and then use a mixing law to estimate the volume fraction of introduced fluid in the formation. In either case, we develop a dynamic estimate of fluid flow in the formation.

The EM measurements give an estimate of the transient saturated flow in the isolated zone, which may be put to use by the reservoir engineer as appropriate. We can demonstrate one approach which is intriguing. Assuming a diagonal hydraulic conductivity tensor, the Darcy equations become

$$v_x = -K_x (\partial h / \partial x),$$

$$v_y = -K_y (\partial h / \partial y),$$

and

$$v_z = -K_z (\partial h / \partial z).$$

Augmenting these equations with the equation of continuity gives the equation of flow through a saturated anisotropic porous medium

$$(\partial / \partial x) (K_x (\partial h / \partial x)) + (\partial / \partial y) (K_y (\partial h / \partial y)) + (\partial / \partial z) (K_z (\partial h / \partial z)) = S_s (\partial h / \partial t),$$

where $S_s = \rho g (\alpha + n\beta)$, α is the aquifer compressibility, n is the porosity, and β is the fluid compressibility.

Assuming that estimates of porosity n^{est} and fluid flow ($v_x^{meas}(\mathbf{x}, t)$, $v_y^{meas}(\mathbf{x}, t)$, $v_z^{meas}(\mathbf{x}, t)$) are made using electromagnetic means, the flow equation becomes

$$(\partial / \partial x) (v_x^{meas}) + (\partial / \partial y) (v_y^{meas}) + (\partial / \partial z) (v_z^{meas}) = S_s (\partial h / \partial t).$$

Since we know S_s and assuming an initial formation head, we can write

$$h = (1/S_s) \int \{ (\partial / \partial x) (v_x^{meas}) + (\partial / \partial y) (v_y^{meas}) + (\partial / \partial z) (v_z^{meas}) \} dt.$$

Then by Darcy's equations, $K_i = -v_i / (\partial h / \partial i)$.

This gives a 3D hydraulic conductivity distribution. Since that the solution involves a temporal and a spatial differentiation, data conditioning will be an issue in the application of the mathematical solution.

Future Plans

We will complete a paper discussing logging in the presence of metallic casing and a paper discussing pumping test flow mapping using EM.

All fracture property characterization using EM must depend on cooperative interpretation of the data with other data sets such as FMS and NMR logs. This task will be emphasized during the remainder of the project.

Technology Transfer/Collaborations

Technology transfer

Our research has been presented in the professional papers referenced below. Our calculations of the triaxial borehole response has been done in

technical support of the EMI, Inc. triaxial tool development.

Collaborations

EMI, Inc. has offered insight into the use and development of triaxial devices. Dr. H. Bertete-Aguirre of Lawrence Livermore Laboratories has collaborated on triaxial modeling under separate DOE funding. Dr. E. Cherkaev, of the University of Utah Department of Mathematics, has collaborated on aspects of mathematical modeling under complementary DOE funding. Prof. Dali Zhang, Visiting Scholar at the University of Utah Dept of Mathematics assisted on aspects of the mathematical analysis at no cost to the project.

Project Publications to Date

Bertete- Aguirre, H., Cherkaev, E., and Tripp, A.C., 2000 , Borehole effects in triaxial induction logging: Proceedings of the Geothermal Resources Council 2000 Meeting.

Bertete- Aguirre, H., Tripp, A.C., and Cherkaev, E., 2001, The borehole environment in triaxial induction logging: Proceedings of the 2001 Stanford Workshop on Geothermal Reservoir Engineering.

Bertete- Aguirre, H., Tripp, A.C., Cherkaev, E., and Jarrard, R.D., 2001, Triaxial induction logging for everyone - credos and caveats: Presented at SAGEEP.

Bertete- Aguirre, H. and Tripp, A.C., 2002 , Imaging triaxial induction logging data: To be submitted to the 2002 Stanford Workshop on Geothermal Reservoir Engineering.

Cherkaev, E. and Tripp, A. C., 2000, Optimal design of focusing inductive arrays for inhomogeneous medium: Proceedings of the 2000 IEEE International Conference on Phased Array Systems and Technology, p. 485-488.

Cherkaev, E., Tripp, A.C., and Jarrard, R.D., 2000, High resolution adaptive induction logging - Petrophysical and electromagnetic considerations: Proceedings of the SPIE 2000, v. 4129.

Tripp, A.C., Moore, J., and Cherkaev, E., 2001, Representation and inductive response of fractal resistivity distributions: Proceedings of the 2001 Stanford Workshop on Geothermal Reservoir Engineering.

Tripp, A.C. and Cherkaev, E., 2001, High resolution EM for petrochemical characterization: Presented at the 2001 AAPG Annual Convention.

Tripp, A.C., 2002 , Borehole casing characterization and calibration: In Preparation.

Tripp, A.C., 2002 , Pumping test permeability determination with electromagnetic: In Preparation.

NUMERICAL ANALYSIS OF THREE-COMPONENT INDUCTION LOGGING IN GEOTHERMAL RESERVOIRS

Principle Investigator - Dr. David L. Alumbaugh
University of Wisconsin-Madison - Geological Engineering Program
2258 Engineering Hall/1415 Engineering Drive
Madison, WI 53706
alumbaugh@engr.wisc.edu

Key Words - Geothermal exploration and characterization, induction logging, borehole effects.

Project Background and Status

This project supported the development of the 'Geo-BILT', geothermal, electromagnetic-induction logging tool that is being built by ElectroMagnetic Instruments, Inc. The tool consists of three mutually orthogonal magnetic field antennas, and three-component magnetic field receivers located at different distances from the source. The source that has a moment aligned along the borehole axis consists of a 1m long solenoid, while the two trans-axial sources consist of 1m by 8cm loops of wire. The receivers are located 2m and 5m away from the center of the sources, and five frequencies from 2 kHz to 40 kHz are being employed. This study numerically investigated the response of the tool to situations that might be encountered in a geothermal field. The results will lead to a better understanding of the data that the tool produces during its testing phase and an idea of what the limitations of the tool are when characterizing geothermal reservoirs. The project was completed as of 8/31/01.

Project Objectives

- 1) To understand the effect of the borehole on the measurements and to test methods for removing the effects. Measurements where both the source and receivers are oriented perpendicular to the borehole (here referred to as the coplanar configuration) are known to be more sensitive to conductivity contrasts between the borehole and the formation than traditional coaxial data. The project numerically determined how significant these effects were and analyzed methods for reducing the effects.
- 2) To test the sensitivity of the Geo-BILT tool to different fracture zone geometries. Here the objective was to run a series of numerical models and analyze the depth sensitivity of the Geo-BILT tool configurations, the effects of fracture zone dip on measurements, the vertical resolution of the tool, the response differences between point dipole and finite-sized sources,

and the effects of fracture zone anisotropy on the results.

Approach

In order to simulate the response of the Geo-BILT tool to a variety of realistic borehole and fracture zone scenarios, we employed a 3-D finite difference code developed at Sandia National Laboratories (Newman and Alumbaugh, 1995) as well as a 1D analytical algorithm developed under another project at the University of Wisconsin (Lu and Alumbaugh, 2002). The models are based on simplified borehole and fracture zone geometries, and both point dipole and finite-length sources have been simulated. The finite-source simulations were performed to determine how the source-dimensions employed in the EMI tool produce fields that differ from point sources that are often used to theoretically analyze the data.

Simulations used to investigate borehole effects included borehole geometries with diameters of 10, 20 and 40 cm, invasion zone diameters of 80 and 120 cm, and different borehole and background conductivities. In addition one model included both a horizontal fracture and an intersecting borehole. The complete borehole analysis involved the computation of approximately 40 different model simulations, each at 2 kHz and 20 kHz. The results have been analyzed by comparing the calculated tool responses with and without the borehole/invasion zone to determine the magnitude of the borehole response. In addition, two different data differencing techniques were applied to the data from models containing the borehole to determine if borehole effects could be mitigated.

For fracture-zone simulations, four fracture models included a thin infinite layer, a thin half-infinite layer truncated at the borehole, a finite-width layer (16m), which is centered about the borehole, and a five-layer model with two conductive fractures. All conductors had a thickness of 1 meter and extended

infinitely in the Y direction. A 1 meter thickness was chosen based on logging data presented by Barton et al. (1998) for the Dixie Valley, Nevada geothermal field. The results were analyzed to determine the sensitivity of the Geo-BILT tool to fracture-features away from the borehole, the fracture conductivity and dip angle effects, and the response of the tool to fracture-zone-anisotropy. Each simulation included two source frequencies: 4 kHz and 40 kHz, and source-receiver offsets of 2 and 5 m. In all approximately 250 forward model simulations were required to complete the analysis.

Research Results

1) Modeling Borehole Effects

One of the main concerns with Geo-BILT data collection is that boreholes filled with conductive drilling mud will produce distortions in the measurements that, if not corrected, will lead to improper interpretation. It was determined from the simulations described above that data collected with both the ‘coaxial’ (source and receiver moments are aligned with the borehole axis) and the ‘coplanar’ (moments are aligned with each other but are perpendicular to the borehole) configurations show distortions caused by the presence of a conductive drilling mud and invasion zone. It was also determined that the effects are more severe for the coplanar component, and that the effect increases with $f\Delta\sigma r^2$, where f is the frequency of operation, $\Delta\sigma$ is the difference between the borehole and formation conductivities, and r is the radius of the borehole.

To illustrate the ‘borehole effect’ on Geo-BILT measurements, we employed a model consisting of

a borehole that penetrates a 2 S/m fracture zone within an otherwise 1 S/m homogenous formation. The borehole is 10cm in diameter, and is filled with 10 S/m mud. The invasion zone above and below the fracture has a conductivity of 3 S/m and is 0.8 m in diameter. Within the fracture, the invasion zone conductivity is 6 S/m and has a diameter of 1.6 m. The synthetic data resulting from the simulations at 20 kHz are shown in Figures 1a and 1b. Note that the response due to the fracture is larger for the coplanar configuration in 1a when compared to the coaxial configuration in 1b. Also note a significant ‘static’ shift in field magnitude caused by the presence of the borehole.

To reduce the borehole effect, a frequency differencing technique (Kaufman and Keller, 1989) has been applied to the data. This technique differences the measurements made at higher and lower frequencies where the latter is normalized by the ratio between the two frequencies. According to Kaufman and Keller, this reduces the effect of the borehole/invasion zone on the data as both frequencies are sensitive to the region immediately between the source and receiver, while the lower frequency has greater sensitivity further out into the medium. Figure 1c shows the results of this differencing process for synthetic data calculated at 20 kHz. Note that although the curves corresponding to models with and without the borehole do not lie exactly on top of each other, the ‘static shift’ has largely been removed. This technique shows promise for reducing these types of effects in data collected with the Geo-BILT tool.

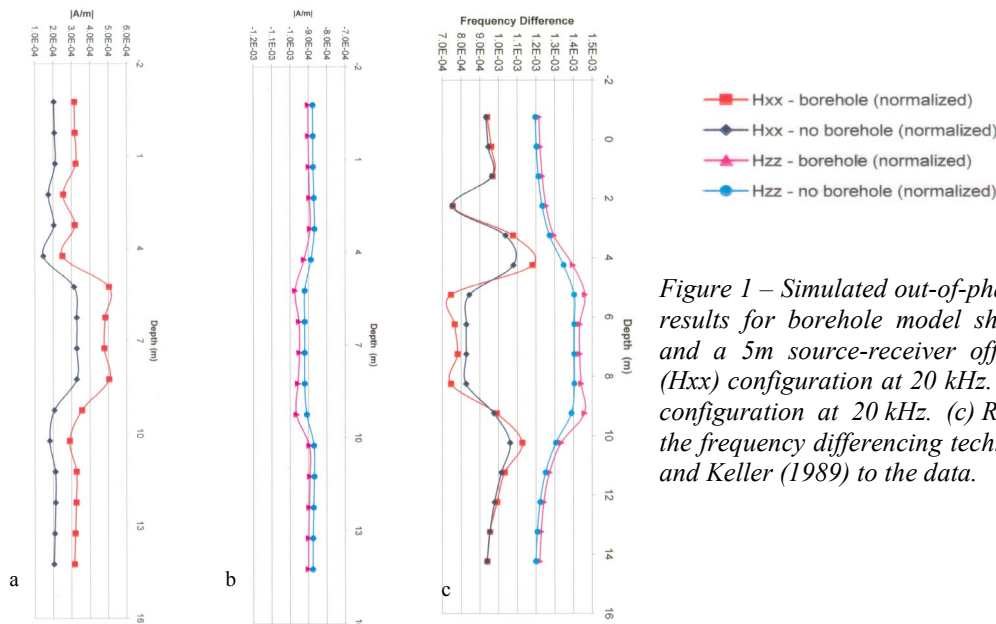


Figure 1 – Simulated out-of-phase magnetic field results for borehole model shown in Figure 2, and a 5m source-receiver offset. (a) Coplanar (Hxx) configuration at 20 kHz. (b) Coaxial (Hzz) configuration at 20 kHz. (c) Result of applying the frequency differencing technique of Kaufman and Keller (1989) to the data.

2) Analysis of Fracture Resolution and the Effects of Anisotropy

The depth to which typical coaxial induction logging tools are sensitive to formation properties has been determined to be approximately twice the source-receiver separation (e.g., Moran, 1982). Alumbaugh and Wilt (2001) presented effective imaging depth sensitivities for the multi-component induction tool for all source-receiver configurations used in our simulations. We have extended the work of Alumbaugh and Wilt to investigate the effective depth of investigation in the presence of thin conductors. We simulated the tool response to a half-infinite conductor terminated at varying lateral depths from the borehole axis for the coaxial, coplanar, and coaxial null-coupled configurations.

As predicted by Moran (1982) for the coaxial configurations, the investigation depth is approximately twice the source-receiver separation. This is evident in Figure 2a for a source-receiver separation of 2m where the difference between the coaxial response for fractures terminating 4m and 6m away from the borehole is less than 1%. Similar results were observed when a 5m offset was employed. The coplanar responses are plotted in Figure 2b and demonstrate a contrasting result. This configuration is sensitive to a depth of approximately one source-receiver offset. This can be predicted, since the whole-space sensitivities for this configuration are more focused near the borehole than for the coaxial configuration (See Alumbaugh and Wilt, 2001). The coaxial null-coupled response shows similar depth dependence to the coaxial configuration.

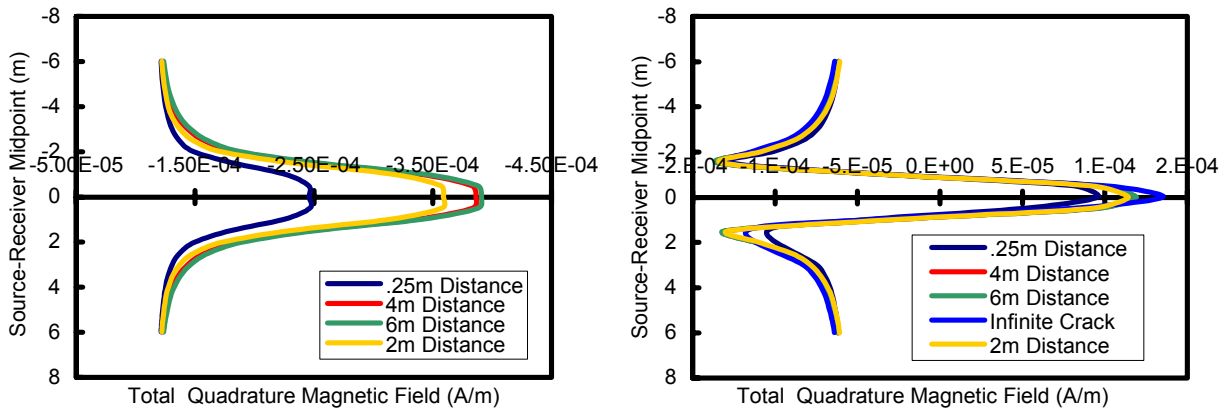


Figure 2. Simulated out-of-phase magnetic field data showing the effective depth sensitivity for the 2m offset tool configuration at 4 kHz. Data represent the half-infinite conductor model, which has varying lateral extent from the borehole axis and is ten times more conductive than the background. (a) Coaxial configuration. (b) Coplanar configuration.

Sixteen sets of calculations were performed simulating infinite and half-infinite fracture geometries in order to determine the affect of anisotropy on the multi-component tool response. The dip angle was varied from 0° to 60°, and for all simulations, the fracture-parallel conductivity was five times that of the background medium and 2.5 times that of the fracture-perpendicular conductivity. Results presented in Figures 3 and 4 for both the coaxial and coplanar configurations and two fracture-dip angles show deviations in amplitude caused by the presence of anisotropy. At 0°, the computed total magnetic fields are equal to or larger for the anisotropic conductor compared to the isotropic case even though both have the same maximum horizontal conductivity (Figures 3a and

4a). However, at 60° the coaxial configuration yields smaller total field amplitudes for the anisotropic conductor model within the 2m thick layer (Figure 3b). This may be explained by the decrease in effective horizontal conductivity due to the conductor dip or to a sensitivity sign change at high dip angles. For the coaxial configuration, the near-borehole sensitivity changes from strongly negative to positive as dip angle increases leading to a decrease in the magnitude of the quadrature component of the magnetic field (Lu and Alumbaugh, 2001). Also note that the effects of anisotropy are not observable in the 1m thick layer, suggesting that this property is not observable when the thickness of the zone is less than the source-receiver separation.

The coaxial response contrasts the coplanar and coaxial null-coupled configurations which always yield higher amplitude values for the anisotropic conductors regardless of dip angle (Figure 4). These results suggest that the scattered currents for the coplanar and null-coupled configurations are focused or channeled in the conductor, which leads to elevated magnetic field amplitudes. This is probable, since anisotropy distorts the coplanar sensitivities affecting them more in the plane of maximum conductivity (Lu et al., 2002). Again note that the thin anisotropic layer produces a response that is indistinguishable from the isotropic response.

Because anisotropy has the effect of altering the total field amplitude over the isotropic case, assumptions used in inverting multi-component data for near-borehole properties can result in error. For example, if only the coaxial data is employed, the formation conductivity will be underestimated, and

the magnitude of this error will depend on the magnitude of the conductivity anisotropy coefficient ($\lambda = \sqrt{\sigma_h/\sigma_v}$) and the dip angle of the formation. The opposite will be true if only coplanar data is used. In our simulations, the maximum error in measured magnetic field amplitude associated with the coaxial component at 60° dip is approximately 35% to 40% of the isotropic field amplitude. It is similar for the coplanar response.

Future Plans

A proposal has been submitted to the most recent DOE call for University Research on Geothermal Energy. If funded, the proposed work will yield a fast scheme for imaging 3D geology about the borehole using data collected with the GeOBILT tool.

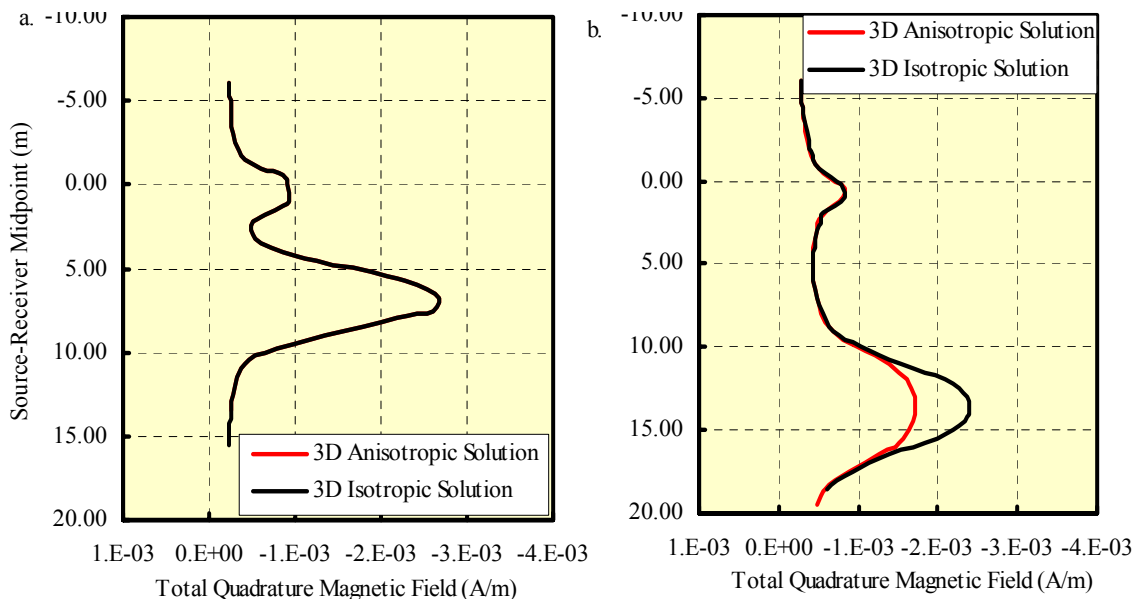


Figure 3. Coaxial out-of-phase magnetic field responses for a five-layer model given by Wang and Fang (2001). a) Response for 0 degree dip. b) Response for 60 degree dip. Layers 1, 3, and 5 are isotropic and have a conductivity of 0.02 S/m. For the anisotropic model, layers 2 and 4 have a parallel-to-layer conductivity of 0.33, and a perpendicular-to-layer conductivity of 0.067 S/m. For the isotropic case, the layer conductivities are 0.33 S/m. Layer 2 has a thickness of 0.73m, and layer 4 a thickness of 3.66m. For the 0 degree dip in a), layer 2 is centered at 0.32 m depth along the borehole, and layer 4 at 6.8 m depth. For the 60 degree dip in b), the corresponding along-borehole depths are 0.5 m and 13.5 m.

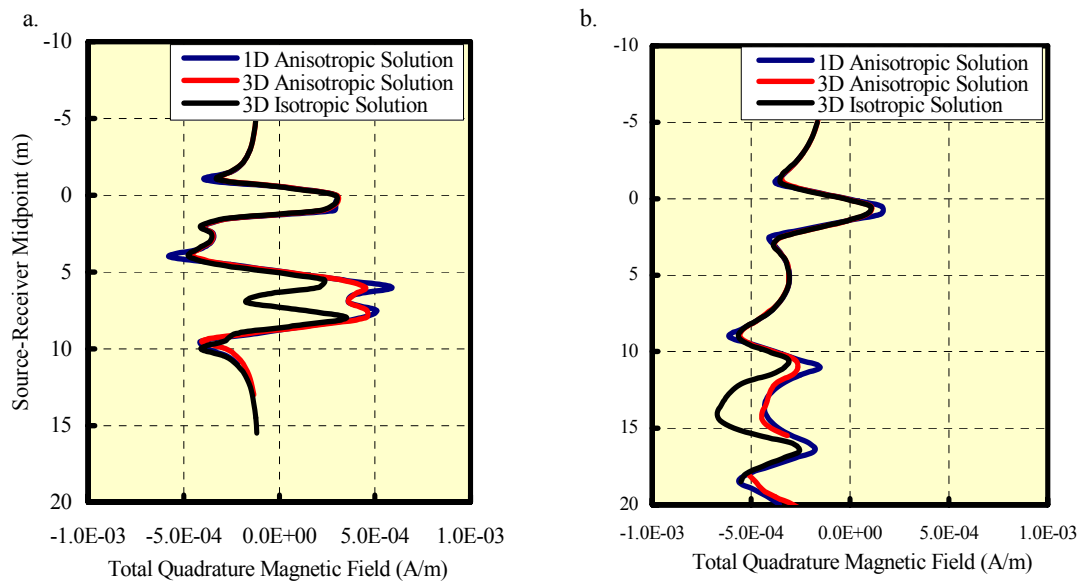


Figure 4. Coplanar out-of-phase magnetic field responses for the five-layer model described in Figure 3. The 1-D analytical solutions for the anisotropic case are provided along with the finite-difference results. a) Coplanar responses for the five-layer model at 0 degree dip. b) Coplanar responses for the five-layer model at a 60 degree dip.

Technology Transfer/Collaborations

This work has been completed in conjunction with ElectroMagnetic Instruments, Inc., who have provided specifications on the tool construction that were employed in the simulations. EMI has received a copy of the report that outlines the results, which will be employed as they see fit. The borehole work was presented at the SEG annual meeting in September (Stanley and Alumbaugh, 2001), and two peer-reviewed publications are in preparation. This project funded two students for a period of one year.

References

- D.L. Alumbaugh, and M.J. Wilt, 2001, A numerical sensitivity study of three-dimensional imaging from a single borehole, *Petrophysics*, 42, 19-31.
- C.A. Barton, S. Hickman, R. Morin, M.D. Zoback, and D. Benoit, 1998, Reservoir-scale fracture permeability in the Dixie Valley, Nevada geothermal field, *Proceedings*

Twenty-Third Workshop on Geothermal Reservoir Engineering, Stanford University, CA

- A.A. Kaufman, and G.V. Keller, 1989, *Induction Logging, Methods in Geochemistry and Geophysics*, 27, Elsevier, Amsterdam.
- Lu, X., and D.L. Alumbaugh, 2002, Electromagnetic fields of dipole sources embedded in stratified anisotropic media, in preparation for submittal to the IEEE Transactions on Antennas Propagation.
- Lu, X., Alumbaugh D.L., and Weiss C., 2002, Three-dimensional sensitivity analysis for multi-component induction logging in anisotropic media, Sandia National Laboratories Technical Report, in preparation.
- Lu, X., and D.L. Alumbaugh, 2001, Three-dimensional sensitivity analysis of induction logging in anisotropic media; *Petrophysics*, 42, 566-579.
- J.H. Moran, 1982, Induction logging-geometrical factors with skin effect, *The Log Analyst*, v. 32, 4-10.

- G.A. Newman and D.L. Alumbaugh, 1995, Frequency-domain modeling of airborne electromagnetic responses using staggered finite differences: *Geophysical Prospecting*, 43, 1021-1042.
- D. Stanley, and D. Alumbaugh, 2001, Numerical modeling of the effects of borehole reflections on 3-component EM induction logging, presented at the Society of Exploration Geophysicists Annual Meeting, September 9-14, San Antonio, Texas.

CORE ANALYSIS FOR THE DEVELOPMENT AND CONSTRAINT OF PHYSICAL MODELS OF GEOTHERMAL RESERVOIRS

Principal Investigator - G. N. Boitnott
New England Research Inc.
331 Olcott Drive, Suite L1
White River Junction, VT, 05001
e-mail: boitnott@ner.com

Key Words - Awibengkok, Geysers, Velocities, Electrical Properties, Physical Models, Geophysics

Background and Status

This project was initiated in May of 1999 as a 5 year project. The project is 50% complete, but currently slated to be ended prematurely as of October 1, 2002, after expending 64% of the initially committed funds. Ending the project in this fashion significantly reduces return on investment.

Project Objectives And Approach

Development of effective exploitation strategies requires the ability to sufficiently characterize geothermal reservoirs. Effective characterization and monitoring of geothermal reservoirs requires a fundamental understanding of the geophysical properties of reservoir rocks and fracture systems. Unfortunately, spatial variability in porosity, fracture density, salinity, saturation, tectonic stress, fluid pressures, and lithology can all potentially produce and/or contribute to geophysical anomalies, causing serious uniqueness problems in interpreting anomalies. The problem is compounded by the fact that geothermal reservoirs are commonly complex, fractured systems with architectures unlike those encountered by the oil and gas industry.

While the extensive and advanced knowledge base of the oil and gas industry is typically applied to geothermal exploration and production workflows, many problems arise due to fundamental differences between geothermal and hydrocarbon reservoirs. To overcome (and/or avoid) these problems, an accurate foundation for the physical understanding of rocks from geothermal reservoirs must be established.

This work is aimed at providing fundamental core measurements to improve interpretations of geophysical measurements. Laboratory data on core samples is being collected and analyzed to constrain models for geophysical properties which will lay a foundation for interpretation of log and field scale measurements. The work has resulted in the recognition that illite, a common mineral phase in

most geothermal reservoirs, plays a controlling role in influencing fundamental geophysical properties.

Results

Overview

Velocities and electrical properties are being measured on core plugs from the Awibengkok Geothermal field in Indonesia and The Geysers Geothermal field in California. The high-temperature (240-315°C), Awibengkok geothermal system is hosted by porous, felsic to intermediate-composition, late Cenozoic volcanic rocks intensely altered to a variety of hydrothermal assemblages. In contrast, The Geysers system is hosted by low porosity metagreywackes and metashales, providing a suite of cores which are mineralogically similar but texturally quite different.

The measured formation factors, ultrasonic velocities, and dynamic bulk and shear moduli all exhibit normal trends with porosity, however scatter in these relationships is relatively large. The laboratory measurements, evaluated in the context of routine porosity determinations as well as petrographic and modal-mineralogic analysis, have enabled the identification of compositional and textural factors affecting the seismic and electrical characteristics of these rocks which appear to produce much of the observed scatter in the relationships with porosity.

Here we quantify those factors in order to produce a generalized model of seismic and electrical properties of geothermal reservoir matrix. The resulting model provides a means with which one can study and understand the relative importance of different variables (namely porosity, mineralogy, and texture) on the core scale physical properties. Systematic evaluation indicates that, with the exception of the bulk modulus, illite plays an important role in influencing all of the measured properties.

Velocities and Moduli

Ultrasonic velocities measured on dry plugs exhibit a relatively weak correlation with porosity. The Geysers cores, spanning the porosity range from 1 to 4 percent, fall on the same general trend with porosity as do the more variable Awibengkok cores which range in porosity from a fraction of a percent to nearly 20 percent. Also of notice is that the velocity/porosity relationship does not distinguish different lithologies from one another. Based on mineralogic analyses from adjacent pieces of core (courtesy of Jeff Hulen at EGI), it is found that the velocities of the high porosity Awibengkok cores (i.e. cores with porosity greater than 10 percent) exhibit a suggestive relationship with illite content. In general, high illite content correlates with low velocities.

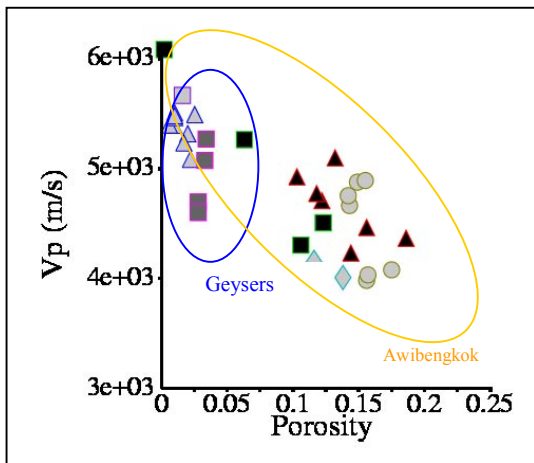


Figure 1: Cross plot of Dry V_p versus porosity for the Awibengkok and Geysers data sets at 10 MPa effective pressure. Different symbols indicate different rock types.

This observation motivated the use of an empirical model for velocities which consists of a linear combination of porosity, illite, and chlorite concentration. Similar relationships are justified for shear velocity (V_s), dynamic bulk modulus (K), and dynamic shear modulus (G). Thus we adopted a generic model of velocities and moduli of the general form

$$(1a) P = A \phi + B I + C X + D$$

where P is the property being studied, ϕ is the volume fraction of porosity, I is the weight fraction illite, and X is the weight fraction of chlorite. Fits to the data were derived using an iterative search

method to find the coefficients that minimize $\Sigma(P_m - P_p)^2$, where P_m is the measured property and P_p is the predicted property from equation 1a. The relative significance of the different parameters was systematically studied by fitting the data to models with certain terms removed, such as

$$(1b) P = A \phi + B I + D$$

$$(1c) P = A \phi + D$$

Best fitting parameter sets are shown in Table 1. Comparative measures of goodness of fit are made by computing the RMS error in predicted porosities for each relationship. An example comparison of these errors for the various properties is shown in Figure 2. From this analysis, we see that in general both the velocities and moduli are fit equally well by the simple empirical model (i.e. the RMS porosity errors are comparable for each property). For the velocities and the shear modulus, the addition of illite dependence reduces the RMS porosity error by nearly a factor of two, while the addition of chlorite produces only marginal improvements. In contrast, the bulk modulus, which exhibits the strongest correlation with porosity alone, exhibits little improvement when illite and/or chlorite are added to the model.

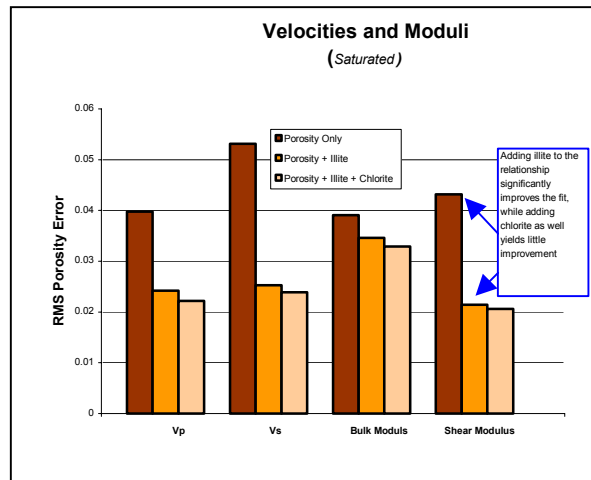


Figure 2: Comparison of RMS porosity errors for fits of saturated velocities and moduli to equations 1(a,b,c). For V_p , V_s , and G_{sat} , the addition of illite significantly reduces errors, indicating that illite is a controlling variable.

Electrical Properties

At present, only the Awibengkok core has been studied using reservoir strength brines. Electrical formation factors (F) of these cores follow a typical

Archie porosity trend, $F = \phi^m$, with ϕ being the porosity and m ranging between -2.6 and -1.8 (see Figure 3).

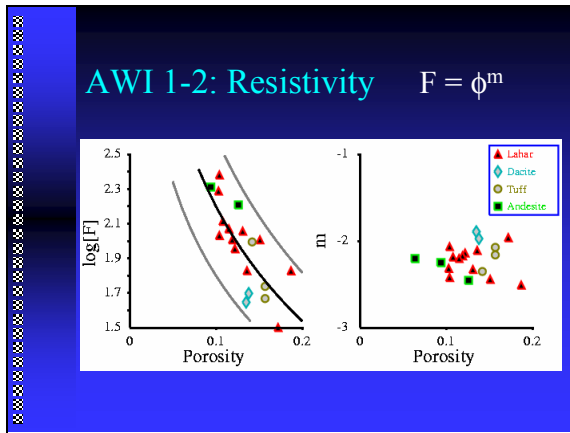


Figure 3: Cross plot of logarithm of formation factor and the Archie exponent m as a function of porosity for the Awibengkok cores saturated with 12000 ppm NaCl.

Based on qualitative analysis of crossplots versus mineralogy and porosity, a simple empirical relationship was selected of the form

$$(2a) F = \phi^m + B I + C X$$

Following a similar procedure to that used for the velocities and moduli, we again find that the inclusion of illite in the relationship significantly reduces the RMS porosity error, while the addition of chlorite along with porosity and illite produces no additional advantage (see Figure 4).

Physical Modeling and Insight

Poroelectricity

Previously, we have shown that the measured velocities of individual cores from both the Awibengkok and Geysers geothermal fields can be fit by a modified low frequency poroelectric model derived by adding a shear weakening term to low frequency Biot-Gassmann theory (Boitnott and Boyd, 1996; Boitnott and Johnson, 1999). The model can be described by the following equations, which describe the effect of saturation on the elastic moduli of the matrix material.

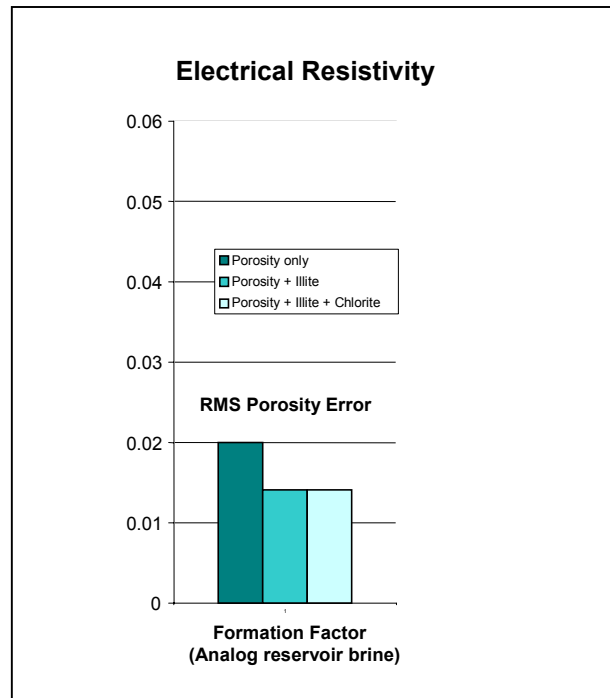


Figure 4: Comparison of RMS porosity errors for fits to equation 2 (see Table 1). As with velocities and moduli, the addition of illite significantly improves the fit, while chlorite has little effect.

$$(3a) K_{sat} = K_{dry} + \Delta K \quad ; \quad (3b) G_{sat} = G_{dry} + \Delta G$$

$$(3c) \Delta K = \frac{(K_{solid} - K_{dry})^2}{[K_{solid}(1 - \phi - (K_{dry}/K_{solid}) + \phi(K_{solid}/K_f))]}$$

It turns out, as we will now show, that the empirical relationships derived in Table 1 are themselves internally consistent with this same poroelectric model, indicating that the data set is consistent with a generalized model which links velocities and their saturation dependence to porosity and illite content. The resulting model provides a foundation upon which to interpret well logs as well as a matrix model upon which to construct field scale models for seismic properties.

In order to be generally applicable, the model needs definition of four parameters. From a physical modeling point of view, the natural parameter set to choose is K_{dry} , K_{solid} , G_{dry} , and ΔG , since K_{dry} , K_{solid} , and G_{dry} do not involve fluid/rock interactions.

K_{dry} and G_{dry} can be defined directly by their best fitting empirical relationships in Table 1. There is no evidence that K_{dry} is influenced by illite or

chlorite, so for simplicity we suggest adoption of equation 1c for K_{dry} . For the shear modulus, G_{dry} does appear to have significant illite dependence, but chlorite dependence is not significant, so equation 1b is used here. The illite dependence of G_{dry} , combined with the lack thereof for K_{dry} is an interesting observation which warrants more study aimed at understanding this observation in the context of a physical model.

ΔG can best be defined empirically by subtracting the equation 1b relationships for G_{sat} and G_{dry} from Table 1, yielding

$$\Delta G = A\phi + BI + D$$

$$A = -3.4$$

$$B = -10.3$$

$$D = -0.1$$

Note that $|B| > |A|$ and $|D| \ll |BI|$ for typical I , and thus illite content dominates ΔG . This is evident in a cross plot of ΔG versus illite, which exhibits a well defined trend despite highly variable porosities (see Figure 5). Note also that the Awibengkok and Geysers cores both follow the same trend, suggesting that textural influences are not important for this phenomenon. While the physical mechanism for this shear weakening remains poorly understood, there is ample evidence that the effect is a chemo-mechanical one, as it is not observed in kerosene saturated samples (see Boitnott and Johnson, 1999).

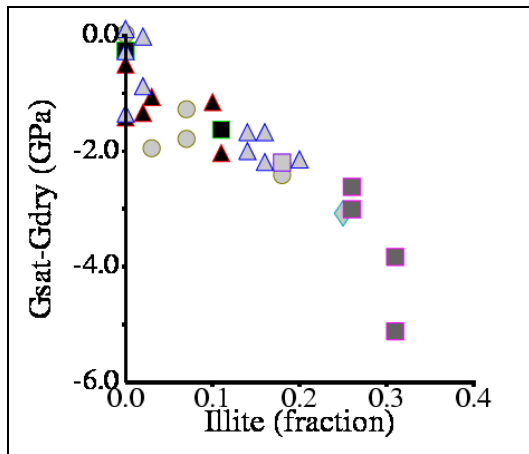


Figure 5: Cross plot of $\Delta G = G_{sat} - G_{dry}$ versus weight fraction illite for the Awibengkok and Geysers data sets. Symbols are the same as in Figure 1. A strong linear trend is clearly seen, consistent with the prediction $\Delta G \sim -10.3I$ using the empirical relations in Table 1.

For the dynamic bulk modulus, the equation 1c relationships in Table 1 indicate that

$$\Delta K = A\phi + D ;$$

$$A = 3$$

$$D = 6.7.$$

In this case we note that $D \gg A\phi$ for typical ϕ , indicating that ΔK is nearly constant independent of porosity. From first glance at equation 3c, one might think that porosity would be a controlling factor on ΔK , however, taking $K_{solid} = 58$ GPa (a typical value used when modeling data from individual cores), we find that ΔK is predicted to be of the correct magnitude and nearly independent of porosity (see Figure 6). This result indicates that low frequency Biot theory described by equations 3(a,c) is consistent with our empirical relationships for K_{dry} and K_{sat} in Table 1, providing justification for use of this well studied physical model for these rocks.

Electrical Properties

Experiments on the Awibengkok cores using different brines suggest a surface conductivity which is roughly proportional to illite content (Boitnott and Hulen [2001]). While significant, this surface conductivity term does not appear to be

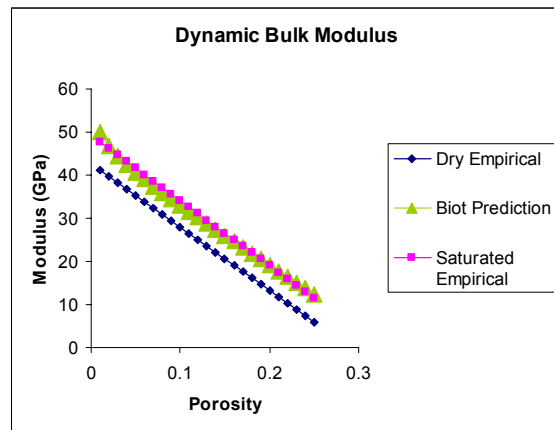


Figure 6: Comparison of K_{sat} from Table 1 with K_{sat} predicted from equation 3c using K_{dry} from Table 1 and $K_{solid} = 58$ GPa.

large enough to fully explain the empirically observed dependence of F on illite, but certainly contributes to some extent. Efforts to construct a physical model incorporating surface conductivity are underway to better understand the illite dependence. It is also of interest to note that in previous studies of The Geysers core (Boitnott and Boyd, 1996), a correlation between sample conductivity and shear weakening was observed. In that work, conductivity measurements were made using distilled water as the pore fluid, so that the

measured sample conductivities are dominated by surface conductivity. Since shear weakening is strongly correlated with illite content, the Geysers data again suggests a correlation between surface conductivity and illite concentration. However, surface conductivities for The Geysers cores are notably less than the inferred surface conductivities of the Awibengkok cores, indicating textural controls are important. More study, particularly with regards to the Geysers cores using brines of variable strength is needed to see if these relationships are similar, and if so, combine them into a unified model.

Joint Interpretation of Velocities and Electrical Properties

One potential application of these relationships is for improved log analysis, such as characterization of porosity and illite concentration from resistivity and velocity logs. Figure 7 illustrates saturated V_p and formation factor contours based on the empirical relationships of each property. This graph illustrates some important interrelationships between these two commonly logged properties. At low porosities, formation factor is found to be relatively insensitive to illite content. For saturated matrix, if F is known, porosity can be inferred directly from F and velocities can be used to infer illite content. High porosity materials have different systematics owing to the fact that porosity effect on F decreases at higher porosities while the illite effect retains its strength. In this case, resistivity becomes a poor predictor of porosity, but in combination with velocities, could again be used to constrain both porosity and illite. Also of significance at moderate porosities, F and V_p contours are relatively parallel, indicative of a regime where porosity and illite cannot be distinguished even using a joint interpretation approach. The Awibengkok reservoir contains a number of units in this regime.

Core Scale Heterogeneity

Another key aspect of the measurement program is the characterization of spatial heterogeneity of electrical properties. A micro-resistivity mapping apparatus has been developed and the resulting images are rich in information, illustrating a wide variety of "anomalies" ranging from conductive or resistive clasts to fractures and porous veins. Importantly, the results illustrate that the samples commonly have intrinsic variability on the order of a factor of three or more, with significant correlations at length scales of a few centimeters.

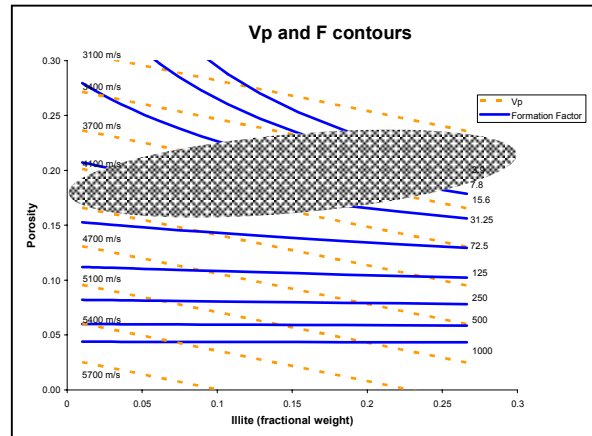


Figure 7: Contours of saturated V_p and F based on Table 1. A zone of parallel contours highlighted in green indicates a region where porosity variations cannot be distinguished from illite variations. Below this zone (i.e. low porosity) F is the best indicator of porosity and V_p can be used to constrain illite.

This suggests that core scale heterogeneity (and its structural details) may give rise to significant resistivity signatures, and may explain much of the remaining scatter in the laboratory scale data.

Viewed in the context of the relationships shown above, we can postulate that resistivity anomalies with $F > 100$ are largely controlled by porosity variations. Illite and porosity are equally likely to contribute significantly to anomalies for $F < 100$. Work is in progress to correlate the observed anomalies with detailed petrographic observations, yielding important constraint on textural controls.

One qualitative conclusion of importance is that resistivity variation is a poor indicator of lithology. Somewhat surprisingly, resistivity maps of lahar samples with conspicuous heterogeneity in the form of clasts of various rock types, illustrate that the clasts are not resolved well by resistivity alone. This same conclusion can be drawn from measurements on plugs of various lithologic units (Figure 3), where lithologies are shown to span wide ranges of porosity and F.

Complex impedance, however, appears to do a reasonable job in identification of discrete clasts and/or beds in many cases, and thus as resistivity logging tools become more advanced, complex impedance may prove a useful reservoir characterization tool. Furthermore, these observations suggest that for these rocks, porosity may reflect a combination of weathering prior to lithification and degree of hydrothermal alteration,

rather than being linked to primary porosity of the host matrix.

Field Scaling

The next step in applying this core scale information is to use it to help constrain and interpret field scale data. The usefulness of matrix velocity information in interpreting field scale velocities has been demonstrated previously in Boitnott [1995]. With knowledge of the matrix properties, differences between field scale and matrix scale velocities and resistivities can be interpreted as the effect of the fracture system. This process is greatly simplified by the fact that the effect of pressure on velocities and resistivities of the matrix is in general quite small, indicating that depth dependence (due to pressure) of matrix properties can be largely neglected for most applications.

Field scale seismic tomography data exhibits similar patterns as observed in the matrix, evidence that saturation effects at the Geysers may be influenced by a field scale shear weakening phenomena similar to that observed in the matrix (see Boitnott and Kirkpatrick, [1997]). The mechanical properties of a single fracture are known to be controlled by the morphology of the fracture and the elastic properties of the host matrix. Thus the poroelastic model for the matrix outlined here provides a necessary component of a physical model for fractured rock as well. A fractured rock model for seismic properties linking fracture network geometry and matrix properties using an effective medium approach is currently under development.

Similarly, pressure and temperature dependence of F is in general relatively small, indicating that the observed systematics should be persistent at all depths. Frequency dependence of resistivity is variable and can lead to relatively strong dispersions at logging frequencies. The available data suggests that the observed dispersion, which can lead to a 20% reduction in resistivity between 1 Hz and 10 kHz, is relatively insensitive to changes in temperature and pressure. Thus the effects of temperature, pressure and frequency are all second order effects when compared to the observed systematics between F , Φ , and illite, indicating that the empirical relationships presented here are directly relevant to field observations. As with for seismic properties, an effective medium model is now being developed to combine the matrix and fracture system effects on field scale measurements.

Future Plans

Initial plans were to extend the data set where needed (partial saturation and temperature), and to

begin adding data from other geothermal reservoirs to test portability of the observed relationships. More work was planned in the areas of integrating petrography, physical properties maps, and core data to further investigate textural controls on seismic and electrical properties. Emphasis on physical models was also planned now that the empirical approach has identified the variables which control key properties. A key aspect of this physical modeling was to be the integration of fractured rock models with matrix models to make the work applicable to field scale geophysical measurements. Also planned was development of methods of mechanical properties mapping of core scale heterogeneity.

While we plan to try to convince DOE that funding for this project should be restored, at present these original goals and plans have been scaled back to reflect DOE's reduced commitment to the project. Efficiencies will be gained by continuing work on the Awibengkok core (already studied and documented) rather than executing another self contained case study. The Awibengkok work will be supplemented with selected samples from other fields to assure that conclusions are not reservoir specific.

This work will continue through September 30, 2002. A final report will be produced and presented at the Geothermal Resources Council (GRC) meeting.

Technology Transfer

Technology transfer is being facilitated through participation in technical meetings, publications in technical journals and through direct collaboration and interaction with researchers working within industry and the DOE program. Data and interpretations are being posted on NER's web page (www.ner.com/geothermal.shtml). The work is being performed in informal collaboration with Dr. J. Hulen at EGI providing expertise in petrographic and mineralogic interpretations of the core samples being studied. Laboratory measurements are also being performed with the intent to compliment the work of others working on related issues, such as J. Roberts and B. Bonner at LLNL who are working on electrical properties during boiling in similar cores.

As a direct result of this project, the microresistivity mapping probe has been commercialized, with the first sale expected this year. The probe is also available for service work for government and industry.

References

Boitnott, G. N., (1995) Laboratory measurements on reservoir rocks from The Geysers geothermal field, *Proceedings, 20th Workshop on Geothermal Reservoir Engineering*, SGP-TR-150, 107-114.

Boitnott, G. N., and P. J. Boyd, (1996), "Permeability, Electrical Impedance, and Acoustic Velocities on Reservoir Rocks from The Geysers Geothermal Field," *Proceedings, 21st Workshop on Geothermal Reservoir Engineering*, SGP-TR-151, 343-350.

Boitnott, G. N. and A. Kirkpatrick, (1997) Interpretation of field seismic tomography at the Geysers geothermal field, California, *Proceedings, 22nd Workshop on Geothermal Reservoir Engineering*, SGP-TR-155 391-398

Boitnott, G. N.. and J. Johnson, (1999) Laboratory measurements of ultrasonic velocities on core samples from the Awibengkok geothermal field, Indonesia, *GRC Transactions*, vol. 23, p. 9-12.

Boitnott, G. N., and J. B. Hulen, (2001), Petrographic controls on electrical properties of core samples from the Awibengkok geothermal field, *GRC Transactions*, vol 25, p-391-394.

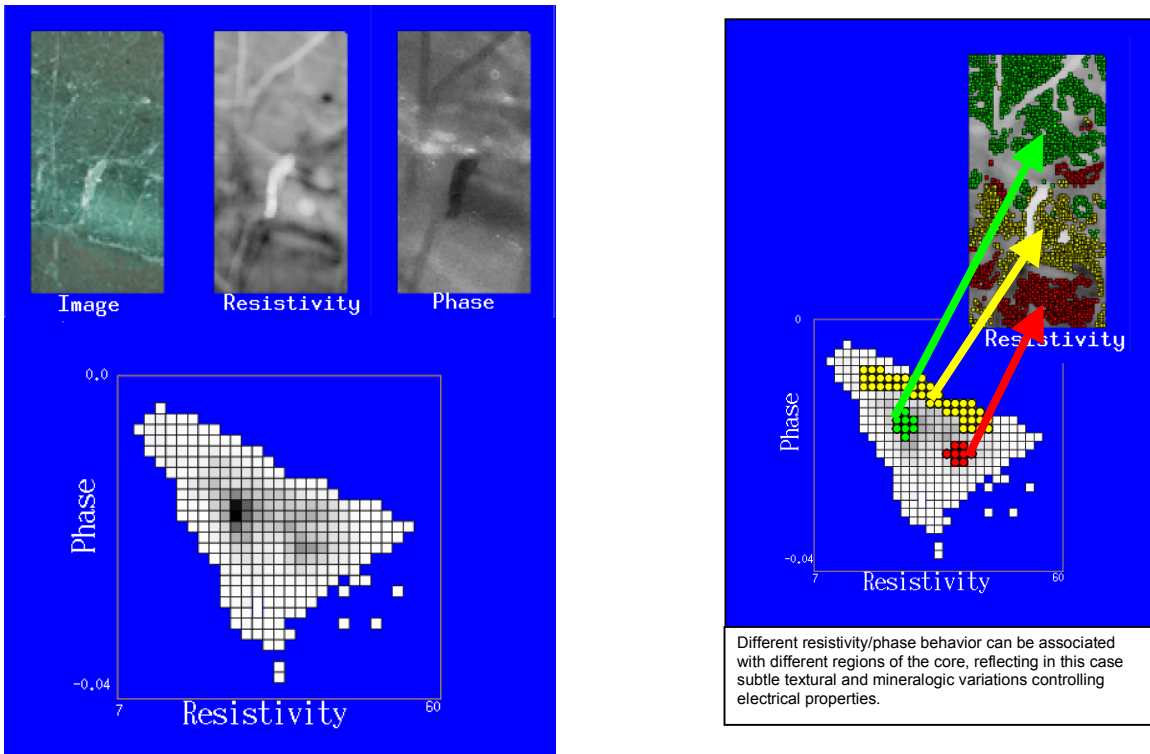


Figure 8: Example resistivity map of a slabbed tuff sample from AWI 1-2. Image dimensions are 6 m by 12 cm. Using a true 4-electrode contacting probe moved in a 1 mm grid, the local complex impedance (plotted here as resistance and phase shift) is measured as a function of position on the slabbed core. Work is in progress relating the various features to detailed petrographic descriptions of the sample. The maps can be used to associate resistivity/phase characteristics with particular textures and mineral assemblages.

Table 1 : Empirical Models of Matrix Properties						
Velocities and Moduli : $P = A\phi + BI + CX + D$						
Property	Dataset	A	B	C	D	RMS Porosity error
Dry V_p (m/s)	Awibengkok and Geysers	-6940			5460	0.0454
		-7610	-1870		5720	0.0345
		-8000	-1750	1320	5540	0.0316
Dry V_s (m/s)	Awibengkok and Geysers	-3520			3270	0.0441
		-3960	-1230		3440	0.0261
		-4090	-1190	441	3370	0.0246
K_{dry} (GPa)	Awibengkok and Geysers	-134			42.4	0.0440
		-141	-19.8		45.2	0.0396
		-147	-18.0	19.8	42.4	0.0373
G_{dry} (GPa)	Awibengkok and Geysers	-76.5			29.0	0.0309
		-83.0	-18.1		31.5	0.0196
		-85.5	-17.4	8.2	30.3	0.0183
Saturated V_p (m/s)	Awibengkok and Geysers	-7580			5620	0.0398
		-8530	-2360		5940	0.0242
		-8980	-2300	1110	5790	0.0222
Saturated V_s (m/s)	Awibengkok and Geysers	-4200			3180	0.0531
		-4990	-1970		3450	0.0253
		-5190	-1940	500	3380	0.0239
K_{sat} (GPa)	Awibengkok and Geysers	-137			49.1	0.0391
		-145	-20.3		51.9	0.0346
		-151	-19.4	14.6	49.9	0.0329
G_{sat} (GPa)	Awibengkok and Geysers	-75.1			27.5	0.0432
		-86.4	-28.4		31.4	0.0214
		-88.8	-28.1	5.8	30.6	0.0206
Formation Factor : $F = \phi^m + BI + CX$						
Property	Dataset	m	B	C	RMS Porosity Error	
F (12000 ppm NaCl)	Awibengkok only	-2.15			0.0200	
		-2.21	-110		0.0141	
		-2.11	-113	121	0.0141	

A THERMOELASTIC HYDRAULIC FRACTURE DESIGN TOOL FOR GEOTHERMAL RESERVOIR DEVELOPEMENT

Principal Investigator - A. Ghassemi
Department of Geology and Geological Engineering
University of North Dakota
Grand Forks, ND 58202
e-mail: ahmad_ghassemi@mail.unda.nodak.edu

Key Words – fractures, fracture networks, fracture mechanics.

Project Background

Geothermal energy recovery from hot dry rocks involves extraction of heat by circulating water through heat exchange areas within the rock mass. Geothermal reservoir rock masses generally consist of igneous and metamorphic rocks that have low matrix permeability. Therefore, cracks and fractures are the major pathways for fluid flow and provide the necessary heat exchange surfaces and play a significant role in extraction of geothermal energy. Thus, knowledge of conditions leading to formation of fracture and fracture networks is of paramount importance. Furthermore, in the absence of natural fractures or adequate connectivity, artificial fracture are created in the reservoir using hydraulic fracturing. Propagation of hydraulic fractures in a geothermal setting is a complex process involving interaction of high pressure fluid with a stressed and hot rock mass, mechanical interaction of induced fractures with existing natural fractures, the spatial and temporal variations of in-situ stress, and rock heterogeneities.

Fracture initiation, propagation, and stability (for induced and natural fractures) are very significant in understanding the response of the reservoir to fluid injection/extraction and need to be considered (see the special issue of *Geothermics* on HDR/HWR in 1999 & Rock Fracture & Fluid Flow, NRC Publication, 1996). Artificial and natural fractures can be better understood through modeling and application of rock fracture mechanics. This can lead to better estimates of the pressure conditions, resulting fracture permeability, fracture networks, fluid flow, and ultimately results in more effective extraction strategies. Moreover, improved understanding of fractures and their properties allows us to design tools for their detection. (e.g., using shear-wave propagation). These insights will also facilitate assessing the importance of fractures for subsurface flow and heat production.

Modeling fracture propagation is an integral part of a comprehensive approach to studying fractures and

is essential to optimum design of hydraulic fractures for geothermal reservoir development. Therefore, we are developing advanced thermo-mechanical models for design of artificial fractures and rock fracture research in geothermal reservoirs. The technology development aspect nicely complements other models used solely for heat extraction aspects of reservoir management (e.g., GEOCRACK).

Project Objectives

The research objectives consist of:

1. Analysis of fracture initiation from a wellbore;
2. Development of a two-dimensional coupled thermoelastic boundary element code for modeling fracture propagation;
3. Theoretical study of fluid flow and heat exchange in induced fractures;
4. Analyses of the influence of variations in reservoir temperature/stress on fractures propagation and geometry;
5. Integration of the analytic and numerical algorithms into a user-friendly software package.

Approach

In view of the number and complexity of the processes involved in drilling and stimulation it is impractical to have a single model for treatment and analyses of various problems of interest. Thus, it is necessary to develop a number of numerical models to investigate various aspect of the problem.

Borehole Failure & Fracture Initiation

Fracture initiation from a wellbore may be treated using a classical strength of materials approach (Hubbert and Willis, 1957; Haimson and Fairhurst, 1967; Pine et al., 1983) or a fractures mechanics approach (McGarr, 1978; Abou-Sayed et al., 1978; Rummel and Hansen, 1989; Ito and Hayashi, 1991). Because of its practicality, the former is the one that is widely used. Using the classical approach, Stephens and Voight (1982) considered fracturing of a vertical well in a cooled rock and found that thermal stresses can impose a significant influence

of on hydraulic fracturing and interpretation of its results to determine the maximum far-field stress. Cooling the rock induces tensile stresses and results in a lower wellbore pressure for fracture initiation. We have developed an analytical model that can calculate the stress distribution around a wellbore of arbitrary orientation while considering, thermoelastic, and poroelastic effects. This work can be used to calculate the failure pressure and its location around the wellbore based on the classical approach. The governing equation and solution methodology can be found in Wolfe (2002) and Ghassemi and Diek (2002).

A fracture mechanics approach can be considered by using a fracture propagation model based on the principles of fracture mechanics. In some instances it provides a better estimate of the breakdown pressure.

Fracture Propagation

Once a fracture is initiated or a natural flaw exists at the wellbore wall, it is of interest to determine the fracture propagation pressure and the propagation path and their determinants.

A fracture propagation model has been developed based on the *complex variable* displacement discontinuity method. The DD's are defined at each step from the numerical solution of a complex hypersingular integral equation written for a fracture of a given configuration and loading (Linkov and Mogilevskaya, 1994; Koshelev and Linkov, 1999). The main advantages of the complex variable approach are the possibility to consider natural discontinuities and heterogeneities in rock and model smooth crack growth. The latter is made possible by using a circular arc to model the crack path increment at each propagation stage.

There are two distinct variants of the CV-BEM. The first type is called the *non-periodic* formulation (Linkov and Mogilevskaya, 1994; Mogilevskaya, 1996) and the second type is the *double-periodic* CV-BIE (Koshelev and Linkov, 1999). In the former approach, a finite number of cracks and/or holes can be considered whereas the latter can consider a rock mass with numerous pores, cracks and/or inclusions. The rock mass is subdivided into blocks having different elastic properties. For infinite bodies, one additional external (infinite) block is introduced to take into account the infinite nature of the domain. Different external forces such as weight of the rock mass, water pressure in some holes or cracks, and the temperature field are also considered.

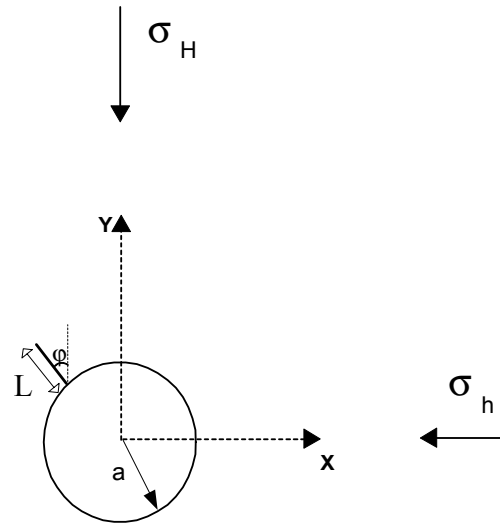


Figure 1. Problem geometry for studying fracture initiation and propagation from a wellbore in a non-hydrostatic stress field.

Our current computer model is based on the non-periodic formulation developed by Mogilevskaya et al., 2000 (see NDRM-00-01 for details). The fracture propagation scheme used consists of two procedures. First, the propagation direction is determined by assuming that a fracture propagates in the direction perpendicular to the maximum circumferential tensile stress. Then, one exploits the fact that the mode II stress intensity factor, K_{II} , is equal to zero at the current crack tip. The crack is extended from the previous tip once the condition for crack propagation $K_I = K_{Ic}$ is satisfied (where K_I is the mode I stress intensity factor, and K_{Ic} the toughness). The stress intensity factors K_I and K_{II} are calculated at each step of propagation using the known displacement discontinuities (DD's) at the fracture surfaces.

Fluid Flow & Heat Extraction

Heat extraction from a fracture in a geothermal reservoir is typically modeled based on the assumption that heat conduction is one-dimensional and perpendicular to the fracture. In our work, an integral equation formulation is used to model two- and three-dimensional heat flow in the reservoir. This method results in a numerical procedures in which subdivision of the reservoir geometry is entirely eliminated, leading to a much more efficient scheme. In addition to providing the temperature distribution in the reservoir, the multi-dimensional boundary integral equation formulations provide an efficient means for calculating the induced thermal stresses on the fracture surface and in the reservoir.

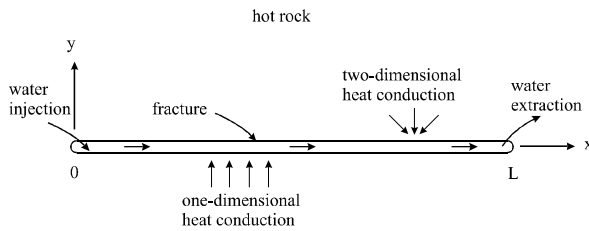


Figure 2. Two-dimensional heat flow model for injection/extraction operation.

The details of the mathematical approach and solution methodology for the problem of heat and fluid flow using a two-dimensional BEM can be found in Cheng et al., 2001. It is assumed that the fracture walls are impermeable and the fracture aperture is constant. All thermal properties such as heat capacity and conductivity are considered constant and water is assumed to be incompressible. Furthermore, the numerical model has been extended to three-dimensions (NDRM-01-07) to model 2D fluid flow in the fracture and 3D heat flow in the rock (Figure 3). The resulting boundary element equations have been solved numerically for a single fracture in HDR (Ghassemi et al., 2002).

We have also studied the heat extraction problem analytically. The analytical solutions have been used to investigate the influence of fluid leak-off and mechanisms such as heat transport, heat storage, advection, and longitudinal dispersion in the fracture.

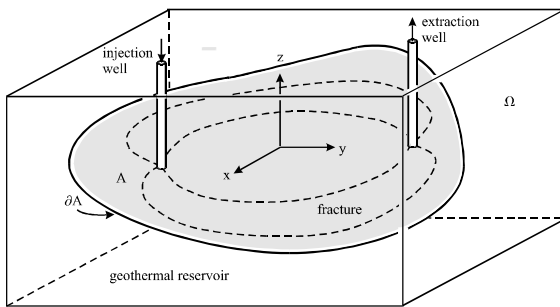


Figure 3. Three-dimensional heat flow model for injection/extraction operation.

Thermal Stresses Due to Heat Extraction

The induced thermal stresses modify the in-situ stress state and can significantly influence fracture growth and propagation. An estimate of the stress field variation with water injection in conjunction

with observing seismicity in geothermal fields can be used to ascertain reservoir growth due to stimulation. In addition, the thermal stresses can be used in determining the change in the permeability of a fracture due to cooling.

A boundary element approach is also used to calculate the thermal stresses in the reservoir and to study its impact on joint aperture change, slip, and fracture propagation. Currently a two-dimensional constant element displacement discontinuity model is used for this purpose. The model assumes that the reservoir is homogeneous with respect to thermal properties. The thermal stresses are calculated from the thermal source strengths obtained from the 2D boundary element solution of heat extraction from a fracture and the fundamental solution for the stresses due to unit continuous heat source (NDRM-01-08).

Research Results

Borehole failure & fracture initiation

An example is shown in Figure 4; it illustrates the large tensile stresses that are induced around the wellbore when cooling the rock by 220 °C.

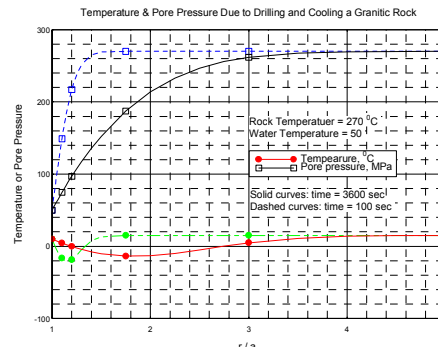


Figure 4. Temperature and pore pressure distribution around a wellbore drilled in a geothermal reservoir using a cooler fluid.

Figure 5 illustrates the distribution of pore pressure and stresses at various times. Note that the zone of tension propagates into the rock and enhances fracturing.

The sum of the thermal and in-situ stress is tensile even when the internal pressure is excluded. Note that although the maximum tensile (tangential) stress always occurs at the wall, a zone of tension also develops and extends into the formation with increasing cooling time.

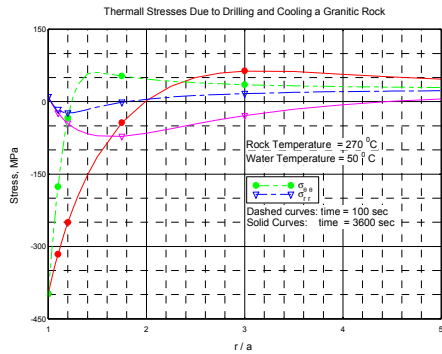


Figure 5. High tensile stresses are developed around the well in a hydrostatic stress field (26 MPa), as a result of cooling. The tensile zone expands into the reservoir with time resulting in fracture initiation and propagation.

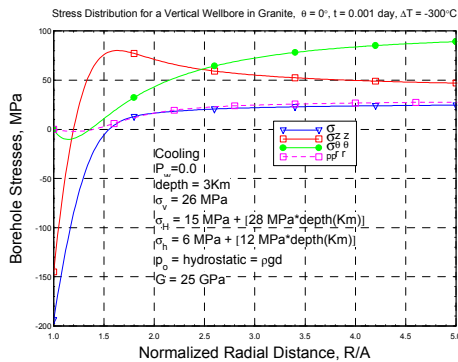


Figure 6. Tensile stresses around a well in a non-hydrostatic stress field (cooled by 300 °C).

Fracture propagation

As an example of the application of our current model, consider the problem of fracture propagation from a wellbore in a homogeneous elastic isotropic medium (Mogilevskaya et al., 2000; NDRM-00-02). A wellbore of radius a is drilled in a compressive stress field. It is assumed that the wellbore boundary contains a preexisting crack of length L that is inclined at an angle ϕ to the direction of maximum principal stress (Figure 1). Several fracture paths for different values of $\beta = [a^{1/2} \cdot (\sigma_H - \sigma_h) / K_{IC}]$ are plotted in Figure 7. When pressure is applied at a slow rate, for a fixed value of β , the fracture tends to return to a straight path as illustrated in the figure. As β increases, the fracture undergoes a sharper turn and reaches the favorable path faster.

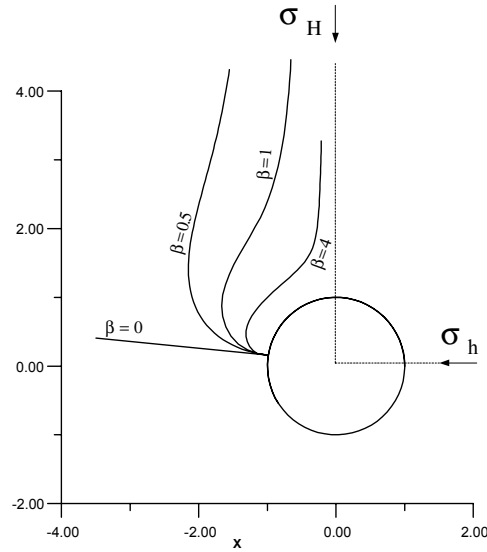


Figure 7. Fracture propagation path depends on in-situ stress difference.

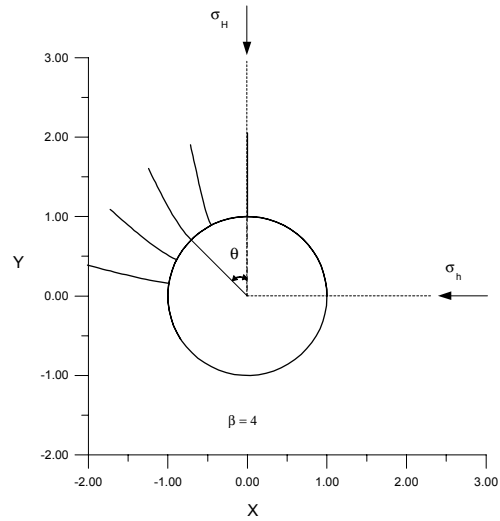


Figure 8. For a given β , fractures tend to propagate in their original direction defined by θ , if the fracturing fluid cannot enter them (e.g., when using explosives or injecting liquid at a high rate into the well).

When calculations are carried out without fluid pressure penetrating the crack, fractures generally tend to follow the path along the initial radial direction without much curvature (Figure 8). This type of behavior has been observed in laboratory experiments (Zoback et al., 1977).

User interface allowing real time, interactive fracture propagation modeling

Experience has shown that an appropriate medium through which models can be applied and results studied is paramount to successful utilization of advanced scientific knowledge and technical solutions. Therefore, in order to maximize the efficacy to the industry, our design codes and analytical solutions are being integrated to form a multi-component model. As part of this effort a graphics user interface (GUI) has been developed to enhance the fracture propagation modeling capabilities. In short, GUI is a graphical representation of the software that gives it a friendly look and helps the user to experience the “feel” and “power” of the software. The system architecture and the GUI have been described elsewhere (NDRM-00-04, NDRM-00-05, NDRM-01-06). The user interface has graphics routines, and dialog boxes for conveniently selecting a desired program and entering data. Graphics capabilities have been implemented to assist the user in problem definition. Post-processing routines allow program output to be viewed directly through graphic presentations or saved in data files for later use. The fracture propagation model can be accessed through client-server architecture. The server, as the name suggests, provides services to clients. In a typical case, client-server architecture consists of one server and one or more clients. The services can range from performing a simulation requested by the client to “asking” other client(s) connected to that system to conduct simulations and to provide the results to the client.

Figures 9-11 are examples of the model interface showing real time fracture propagation. Figure 9 illustrates the influence of inclusions (e.g. rock grains or other material inhomogeneity) on fracture interaction. It shows the capability of the model to consider rock heterogeneity. The upper inclusion is five times stiffer than the lower one, which has a stiffness that is twice that of the rock matrix.

Compressive stresses are imposed in both directions ($\sigma_{xx}=12.5$ MPa, ($\sigma_{yy}=10.0$ MPa, and $\nu=0.25$, $G=1$ GPa). A pressurized fracture is propagating in the direction of maximum stress. Note that the fracture’s path is altered due to variation in stress distribution caused by the stiffer and softer (upper & lower) inclusions.

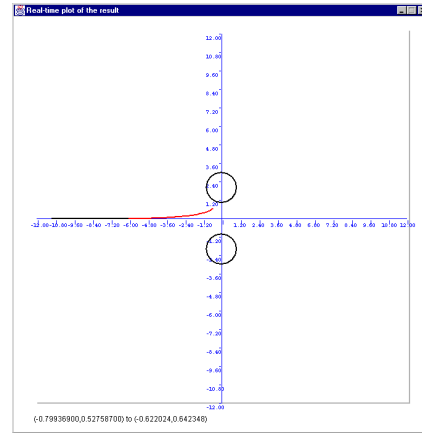


Figure 9. Fracture propagation in heterogeneous rock.

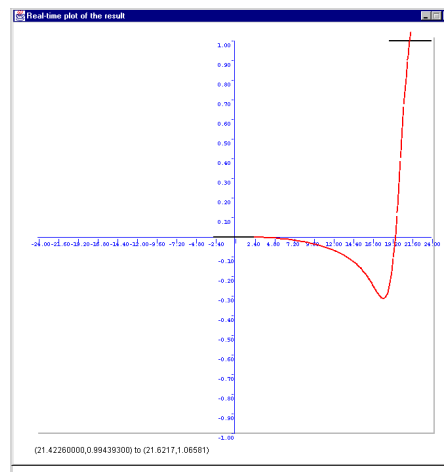


Figure 10. Interaction of an echelon fracture systems.

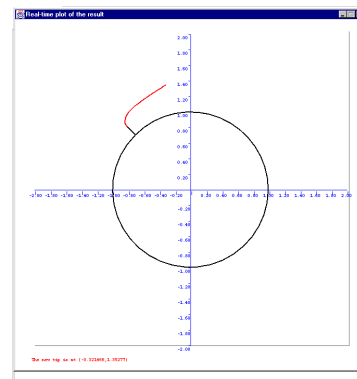


Figure 11. Hydraulic fracture propagation from a wellbore. The interface also shows a graph of the pressure history.

Figure 10 illustrates a typical fracture interaction problem namely, the en echelon fracture geometry comprised of two cracks separated by a small distance (1 cm). The lower crack is allowed to propagate under the influence of a far-field isotropic tensile stress. The fracture initially propagates in a straight direction, as it reaches the vicinity of the left tip of the upper fracture it turns away from it. However, as a result of mechanical interaction with the free face of the upper crack, it turns up and intersects the upper crack. This is in very good agreement with experimental observation (Thomas and Pollard, 1993).

The real time analysis of the hydraulic fracturing problem described previously is shown in Figure 11. The user can also study the pressure history and the stress intensity factor as the crack propagates. These are useful for monitoring stable and unstable fracture growth and pressure requirements. They are not shown here due to space limitations.

Fluid flow and heat extraction

We have developed analytical solutions for heat extraction from a fracture in order to study the influence of various plausible mechanisms such as heat dispersion in the fracture, heat storage in the fracture, and fluid leak-off into the rock mass. We have found that all but fluid leak-off has negligible influences on the extraction temperature. Fluid loss has the effect of reducing power generation by reducing the total amount of heat extracted per unit time (because less fluid is extracted). Figure 12 illustrates the rate of heat energy extracted per unit height of fracture for the 50% leak-off and no leak-off cases. Clearly the no leak-off case extracts more heat (Cheng and Ghassemi, 2001).

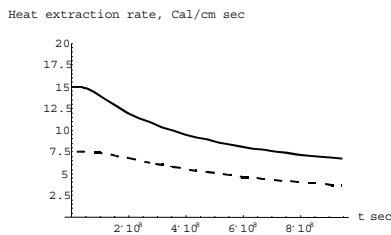


Figure 12. Heat extraction rate per unit height of fracture. (Dash line: 50% leak-off loss; solid line: no leak-off)

The numerical boundary element solutions, described previously, have been used to study heat extraction from line and circular fractures. Figure 13 shows the normalized temperature of water from a fracture in hot dry rock using a two-dimensional boundary element model. The one-D solution of Lowell is also shown. Note that the difference

between 1D and 2D solutions is insignificant for longer fractures for the same injection rate. This is to be expected as the rate of heat extraction from the rock decreases. Thus, it takes a much longer time for the two-dimensional diffusion mechanism to develop in the rock mass. This explains the large differences between the 3D and 1D heat extraction from a circular fracture reported by the Kolditz (1995). Such differences seem to be observed only under high water injection rates

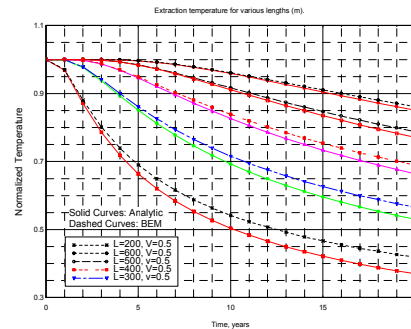


Figure 13. Normalized temperature of water extracted from a fracture in hot dry rock using a two-dimensional heat boundary element model (fluid velocity of 0.5 cm/sec, see Cheng et al., 2001 for fluid & rock properties).

Figures 14 illustrates the result of our three-dimensional boundary element heat extraction model. The rock temperature distribution is shown after 3 days of injection/production (see Rodemman, 1982 for rock and fluid data).

Thermal stresses due to heat extraction (2D solution)

The problem involves injecting water at one end of a fracture. It is assumed that water is pumped out of the fracture, at the other end, at same rate as it is injected. It is of interest to calculate the tractions that are induced along the fracture(s) by the perturbation of the temperature field due to extraction of heat. This is achieved using a two-dimensional constant element displacement discontinuity model (Savitski, 2001). The thermal stresses are calculated from the source strengths obtained from the 2D boundary element solution of heat extraction. Figure 15 illustrates the thermal stresses for the heat extraction problem treated above. Note that significant stresses are generated on the fracture face (increasing with time). This suggests that when compared to pore pressure, the thermal stresses play a significant role in joint and fault slip and associated seismicity, as observed by Mossop and Segall (2001) for an injection well.

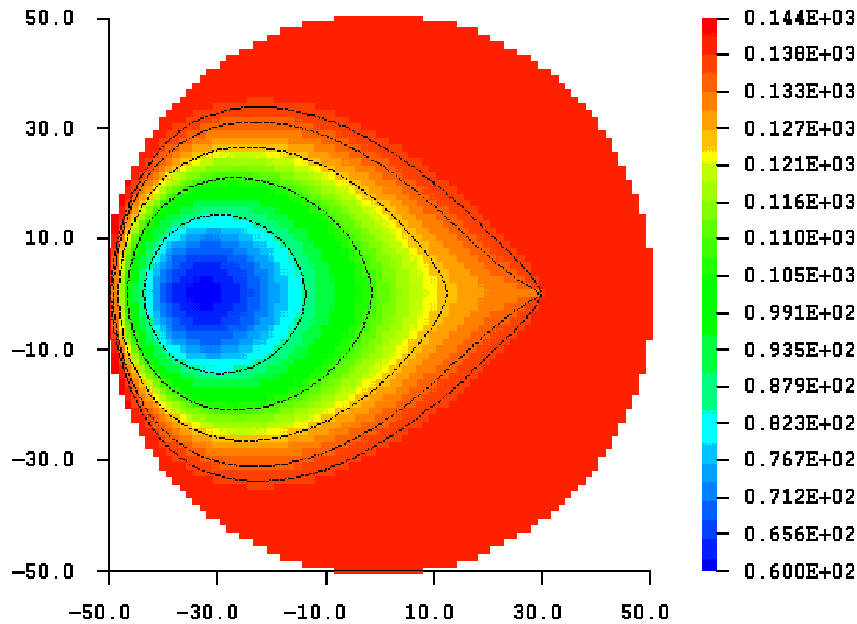


Figure 14. Rock temperature contours of Rodemann (1982) based on our 3D BEM results. The black contour lines are in good agreement with Rodemann's curves.

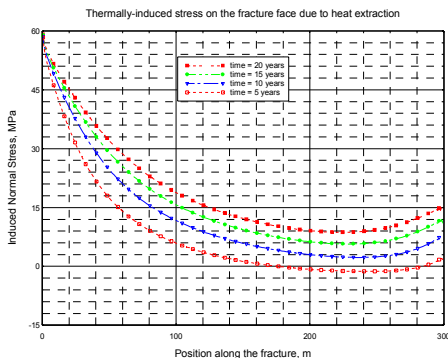


Figure 15. Thermal stress on the face of a line crack due to injection/extraction.

Future Plans

Future activities include application of the current models to geothermal problems of interest and comparison with laboratory experiments.

The current fracture propagation model (i) does not rigorously consider thermoelastic stresses (ii) is unable to model injection into a fault and treat fracture *intersection and termination* at interfaces such as joints and faults, (iii) cannot consider an infinite number of cracks and pores and their effect on elastic properties of the rock mass, and

(iii) cannot address three-dimensional effects. Thermoelastic effects are being introduced as part of an ongoing effort. The other limitations will be remedied in the future phases of the project namely:

- A. Development of a two-dimensional thermoelastic complex-variable boundary element method (CV-BEM) for *naturally fractured* reservoirs:
 - a. Develop and apply CV-BEM algorithms for calculating the effective elastic properties of fractures reservoirs;
 - b. Analyze and model hydraulically driven fractures intersecting other surfaces such as faults, joints, and bedding planes
- B. Development of a three-dimensional thermoelastic hydraulic fracture model
 - a. 3D displacement discontinuity fracture model;
 - b. Couple fluid flow/heat extraction to 3D fracture propagation.

In addition, geothermal areas commonly are located in the zones of intensive tectonic movements. Complicated coupled tectonic and poro-mechanical processes lead to the creation of pore and fracture spaces at depth, forming deep-

seated geothermal systems. To describe the development and evolution of the pore space and fractures in shear zones, we are using a viscoelastic rheology to develop a viscoporoelastic FEM model for studying the formation of deep-seated geothermal systems.

Publications/Collaborations

Ghassemi, A., Cheng, A., H.-D., and Tarasovs, S., 2002. A three-dimensional solution for heat extraction from a fracture in hot dry rock using the boundary element method. 27th Annual Stanford Geothermal Workshop.

Cheng, A. H.-D & Ghassemi, A. 2001. Effect of fluid leak-off on heat extraction from a fracture in hot dry rock. GRC 2001 Annual Meeting, San Diego, CA.

Cheng, A. H.-D., Ghassemi, A., and Detournay, E. 2001. A two-dimensional solution for heat extraction from a fracture in hot dry rock. *Int. J. Numerical & Analytical Methods in Geomech.*, 25, 1327-1338.

Simakin, A. and Ghassemi, A. 2002. Heat Pipe in Porous Brine Saturated Rock: Quasi Steady-State Operation and Related Heat and Mass Transport. 27th Annual Stanford Geothermal Workshop.

NDRM-00-01. Modeling two-dimensional fracture propagation using a complex variable displacement discontinuity method. Quarterly Report Submitted to DOE by Department of Geology & Geological Engineering, University of North Dakota, 2000.

NDRM-00-02. Modeling fracture propagation from a wellbore & heat extraction from a fracture in HDR. Quarterly Report Submitted to DOE by Dept. of Geology & Geological Engineering, University of North Dakota, 2000.

NDRM-00-03. Numerical analysis of hydraulic fracture propagation under a thermoelastic perturbation of the state of stress & A two-dimensional solution for heat extraction from a fracture in hot dry rock. Quarterly Report Submitted to DOE by Dept. of Geology & Geological Engineering, University of North Dakota, 2000.

NDRM-00-04. User interface development & Three-dimensional heat extraction from a fracture in HDR. Quarterly Report Submitted to

DOE by Dept. of Geology & Geological Engineering, University of North Dakota, 2000.

Three additional papers are being prepared for submission to journals. Also, we have begun discussions with Steve Glaser at UC Berkeley to compare numerical results with their experimental observations as soon as they become available.

References

Abou-Sayed, A.S., Brechtel, C.E., and Clifton, R.J. 1978. In-situ stress determination by hydrofracturing: a fracture mechanics approach. *J. Geophys. Res.*, 83 (B6), 2851-2862.

Cheng, A. H.-D., and Ghassemi, A. 2001. Effect of fluid leakoff on heat extraction from a fracture in hot dry rock. GRC 2001 Annual Meeting, San Diego, CA.

Cheng, A. H.-D., Ghassemi, A., and Detournay, E. 2001. A two-dimensional solution for heat extraction from a fracture in hot dry rock. *Int. J. Numerical & Analytical Methods in Geomech.*, 25, 1327-1338.

Ghassemi, A., Cheng, A., H.-D., and Tarasovs, S., 2002. A three-dimensional solution for heat extraction from a fracture in hot dry rock using the boundary element method. 27th Annual Stanford Geothermal Workshop.

Ghassemi, A., and Diek, A., 2002. Porothermoelasticity for shales. *J. of Pet. Sci. & Engrg.* (in Press).

Haimson, B.C., and Fairhurst, C. 1967. Initiation and extension of hydraulic fractures in rocks. *Soc. Pet. Eng. J.*, 310-318.

Hubbert, M.K., and Willis, D.G. 1957. Mechanics of hydraulic fracturing. *Trans. Am. Inst. Min. Engrs*, 210, 153-168.

Ito, T., and Hayashi, K. 1991. Physical background to the breakdown pressure in hydraulic fracturing tectonic stress measurements. *Int. J. Rock Mech. Min. Sci. & Geomech. Abstr.*, 28 (4), 285-293.

Koshelev, V. F., and Linkov, A.M. 1999. Complex BEM in periodic and double-periodic elasticity problems. Proc. 13th ASCE Engrg. Mech. Conf., CDROM.

Linkov, A. M., and Mogilevskaya, S. G. 1994. Complex hypersingular integrals and integral equations in plane elasticity. *Acta Mechanica*, 105, pp. 189-205.

- Linkov A.M., Koshelev V.F. 1999. Complex variable BIE and BEM for a plane doubly periodic system of flaws. *J. Chinese Inst. Engineers*, 22, No.6, 709-720.
- Mogilevskaya, S.G., Rothenburg, L., and Dusseault, M.B. 2000. Interaction between a circular opening and fracture originating from its boundary in a piecewise homogeneous plane. *Int. J. Numer. Anal. Meth. Geomech.*, 24, 947-970.
- Mogilevskaya, S.G. 1996. The universal algorithm based on complex hypersingular integral equation to solve plane elasticity problems. *Computational Mechanics*, 18, 127-138.
- Mossop, A. and Segall, P. 2001. Induced seismicity in geothermal field. I- A thermoelastic injection model (on the Web; to be published).
- NDRM-00-02. Modeling fracture propagation from a wellbore & heat extraction from a fracture in HDR. Quarterly Report Submitted to DOE by Dept. of Geology & Geological Engineering, University of North Dakota, 2000.
- Pine, R.J., Ledingham, P., and Merrifield, C. 1983. In-situ stress measurements in the Carnmenellis granite- II. Hydrofracture tests at Rosemanowes quarry to depths of 2000 m. *Int. J. Rock Mech. Min. Sci. & Geomech. Abstr.*, 20, 63-72.
- Rodemann, H., 1982. Analytical model calculations on heat exchange in a fracture, in Haenel, R. (ed.), *Urach Geothermal Project*, pp. 351-353. Stuttgart.
- Rummel, F., Hansen, J. 1989. Interpretation of hydrofrac pressure recordings using a simple fracture mechanics simulation model. *Int. J. Rock Mech. Min. Sci. & Geomech. Abstr.*, 26 (6), 483-488.
- Savitski, A. 2001. Calculation of thermal stress due to heat extraction from HDR. Report to the Dept. of Geology & Geological Engineering, University of North Dakota.
- Stephens, G., and Voight, B. 1982. Hydraulic fracturing theory for conditions of thermal stress. *Int. J. Rock Mech. Min. Sci. & Geomech. Abstr.*, 19, 279-284.
- Thomas, A. L., and Pollard, D. D. 1993. The geometry of echelon fractures in rock: implications from laboratory and numerical experiments. *J. Struct. Geol.*, 15, (3-5), 323-334.
- Wolfe, C. A., 2002. Borehole Stability in shale. MS thesis, Dept. of Geology & Geological Engineering, University of North Dakota.
- Zoback, M. D., Rummel, F., Jung, R., and Raleigh, C.B. 1977. Laboratory hydraulic fracturing experiments in intact and pre-fractured rock, *Int. J. Rock Mech. and Min. Sci.*, 14, 49-58.

MODELING PRODUCTION/INJECTION STRATEGIES IN FRACTURE-DOMINATED GEOTHERMAL RESERVOIRS

Principal Investigator - Dr. Daniel Swenson
Mechanical and Nuclear Engineering Department
Kansas State University
Manhattan, KS 66502
e-mail: swenson@ksu.edu

Key Words - Geothermal, Finite Element, Fractures, Faults, Fluid Flow, Heat Transfer, Deformation, Multi-Physics

Background and Status

Realistic models of flow in fractured reservoirs are needed because long-term, economic operation of geothermal reservoirs requires that re-injection be used to recharge fluid and recover additional thermal energy. However, re-injection in fractured reservoirs can cause short-circuits and prematurely cool the produced fluid. Understanding and controlling this flow is critical for successful reservoir operation. Realistic fracture models can help both in designing re-injection strategies and in operation of fractured reservoirs.

This research is an extension of previous work at Kansas State University developing the Geocrack2D reservoir simulation program (Swenson, 1997). Geocrack2D includes the complex interactions between rock deformation, fluid flow, and heat transfer, where flow paths and reservoir pressures change as a result of heat removal. A primary goal of this project was to develop similar capability in three dimensions.

The project included numerical model development at Kansas State University, tracer analyses at the Energy & Geoscience Institute at the University of Utah, and oversight and industrial collaboration with Oxbow Power Services.

Objectives

The specific objective of this project is to improve modeling of flow in fracture-dominated reservoirs, leading to increased reservoir energy production. In a larger sense, this project complements broader investments being made by the Department of Energy in reservoir diagnostic technologies. Significant effort is being applied to improved tracer data, borehole imaging, tomographic imaging (such as Electrical Resistance Tomography), and micro-seismic data analysis. All of these technologies are beginning to make it possible to map major features in a reservoir. When these technologies come to fruition, it will be possible to create a model that incorporates the major features

of a reservoir before the reservoir is brought into production. At the same time, future computer power will make it possible to perform complex calculations in a much more routine manner than is now possible. Our goal is to make future reservoir modeling have the same engineering usefulness that structural analysis has today.

Approach

The three-dimensional model (Geocrack3D) developed in this research explicitly represents the fractures as flow paths in the model. The user interactively defines geometric features (the boundaries, wellbores, and fractures) of the reservoir and Geocrack3D then stores a valid geometric model. Using the geometric data, a finite element is created and solved and results are then displayed.

Several tasks were completed in reaching the goal of developing a general 3D finite element analysis for fractured reservoirs. These include:

1. **Use of a Geometric Model to Represent a Reservoir:** A geometric model is a high-level, geometry-based representation of an object and was a key component in the development of Geocrack3D (Hardeman, 1998; Hardeman and Swenson, 1998). The geometric model allows the reservoir to be described independent of the details of how the problem will be meshed and solved.
2. **Implementation of Coupled Hydro-Thermal-Structure Finite Element Program:** Object-oriented software methods were used to design a finite element program framework to implement solution of the coupled hydro-thermal-structure problem, while allowing extension and application to other problems (Hardeman, et al., 1999).
3. **Interactive Cross-Platform User Interface:** The user interface provides functionality to create the model and to define all the other information needed for an analysis (material

properties, boundary conditions, etc.). The interface was implemented in Java, interfacing to a C++ model, to allow cross-platform capability (Kulkarni, 1999).

4. **Meshing of 2D Surfaces and 3D Volumes:** Automatic meshing of 2D surfaces and 2D volumes was needed to implement the finite element solution. To accomplish this, we extended 2D and 3D meshing software developed at Cornell University.
5. **Logarithmic Well Element:** The solution for flow in the vicinity of a well has a logarithmic pressure distribution. We implemented a new finite element that uses logarithmic shape functions, thus ensuring that the correct analytic solution is obtained near a well (Liu and Swenson, 2001).
6. **Implementation of Upwinding:** When two fractures intersect, the fluid flowing in one fracture can be hot and flow in the other fracture cold. To allow reasonable elements to be used in the 3D mesh, we implemented upwinding in Geocrack3D using the SUPG method described in Mizukami and Hughes, 1985.

Research Results

Example of Flow on Single Fracture

An injection/production analysis was performed representing the 2D flow on the fracture with 3D heat conduction in the rock. The 2D mesh on the fracture is shown in Figure 1 and the corresponding 3D mesh is shown in Figure 2. Temperature contours on the 3D single fracture calculation are given in Figure 3 and Figure 4 at 1000 days.

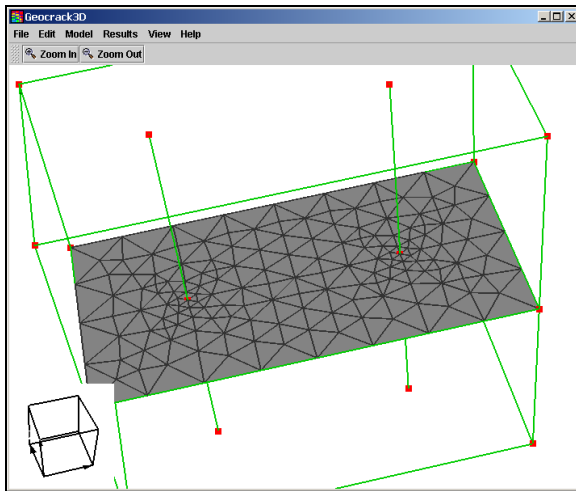


Figure 1: Mesh on fracture

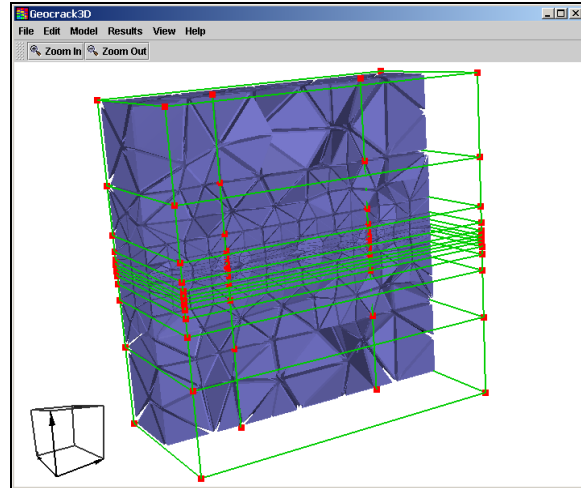


Figure 2: 3D mesh used for single fracture analysis

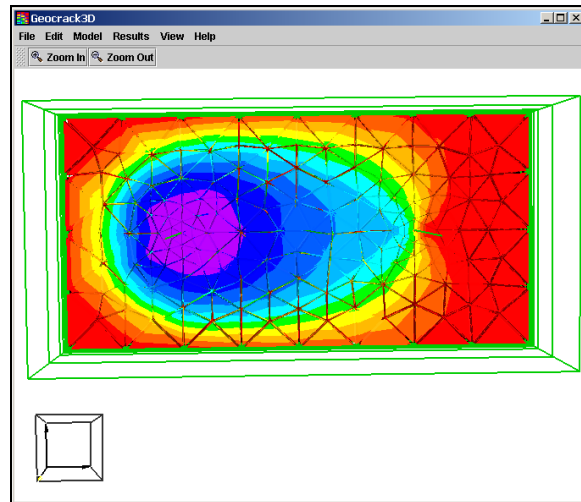


Figure 3: Temperatures on single fracture at 1000 days

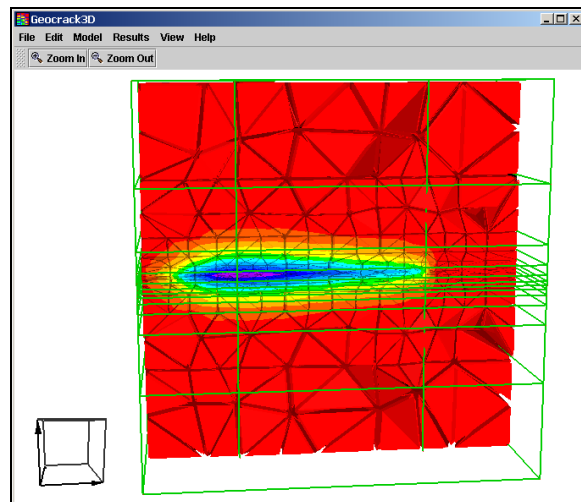


Figure 4: Section showing single fracture temperatures at 1000 days

These results, especially Figure 4, show why flow on fractures can lead to more rapid cooling than expected. Rock is a relatively poor heat conductor; consequently it is possible to cool the surface of a fracture but only remove heat from a relatively small volume of rock adjacent to the fracture. As a result, the temperature of the produced fluid can drop before the potentially available heat is removed from the reservoir.

Fault-Dominated Example Analysis

In the Dixie Valley geothermal field, reservoir permeability is closely associated with the extensive Stillwater fault, a normal fault with little or no strike slip movement. Well logs indicate that the reservoir permeability is due to the presence of the fault and concomitant fracturing of the brittle members of the reservoir rocks adjacent to the fault. The specific geometries of some faults and fractures that contribute to reservoir productivity are uncertain, however, well logs show that flow is transmitted through fractures with large apertures. It is therefore appropriate to employ a numerical model with fractures represented as discrete features, and to calculate the heat exchanged between the rock matrix and the fluid without assuming thermal equilibrium. This allows fluid and heat to flow in a simulation at different physical rates, by slow conduction in impermeable rock, and by convection with the fluid in fractures.

We have constructed a simple model and used it only for an example analysis; more effort is required to include the latest conceptual models and historical data. In this effort, our goal is to demonstrate the capacity for modeling Dixie Valley with Geocrack3D, not to make any realistic simulation or predictions for this reservoir.

In this Geocrack3D model, we have used only a few planes to represent the Stillwater fault in the reservoir region, and connected another single fault that dips at a shallower angle to intersect all the wells near the productive reservoir depth. All of these fractures were assigned a single aperture that corresponds to a transmissivity of 70,000 md ft, which came from a conceptual model developed in the late 1980's. Even though Geocrack3D can model heterogeneity in fracture apertures, the apertures in the Dixie Valley model are uniform. Also, homogenous properties were assumed for the entire rock matrix in the model. Figure 5 shows the 3D mesh used for the analysis. Logarithmic elements are used where the wells intersect the fracture planes.

The wells were given flow boundary conditions. There is no recharge flow in the analysis. Temperature results at 10 years are shown in Figure 6. Note that the injection was simplified to representative sections for the thermal analysis. The initial temperature of the reservoir was assumed to be 250 °and the injection temperature was assumed to be 150 °C. The figure shows the cooling that starts near the injection wells and gradually extends on the fracture.

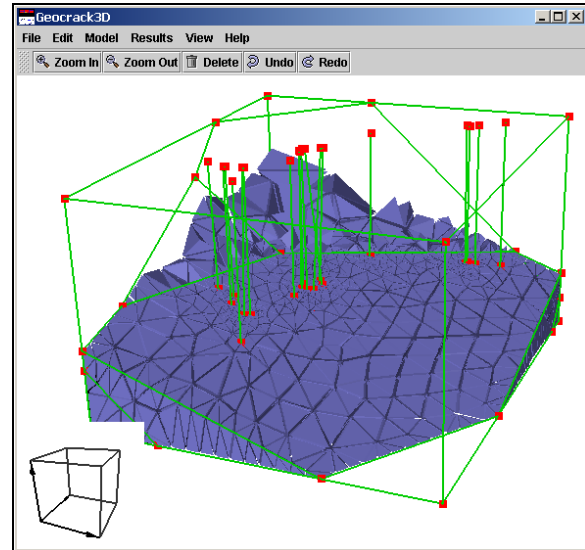


Figure 5: 3D mesh

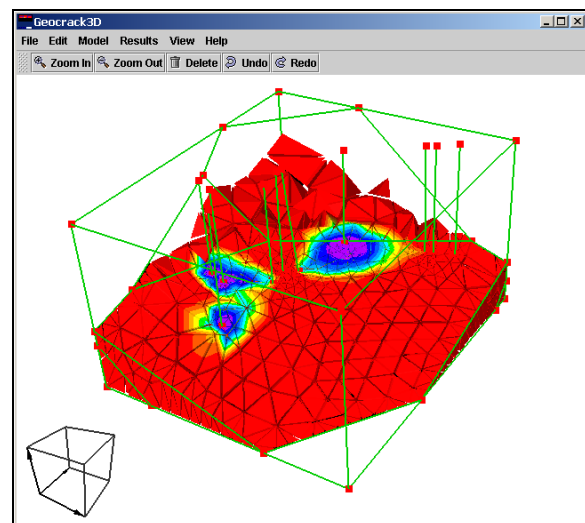


Figure 6: Temperature contours on fracture after 10 years using simplified model without recharge

Summary of Accomplishments

The major goal of this research, developing a 3D model of fluid flow in fractured rock, has been accomplished. To develop the model, the following tasks were completed:

1. Implementation of a geometric model to describe the reservoir. This geometric model allows the user to work with features at a high level when defining the reservoir. For example, the user does not manipulate details of the mesh when describing the geometry, but instead defines the problem boundaries, fractures, and wells. The mesh is then automatically created from this high level description. The geometric model uses a non-manifold topological database to store the model description.
2. Development of a cross-platform, interactive interface for defining and viewing the model and results.
3. Implemented algorithms to mesh both the 2D bounding surfaces and the 3D volumes of the model. This mesh is created automatically from the high level geometric description.
4. Implemented an object-oriented finite element program to perform the analysis. The input to this program is written from the data stored in the geometric model and mesh.
5. Developed a new logarithmic element to ensure accurate solutions near the intersection of the well with a fracture.
6. Implemented 3D post-processing of results.
7. Performed verification of the solution.

Users of Geocrack3D

At this point, Geocrack3D is a research code, nevertheless, response to the code has been positive. Some users include:

1. Geocrack3D has passed an initial evaluation by Shell Technology EP, Rijswijk, (Coumou, 2001) in which the conclusions state "Although Geocrack3D is still being developed, it has proved to be a suitable modeling code for HFR systems." Additional Sultz models are presently being developed by Shell researchers.
2. Geocrack2D and Geocrack3D are being used by the Engineering Geology and Geophysics Research Group, Teknikringen, Sweden, for research in hot-dry-rock geothermal reservoir simulation.

3. The Australian Hot Dry Rock project used Geocrack2D for initial reservoir simulations (Henschke, 2001) and will use Geocrack3D in the future.
4. Geocrack2D was used for analysis of the Hijiori reservoir (Okabe, et al., 2000) and a Geocrack3D is presently being developed.
5. The rock deformation effects provide capability for well test analysis. We have been contacted for use of Geocrack2D for well analysis in the Middle East.

Spin-Off Technology

In addition to the direct focus of the work, this research has resulted in a spin-off application of the technology to develop a pre- and post-processor for the TOUGH2, TETRAD, and STAR programs. This software will be released commercially in 2002.

The new program (PetraSim) builds on the visualization and modeling tools in Geocrack3D. The program can be found at www.thunderheadeng.com.

Future Plans

Based on the positive response, we propose to continue development of Geocrack3D. We are part of a proposal submitted by the Energy & Geoscience Institute at the University of Utah for Enhanced Geothermal Systems research. We will also respond to the Department of Energy request for proposals for University research in geothermal energy.

Collaboration

In this project, we made a significant effort to collaborate with industry and internationally. Some of these are listed below.

Booth at Annual GRC Meetings

One form of interaction with industry was through attendance at the annual Geothermal Resources Council meeting. Kansas State University manned a booth at the 1998, 1999, 2000, and 2001 meetings. This booth allowed us to display Geocrack2D, Geocrack3D, and our other work at Kansas State University.

Participation in Stanford Geothermal Workshops

During the project, we also attended all Stanford Geothermal Workshops and presented the results of our research in papers.

International Collaboration

World Geothermal Congress 2000

Three papers were presented at WGC 2000 in Tohoku, Japan, that used the Geocrack software. The papers were:

"Initial Calculations of Performance for an Australian Hot Dry Rock Reservoir," Prame Chopra, Doone Wyborn, and Daniel Swenson

"Analysis in Preparation for Hijiori Long Term Circulation Test," T. Okabe, K. Kirihara, K. Hayashi, K. Karasawa, D. Swenson, and R. Schroeder

"A 3-D Finite Element Model of Flow in Fractured Reservoirs," B. Hardeman, S. Kulkarni, and D. Swenson

Work with Tohoku University

Professor Takatoshi Ito from the Institute of Fluid Science, Tohoku University, spent most of August, 2000, at Kansas State University, working with us on Geocrack2D and Geocrack3D. He used Geocrack2D to simulate the effect of changes in temperature on permeability of rock. As a result of different thermal expansion coefficients of the minerals in rock, it is hypothesized that microfractures will open as temperatures are changed. He completed initial analyses of this effect.

Murphy Project

The work on Geocrack3D was partially supported as part of the Murphy Project funded by NEDO, Japan, (www.earth.tohoku.ac.jp/Niitsumalab/mte-e.html). The goal is to extract more detailed fracture information from the micro-seismic data and use it to create more detailed models of the reservoir.

Web Site

The Geocrack web site

(www.mne.ksu.edu/~geocrack) provides access to Geocrack3D. It includes 3D example problems and a description of the software.

References

Coumou, D., "Modeling Hot Fractured Rock systems. Case study of Soultz-sous-Forets HFR reservoir," EP 2001-5289, Shell Technology EP, Rijswijk, 2001.

Coumou, D., Harris, C. K., vd Berg, A. P., "Application of Geocrack-2D and -3D to Modeling Thermal Drawdown in the Soultz

Hot Dry Rock System," GRC Annual Meeting, 2001.

Hardeman, B. "A Geometric Modeling Framework for the Analysis of Fractured Rock Volumes." M.S. Thesis, Kansas State University, May, 1998.

Hardeman, B. and D. Swenson, "A Geometric Modeling Framework for the Numerical Analysis of Geothermal Reservoirs," PROCEEDINGS, Twenty-Third Workshop on Geothermal Reservoir Engineering Stanford University, Stanford, California, January 26-28, 1998.

Hardeman, B., Kulkarni, S., and Swenson, D., "A 3-D Finite Element Model of Flow in Fractured Reservoirs," Proceedings of the World Geothermal Congress, Kyushu-Tohoku, Japan, May 28 - June 10, 2000.

Hardeman, Brian, Kulkarni, Sarang, Swenson, Daniel, and James, Mark, "Design of an Object-Oriented Finite Element Framework for Multi-Physics Problems," 5th U.S. National Congress on Computation Mechanics, August 4-6, 1999, University of Colorado, Boulder.

Henschke, Julian, "Modeling of an Australian Hot Dry Rock Reservoir Using Geocrack2D," The Australian National University, Department of Engineering, ENGN4200 – Individual Project, June, 2001.

Kulkarni, Sarang Mukund, "An Object-Oriented 3-D Finite Element Model of Fluid Flow in Fractured Rock," M.S. Thesis, Kansas State University, May, 1999.

Liu, Tan and Swenson, Daniel, "An Effective Logarithmic Finite Element for Flow Near a Well," Twenty-Sixth Workshop on Geothermal Reservoir Engineering, Stanford University, Stanford, California, January 29-31, 2001.

Mizukami and Hughes, "A Petrov-Galerkin Finite Element Method for Convection-Dominated Flows: An Accurate Upwinding Technique for Satisfying the Maximum Principal," *Computer Methods in Applied Mechanics and Engineering*, 50, 181-193, 1985.

Okabe, T., Kirihara, K., Hayashi, K., Karasawa, K., Swenson, D., Schroeder, R., "Analysis in Preparation for Hijiori Long Term Circulation Test," Proceedings of the World Geothermal Congress, Kyushu-Tohoku, Japan, May 28 - June 10, 2000.

Swenson, D. V., 1997, "User's Manual for GEOCRACK: A Coupled Fluid Flow/Heat Transfer, Rock Deformation Program for Analysis of Fluid Flow in Fractured Rock," Mechanical Engineering Department, Kansas State University, Manhattan, KS, 66505, available for download at:
<http://www.mne.ksu.edu/~geocrack>.

FUNDAMENTALS OF STEAM-WATER FLOW IN POROUS MEDIA

Principal Investigator - Roland N. Horne
Stanford Geothermal Program, Stanford University

Collaborating Investigator - Kewen Li
Stanford Geothermal Program, Stanford University

Key Words - water injection; production performance; steam-water flow; relative permeability; capillary pressure.

Project Background and Status

The Stanford Geothermal Program (SGP) is focusing on the understanding of the fluid flow theory that governs geothermal reservoir performance. One of the most important concerns in the geothermal industry in recent years is reservoir decline. Injection of condensate and waste water in geothermal reservoirs is an important and practical solution. Accordingly, SGP has been investigating the problems related to liquid injection into geothermal reservoirs. The research has also focused on the estimation of recoverable reserves in geothermal reservoirs by developing methods of decline curve analysis based on fluid flow theory. SGP completed the projects that planned in the previous fiscal year.

Project Objectives

The main objective is to improve the ability of engineers and scientists to forecast the future performance of geothermal reservoirs. By understanding the production characteristics, development decisions can be made sooner and with greater certainty. This will result in more efficient utilization of the geothermal energy resource. Another objective is to provide engineers and scientists direct methods to estimate the energy production rate of geothermal reservoirs and practical models of steam-water flow properties, including steam-water relative permeability and capillary pressure models.

Approaches

The Stanford Geothermal Program uses both theoretical and experimental approaches to conduct the research. We use numerical simulation for modeling work and we use an X-ray CT scanner as one of our main experimental tools to measure in-situ water saturation and its distribution. We also design and construct purpose-built apparatus to conduct the experiments needed.

Research Results

SGP completed the projects that were planned in the previous fiscal year. The main accomplishments are as follows:

Decline Curve Analysis Method Based on Fluid Flow Mechanisms

As pointed out by Raghavan (1993), "Until the 1970s, decline curve analysis was considered to be a convenient empirical procedure for analyzing performance; no particular significance was to be attributed to the values of D_i and b . To an extent this is still true even today."

To this end, an analytical decline curve analysis model was developed based on the theory of fluid flow mechanisms with relative permeability, capillary pressure, and gravity included. We avoided the empiricism in the papers by Arps (1945) and by Fetkovich (1980). The model reveals a linear relationship between the production rate and the reciprocal of the cumulative production. The present work developed the theoretical significance for the two constants describing the decline rate (although actually these are not the same parameters as D_i and b).

We applied the model to the production data of over 20 production wells in The Geysers geothermal field and found a linear relationship between the production rate and the reciprocal of the cumulative production for most of the wells, especially at the late period of production. An example of the application is shown in Fig. 4.1.1. This implies that we may be able to estimate the reservoir properties and the reserves.

Wettability of Geothermal Fluid-Rock Systems

Wettability of geothermal systems is one of the important parameters governing the efficiency of water injection. The more the rock is water wet, the more the water can be imbibed and the greater the water injection efficiency. The wettability in

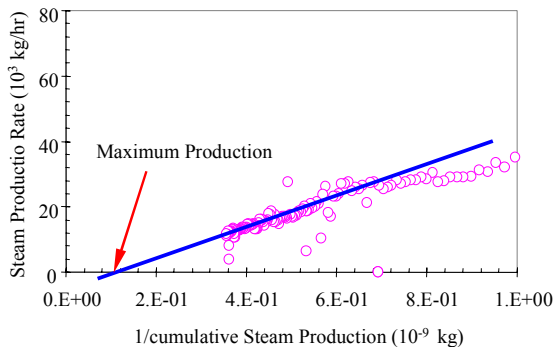


Figure 1. Relationship between the steam production rate and the reciprocal of the accumulative steam production (Well 1).

different gas-liquid-rock systems may not be the same (as is often assumed). However, few approaches are available to evaluate the wettability in gas-liquid-rock systems. For this purpose, a method was developed to infer the wettability of steam-water-rock systems based on the relationship between permeability and capillary pressure by Purcell (1949). The Purcell model was extended to two-phase flow to verify whether the wettability is a function of water saturation. The results calculated using the experimental data showed that the wettability index in drainage was greater than that in imbibition, which has been proven experimentally. Both the receding (drainage) and advancing (imbibition) contact angles in steam-water-rock systems were reasonably independent of water saturation ranging from about 25 to 85%. It was also found that the wettability model could be reduced to the model reported by Slobod and Blum (1952) in specific cases. The method developed in this study to estimate wettability of steam-water-rock systems could be applied directly to other gas-liquid-rock and liquid-liquid-rock systems.

Figure 2 shows the values of the wettability index of steam-water-rock systems in both drainage and imbibition calculated using our model.

We may be able to determine where the water should be injected in geothermal reservoirs once the distribution of the wettability index is available. We may also be able to explain why water injection yields greater increase of energy production in some reservoirs but not in others.

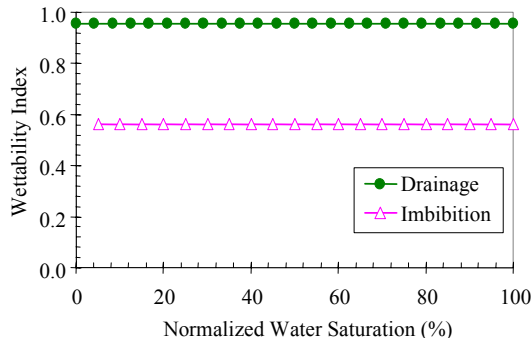


Figure 2. Wettability indices calculated using the experimental data from Li and Horne (2001) and Mahiya (1999).

Steam-Water Relative Permeability from Capillary Pressure Data

Steam-water relative permeability plays important role in controlling reservoir performance for water injection into geothermal reservoirs. However, it is very difficult to measure steam-water relative permeability due to the phase transformation and the significant mass transfer between the two phases as pressure changes. It would be helpful for reservoir engineers to be able to calculate steam-water relative permeability once steam-water capillary pressure is available.

Various capillary pressure approaches were used to calculate steam-water relative permeabilities using the measured data of steam-water capillary pressure in both drainage and imbibition processes. The calculated results were compared to the experimental data of steam-water relative permeability measured in sandstone core samples. The steam-water relative permeability and capillary pressure were measured simultaneously. The differences between the Purcell model (1949) and the measured values were almost negligible for water phase relative permeability in both drainage and imbibition but not for the steam phase. The lack of significance of the effect of tortuosity on the wetting phase was revealed. A physical model was developed to explain the insignificance of the tortuosity. Steam phase relative permeabilities calculated by other models were very close to the experimental values for drainage but very different for imbibition as expected. The same calculation was made for nitrogen-water flow to confirm the observation in steam-water flow. The results showed that it would be possible and useful to calculate steam-water relative permeability using the capillary pressure method, especially for the drainage case. One of the comparisons between

calculated and measured steam-water relative permeabilities is shown in Figure 3.

The general conclusion based on this study was that the Purcell model (1949) can be used to calculate the water phase relative permeability and the Corey model (1954) can be used to calculate the steam phase relative permeability.

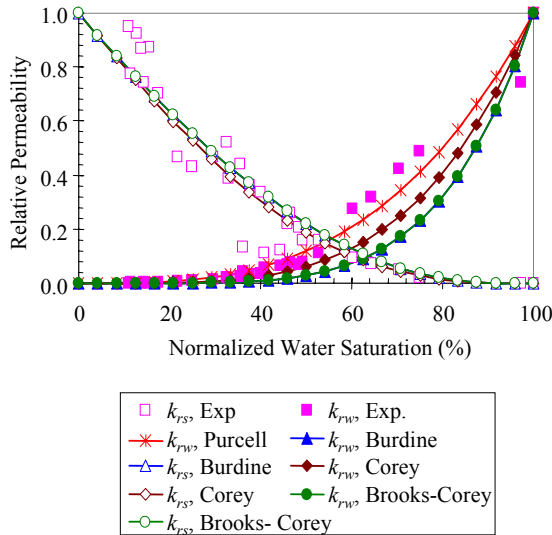


Figure 3. Calculated steam-water relative permeability and the comparison to the experimental data in the drainage case.

Water Injection into Geothermal Reservoirs

Water injection has proven to be a successful engineering technique to maintain reservoir pressure in geothermal reservoirs and to sustain well productivity. However, many questions related to water injection into geothermal reservoirs still remain unclear. For example, how the in-situ water saturation changes with reservoir pressure and temperature, and the reservoir pressure influences well productivity. To answer these questions, we studied the effects of temperature and pressure on the in-situ water saturation in a core sample using an apparatus developed for the purpose. The in-situ water saturation decreases very sharply near the saturation pressure but not to the residual water saturation. When the mean pressure in the core sample decreases further, the in-situ water saturation decreases sharply again to the residual water saturation at a pressure much less than the saturation pressure. This demonstrated the significant effects of steam-water capillary pressure and physical adsorption on the in-situ water saturation.

Also investigated were the effects of pressure on the well productivity index (see Figure 4 as an example). The well productivity increased with an increase of mean reservoir pressure within a certain range and then decreased. The well productivity reached the maximum value at a pressure close to the saturation pressure. The results of this study should be useful to evaluate projects such as the waste water injection scheme at The Geysers.

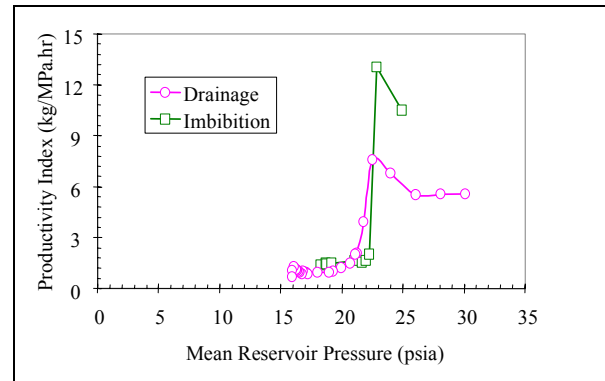


Figure 4. Effect of reservoir pressure on the productivity index.

Relative Permeability in Fractures

The mechanism of two-phase flow through fractures exerts an important influence on the behavior of geothermal reservoirs. Currently, two-phase flow through fractures is still poorly understood. In this study, nitrogen-water experiments were conducted in both smooth- and rough-walled fractures to determine the governing flow mechanisms. The experiments were done using a glass plate to allow visualization of flow. Digital video recording allowed instantaneous measurement of pressure, flow rate and saturation. Saturation was computed using image analysis techniques. The experiments showed that the gas and liquid phases flow through fractures in nonuniform separate channels (see Figure 5).



Figure 5. Examples of gas-water flow channels.

The data from the experiments were analyzed using Darcy's law and using the concept of friction factor and equivalent Reynold's number for two-phase flow. For both smooth- and rough-walled fractures a clear relationship between relative permeability and saturation was seen. The calculated relative permeability curves follow Corey-type behavior, as shown in Figure 6. The sum of the relative permeabilities of the two phases is not equal to one, indicating phase interference. The equivalent homogenous single-phase approach did not give satisfactory representation of flow through fractures. The graphs of experimentally derived friction factor with the modified Reynold's number do not reveal a distinctive linear relationship.

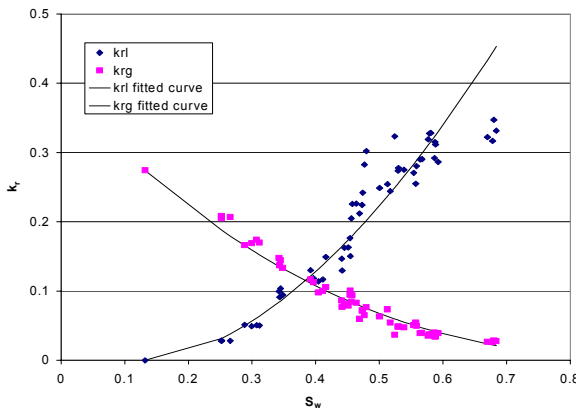


Figure 6. Drainage relative permeability curves in a rough-walled fracture.

Constant-Pressure Measurement of Steam-Water Relative Permeability

A series of steady-state experiments established the relative permeability curves for two-phase flow of water in a porous medium. These experiments have minimized uncertainty in pressure, heat loss, and saturation. By maintaining a constant pressure gradient, the experiments have provided a baseline from which to determine the effect of temperature on relative permeability. The experimental data of steam-water relative permeability from this study and the comparison to the published data are shown in Figure 7.

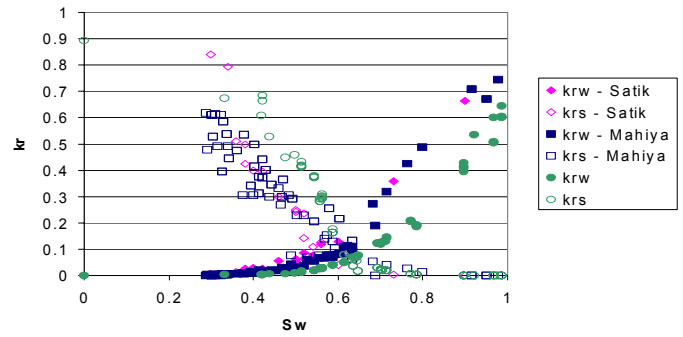


Figure 7. Comparison of results with previous experiments.

Summary

1. Eight papers and two major reports were published in the last fiscal year.
2. Four graduates and one research associate were funded; two students graduated from the Stanford Geothermal Program and obtained the M.S. degree, with two more still working on their degrees.
3. Three different sets of laboratory apparatus were developed.

Future Plans

Our future research plans are addressed as follows:

1. Application of the analytical decline curve analysis method in geothermal reservoirs.
2. Scaling of experimental data of spontaneous water imbibition.
3. Measurement of steam-water relative permeability through fractures.
4. Effect of initial water saturation on spontaneous water imbibition.
5. Development of apparatus and techniques to measure relative permeability in extremely low permeable geothermal rocks.

Major Papers Published in Fiscal Year

Li, K., Nassori, H., and Horne, R.N.: "Experimental Study of Water Injection into Geothermal Reservoirs," proceedings of the GRC 2001 annual meeting, August 26-29, 2001, San Diego, USA; *GRC Trans.* V. 25 (2001).

- Li, K. and Horne, R.N.: "An Experimental Method of Measuring Steam-Water and Air-Water Capillary Pressures," proceedings of the Petroleum Society's Canadian International Petroleum Conference 2001, Calgary, Alberta, Canada, June 12 – 14, 2001.
- Li, K. and Horne, R.N.: "Steam-Water Relative Permeability by the Capillary Pressure Method," proceedings of the International Symposium of the Society of Core Analysts, Edinburgh, UK, September 17-19, 2001.
- Li, K. and Horne, R.N.: "Differences between Steam-Water and Air-Water Capillary Pressures," presented at the 26th Stanford Workshop on Geothermal Reservoir Engineering, Stanford University, Stanford, CA 94043, USA, January 29-31, 2001.
- Li, K. and Horne, R.N.: "Gas Slippage in Two-Phase Flow and the Effect of Temperature," SPE 68778, presented at the 2001 SPE Western Region Meeting, Bakersfield, CA, USA, March 26-30, 2001.
- Li, K. and Horne, R.N.: "Wettability Determination of Geothermal Systems," presented at the 27th Stanford Workshop on Geothermal Reservoir Engineering, Stanford University, Stanford, CA 94043, USA, January 28-30, 2002.
- Li, K. and Horne, R.N.: "An Experimental and Theoretical Study of Steam-Water Capillary Pressure," *SPEREE* (December 2001), p.477-482.
- Li, K. and Horne, R.N.: "Characterization of Spontaneous Water Imbibition into Gas-Saturated Rocks," *SPEJ* (December 2001), p.375-384.
- Corey, A. T.: "The Interrelation between Gas and Oil Relative Permeabilities", *Prod. Mon.*, (1954), 19, 38.
- Fetkovich, M.J.: "Decline Curve Analysis Using Type Curves," *JPT* (June. 1980) 1065-1077.
- Li, K. and Horne, R.N.: "An Experimental and Theoretical Study of Steam-Water Capillary Pressure," *SPEREE* (December 2001), p.477-482.
- Mahiya, G.F.: "Experimental Measurement of Steam-Water Relative Permeability," MS report, Stanford University, Stanford, CA, USA, 1999.
- Purcell, W.R.: "Capillary Pressures-Their Measurement Using Mercury and the Calculation of Permeability", *Trans. AIME*, (1949), 186, 39.
- Raghavan, R.: *Well Test Analysis*, PTR Prentice Hall, 1993, p.519.
- Satik, C., "A Measurement of Steam-Water Relative Permeability," Proceedings of 23rd Workshop on Geothermal Reservoir Engineering, Stanford University, Stanford, California (1998).
- Slobod, R.L. and Blum, H.A.: "Method for Determining Wettability of Reservoir Rocks", *Trans. AIME*, (1952), 195, 1.

Major Reports Published in Fiscal Year

- Diomampo, G.P.: "Relative Permeability Through Fractures," June 2001.
- O'Connor, P.A.: "Constant-Pressure Measurement of Steam-Water Relative Permeability Through Fractures," June 2001.

References

- Arps, J.J.: "Analysis of Decline Curves," *Trans. AIME* (Dec. 1945) 160, 228-247.

A GEOCHEMICAL AND MICROANALYTICAL STUDY OF SILICA SCALE DEPOSITION IN GEOTHERMAL BRINES

U.S. DEPARTMENT OF ENERGY, GEOTHERMAL ENERGY PROGRAM

Principal Investigators - Peter J. Heaney

Organization: The Pennsylvania State University

Address: Dept. of Geosciences, Deike Bldg., University Park, PA 16802

Email: heaney@geosc.psu.edu

Collaborating Investigator - Susan L. Brantley

Organization: The Pennsylvania State University

Address: Dept. of Geosciences, Deike Bldg., University Park, PA 16802

Email: brantley@geosc.psu.edu

Key Words - silica scale, hydrothermal brines, nanocolloidal silica

Project Background and Status

The tendency of siliceous sinters to precipitate from geothermal fluids presents both industrial and environmental challenges. The deposition of silica scale on metal surfaces leads to the clogging of re-injection pipes and the corruption of fluid handling equipment (Axtmann, 1976). If uncorrected, the precipitation of the silica-rich scales can necessitate the costly extraction and replacement of pipes, wellheads, and other processing components. In brines of especially high ionic strength, uncontrolled deposition can be extreme; Salton Sea fluids, for example, may precipitate silica scale in excess of 50 cm yr⁻¹ (Gallup, 1989). Moreover, if fluids are re-injected into the ground rock after their withdrawal, silica precipitation may diminish the porosity of the reservoir, thereby degrading the flow characteristics of the field. As silica deposition concentrates heavy metal ions into the solid phase, disposal of silica scales in an environmentally acceptable fashion also can prove problematic.

We have completed a series of baseline experiments using a model brine solution in which we monitored the evolution of colloidal silica and silica precipitate. These results will serve as a reference for our current investigations of silica coagulation in the presence of scale inhibitors. By comparing the behavior of dissolved silica in the presence and in the absence of inhibitors, we will be able to determine the mechanisms by which the inhibitors operate and to suggest new approaches for scale inhibition.

Project Objectives

The overarching question that we are addressing for this project is as follows:

What factors control the condensation of colloidal silica to form amorphous precipitates in geothermal brines?

Researchers have proposed a number of hypotheses to account for the coagulation of silica polymers and the resultant formation of silica gels in aqueous fluids of high ionic strength. Hypotheses have included: 1) a lowered activity of the water component in brines due to electrolyte hydration (Marshall and Warakowski 1980); 2) a decrease in the "shielding" of the silica surface by water molecules in response to surface dehydration at neutral to high pH (Matijevic 1973); 3) an increase in the effective zpc of silica due to the incorporation of metal cations in the surfaces of silica colloids (Yokoyama et al. 1993); and 4) interparticle coagulation based on the inner-sphere bonding of sorbed metal cations (Yates et al. 1998).

In collaboration with research scientists from the Geothermal and Power Operations Division of the Unocal Corporation, we are performing experiments that will allow us to test these hypotheses. Specifically, we will examine individual steps in the reaction sequence by which monomeric silica transforms to amorphous opal. By separating this reaction pathway into discrete events, we will be able to monitor with high specificity the interactions between aqueous silica with dissolved metal ions of interest. Once the nature of these sub-reactions is established, geothermal industries will be able to inhibit the formation of scale by targeting those factors that induce coagulation with precision.

Approach

We are approaching the formation of silica scale by a combination of exhaustive wet-chemical

analytical assays that can distinguish monomeric and polymeric silica and by novel chromatographic methods that we have helped to develop. The chemical parameters of our experiments were designed with the participation of Dr. Darrell L. Gallup, a Consulting Chemist with the Unocal Corporation, and the fluids are based on brine compositions from the Salton Sea Known Geothermal Resource Area (SSKGRA) in southern California's Imperial Valley, a site with 10 generating plants and a 330 MW net capacity.

Using the Salton Sea Brine composition (4598 ppm Na⁺, 978 ppm K⁺, 200 ppm Ca²⁺, 8330 ppm Cl⁻, 45 ppm HCO₃⁻), we are systematically exploring the effects of time, pH, ionic strength, and initial silica concentration on the deposition of silica precipitates. Silica solutions with initial concentrations of 250, 750, and 1250 mg/L silica (SiO₂) were prepared from pH 3 to pH 11 and with ionic strengths of 0.015 and 0.24. Silica concentrations of 250, 750, and 1250 mg/L SiO₂ were chosen for these experiments because they encompass the range of concentrations observed in hydrothermal fluids at the geothermal sites of interest to the Unocal Corporation. Values of pH include 3, 4, 5, 6, 7, 9, and 11. Silica sols exhibit maximum stability between pH 2 and 3. Above pH values of 11, silica becomes extremely soluble. Between these pH limits, silica coagulates most rapidly.

Results

Nanocolloidal Silica Characterization

We have tested ultrafiltration and developed other techniques for sizing nanocolloids. In our previous efforts to size silica colloids using calibrated gel filtration chromatography (GFC), we observed that the first colloids to appear in solutions containing 500 to 1000 mg/kg silica at pH 7 for both low (0.005 M) and relatively high (0.24 M) ionic strengths measured 20 to 40 kD. We determined that these weights correspond to sizes of 3 to 4 nm for these incipient colloids, and we confirmed these results by light scattering, atomic force microscopy (AFM), and transmission electron microscopy (TEM).

Wet Chemical Experiments

Typical results from our wet chemical baseline analyses of the concentrations of monomeric silicic acid, nanocolloidal silica, and silica precipitate are presented in Figure 1. These results yield the following insights:

1) For all silica concentrations and ionic strengths, the deposition of precipitate is extremely dependent on solution pH. The sensitivity is slightly less pronounced with higher ionic strength, but, in all cases, reaction rates are maximized between pH 5 and 7 and markedly lower outside this range.

2) Relatively small increases in silica concentration and in ionic strength can dramatically enhance the deposition of silica scale. Whereas no precipitate appears over several months in 0.015 M solutions with 250 mg/L silica, the deposition of scale occurs over hours when ionic strength is 0.25 M or silica concentrations are 1250 mg/L.

3) Nanocolloidal silica consistently appears as an intermediate reaction product. Even in solutions that deposit silica precipitate within hours, a transient nanocolloidal population can be detected.

Our initial studies of the effects of a sulfite inhibitor (50 mg/L) on the nucleation and precipitation of nanocolloidal silica (Fig. 2) lead to the following conclusions:

1) The magnitude of the sulfite inhibition of silica precipitation is strongly dependant on the pH of the solution. Sulfite is more effective at inhibiting precipitation at pH values of 5 and below.

2) The magnitude of sulfite inhibition on silica precipitation is strongly dependant on the initial concentration of silica. Sulfite is less effective at inhibiting silica precipitation at higher concentrations than at lower concentrations.

3) Monomeric and nanocolloidal silica fractions were stabilized by sulfite in all solutions.

Planned FY 2002 Milestones

The major goals for the coming year are as follows:

1) Inhibition of silica polymerization by carboxylic acids. Silica solutions with concentrations of 250, 750, and 1250 mg/L ppm silica will be prepared as standard Unocal brines with EDTA, acetic acid, and citric acid. Polymer evolution will be assayed by wet chemical analysis and ICP-AES to ascertain the stages of polymerization that are interrupted by these inhibitors. 2) Titration of coagulated silica solutions. Solutions with concentrations of 2000 mg/L silica will be prepared and allowed to achieve steady state monomer/polymer concentrations. A suite of Groups I and II and transition metal cations will be added to these solutions in a range of concentrations to determine CCCs.

Technology Transfer/Collaborations

The Geothermal and Power Operations Division of the Unocal Corporation has sponsored basic and applied research on the formation of silica scale for 23 years. In 1996, Unocal awarded a 2-year grant to one of the principal investigators (Heaney) to investigate the feasibility of soft-gel chromatography for geothermal fluid analysis. This grant provided half-support for a postdoctoral scholar (Dr. Douglas M. Yates), who refined the technique and performed a series of experiments in conjunction with Unocal. Results of this work have been presented at national meetings (Yates and Heaney 1997, 1999; Heaney and Yates 1997, 1998) and in written and oral Final Reports to Unocal.

For this DOE-sponsored project, we are maintaining our strong partnership with Unocal. As noted above, we are studying brine compositions specified by Unocal, and we are performing research along avenues developed in collaboration with research scientists at Unocal, particularly Drs. Darrell L. Gallup and Philip A. Molling. None of our research results are proprietary. The DOE grant supports one undergraduate student and one postdoctoral researcher. The postdoctoral researcher, Dr. Gary Icopini, has presented our initial colloidal sizing data at the 11th Annual Goldschmidt Symposium in May 2001 (Icopini et al. 2001), and shortly we will be submitting two papers on our work to date to *Geochimica et Cosmochimica Acta* and to *Geothermics*.

References

Axtmann, R.C. (1976) Chemical aspects of the environmental impact of geothermal power. Proceedings, Second United Nations Symposium on the Development and Use of Geothermal Resources, San Francisco, vol. 2, 1323-1327.

Chan, S.H. (1989) A review on solubility and polymerization of silica. *Geothermics*, 18, 49-56.

Crerar, D.A., Axtmann, E.V., and Axtmann, R.C. (1981) Growth and ripening of silica polymers in aqueous solutions. *Geochimica et Cosmochimica Acta*, 45, 1259-1266.

Darragh, P.J., Gaskin, A.J., and Sanders, J.V. (1976) Opals. *Scientific American*, 234, 84-95.

Gallup, D. L. (1989) Iron silicate scale formation and inhibition at the Salton Sea geothermal field. *Geothermics*, 18, 97-103.

Gallup, D. L. (1997) The interaction of silicic acid with sulfurous acid scale inhibitor. *Geothermal Resources Council Transactions*, 21, 49-53.

Gallup, D. L. (1998) Aluminum silicate scale formation and inhibition (2): scale solubilities and laboratory and field inhibition tests. *Geothermics*, 27, 485-501.

Heaney P.J. and Yates, D.M. (1997) Sorption of polymeric silica to cellulose: Mechanism for wood fossilization. *Eos*, F738.

Heaney P.J. and Yates D.M. (1998) Adsorption of toxic metal cations to aqueous polymeric silica. IMA abstracts, A46.

Icopini, G., Heaney, P.J., Mellott, N.P., Brantley, S.L., and Yates, D.M. (2001) Sizing silica nanocolloids: A comparison of gel filtration chromatography with diffraction and imaging methods. Abstracts, Eleventh Annual Goldschmidt Conference, May 2001.

Iler, R.K. (1979) *The Chemistry of Silica: Solubility, Polymerization, Colloid and Surface Properties, and Biochemistry*. John Wiley, New York.

Marshall, W.L. and Warakowski, J.M. (1980) Amorphous silica solubilities -- II. Effect of aqueous salt solutions at 25°C. *Geochimica et Cosmochimica Acta*, 44, 915-924.

Matijevic, E. (1973) Colloid stability and complex chemistry. *Journal of Colloid and Interface Chemistry*, 43, 217-245.

Tarutani, T. (1970) Chromatographic behavior of silicic acid on Sephadex columns. *Journal of Chromatography*, 50, 523-526.

Thomas, D.M. and Gudmundsson, J.S. (1989) Research directions in solids deposition in geothermal systems. *Geothermics*, 18, 337-341.

Weres, O. and Tsao, L. (1981) Chemistry of silica in Cerro Prieto brines. *Geothermics*, 10, 255-276.

Yates, D.M. and Heaney, P.J. (1997) Polymerization of silica in solution: Mechanism for the formation of amorphous silica. *Eos*, 78, F834.

Yates, D.M. and Heaney, P.J. (1999) Comparison of size-exclusion chromatographic gels for the characterization of polymeric silica. Abstracts, Ninth Annual Goldschmidt Conference, 334.

Yates, D.M., Joyce, K.J., and Heaney, P.J. (1998)
Complexation of copper with polymeric silica
in aqueous solution. *Applied Geochemistry*,
13, 235-241.

Yokoyama, T., Sato, Y., Maeda, Y., Tarutani, T.
and Itoi, R. (1993) Siliceous deposits formed
from geothermal water. I. The major
constituents and the existing states of iron and
aluminum. *Journal of Geochemistry*, 27,
375-384.

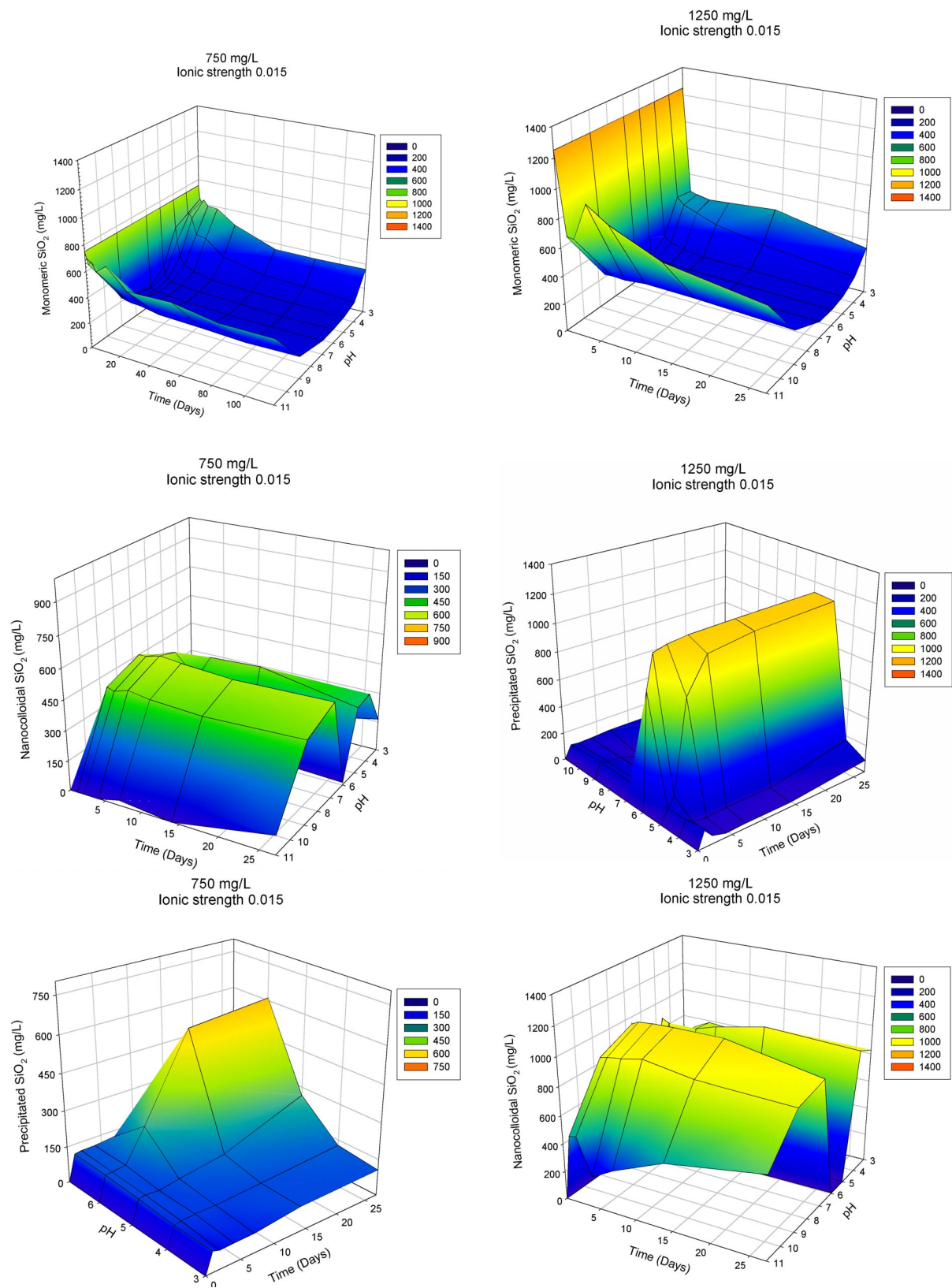


Figure 1. Variation of monomeric, nanocolloidal, and solid silica concentrations as a function of time and pH for solutions of low ionic strength (0.015 M) and an initial concentration of 750 and 1250 mg/L SiO₂.

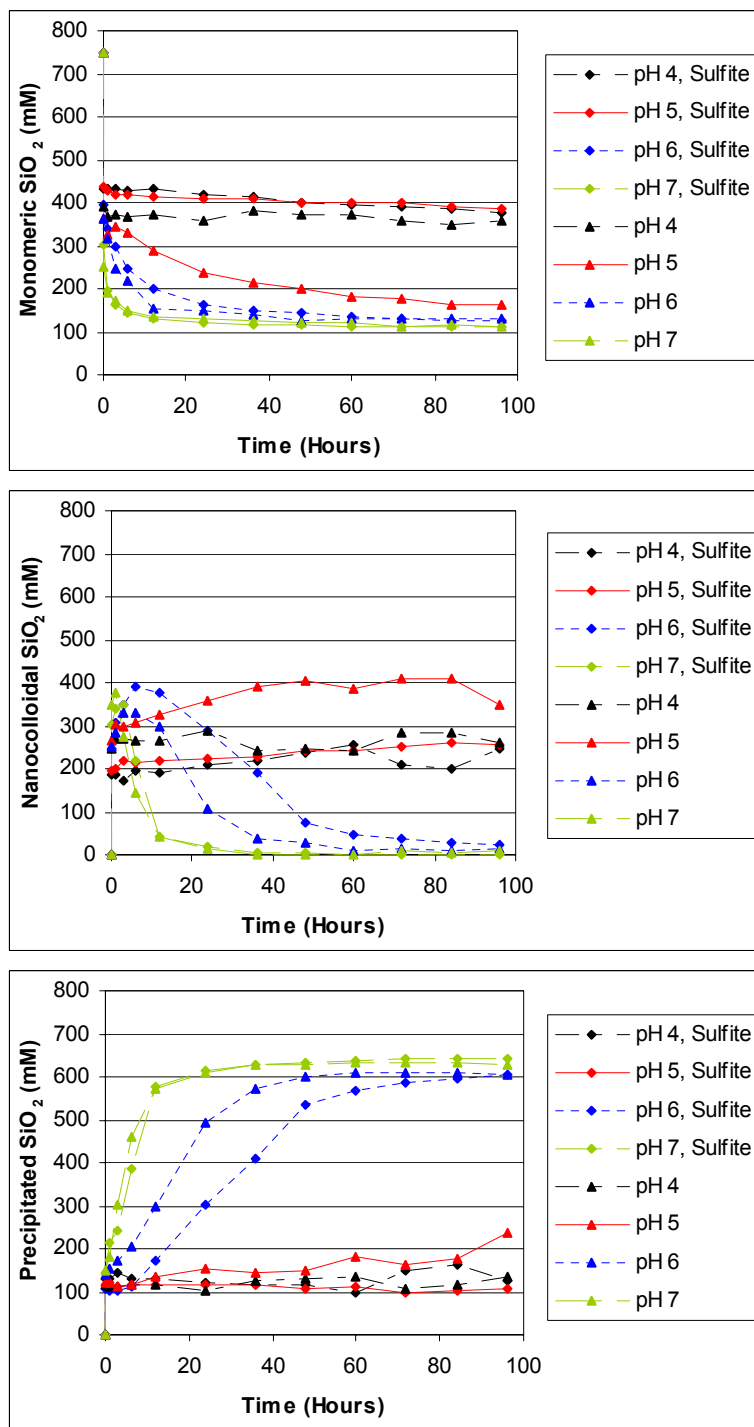


Figure 2. Variation of monomeric, nanocolloidal, and solid silica concentrations as a function of time and pH for solutions of high ionic strength (0.24 M) and an initial concentration of 750 mg/L SiO₂. The diamonds indicate solutions to which 50 mg/L sulfite was added to the simulated brine.

TRACING GEOTHERMAL FLUIDS: TWO-PHASE TRACER DEVELOPMENT

Principal Investigator - Michael C. Adams

Energy & Geoscience Institute

423 Wakara Way, Suite 300, Salt Lake City UT 84108

madams@egi.utah.edu

Key Words - Tracers, Vapor-Phase Tracers, Two-phase tracers, Geysers, Fluorinated alcohols, Hydrofluorocarbons

Abstract

The development of geothermal tracers is a vital component of geothermal research. Industry uses these compounds to maximize power production from geothermal fields. All of the tracers currently in use have been developed at EGI. These tracers are designed to tag either steam or liquid. Research under the current contract is focused on developing two-phase tracers, which will be used to trace both steam and liquid. Candidate compounds have been chosen and appear to be thermally stable. The detection limit and acidity of these compounds still needs to be determined.

Project Background and Status

Geothermal Tracers

Tremendous volumes of water are cycled through any power plant that produces electrical power from geothermal water. This water must be injected back into the reservoir to maintain power production and avoid contamination of local groundwater. Injection can dramatically increase the number of years that power can be produced from a geothermal field. The direction and rate of the injectate must be controlled so that it provides fluid recharge but does not cool the fluid that is being produced from the wells. Tracers are the only method of tracking the speed and pathways of the injected water. Before 1983, when the DOE-sponsorship of injection research began, few tracers were available to the industry (Adams, 1985). Since 1983, research performed at EGI has defined the stability and use of the tracers fluorescein (Adams et al., 1989; Adams and Davis, 1991), rhodamine WT (Rose and Adams, 1994), and many aromatic acids (Adams et al., 1992). Dr. Peter Rose has extended this research to the development of the very stable naphthalene sulfonates under a separate DOE contract to EGI (e.g., Rose et al., 2001).

Vapor-Phase Tracers

Research under this contract has branched to the development of tracers that are capable of following steam and/or liquid water. In 1989 the operators at The Geysers asked DOE for research that would help them stem reservoir pressure decline and maintain production from this important resource.

Tracers were specifically called out. Several CFC gas tracers were quickly developed by us (Adams et al., 1991b) and deployed at The Geysers. (Adams et al., 1991a). From 1991 to 1997, several tests were performed with one of these gas tracers, R-13 (Beall et al., 1994). When production of the chlorofluorocarbon R-13 was cut back because of international agreements to alleviate ozone depletion, two hydrofluorocarbons, R-134a and R-23, were chosen to replace it (Beall et al., 1998; Adams, 1999). Since their introduction, both R-134a and R-23 have been used in multiple tracer tests to quantify the benefits of injecting water from Clear Lake and Lake County effluent into the reservoir at The Geysers (Goyal, 1999).

Vapor-phase tracers are much more soluble in the steam than the liquid phase. This is a necessary attribute that allows the tracers to track the steam through the reservoir. This increased volatility makes vapor-phase tracer tests more difficult to design and interpret than liquid-phase tests (Adams et al., 2001). The primary effect of the high volatility is that steam is the only phase that comes out of the production wells, but liquid water is only phase injected back into the reservoir. Therefore, vapor-phase tracers, which are sparingly soluble as a consequence of their high volatility, must be injected at low concentrations. When the injection water reaches boiling temperature in the reservoir, the tracers immediately transfer into the steam phase. Very little is left in the residual water to track it to its ultimate destination. A secondary effect of the high volatility is that different tracers enter the steam phase at different rates. The rate for each compound depends on its solubility, which vary considerably from compound to compound (Fig. 1). Consequently, the decay rate of vapor-phase tracers cannot be used to define pre-decay concentrations or any temperature parameters of the flow path, because there is no index compound to compare them to. This situation creates a solubility-dependent ratio in production steam of any two volatile tracers that were simultaneously injected. This has been detected in two tests conducted at The Geysers, in which tritiated water was injected simultaneously with a vapor-phase tracer (Adams, 1999).

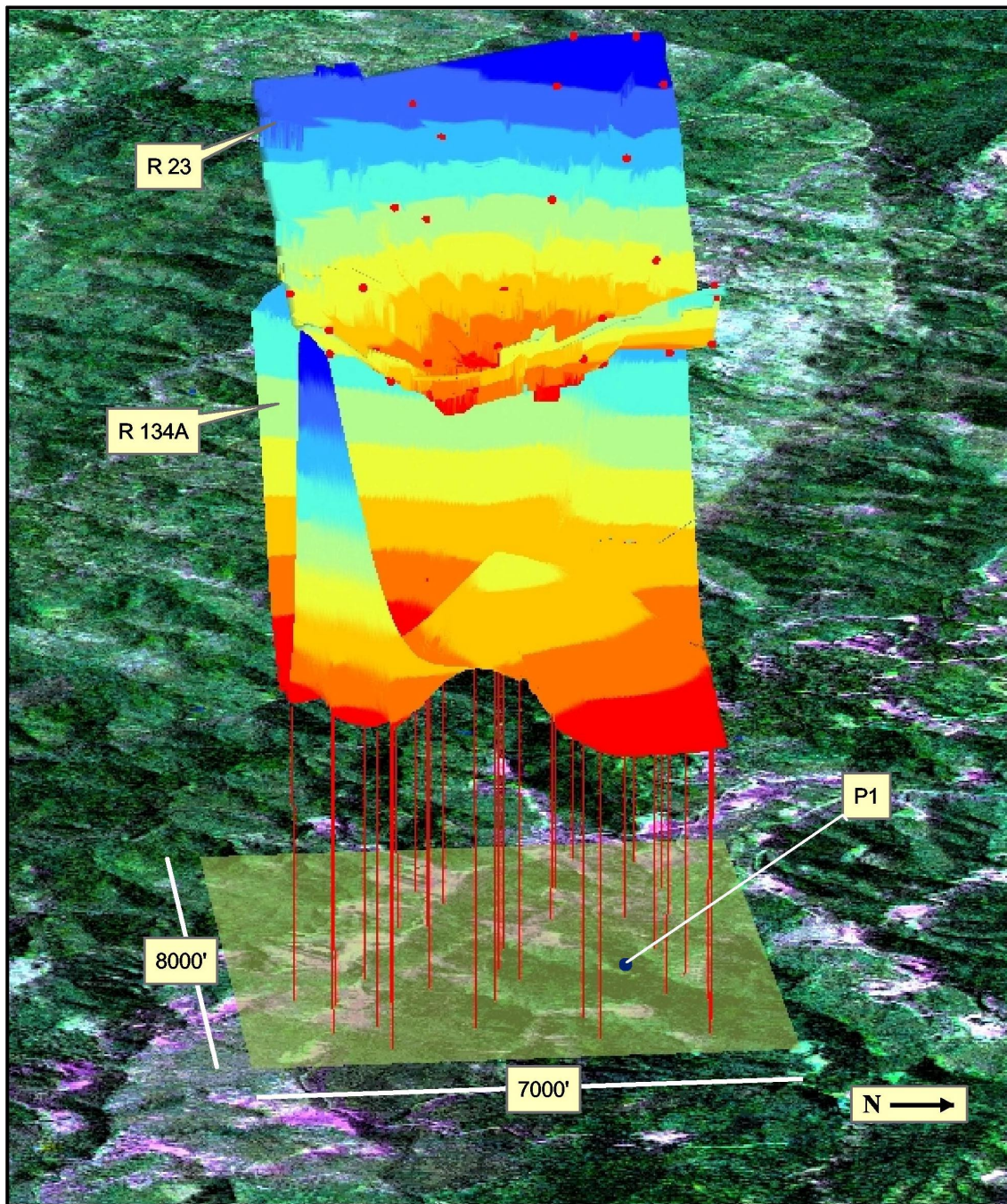


Figure 7. Results of one day of the P-1 tracer test at The Geysers in which two different tracers, R-134a and R-23, were used.. The colored surfaces represent the concentrations of the tracers in a logarithmic scale. Blue is the highest concentration, red the lowest. The surfaces are overlain on a satellite photograph of The Geysers. The locations of wells involved in the test are shown by the vertical lines and the dots on the upper surface.

Because of their volatility, vapor-phase tracers do not always follow the same path as the majority of the injected water. For example, Adams et al. (1999) has shown that in one tracer tests the vapor-phase tracers had a different geographic distribution than the tritium tracer, even though the two tracers were simultaneously injected. Calculations of injectate recovery using the two different tracers differ when this situation occurs. This is an important consideration, one that will become increasingly relevant as the amount of injection increases due to the Lake and Sonoma County pipelines. It should be noted, however, that the path of the vapor-phase tracers and the bulk of the injection-derived steam coincide in many cases (Adams et al., 1991a; Beall et al., 1994; Adams, 1999).

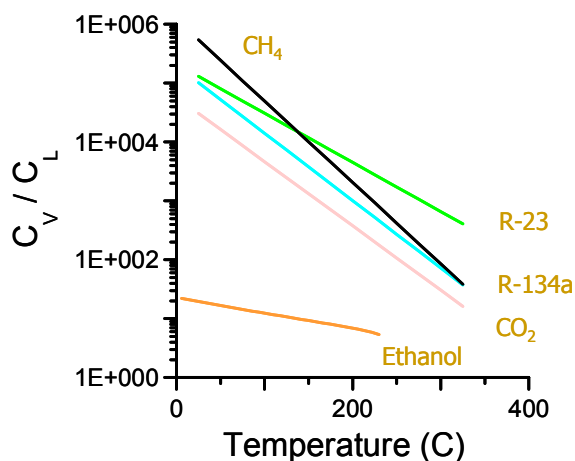


Figure 8. Solubility of some vapor-phase tracers in steam. C_v = concentration in steam, C_L = concentration in liquid. Ethanol, a two-phase tracer, has a much lower solubility in steam and thus will stay with the water much longer during a tracer test.

A tracer with significant solubility in water but which volatilizes at a rate near that of water can be termed a two-phase tracer (water and steam) (e.g., ethanol in Fig. 2). Our initial investigations indicate that alcohols have the most potential for use as two-phase tracers. They have significant solubility in both the liquid and steam phases and appear to be relatively stable at geothermal temperatures. Alcohols, especially ethanol, have low toxicity. The Threshold Limit Value for ethanol, which is an OSHA standard for continuous exposure, is 1000 ppm in the vapor phase (ACGIH, 1979). Under most circumstances the human body can eliminate ethyl alcohol at the same rate that it is absorbed (Lester and Greenberg, 1951).

Alcohols were also chosen because of their low acid dissociation constant. This implies that the compound will not ionize until the pH of the water is quite high. This is important because water can get quite basic when it boils, due to the loss of carbon dioxide. This is a strong limitation on the type of compound that will be suitable as a two-phase tracer. For example, organic acids can be quite stable but they are ionized at the pH typical of a geothermal reservoir.

To date we have tested several alcohol-water solutions in our pressurized autoclaves at temperatures of up to 320°C for periods ranging up to one month (Adams, 1995). The results display an inverse relationship between the thermal stability of straight-chain alcohols and the number of carbons in the molecule. The one branched alcohol tested, isopropanol, decayed rapidly at temperatures as low as 240°C. Isopropanol was also detected as a decay product of n-propanol. The rapid reaction of isopropanol and its shallow temperature dependence imply that the decay of secondary alcohols will reach equilibrium within the time span of a tracer test, and should not be used as tracers. Decay of the straight-chain alcohols, in contrast, are kinetically controlled and can be used as tracers, especially in moderate-temperature systems such as The Geysers.

However, the alcohols by themselves are very difficult to use in the field because they have no properties that make them strongly detectable. We believe that the addition of fluorine to the alcohols would provide a much lower detection limit. For instance, some of the detection techniques developed for use with the hydrofluorocarbons that we developed for use at The Geysers might be used to analyze fluorine-containing molecules at extremely low levels (Adams, 1999). Therefore, we are currently examining the potential of fluorinated alcohols as two-phase tracers.

Project Objectives

The overall objective of this research is to develop tracers that will help increase and maintain the power production of geothermal systems through injection management. Specifically, our objectives are to:

- 1) Identify a class of compounds with the desired properties of a two-phase tracer.
- 2) Select several members of this class and test them in the laboratory.
- 3) Perform a field test at The Geysers.
- 4) Transfer the technology to industry.

Approach

The first task was to identify the necessary or desired properties of a two-phase tracer. These include stability, toxicity, detection limit, solubility, volatility, acidity, and cost. The criteria were:

- 1) Stability – The compounds should be stable in a simple water-tracer system for 50 days at 240°C. If they decay, they should follow a first-order rate law and decay no more than 20%.
- 2) Toxicity – Compounds with specific toxicity will not be considered. Compounds labeled as irritants will be considered.
- 3) Good detection limit – Detection limits should be in the parts per trillion range. The search for two-phase tracers will focus on fluorinated compounds because the gas chromatography detectors adapted for fluorine detection have been successfully optimized for use with fluorinated vapor-phase tracers.
- 4) Solubility – Compounds with infinite or limited solubility will be considered. This implies that the elements should include hydrogen, oxygen, , and carbon to raise the polarity of the tracer. Fluorine will be included for detectability.
- 5) Volatility – Compounds should be neutral at reservoir boiling pH's
- 6) Inertness – Any ions that can be naturally produced by the compounds should be negative to avoid interaction with the reservoir rock.
- 7) Acidity – The compounds should not be so acidic that it interferes with volatility.
- 8) Cost -- Ultimately cost will be an issue. It will not be considered in the initial stages of the investigation.

A class of compounds with attributes that are closest to the desired properties will be chosen, and a few tested for thermal stability. These will be run in pressurized autoclaves at 280°C for four days as a screening test. We will continue testing the most stable compounds to determine the kinetic parameters in simple water-tracer systems.

Research Results

The results of the literature survey are shown in Figure 3. At the present time we are restricting our selections to soluble compounds due to a lack of high-temperature EOS for fluorinated compounds at

high temperatures. Thus, the most suitable compounds are the soluble alcohols.

Three fluorinated alcohols were chosen for laboratory testing. These are the most soluble of this class of compounds. Specifically, 1,1,1-trifluoro-2-propanol, 1,1,1-trifluoro-2-propanol, 4,4,4-trifluoro-1-butanol were selected. The structures of these compounds are shown in Figure 4.

The results so far are encouraging. The preliminary data on the stability of all of the compounds indicates that they are sufficient for tracing in moderate-temperature systems (Fig. 5). However, the detection limit and acidity of these compounds still needs to be determined.

Future Plans

We hope to finish the qualifying autoclave tests during FY2002. During this time the detection limits will be determined. If the detection limits can be pushed low enough for use in tracing, the acidity will be determined experimentally during FY2003.

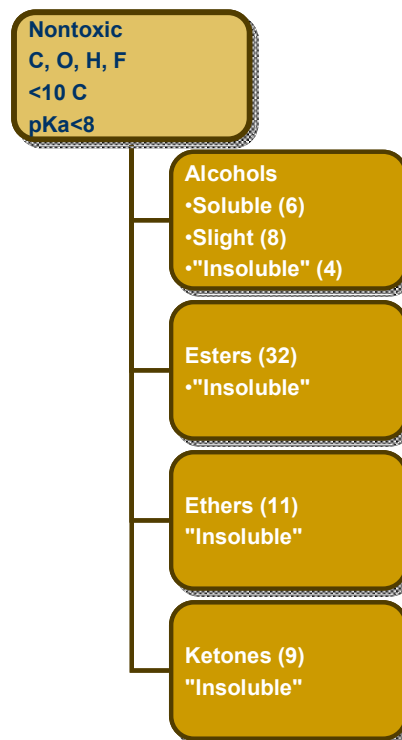


Figure 9. Results of the search for potential two-phase tracers. The criteria for the search are given in the top box, and the results for the various compound classes are given in the lower boxes.

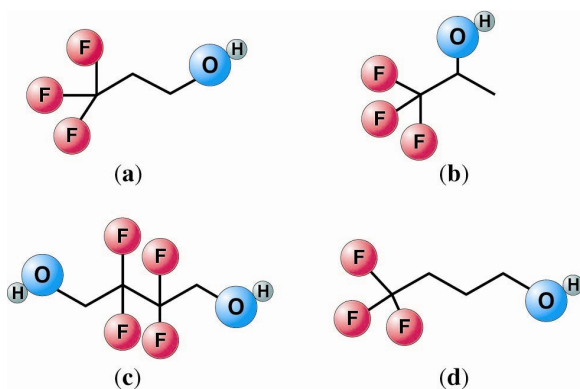


Figure 10. Structure of the fluoroalcohols chosen for the screening tests. (a) 3,3,3-trifluoro-1-propanol; (b) 1,1,1-trifluoro-2-propanol; (c) 4,4,4-tetrafluoro-1,2-butandiol; and (d) 4,4,4-trifluoro-1-butanol. The tests on the dialcohol (c) have not yet begun because of analytical difficulties.

Table 1. Results of the laboratory experiments.

1,1,1-trifluoro-2-propanol		
Temperature	Time	% Remaining
280°C	4 days	99.91%
320°C	7 days	97.15%
320°C	10 days	76.05%
330°C	7 days	91.45%
330°C	10 days	91.26%
330°C	14 days	59.56%
3,3,3-trifluoro-1-propanol		
280°C	4 days	8.13%*
320°C	4 days	42.16%
320°C	7 days	28.85%
4,4,4-trifluoro-1-butanol		
280°C	4 days	81.44%
300°C	4 days	82.84%
300°C	7 days	75.16%
320°C	7 days	72.20%

*Excessive decay from oxygen contamination

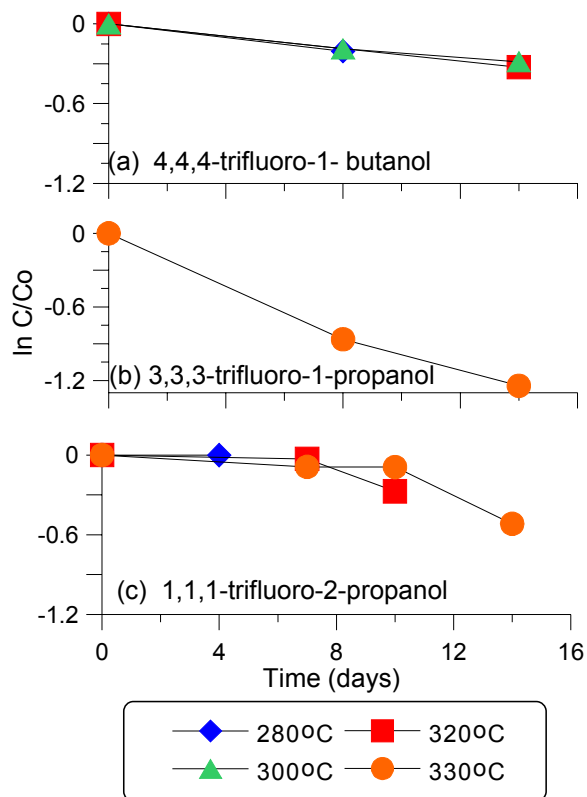


Figure 11. Thermal stability of fluorinated alcohols. C/C_0 is the fraction left after heating at the specified temperature and time.

Collaborations, Papers Published and Technology Transfer

This project has been strongly collaborative with industry. As stated by Paul Hirtz of Thermochem, Inc. in June, 1998:

“To date at least 30 liquid and vapor-phase tracer tests have been performed using tracers developed by EGL. Of these tests, 10 were funded entirely by private industry. This demonstrates the value and overall acceptance of the tracer technologies for solving important geothermal development and utilization problems. I am not aware of any other DOE-funded geothermal program that has resulted in such widespread use by industry.”

“The reservoir tracers are now used routinely to monitor important water injection projects, such as the wastewater injection programs at The Geysers. The results are used to optimize injection strategy for maximum conversion of wastewater to steam. The liquid tracers have been used to monitor brine injection breakthrough in fields such as Dixie Valley and Coso, and both liquid and vapor tracers have been recently used in high-temperature

systems in Hawaii and Indonesia. The results of these tests weigh heavily in multi-million dollar decisions by developers regarding injection placement and the drilling of new injection wells."

The tracer tests mentioned by Hirtz were performed in conjunction with Calpine Geothermal, Northern California Power Authority, Unocal Geothermal, California Energy Corporation, and Caithness Corporation.

All of the major papers on tracer development have been published by EGI. During the last three years eight were published under the current contract (Adams et al., 1999; Adams and Kilbourn, 2000; Adams et al., 2000; Moore et al., 2000; Adams, 2001; Adams et al., 2001; Beall et al., 2001; Nash and Adams, 2001). A special issue of the journal *Geothermics* devoted to the topic of tracers was published this year as a task under the current contract.

References

- ACGIH, 1979. TLV's - Threshold limit values for chemical substances and physical agents in the workroom environment. American Conference of Governmental Industrial Hygienists, Cincinnati OH.
- Adams, M.C., 1985. Tracer stability and chemical changes in an injected geothermal fluid during injection-backflow testing at the East Mesa geothermal field. Tenth Workshop on Geothermal Reservoir Engineering, Stanford University, Stanford CA, 247-252.
- Adams, M.C., 1995. Vapor, liquid, and two-phase tracers for geothermal systems. World Geothermal Congress 3, Florence, Italy, 1875-1880.
- Adams, M.C., 1999. Tracing the flow of effluent into The Geysers geothermal field, U. S. Department of Energy, Office of Geothermal Technologies
- Adams, M.C., 2001. A comparison of two multiple-tracer tests conducted at The Geysers. Twenty-Sixth Workshop on Geothermal Reservoir Engineering, Stanford University, Stanford, CA,
- Adams, M.C., Beall, J.J., Eney, S.L. and Hirtz, P., 1991a. The application of halogenated alkanes as vapor-phase tracers: A field test in the Southeast Geysers. Transactions, Geothermal Resources Council 15, 457-463.
- Adams, M.C., Beall, J.J., Eney, S.L., Hirtz, P.N., Kilbourn, P., Koenig, B.A., Kunzman, R. and Smith, J.L.B., 2001. Hydrofluorocarbons as geothermal vapor-phase tracers. *Geothermics* 30, 747-775.
- Adams, M.C., Beall, J.J., Hirtz, P., Koenig, B.A. and Smith, J.L.B., 1999. Tracing effluent injection into the SE Geysers - a progress report. Transactions, Geothermal Resources Council 23, 341-345.
- Adams, M.C., Benoit, W.R., Doughty, C., Bodvarsson, G.S. and Moore, J.N., 1989. The Dixie Valley, Nevada tracer test. Transactions, Geothermal Resources Council 13, 215-220.
- Adams, M.C. and Davis, J., 1991. Kinetics of fluorescein decay and its application as a geothermal tracer. *Geothermics* 20, 53-66.
- Adams, M.C. and Kilbourn, P.M., 2000. Thermal stability of the vapor-phase tracer R-134a. Twenty-Fifth Workshop on Geothermal Reservoir Engineering, Stanford University, Stanford CA,
- Adams, M.C., Moore, J.M. and Hirtz, P., 1991b. Preliminary assessment of halogenated alkanes as vapor-phase tracers. Sixteenth Workshop on Geothermal Reservoir Engineering, Stanford University, Stanford CA, 57-62.
- Adams, M.C., Moore, J.N., Fabry, L. and Ahn, A.H., 1992. Thermal stabilities of aromatic acids as geothermal tracers. *Geothermics* 21, 323-339.
- Adams, M.C., Yamada, Y., Yagi, M., Kondo, T. and Wada, T., 2000. Stability of methanol, propanol, and SF6 as high-temperature tracers. World Geothermal Congress, 3015-3019.
- Beall, J.J., Adams, M.C. and Hirtz, P.N., 1994. R-13 tracing of injection in The Geysers. Transactions, Geothermal Resources Council 18, 151-159.
- Beall, J.J., Adams, M.C. and Hirtz, P.N., 1998. Evaluation of R-134a as an injection tracer in the Southeast Geysers. Transactions, Geothermal Resources Council 22, 569-573.
- Beall, J.J., Adams, M.C. and Smith, J.L.B., 2001. Geysers reservoir dry out and partial resaturation evidenced by twenty-five years of tracer tests. Transactions, Geothermal Resources Council 25, in press.
- Goyal, K.P., 1999. Injection experience in The Geysers, California -- A summary. Transactions, Geothermal Resources Council 23, 541-547.

- Lester, D. and Greenberg, L., 1951. The inhalation of ethyl alcohol by man. *Quart. J. Studies Alc.* 12, 167-178.
- Moore, J.N., Adams, M.C., Sperry, T.L., Bloomfield, K.K. and Kunzman, R., 2000. Preliminary results of geochemical monitoring and tracer tests at the Cove Fort-Sulphurdale geothermal system, Utah. Twenty-Fifth Workshop on Geothermal Reservoir Engineering, Stanford University, Stanford CA,
- Nash, G.D. and Adams, M.C., 2001. Cost effective use of GIS for tracer test data mapping and visualization. *Transactions, Geothermal Resources Council* 25, in press.
- Rose, P.E. and Adams, M.C., 1994. The application of rhodamine WT as a geothermal tracer. *Transactions, Geothermal Resources Council* 18, 237-240.
- Rose, P.E., Benoit, W.R. and Kilbourn, P., 2001. The application of the Polyaromatic sulfonates as tracers in geothermal reservoirs. *Geothermics* 30(6), 617-640.

TECHNOLOGY FOR INCREASING GEOTHERMAL ENERGY PRODUCTIVITY

Principal Investigator - Nancy Møller
Chemistry Department (0340)
University of California at San Diego
La Jolla, CA 92093

Collaborating Investigators - John H. Weare
Chemistry Department (0340)
University of California at San Diego
La Jolla, CA 92093

Key Words - Breakout, computer models, EOS, heat content, hot/dry rock, hydrothermal, injection chemistry, phase coexistence, production chemistry, reservoir, scaling, simulations, solubility, technology transfer, thermodynamic properties

Project Background and Status

The development of a geothermal resource requires considerable financial investment that can be jeopardized by the uncertain chemistry of the resource and energy production processes. For example, current subcritical operations can encounter mineral sealing and injection incompatibilities in aquifers and scaling and toxic gas discharge during energy extraction. Therefore, the ability to predict the chemical behavior and energetics of the various geothermal heat sources - hydrothermal, hot dry rocks, geopressured zones and magma - and associated energy extraction processes would significantly promote the economical production and expanded use of geothermal energy.

The DOE Geothermal Program has funded the UCSD Chemical Geology Modeling Group (CGMG) to carry out research projects designed to provide the geothermal industry with easy-to-use model technologies that can correctly predict resource and process chemistry for a wide array of operating conditions. This chemistry reflects solid-liquid-gas interactions that are complicated functions of pressure, temperature, volume and composition (PTVX). Utilizing recent advances in physical chemistry and careful parameterization procedures, we have demonstrated (e.g., see Møller et al. (1998); Duan et al. (1995)) that semi-empirical equations of state (EOS) models can be constructed that reliably reproduce the complex chemistry of geothermal systems - scaling, breakout, steam fractions, heat content, gas emission, phase coexistence, miscibility, pH, formation temperatures, downhole brine concentrations - for a wide range of PTVX variables. New equation of state models have been developed that can treat compressible phases and the chemical behavior occurring in untapped

very high T, P (including low permeability) resources.

To facilitate the transfer of our modeling technologies, we develop extensive user interface software so that our models can be bundled into easy-to-use application packages: TEQUIL (predicts scaling and reservoir chemistry as a function of composition for temperatures below 300°C); GEOFLUIDS (predicts processes, such as flashing and miscibility, to high TP) and GEOHEAT (predicts enthalpies of complex mixtures). These models are implemented on our interactive Internet website: geotherm.ucsd.edu. This site is accessed by the geothermal community and by many researchers in other areas of interest. Accurate models of chemical fluids have broad applications, many of which are important to the American public. Examples include: the integrity of nuclear waste storage facilities, the transport of hazardous materials via aqueous phases, mineral and oil recovery.

Our research program - to develop critical chemical model technologies for significantly expanding geothermal energy production - benefits from the synergistic relationship between applied and fundamental research present at a research university. Located at UCSD, a university that repeatedly ranks as one of the top five research institutions, we have the opportunity to collaborate on a daily basis with leaders in the fields of mathematics, science, computer technology and engineering. In addition, graduate and post-doctoral students can be trained in advanced fluid chemistry for application to various fields, including geothermal energy production.

Project Objectives

Heat beneath the Earth's surface is an enormous source of clean, sustainable energy for meeting the needs of the United States. The 1998 DOE Strategic Plan for the Geothermal Energy Program calls for new technologies to significantly expand the use of geothermal energy by reducing the financial risks associated with current energy production operations and the future exploitation of deep and low permeability heat resources. Since many of the significant problems that limit geothermal energy production are related to complicated resource and production chemistry, the objectives of our research projects are:

- To develop thermodynamic models that describe the interactions between solid/gas/liquid interactions and heat properties encountered in present-day geothermal energy extraction processes (e.g., prediction of solubilities, phase equilibria, gas breakout, pH).
- To develop new cutting-edge thermodynamic-modeling technologies that can successfully treat problems encountered in the exploitation of future higher T-P and fluid-limited resources.
- To develop advanced methodologies that reduce the dependence on experimental data in model construction.
- To develop extensive user interfaces so that our model codes can be incorporated into user-friendly modeling software packages for the rapid transfer of technology and education.
- To increase the fundamental understanding of the complex chemistry of a wide variety of present-day and future heat sources and energy extraction operations.
- To train students in earth science with expertise in hydrothermal resources.

Approach

Utilizing advances in physical chemistry, we develop equation of state (EOS) descriptions of the thermodynamics of mixed natural fluid systems. This approach allows the construction of chemical models that yield highly useful information (e.g., solubilities, phase equilibria and heat properties)

about geothermal reservoir behavior and energy production processes as a function of PVTX. Our modeling approaches, based on fundamental theory of the liquid state, support accurate extrapolation and interpolation of the data used in the model parameterization.

For current, relatively near surface, geothermal operations ($P \approx 1$ atm), the principal variation of the liquid density phase free energy is due to concentration changes of the solutes. For these conditions, we use modified Pitzer equations and accurate laboratory measurements to construct models of complex rock-water-gas equilibria accurate to high concentration and temperature (see Solution Activity Equations, below). In these equations, the coefficients, B , Z , Φ , ψ , etc., are parameters to be evaluated from data. Pressure corrections can be calculated from partial molal volumes.

New chemical problems are expected to arise in the future development of higher T-P reservoirs. To treat these systems and other problems requiring density variation (e.g., miscibility, subsurface boiling, 2-phase flow in reservoirs), we have developed more advanced equations of state (see EOS for Compressible Phases, below). In these equations the parameters, A , B , D , a , etc., are established from data and polynomial mixing rules. η and v are functions of the molar volume. These new EOS descriptions yield free energies that are correct at liquid and vapor densities and can describe the large changes in composition and very high solute mole fractions that can occur during phase separation at high T and P.

Simulation studies of reservoir chemistry indicate that geothermal fluids evolve to near critical conditions. New methods are being developed to describe the unusual behavior of fluids in the critical region.

Semiempirical models, even when based on physical chemistry theory, require thermodynamic data for parameterization. There are much fewer experimental data available for model parameterization of high T-P systems. Therefore, we use molecular level approaches (e.g., molecular dynamics and Monte Carlo simulations) to meet this challenge. We have shown that these approaches can be used successfully to generate the accurate thermodynamic information needed to model brine behavior.

Solution Activity Equations

$$\ln \gamma_M = z_M^2 F^2 \sum_a m_a (2B_{Ma} + ZC_{Ma}) + \sum_c m_c (2\Phi_{Mc} + \sum_a m_a \Psi_{Mca})$$

$$+ \sum_a \sum_{a' < a} m_a m_{a'} \Psi_{aa'M} + |z_M| \sum_c \sum_a m_c m_a C_{ca}$$

$$+ \sum_a m_a (2\lambda_{naM}) + \sum_a \sum_a m_a m_a \zeta_{naM}$$

$$F = -A^* \left\{ I^{1/2} / (1 + 1.2I^{1/2}) + (2/1.2) \ln(1 + 1.2I^{1/2}) \right\}$$

$$+ \sum_c \sum_a m_c m_a B'_{ca} + \sum_c \sum_c m_c m_c \Phi'_{cc} + \sum_a \sum_{a' < a} m_a m_{a'} \Phi'_{aa'}$$

$$B_{Ma} = \beta^{(0)}_{Ma} + \beta^{(1)}_{Ma} g(\alpha I^{1/2}) + \beta^{(2)}_{Ma} g(12I^{1/2})$$

$$g(x) = 2(1 - (1+x)e^{-x})/x^2$$

$$\Phi_{cc} = \Phi_{cc} + F \Phi_{cc}(I)$$

$$C_{ca} = C_{ca} \phi / 2 |z_c z_a|^{1/2}$$

$$Z = \sum_i |z_i| m_i$$

EOS for Compressible Phases

$$Z = \frac{PV}{RT} = Z^{hd} + Z^{dp} + Z^{pr}$$

$$Z^{hd} = \frac{1 + \left[\frac{3DE}{F} - 2 \right] \eta + \left[\frac{3E^3}{F^2} - \frac{3DE}{F} + 1 \right] \eta^2 - \frac{E^3}{F^2} \eta^3}{(1 - \eta)^3}$$

$$Z^{dp} = \eta \frac{\left[1 - \frac{2A_3}{A_2} \right] \frac{\partial A_2}{\partial \eta} + \frac{\partial A_3}{\partial \eta}}{\left[1 - \frac{A_3}{A_2} \right]^2}$$

$$Z^{pr} = -\frac{1}{RT} \left[\frac{a}{v} + \frac{acb}{2v^2} + \frac{3adb^2}{16v^3} + \frac{aeb^3}{16v^4} \right]$$

Results

TEQUIL Models

We have made considerable progress building a comprehensive suite of models for application to current, near surface geothermal operations ($T < 300^\circ\text{C}$) up to high brine concentrations. These models provide important tools for performance assessment (e.g., potential for flashing and scaling in power plants and well bores), predicting downhole chemistry and testing problem abatement strategies. To illustrate our progress in this area, we describe below selected recent developments.

Acid/Base Reactions: The solubilities of minerals (e.g., carbonate and amorphous silica scales) and insoluble gases (e.g., CO_2 , H_2S) in geothermal fluids and the alteration of reservoir rocks (e.g., $3\text{KAlSi}_3\text{O}_8(\text{K-spar}) + 2\text{H}^+ = \text{KAl}_3\text{Si}_3\text{O}_{10}(\text{OH})_2(\text{K-mica}) + 6\text{SiO}_2(\text{quartz}) + 2\text{K}^{2+}$) are often strong functions of the hydrogen ion concentration in solution. To characterize these important rock/water/gas reactions, we are modeling the acid/base behavior of brines. The temperature dependence of the important carbonic and silicic acids are given as a function of brine composition in Figure 1.

The control of amorphous silica ($\text{Si}(\text{OH})_4(\text{s})$) scale is a major production problem for many geothermal power facilities. At equilibrium, the solubility of the solid phases, quartz or amorphous silica, is controlled by the concentration of $\text{Si}(\text{OH})_4$ in solution. $\text{Si}(\text{OH})_4$ is a fairly weak acid with a pK_1 in pure water not much lower than 9 (see Fig. 1). On the other hand, for high salinity brines the pK

decreases dramatically with temperature (Fig. 1), reaching a value as small as 7.5 for brines with ionic strengths of 5 m at 250°C . Therefore, at $\text{pH} > 7.5$, the $\text{Si}(\text{OH})_4(\text{aq})$ species dissociates removing it from solution and silica scale becomes more soluble.

Since the polymerization of silica is relatively slow at low pH, a method of limiting scale formation in geothermal power plants is to lower the pH of the process stream by the injection of a strong acid (pH modification strategy). However, if weak acid anions (e.g. HCO_3^-) are present in the brine they will react with the added protons, reducing the amount of free protons and decreasing the effectiveness of this method. Adding too much acid will damage plant equipment and is expensive. Figure 2 shows the change in pH predicted by TEQUIL when acid is added to a typical low salinity geothermal brine. The effect of carbonate and sulfate buffering is clearly illustrated.

Since the concentration of $\text{Si}(\text{OH})_4$ in equilibrium with quartz in the formation is a function of temperature, measuring its concentration at the wellhead can provide a cost effective estimate of the downhole temperature of the geothermal reservoir. The TEQUIL acid/base model can be applied to predict the change in the solubility of quartz with pH and temperature. The importance of pH variation is shown in Figure 3, below. For example, if the wellhead $\text{Si}(\text{OH})_4$ equals .003 m then (from Fig. 3) the predicted temperature of a $\text{pH} = 9$ brine would be about 230 F; whereas a $\text{pH} = 6$ brine would have a predicted temperature of 460 F.

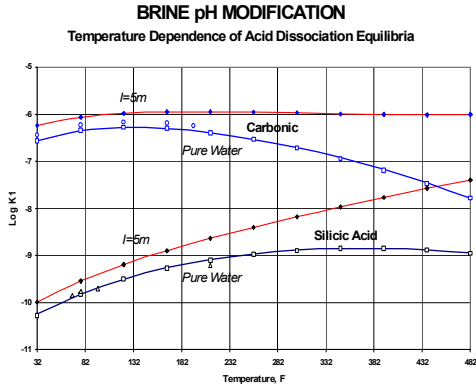


Figure 1

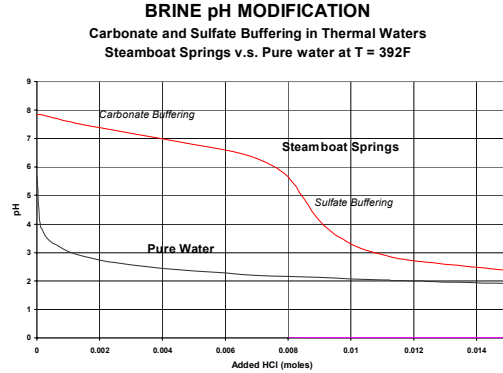


Figure 2

GEOFLUIDS Models

These models can be used to characterize multiple phase processes, such as flashing and immiscibility, and the effects of injectates on deep, low permeability reservoirs. For higher temperature systems, these models are used to predict the evolution of brines via processes such as deep boiling.

An example of predicted high T-P vapor-liquid phase equilibria is given in Figure 4. This figure shows phase coexistence in the geologically important NaCl-H₂O-CH₄ system as a function of concentration at constant T, P. Note that even for

these high T and P conditions there is a large region of immiscibility caused by the presence of CH₄. Such a region would have a substantial effect on the fluid compositions in a deep geothermal system. For example, in Figure 4, a dilute fluid in the immiscible region (point a) would phase separate into a salt-rich brine with composition at b and a vapor phase at composition c.

We (e.g., Duan et al. (1996)) have also made considerable progress developing advanced molecular level technologies (e.g., molecular dynamics and Monte Carlo simulations) that can be used to generate needed “data” for empirical model construction.

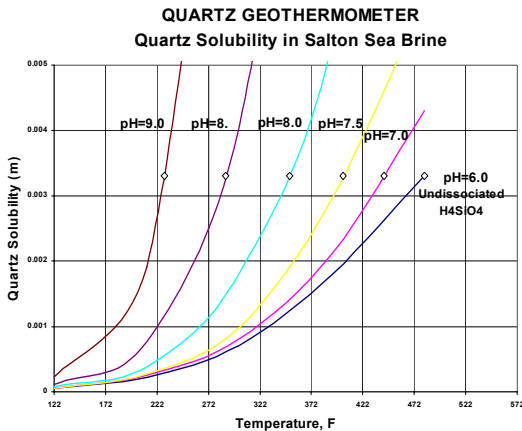


Figure 3

Phase equilibria in the NaCl-H₂O-CH₄ system

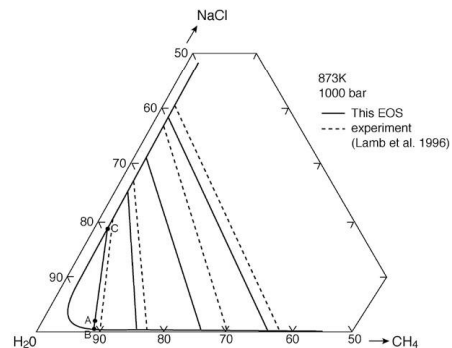


Figure 4

Near critical behavior of fluid mixtures: The region near the critical loci is difficult to model with the usual EOS approaches. The isotherms predicted for the H₂O-CH₄ binary (dashed lines in Fig. 5) by our prior EOS model for the H₂O-CO₂-CH₄ system illustrate this problem. The symbols (dots 633 K, triangles 628 K and circles 626 K) are experimental data. This model is accurate for most of TPX space. However, it would, for example, predict a two phase region at a temperature of 628 K, pressure of about 1000 bar and mole fraction of X = 0.22; whereas the data indicate that at this pressure and mole fraction the system is in a single phase region. The disagreement between model predictions and measured results along the critical loci could have a significant impact on interpretations of geological data (e.g., in fluid inclusion studies). To obtain the correct behavior in the critical region, it is necessary to represent the EOS in this region in terms of scaling laws. In Figure 5 (solid lines), we illustrate the excellent agreement of our application of scaling methods.

GEOHEAT Models

These models provide the enthalpy of fluid phases for geothermal applications such as the prediction of steam ratios and available heat. The present GEOHEAT code includes an accurate enthalpy model of the H₂O-CO₂-CH₄ system for both liquid and vapor phases for a very large T-P range. We also have implemented an accurate model of the liquid state enthalpy for the most common NaCl dominated systems. Fig. 6 shows an enthalpy-pressure diagram calculated with these models for the Salton Sea brine (all the salt concentrations are included in the NaCl component). Because of the reduced vapor pressure of water in the concentrated brine, the steam ratio from flashing in the well bore (boiling) is significantly different from that of a low salt concentration system. This has a major effect on the properties of the fluids at the wellhead. For example, starting at point a (Fig. 6), a constant enthalpy process for this brine with a wellhead pressure of 10 bar would yield a steam ratio (SR) of roughly 20%. Similar conditions for a pure water system would lead to a SR of roughly 29%.

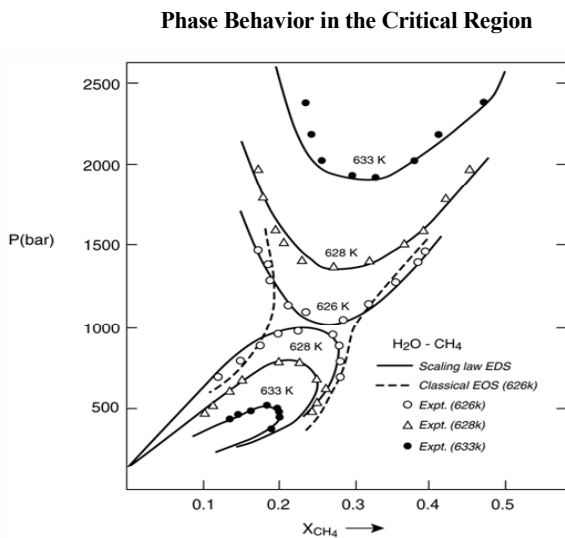


Figure 5

ENTHALPY-PRESSURE RELATIONS IN SALTON SEA GEOTHERMAL BRINE

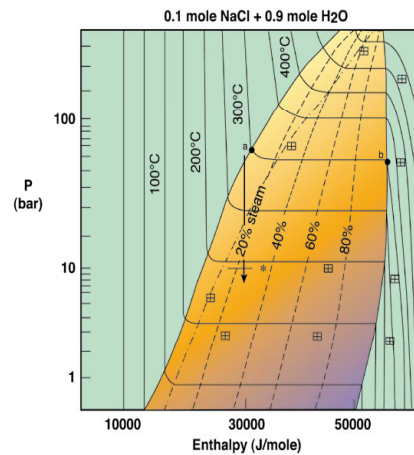


Figure 6

User Interfaces and Website Development

Substantial improvements were made to our <http://geotherm.ucsd.edu> web site. A GEOFLUIDS application for the NaCl-CO₂-CH₄-H₂O system is now available.

Future Plans

In the upcoming project periods, we will continue expanding the compositional flexibility of our rock/water Pitzer-type models ($T < 300^{\circ}\text{C}$). Aluminum hydroxide, silicate and sulfide systems and pressure variability will be added as well as important thermochemical assessment tools, such as heat content, pH prediction. We will complete a model for the NaCl-KCl-CaCl₂-MgCl₂-H₂O system, targeted for 300°-1000°C and to 6000 bars, for characterizing the chemistry of very high T-P reservoirs and describing important geothermal processes such as flashing, phase co-existence and miscibility. Heat property models of supercritical conditions will be developed. We will also explore more theoretically based modeling approaches in order to develop EOS forms that are accurate through the critical range ant to high TPX. Our TEQUIL, GEOFLUIDS and GEOHEAT application packages will be expanded as described above. A new package, GEOTHERM, containing geothermometry software will begin development. User interfaces will be developed for the new model codes, and these codes will be implemented on our web site.

Technology Transfer, FY01 (10/1/00 – 9/30/01)***Web Site Use***

There were 1605 hits on our web site (geotherm.ucsd.edu). In addition, many personal contacts were made and expert advice given.

Technical Meetings

INVITED PRESENTATION: "Thermodynamic Models of Natural Fluids: Theory and Practice." 221st. meeting American Chemical Society, April 1-5, 2001, San Diego, CA.

PRESENTATION: "Monte Carlo Gibbs Ensemble Simulation of Phase Equilibria of the RWK2 Water." 221st. meeting ACS, April 1-5, 2001, San Diego, CA.

PRESENTATION: "Technology for Increasing Geothermal Energy Productivity, DOE Geothermal Subcontractors' Meeting, May 8-10, Albuquerque NM.

PRESENTATION: "From Molecular Models to Equations of State." 11th. Annual Goldschmidt 2001 Conference, May 20-24, 2001, Hot Springs, VA.

INVITED KEYNOTE PRESENTATION: "First Principles Dynamical Simulations of Hydrothermal Solution Behavior." Goldschmidt 2001 Conference, May 20-24, Hot Springs, VA.

INVITED PRESENTATION: "Parallel Implementation of Large-Scale *Ab Initio* Molecular Dynamic Algorithms: Scaling Issues." 1st COMPUTATIONAL CHEMISTRY CONFERENCE, University of Kentucky, Lexington, Kentucky, October 17, 2001.

Selected Publication

"Equation of state for the NaCl-H₂O-CH₄ system and the NaCl-H₂O-CO₂-CH₄ system: phase equilibria and volumetric properties above 573K," submitted for publication in *Geochim. Cosmochim. Acta*.

Education of Scientists

Supervise the research activities of one postdoctoral student and one project scientist in the area of developing chemical models for application to the production of geothermal energy.

References

- Møller, N., Greenberg, J. P. and Weare, John H. (1998) *Transport in Porous Media* 33, 173-204.
- Duan, Z. Møller, N. and Weare (1995) *Geochim. Cosmochim. Acta* 59, 2869-2882.
- Duan, Z. Møller, N. and Weare (1996) *Geochim. Cosmochim. Acta* 60, 1209-1216.

THE DEVELOPMENT OF TRACERS FOR USE IN GEOTHERMAL RESERVOIRS

Principal Investigators - Peter E. Rose
Geoscience Institute at the University of Utah
423 Wakara Way suite 300
Salt Lake City, Utah, 84108

Collaborating Investigators - Phaedra Kilbourn, and Christian Kasteler Energy
Geoscience Institute at the University of Utah
423 Wakara Way suite 300
Salt Lake City, Utah, 84108

Joel M. Harris
Department of Chemistry, University of Utah
2020 HEB
Salt Lake City, Utah, 84112

Key Words - geothermal tracers, naphthalene sulfonates, fluorescein, laser-induced fluorimetry, fluorescence detection, injection

Project Background and Status

Geothermal energy production involves the flow of large volumes of water through hot fractured rock deep underground, where heat is transferred from the rock to the water. The heated water then flows to the surface through production wells and is used to generate electricity in steam turbines. The cooled water is then reinjected via dedicated injection wells to be recirculated through the reservoir. If the injection wells are located too close to the production wells, there develops a risk of premature thermal breakthrough. If the injectors are placed too far from the producers, then the injectate will not return to the reservoir and the result will be a drop in reservoir pressure. *The use of artificial tracers provides the only expedient, reliable and cost effective means of tracking injection fluids and optimizing injection well placement in geothermal reservoirs.*

Project Objectives

The purpose of this project is to increase the thermal stability and detectability of tracers for use in hydrothermal environments. Operators of geothermal reservoirs claim that many more tracers than are currently available are needed in order to effectively track fluid flow in reservoirs having many injection wells. Such tracers must be environmentally benign, resistant to adsorption on geothermal rock, affordable, thermally stable and very detectable. Whereas all of these qualities are essential, only the latter two are design drivers. Therefore, our primary objectives are:

- to identify and qualify two new thermally stable tracers for use in high-temperature (>300°C) geothermal systems

- to demonstrate an increase in the detectability of fluorescent tracers by a factor of at least 100 for intermediate-temperature (<250°C) applications

Approach

We have focused our attention primarily on a new class of uv-fluorescent compounds that have proven to be excellent candidates for use as tracers in high temperature geothermal reservoirs. These compounds, known as the naphthalene sulfonates, are environmentally benign, very detectable by fluorescence spectroscopy, affordable, and thermally stable. Toxicity studies indicate that the naphthalene sulfonates are neither carcinogenic nor mutagenic (Greim *et al.*, 1994).

Our approach was to study two naphthalene sulfonates candidate tracers, 1-naphthalene sulfonate and 2,6-naphthalene disulfonate, under controlled laboratory conditions to determine their suitability for use in geothermal applications. Next, we set out to verify the laboratory results in a field test at the Dixie Valley geothermal reservoir in west-central Nevada. Shown in Figure 1 are the chemical structures of these two compounds in addition to four other naphthalene sulfonates that have recently been tested and shown to be viable geothermal tracers.

In the area of improved tracer-detectability, our experimental approach was first to design and fabricate an innovative analytical instrument, based upon emerging technologies in laser light sourcing, fiber optics and charge-coupled-devise (CCD) spectroscopy (see Figure 2). Using this instrument, we then set out to demonstrate a reduction in the detection limit of fluorescent tracers by a factor of

Compound	Structure	Excitation / Emission (nm)
1-naphthalene sulfonic acid		217 / 333
2-naphthalene sulfonic acid		220 / 336
1,5-naphthalene disulfonic acid		218 / 334
2,6-naphthalene disulfonic acid		225 / 342
2,7-naphthalene disulfonic acid		226 / 339
1,3,6-naphthalene trisulfonic acid		228 / 342

Figure 1. Chemical names, structures, and excitation and emission band maxima of six naphthalene sulfonate geothermal tracers studied in the laboratory and in the field.

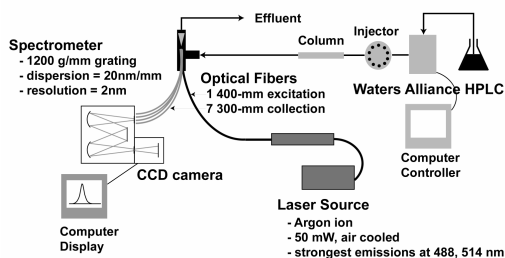


Figure 2. Schematic view of the HPLC/fluorimeter assembly.

100, thereby reducing the quantity of tracer required in a tracer test also by a factor of 100. Second was the evaluation of a family of candidate fluorescent tracer compounds that could be analyzed using the new apparatus. These compounds are not as thermally stable as the naphthalene sulfonates mentioned above. However, they are suitable for use in intermediate-temperature (<250°C) geothermal reservoirs, which constitute a significant fraction of systems in the U.S. In addition, these compounds are sufficiently similar to the geothermal tracer fluorescein that they require the same excitation wavelength as fluorescein, serving to simplify their analysis.

Research Results

This year's results can be summarized as:

- the laboratory demonstration of two new tracers for use in high-temperature (>300°C) reservoirs and verification of those laboratory results in a field test
- the field demonstration of a reduction in the detection limit of fluorescent tracers for intermediate-temperature (<250°C) applications by a factor of 100, resulting in a concomitant reduction in the quantity of tracer required for a tracer test also by a factor of 100.

The high-temperature naphthalene sulfonate tracer candidates were analyzed using High Performance Liquid Chromatography (HPLC) with fluorescence detection (Waters Corporation, Milford, MA). HPLC allows for the separation of the polyaromatic sulfonates not only from each other but also from interferences that occur naturally in the reservoir. Using HPLC, any number of polyaromatic sulfonate tracers can, in principle, be analyzed in each other's presence.

The six naphthalene sulfonate tracers shown in Figure 1 can be analyzed using gradient chromatography in less than 10 minutes, as shown by the chromatogram in Figure 3. The first mobile phase consisted of a solution of 3.17 mM Na₂HPO₄, 6.21 mM KH₂PO₄, and 5.0 mM TBAP in 25%/75% methanol/water. The second mobile phase consisted of the same concentrations of salts in 30% /70% methanol/water.

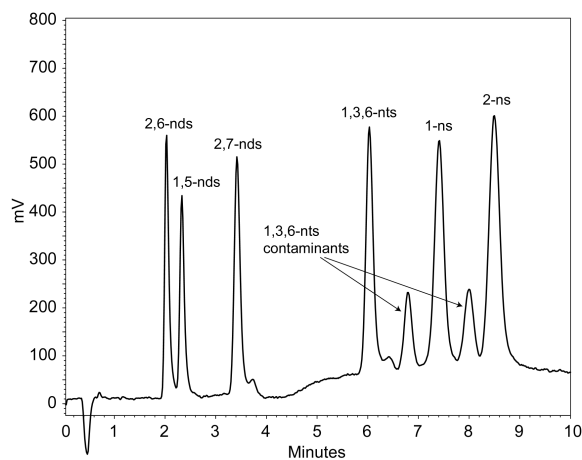


Figure 3. Chromatogram of six naphthalene sulfonate analytes obtained using a gradient method.

The decay kinetics of the two naphthalene-sulfonate tracers was studied using autoclave batch reactors under controlled conditions designed to simulate a geothermal environment.

The naphthalene sulfonate tracers decay according to the first-order differential equation:

$$-dC_n/dt = k_n \cdot C_n \quad (1)$$

where C_n is the concentration of naphthalene sulfonate and k_n is the first-order rate constant. Solution of this equation results in the following relationship between C_n and t :

$$\ln\left(\frac{C_n}{C_n^0}\right) = -k_n \cdot t \quad (2)$$

where C_n^0 is the initial concentration of polyaromatic sulfonate. The temperature dependence of k_n can be described by the Arrhenius relationship:

$$k_n = Ae^{(-E_a/RT)} \quad (3)$$

where A is the pre-exponential factor, E_a is the energy of activation, R is the gas constant and T is absolute temperature.

By solving for the Arrhenius rate-constant coefficients, it is possible to determine the half-life vs. temperature for each compound (see Figure 4). Figure 4 includes data not only for the two naphthalene sulfonate tracers but also for other polyaromatic sulfonate and xanthene-dye tracers that we have studied in our laboratory. No decay was observed for 1-naphthalene sulfonate, 2,6-naphthalene disulfonate, 2-naphthalene sulfonate or 2,7-naphthalene disulfonate upon exposure to simulated geothermal conditions for one week at 330°C. Therefore, we have approximated the half-life data for these four compounds, as shown by the dotted line in Figure 4. We suspect that these compounds are sufficiently stable for use in geothermal reservoirs with fluid temperatures of 330°C or hotter. Since there are no geothermal reservoirs in the U.S. with temperatures that high, these tracers are sufficiently stable to satisfy operator needs.

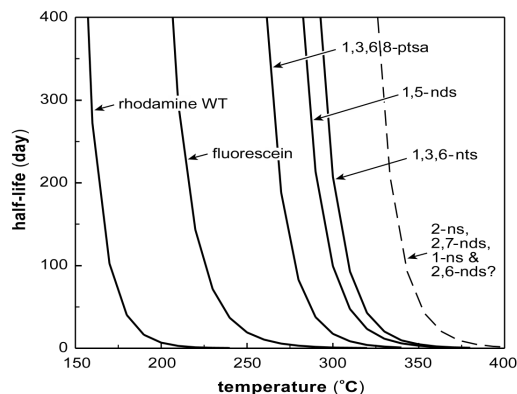


Figure 4. Plots of half-life vs. temperature for several polyaromatic sulfonate tracers as well as for two xanthene dyes as determined from decay kinetics data measured at EGI.

The two naphthalene sulfonates were field tested at the Dixie Valley geothermal reservoir. On July 10, 2001, 143 kg of 1-naphthalene sulfonate (Yick-Vic Chemicals, Hong Kong) was injected into well 45-5, which was flowing at approximately 100 kg/sec. Similarly, on July 10, 2001, 150 kg of 2,6-naphthalene disulfonate (Yick-Vic Chemicals, Hong Kong) was injected into the recently drilled well 38-32, which was flowing at approximately 110 kg/sec. All of the producing wells in the field were subsequently monitored for the two naphthalene sulfonates over the subsequent six months.

A return-curve plot from that test is shown in Figure 5. This represents the return of the candidate tracer 2,6-naphthalene disulfonate that was injected into well 38-32. These return curves show tracer production in the northeast portion of the reservoir only, as no tracer was observed in any of the production wells monitored further to the southwest in section 7. This flow pattern is similar to the one observed from tracer testing of the nearby well 27-32 that was initiated in November 1999 (Rose *et al.*, 2001).

The tracer flow patterns for the two tracers tested this past year, 2,6-naphthalene disulfonate and 1-naphthalene sulfonate, are shown in Figure 6. Also summarized in Figure 6 are the flow patterns of four additional naphthalene sulfonate tracers and one polyaromatic sulfonate tracer (1,3,6,8-pyrene tetrasulfonate) that were recently tested at the Dixie Valley geothermal reservoir. All seven tracers shown in Figure 6 can be analyzed simultaneously by the HPLC methods described in this paper.

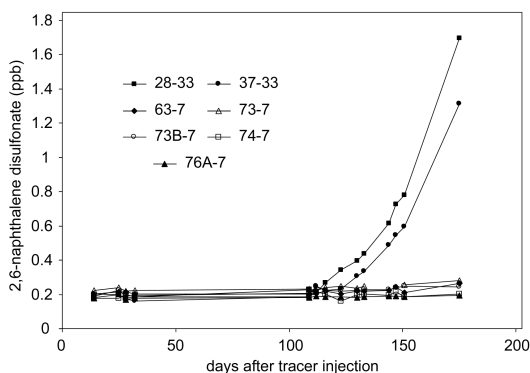


Figure 5. 2,6-naphthalene disulfonate returns observed from the testing of injector 38-32 at the Dixie Valley geothermal reservoir.

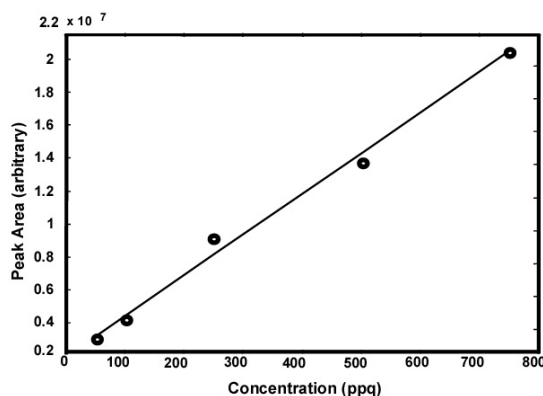


Figure 7. Calibration curve for fluorescein showing a linear relationship between concentration and peak area over the range of interest.

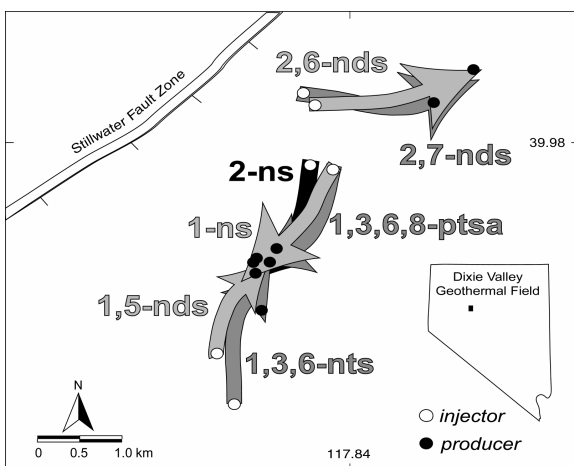


Figure 6. Tracer test results from seven tracer tests recently conducted at the Dixie Valley geothermal reservoir.

The apparatus shown in Figure 2 was used to demonstrate the greatly enhanced detectability of the intermediate-temperature tracer fluorescein in geothermal water. Shown in Figure 7 is a calibration curve for fluorescein between 50 and 750 parts per quadrillion (ppq). The actual limit of detection for fluorescein was 40 ppq, which is the lowest ever reported in the literature for this application and approximately 100-fold lower than what can be obtained by conventional analytical methods.

Having set a new standard for tracer detection in the industry, we then identified a number of tracers that were similar in structure to fluorescein and that, therefore, might possess comparable thermal stability. Shown in Figure 8 are the chemical structures of fluorescein and four similar compounds. The last column in this figure shows the thermal stability of each relative to fluorescein.

The second compound listed in Figure 8, 5-carboxyfluorescein, was chosen for field tests at the Beowawe and Dixie Valley geothermal reservoirs for the purpose of demonstrating in hydrothermal settings the greatly enhanced detectability of the laser fluorimeter over conventional analytical chemistry methods.

Compound	Structure	% Undecayed (2 days at 270°C)
fluorescein		78
5(6)-carboxyfluorescein		83
fluorescein-5-sulfonic acid		59
Oregon Green 488		40
Oregon Green 500 carboxylic acid		30

Figure 8. Compounds of intermediate thermal stability that can be analyzed by the very sensitive laser fluorimeter. The last column lists the percentage of each compound that remains undecayed upon exposure to geothermal conditions for two days at 270°C.

On July 10, 2001, 600 g of 5-carboxyfluorescein was injected into well 38-32 at Dixie Valley as a companion tracer to 2,6-naphthalene disulfonate. The 5-carboxyfluorescein was observed to return to the section 33 wells in similar fashion to the return of 2,6-naphthalene disulfonate as shown in Figure 5. This represents a 150-fold decrease in the quantity of fluorescein tracer used in a previous test at Dixie Valley.

On July 12, 2001, 600 g of 5-carboxyfluorescein was likewise injected into well 85-18 at the Beowawe geothermal field in east-central Nevada. A chemical analysis of returns to the production wells indicated that less than 1 g of 5-carboxyfluorescein would have been sufficient to demonstrate breakthrough at the production wells. This is approximately 100,000 times less than the quantity of tracer used in the previous tracer tests at Beowawe and dramatically illustrates the greatly enhanced detectability of the laser fluorimeter.

Conclusions and Plans for Continued Research

We have made significant progress in identifying and testing a family of tracers for high temperature (>300°C) geothermal applications. These tracers are being used to determine flow processes between injection and production wells within all major U.S. geothermal reservoirs. Since more tracers are needed, however, we plan to continue to identify, test and qualify additional candidates.

We have also made significant progress towards increasing the detectability of geothermal tracers for intermediate temperature (<250°C) tracing applications. We have demonstrated a reduction in the detection limit of these compounds by a factor of 100. We also identified and tested in the laboratory five new intermediate- temperature tracer candidates and demonstrated the greatly enhanced detectability of one of these compounds (5-carboxyfluorescein) in field tests at the Dixie Valley and Beowawe geothermal fields. We plan to continue to demonstrate improved detectability of fluorescent compounds and to use the emerging technologies of laser light sourcing, long pathlength flow cells, fiber optics and CCD spectrometry to implement field deployable detectors for the analysis of fluorescent tracers at the wellhead.

Collaborations, Papers Published and Technology Transfer

The best indication of the utility of technology developed by the R&D community is whether or not that technology gets transferred to the geothermal

industry. Effectively all of the companies operating geothermal reservoirs within the U.S. (and many more companies and institutes internationally) have adopted the use of the naphthalene sulfonate tracers. Shown in Figure 9 is a list of U.S. companies that have either used the new high temperature tracers in their respective reservoirs and/or have developed the ability to chemically analyze the tracers in-house.

Company	In-House Analytical Capability	Field Use
Caithness Energy	yes	yes
Unocal Geothermal	yes	yes
CalEnergy	yes	pending
Far West Capital	no	yes
Puna Geothermal	no	yes
Thermochem	yes	yes

Figure 9. List of U.S. companies that have adopted the use of the high temperature naphthalene sulfonate tracers.

In addition to the direct technology transfer activities summarized in Figure 9, we disseminate our results in peer-reviewed scientific journals and at geothermal conferences and workshops. Listed below are some of our recent publications:

Nimmo, J.R., Perkins, K.S., Rose, P.E., Rousseau, J.P., Orr, B.R., Twining, B.V., and Anderson, S.R., 2001, Kilometer-scale rapid transport of naphthalene sulfonate tracer in the unsaturated zone at the Idaho National Engineering and Environmental Laboratory, submitted for publication.

Rose, P.E., Johnson, S.D., and Kilbourn, P.M., and Kasteler, C. (2002) Tracer Testing at Dixie Valley, Nevada Using 1-Naphthalene Sulfonate and 2,6-Naphthalene Disulfonate: *Proc. Twenty-Sixth Workshop on Geothermal Reservoir Engineering*, Stanford University, SGP-TR-171.

Rose, P.E., Benoit, W.R., and Kilbourn, P.M., 2001, The application of the polyaromatic sulfonates as tracers in geothermal reservoirs: *Geothermics*, 30(6), pp. 617-640.

- Kleimeyer, J.A., Rose, P.E., and Harris, J.M., 2001, Determination of ultratrace-level fluorescent tracer concentrations in environmental samples using a combination of HPLC separation and laser-excited fluorescence multiwavelength emission detection: application to testing of geothermal well brines: *Applied Spectroscopy*, 55(6), 690-700.
- Rose, P.E., Johnson, S.D., and Kilbourn, P.M. (2001) Tracer testing at Dixie Valley, Nevada, using 2-naphthalene sulfonate and 2,7-naphthalene disulfonate: *Proc. Twenty-Sixth Workshop on Geothermal Reservoir Engineering*, Stanford University, SGP-TR-168, pp. 60-65.
- Wong, Y.L. and Rose, P.E. (2000) The testing of fluorescein derivatives as candidate geothermal tracers: *Geothermal Resource Council Transactions*, 24, 637-640.
- Rose, P.E., Benoit, W.R., Bacon, L., Tandia, B., Kilbourn, P.M., (2000) Testing the naphthalene sulfonates as geothermal tracers at Dixie Valley, Ohaaki, and Awibengkok: *Proc. Twenty-Fifth Workshop on Geothermal Reservoir Engineering*, Stanford University, SGP-TR-165, pp. 36-42.
- Rose, P.E., (2000) The application of polyaromatic sulfonates as tracers in geothermal and ground water environments: *Proceedings: American Association of Petroleum Geologists*, New Orleans.
- Rose, P.E., Goranson, C., Salls, D., Kilbourn, P.M. (1999) Tracer testing at Steamboat Hills, Nevada, using fluorescein and 1,5-naphthalene disulfonate: *Proc. Twenty-Fourth Workshop on Geothermal Reservoir Engineering*, Stanford University, SGP-TR-162, pp. 17-23.
- Rose, P.E. (1998) The use of polyaromatic sulfonates as tracers in high temperature geothermal reservoirs: *Proceedings 20th NZ Geothermal Workshop*, 239-243.
- Rose, P.E., Benoit, W.R., and Adams, M.C. (1998) Tracer testing at Dixie Valley, Nevada, using pyrene tetrasulfonate, amino G, and fluorescein: *Geothermal Resource Council Transactions*, 22, 583-587.
- Aquilina, L., Rose, P.E., Vaute, L., Brach, M., Gentier, S., Jeannot, R., Jacquot, Audigane, P., Tran-Viet, T., Jung, R., Baumgaertner, J., Baria, R., and Gerard, A. (1998) A tracer test at the Soultz-sous-Forets Hot Dry Rock geothermal site: *Proc. Twenty-Third Workshop on Geothermal Reservoir Engineering*, Stanford University, SGP-TR-158, 343-347.

References

- Greim H., Ahlers, R., Bias, R., Broecker, B., Hollander, H., Gelbke, H.P., Klimisch, H.J., Mangelsdorf, I., Paetz, A., Schon I., Stropp, G., Vogel, R., Weber, C., Ziegler-Skylakakis, K., and Bayer, E. (1994) Toxicity and Ecotoxicity of Sulfonic Acids: Structure-Activity Relationship: *Chemosphere*, 28(12), 2203-2236.

GAS ANALYSIS OF GEOTHERMAL FLUID INCLUSIONS: A NEW TECHNOLOGY FOR GEOTHERMAL EXPLORATION

Principal Investigators – David I. Norman
Department of Earth and Environmental Science
New Mexico Tech, Socorro, NM 87801, USA
email: dnorman@nmt.edu

Key Words - geothermal, gas, analysis, fluid, inclusion, exploration, monitoring, tracer, technology, stratigraphy, monitoring, plume, reservoir, magmatic, meteoric, air, saturated, water, condensation, condensate, boiling

Project Background and Status

In 1994 ideas about geothermal gas chemistry were vague. Gaseous species are commonly the principal dissolved component in geothermal fluids, but the significance of the gas chemistry was mostly overlooked. Giggenbach presents the basic geothermal equilibrium gas chemistry (Giggenbach 1980) and calculates how boiling might affect CO₂-CH₄-H₂ ratios in geothermal fluids (Giggenbach 1986). However, attempts at using gas equilibrium geothermometers for geothermal exploration largely failed.

I began collaboration with Joe Moore and Jeff Hulen, and later Sue Lutz at EGI, University of Utah, in 1994. We hypothesized that fluid inclusion gas analyses would complement their petrographic and fluid inclusion studies, and thus provide a comprehensive picture of geothermal system processes and evolution. That year I published a paper (Norman 1994), developing an idea brought forth by Giggenbach (1986), which shows that fluid inclusion gas analysis can identify a magmatic component in inclusion fluids. One of our goals was to apply this new tool to the study of active geothermal systems. Our collaboration has resulted in a number of publications that expand the science of geothermal gas chemistry and increase our understanding of geothermal processes and evolution (Moore 1995; Moore 1997; Lutz 1999; Adams 2000; Lutz 2002) (Moore 1997; Moore 1998; Moore 1998; Moore 1999; Moore 2000; Moore, Norman et al. 2001) (Norman 1994; Norman 1996; Norman 1997; Norman 1998; Norman 1999) (Norman 2001; Norman 2001; Norman 2002; Norman 2002)

In 1999 it was evident that with our increased understanding of geothermal gas chemistry that it could be a valuable tool for geothermal exploration. It was also apparent that geothermal gas chemistry had proven to be a valuable instrument for

understanding evolution of geothermal systems, and that it order for Norman to spend more time on this work, funding was required. Therefore, funds were sought from the DOE university Geothermal Program.

Project Objective

The principal objective was to increase our knowledge of gaseous species in geothermal systems by fluid inclusion analysis in order to facilitate the use of gas analysis in geothermal exploration.

Approach

Update the New Mexico Tech fluid inclusion gas analysis facility.

1. Add to the merger data base of magmatic gases by measuring gases in magmatic glass inclusions.
2. Analyze the volatiles in Karaha fluid inclusions studied by Joe Moore.
3. Develop a technology base for the analysis of fluid inclusion organic compounds.
4. Develop methods of applying geothermal gas analysis to geothermal exploration using knowledge gained during the project

Research Results

Sub-objectives 1-4 above were completed and reported on (Blamey Nigel J.F. 2001; Norman 2001; Norman 2001; Blamey 2002; Norman 2002; Norman 2002). Here I will report new methods for applying geothermal gas analysis to geothermal exploration, which is the main subject of the proposal.

The unique approach that was developed is to look at gas chemistry as a product of components from meteoric, crustal, and magmatic sources that are modified by geothermal processes of boiling, mixing, and condensation. Five assumptions are made: 1) gas chemistry of geothermal reservoir fluids is different than gas chemistry of non-thermal waters; 2) reservoir fluids commonly have additions of magmatic volatiles that have specific He-N₂-Ar ratios; 3) there are three sources of volatile compounds: magmas, the crust by wall rock reactions, and the atmosphere; 4) boiling, condensation, and fluid mixing processes result in systematic changes in gas chemistry; and 5) gas chemistry of past geothermal systems may also be determined by fluid inclusion gas analysis. The rationale for the interpretations we use is explained in detail elsewhere (Norman 2001; Blamey 2002; Norman 2002) and references therein. I will discuss examples of applying geothermal gas analysis to grass roots exploration at the Lightning Dock geothermal area, NM; to drill core chips at the Coso

geothermal field; and to monitoring production at the Cerro Prieto field.

Lightning Dock

The Lightning Dock, Animas Valley, New Mexico geothermal area was discovered when a rancher found boiling water while drilling a shallow stock tank well (Elston, Deal et al. 1983). There are no surface manifestations of present or past geothermal activity in the Animas Valley. There is no geophysical low-resistivity anomaly. The only item to investigate is the waters in stock tank wells. Norman and Bernhart (Norman 1982) analyzed the gases, and water chemistry in the discovery well and 15 stock tank wells nearby (Fig. 1). The well temperatures are typical of shallow well waters; we did not know how to interpret the gas analyses at that time, and other geochemical analyses showed no identifiable geothermal input. AMAX Geothermal failed to find reservoir fluids in 8 boreholes drilled there in the late 70's.

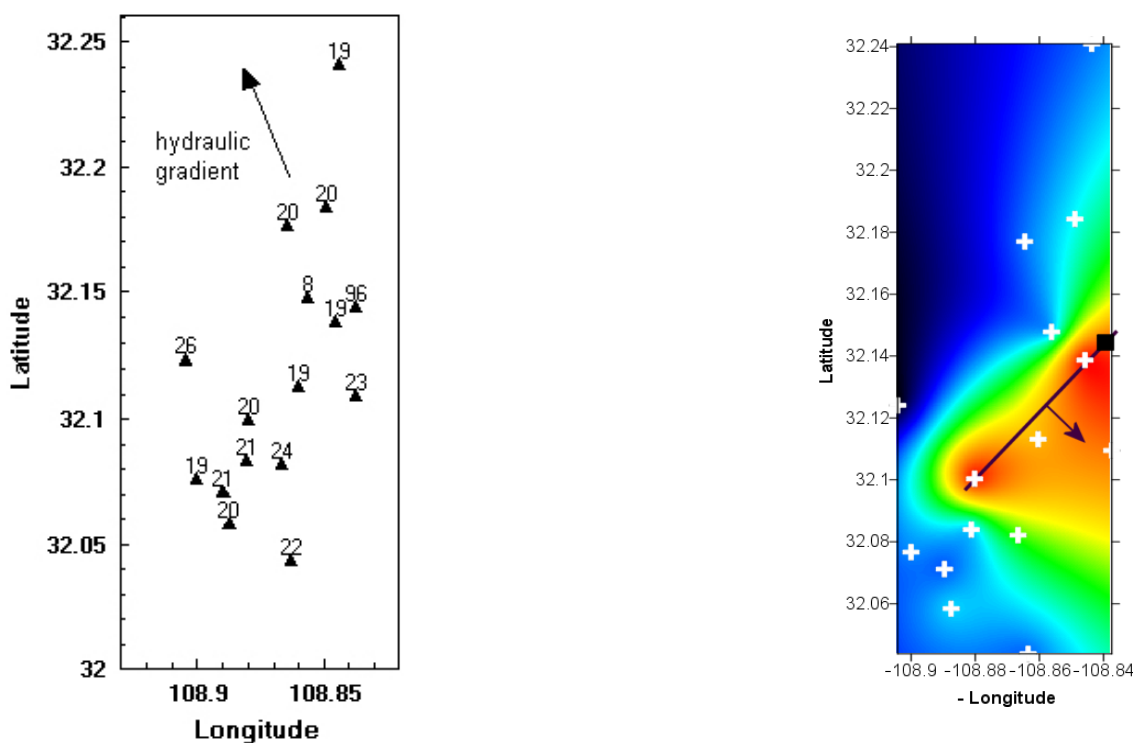


Figure 1 (Left) Location of the wells sampled in the Lightning Dock geothermal area. The number above each well is the measured well temperature. (Right) The right-hand figure is a Surfer® contour-image plot that shows the location of a vapor plume at Lightning Dock. The highest values of total gas are red and lowest values in dark blue. The white crosses are well locations; the black square is the discovery well. An inferred fault is shown with the dip direction. This newly developed method of using gas analyses to find condensed vapor shows a drilling target, whereas common geochemical methods used in geothermal exploration do not work at Lightning Dock..

Reevaluating our analyses now it is apparent that the discovery well gas chemistry indicates boiling. The discovery well water has about 1/1000 the N_2 common in groundwater, which implies that the well fluid was degassed by subsurface boiling. The working assumption is that vapor generated by boiling Lightning Dock waters should exit the surface because there is no sign of vapor blockage and resulting hydrothermal eruptions. This flux of volatiles should condense some soluble species in shallow ground water. A gas mixing-condensation diagram (Norman 2002) was constructed (Fig. 2) that clearly confirms condensation, and as well shows mixing between groundwater and the discovery well. The wells that exhibit fluid mixing are the two wells that are NNE and down the hydraulic gradient from the discovery well. Total gas amounts, save for the discovery well, were projected onto the condensation line, and the values kriged and contoured using Surfer® software (Fig. 1). This analysis shows the location of a gas plume, and suggests a structure trending NE-SW from the discovery site dipping to the SE. There are structures trending NE in the Lightning Dock district (Elston, Deal et al. 1983). However, the structure the gas data suggests is not shown on maps because the Animas Valley is covered by thick gravel.

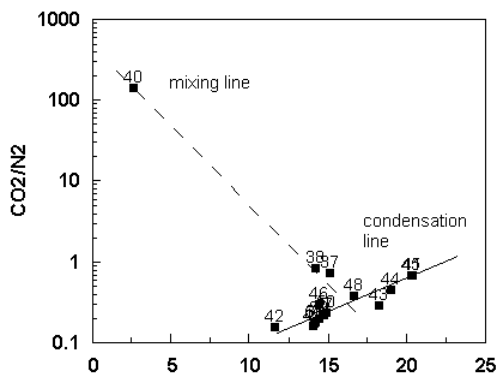


Figure 2. Analyses of Animas Valley wells shown in Figure 1 are plotted on a condensation diagram (Norman 2002). Numbers above data points are the well number. The condensation trend is labeled. A mixing line is constructed from the discovery well #40 through wells # 37 and 38. This diagram shows how gas data may be used to construct a fluid-mixing diagram. Mixing diagrams are a standard tool in interpreting geothermal fluids, however mixing diagrams to date use dissolved solids. Stock-tank well analyses fall on a condensation line (Norman 2002) hence; indicate a rising plume of volatiles modifies groundwater gas compositions.

Exploration Using Drill Chips

Several oil companies routinely use “Fluid Inclusion Stratigraphy” (FIS) whereby fluid inclusion volatiles in exploration-well drill-chips are analyzed at intervals of 10 or 20m (Hall 2002). Gas concentrations are plotted on well strip chart or mudlogs, and the stratigraphic intervals that act as seals and pay intervals for oil and methane are readily apparent (Fig. 3). This type of correlation should work for geothermal system exploration as well. Minor fractures penetrate far into the county rock from major structures in geothermal systems (Hickman, Barton et al. 1998), and they form secondary inclusions as they heal within a few years at geothermal system temperatures. FIS is not used in the geothermal industry because it was not known how to distinguish reservoir fluid inclusions from groundwater-filled fluid inclusions. Hydrocarbon-bearing fluids are easily distinguished by inclusions that contain organic compounds.

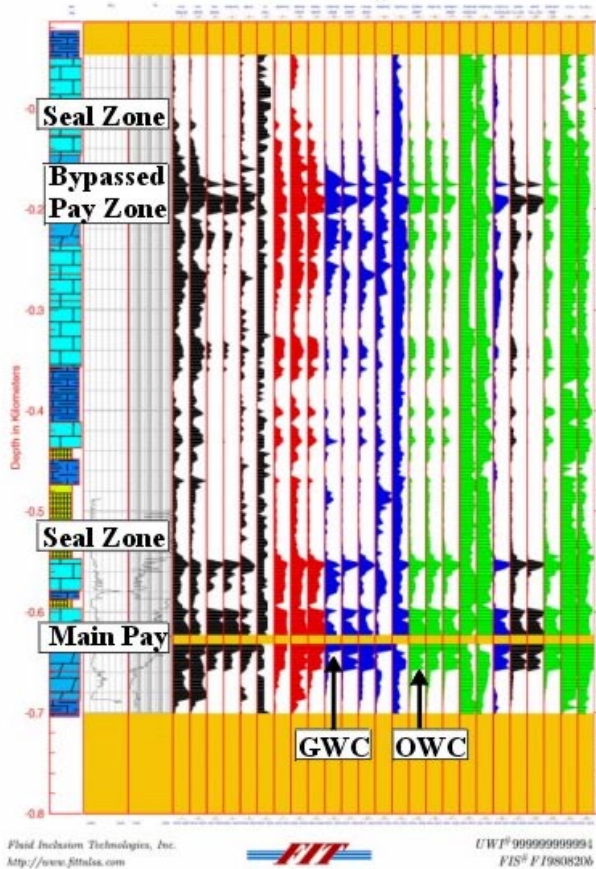
In order to test FIS for geothermal exploration, we analyzed Coso well 83-16 drill chips selected at 1000 ft intervals by Joseph Moore. Sequential crushes done by our CFS (crush-fast-scan) method (Norman 1996) show that chips have a high density of homogeneous fluid inclusions. Analyses were averaged and plotted versus depth (Fig. 4), and interpreted (Figs 4 and 5). Fluid inclusion gas analyses done on vein minerals from drill hole 68-6 that we earlier analyzed (Adams 2000) were plotted for comparison (Fig. 4) in order to confirm that similar analyses are obtained from chips and vein minerals.

It is apparent looking at Fig. 4 that fluid inclusion analysis detects a change in gas chemistry at about 5,500 ft, which is the top of the Coso production zone. Analyses for both wells show: 1) boiling fluids with a magmatic component below about 5000 ft; 2) a change in gas chemistry at 5000-6000 ft; 3) non-boiling, meteoric fluids immediately above 5000 ft; and 4) fluids with a magmatic component or boiling in waters < 1700'. Our interpretation of well 83-16 is that inclusions below 6,000 ft are samples of boiling reservoir waters (Fig. 5). Lack of boiling and meteoric N_2/Ar ratios above 5000 ft indicate the geothermal system is dominated by cooler meteoric waters there. The change in fluid chemistry and drop in fluid temperature at 5000-6000 ft. is best explained by a permeability seal. The indicated gas cap at about 5,500 ft in well 68-6 also indicates a seal. Near-surface fluids have the characteristics of steam-heated waters with elevated H_2S and C_6H_6 and or a magmatic component. The difference in chemistry

between surface waters and the immediately deeper fluid suggests a seal that must be penetrated by a few fractures transmitting steam from boiling reservoir fluids. The interpretation agrees well with the well log for bore hole 83-16 that shows the well cased to 6,000 ft, a decrease in fluid temperatures at depths above 5,500 ft, and an increase in temperatures at depths <1,700 ft. Our trial analyses

roughly indicate the Coso reservoir top. In actual practice, where analyses are done at more closely spaced intervals, we expect much better precision in determining reservoir boundaries. We expect that a greater density of analyses will also identify productive fractures as well.

FIS Example 1



FIS Analysis of a Michigan Basin Discovery Well, SW Ontario:

The top of the targeted Silurian Reef occurs at 626m. FIS data identify the gas-oil contact at approximately 638m and the oil-water contact at about 656m. This information can be used to optimize completion strategies.

A shallower, Devonian section at 176-194m correlates with a zone of stained, porous dolomite. The interval was not logged and is typically drilled overbalanced. Hence, information on petroleum charge from standard wellsite techniques can be misleading. This section is interpreted to represent a bypassed pay interval in the area.

The shallow and deep anomalies are separated by what appear to be effective seal rocks.

FIS Species Key:

- Black** = inorganic volatile compounds
- Red** = gas-range organic volatile species
- Blue** = water-soluble volatile compounds
- Green** = liquid-range organic volatile species

Figure 3. A "Fluid Inclusion Stratigraphy" example for a hydrocarbon well. Fluid inclusion analyses are performed on drill-chips taken at intervals of 30 or 60 feet and the relative heights of mass peaks corresponding to major species are plotted on mudlogs.

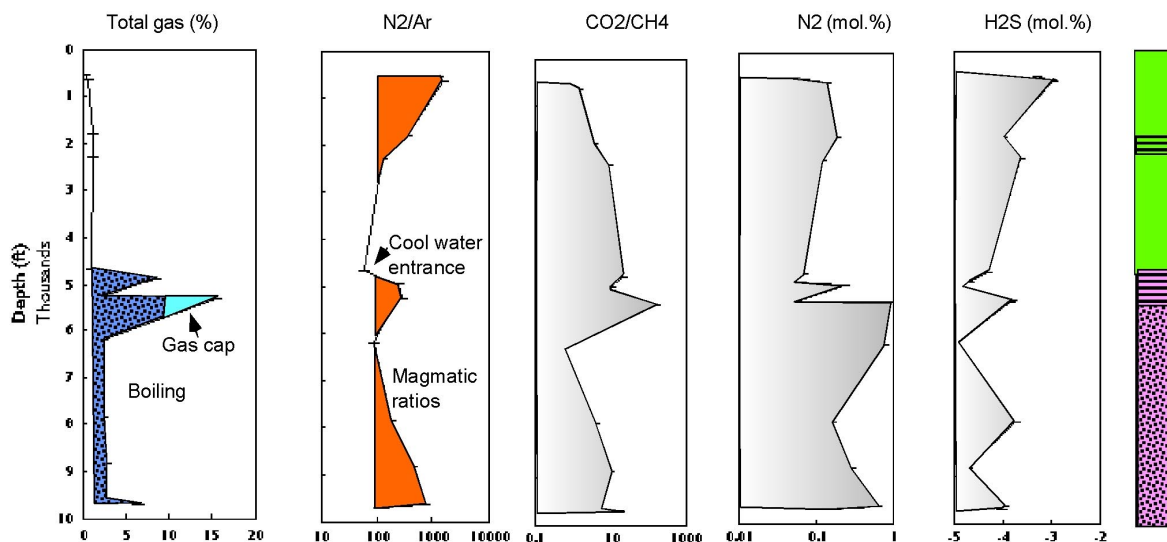


Figure 4 (Upper) Analysis of nine Coso well 83-16 drill-chip samples plotted versus depth in thousands of feet. TOT GAS is total gaseous species, K'' is the Fischer-Tropsch reaction coefficient, and TORG is the sum of C_2 - C_7 organic species. Orange-filled areas indicate magmatic ratios; blue-filled areas on TOT GAS and K'' columns are values that indicate boiling. (Lower) Analyses of twelve vein samples from Coso well 68-6 are plotted versus depth. Filled areas in N_2/Ar columns and total gas columns respectively indicate values for magmatic fluids and fluid boiling. See Fig. 5 for the explanation for the interpretive column at the right.

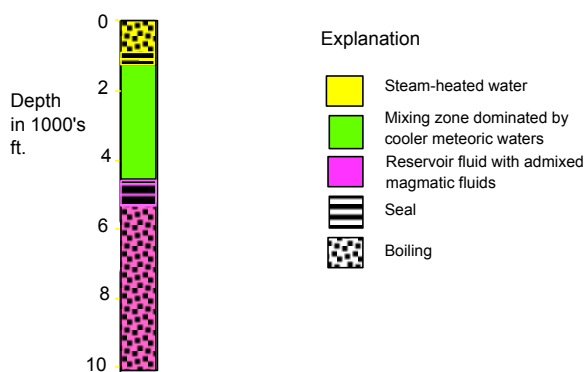


Figure 5. An interpretation of fluid types, fluid processes, and seal locations in Coso well 83-16, based on fluid inclusion gas analysis. The gas data is displayed in Figure 4. See text for an explanation of how the interpretations are made.

The preliminary analyses strongly indicate that FIS stratigraphy can be applied to geothermal systems. FIS will provide the same type of benefits it does in hydrocarbon exploration. It can be used with other well logging tools to maximize well production by showing productive and non-productive bore-hole intervals. Commercial lab analyses are relatively inexpensive at \$2,000 to \$6,000 per bore hole

(Hall 2002), the turnaround is in days, and data from commercial labs are formatted to be accepted by common strip log and mudlogging computer programs.

FIS analyses will have to be plotted differently than is done for the oil industry. Ratios of gaseous species that indicate fluid sources and fluid boiling will have to be added, and analyses of many organic compounds can be reduced. A valuable side benefit of FIS analyses is that analyses from a number of drill holes can be combined to provide a cross-sectional map of the reservoir (see Fig. 6).

Producing Systems - Cerro Prieto

A new way to monitor producing fields is introduced in (Norman 2002). The flow of geothermal fluids is mapped at the production level by use of gas chemistry obtained in routine field monitoring. Cerro Prieto gas analyses collected by Cathy Janik and Alfred Truesdell from 1977 to 1998 are used for the demonstration analyses (Fig. 7). Cerro Prieto CO_2/N_2 and N_2/Ar ratios correlate (N_2/Ar ratios show contributions of magmatic volatiles), thus the sum of these ratios is used to tag magmatic-volatile-rich reservoir fluids.

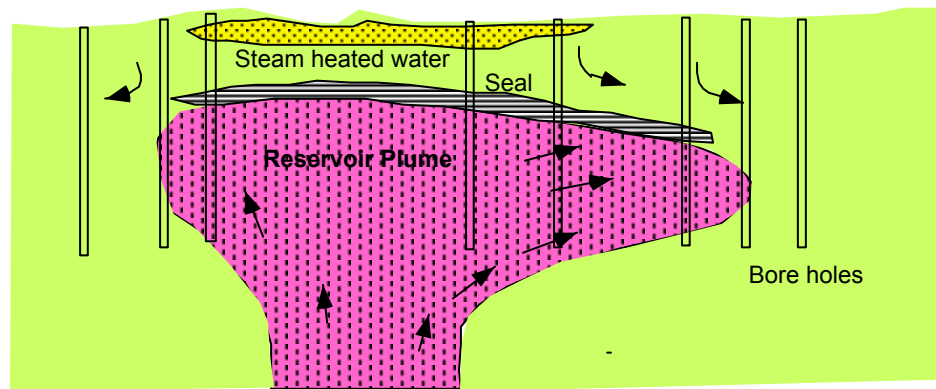


Figure 6. Schematic cross section of a geothermal system like Coso showing conceptually how fluid inclusion stratigraphy interpretations, like those in Figs. 4 and 5, may be used to determine the location of a well site with respect to the center, margin, or outside of the geothermal system.

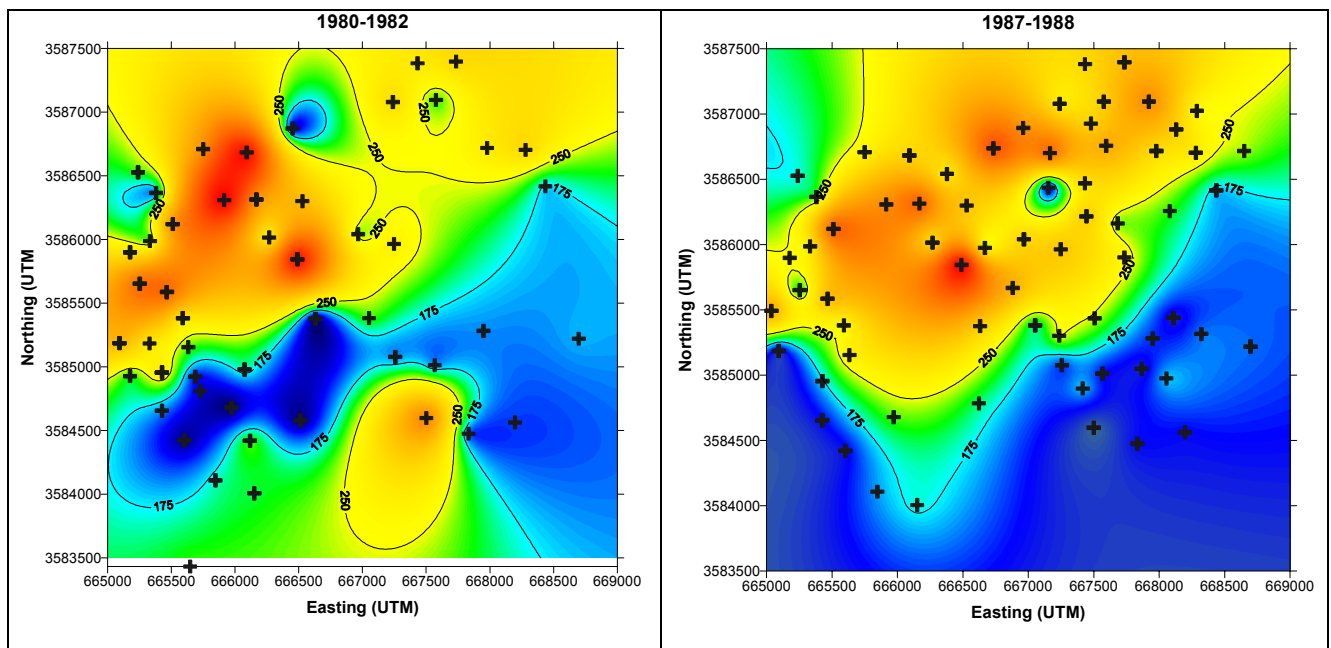


Figure 7. Contour plots of the Cerro Prieto geothermal plume produced by contouring $N_2/Ar + CO_2/N_2$ ratios in gas analyses performed during 1980 to 1982 (left) and 1987-1988 (right). Values below 175 are waters with little or no meteoric component. Values > 250 are fluids with a magmatic component. Gradations of blue to red show the respective proportions of meteoric and magmatic gaseous species. Black crosses locate wells that provided data for the map.

The analyses show that reservoir fluid-flow changes with time, most probably as a result of a changing stress field change. The wells in the red areas on Figure 7 have the highest enthalpies (temperatures), and generally have sustained production for the period 1977-1988. During 1980-1982 there appears to be a NW trending control on magmatic-vapor-rich fluids that coincides with a major NW trending fault. The map for 1986-1988 shows the southern part of the field dominated by meteoric waters, and a shift in the magmatic-vapor-rich waters to a NE trend. Wire frame and shaded image diagrams (Fig. 8) more clearly show the linear features. A vector plot (Fig.9) shows direction of reservoir fluid flow, and should be useful in planning injection well locations.

At Cerro Prieto geophysics and mapping indicates these NE-trending structures (Lippmann 1997). The area of blue-colored meteoric gas-dominated waters that trend NE in the 1980-1982 map (Fig. 7, Left) corresponds to the “H” fault that dips to the SE (Lippmann 1997), which they conclude is an important control on recharge into the reservoir. Contours of Cerro Prieto fluid salinity, enthalpy, and oxygen isotopic compositions (Lippmann 1997) also show a NE trend. Hence, NE-trending structures must be the main controls on Cerro Prieto fluids. Gas data alone (Fig. 8) appear to locate these structures.

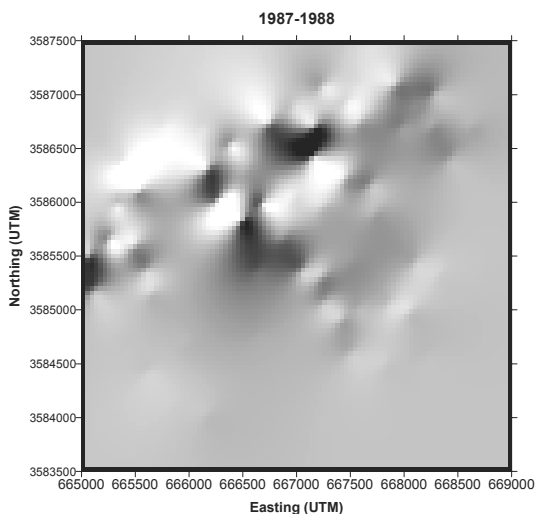


Figure 8. A shaded relief map (upper) produced from 1987-1988 gas analyses using SURFER® software. The map shows the location of structures that control reservoir fluids.

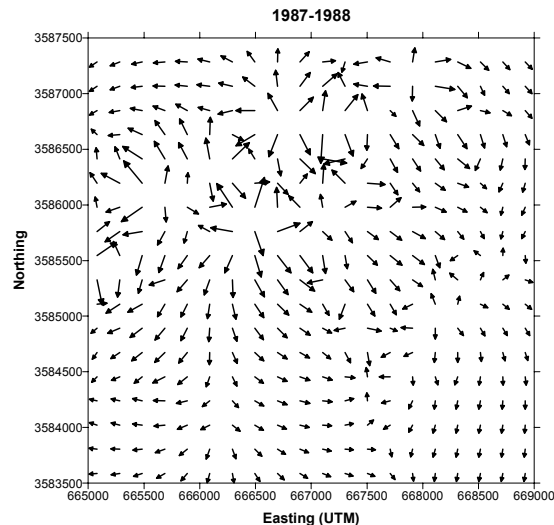


Figure 9. Gas analyses shown in Fig. 7 are shown in a SURFER® vector plot. It shows the maximum rate of change from fluids with a magmatic gas component to fluids with meteoric and crustal gaseous species. Thus, the vectors should indicate the direction and magnitude of reservoir fluid flow.

Our examination of Cerro Prieto gas analyses indicates that the geothermal system structure is changing with time. Gas data appear to be very useful for monitoring changes of geothermal reservoir fluid flow and identifying controlling structures, which should prove useful in maintaining field production. Gas compositions are basically shown to act as free-of-cost tracers, and should work equally well in monitoring reinjection fluids. Gaseous species are routinely measured in most geothermal fields, hence fluid-flow plots as presented here can be accomplished with little cost. Gas analytical data, therefore, are useful in developing management procedures for geothermal fields characterized by complicated, highly-fractured reservoirs where flow patterns may change with time.

Details

Who Thinks the Research is Useful

- Starting May 12, 2002 we are going to work with Lightning Dock Geothermal to do a detailed gas plume map in the same area shown in Fig. 2. The company plans to start a drilling program late summer 2002.

- We will be analyzing chips on the new holes being drilled at Coso by the US Navy. We are planning with Caithness Energy on performing FIS analysis on chips from about 40 Coso boreholes. Analyses will be made by a commercial lab. We will help interpreting the analyses.
- Ridgeway Petroleum Corp. of Calgary, Canada who is drilling in New Mexico for CO₂-He gas wishes to have drill chip analyses made during their drilling program.

Collaborations

Principal collaborations are with Joe Moore, Jeff Hulen, and Sue Lutz at EGI, University of Utah, and the companies mentioned above Lightning Dock Geothermal, US Navy, Caithness Energy, and Ridgeway Petroleum Corp.

Papers Published: Papers published are: (Blamey Nigel J.F. 2001; Moore, Norman et al. 2001; Norman 2001; Norman 2001; Blamey 2002; Lutz 2002; Norman 2002; Norman 2002)

Students Supported: Nigel J.F. Blamey, Postdoc and Penny Ortiz, undergraduate Research Assistant

References

- Adams, M. C., Moore, J. N., Bjornstad, Norman, D.I (2000). "Geologic history of the Coso geothermal system." Transactions, Geothermal Resources Council 24: 205-209.
- Blamey, N., Norman, David I. (2002). New Interpretations of Geothermal Fluid Inclusion Volatiles: Ar/He and N₂/Ar ratios - A Better Indicator of Magmatic Volatiles, and Equilibrium Gas Geothermometry. PROCEEDINGS, Twenty-Seventh Workshop on Geothermal Reservoir Engineering Stanford University, Stanford, California.
- Blamey Nigel J.F., D. I. N. (2001). " Fluid Inclusion Evidence for a Supercritical Magmatic Fluid, Modified by Wall-rock Interaction and Mixing with Meteoric Waters." PROCEEDINGS, Twenty-Sixth Workshop on Geothermal Reservoir Engineering Stanford, California, January 29-31, 2001: 243-251.
- Elston, W. E., E. G. Deal, et al. (1983). Geology and geothermal waters of Lightning Dock region, Animas Valley and Pyramid Mountains, Hidalgo County, New Mexico, New Mexico

Bureau of Mines and Mineral Resources, United States.

Giggenbach, W. F. (1986). The use of gas chemistry in delineating the origin of fluids discharges over the Taupo Volcanic Zone: A review. International Volcanological Congress, Hamilton, New Zealand,.

Giggenbach, W. F. T. G. g. e. (1980). "Geothermal gas equilibria." *Geochimica et Cosmochimica Acta* 44(12): 2021-2032.

Hall, D. (2002). Fluid Inclusion Technologies, Inc.

Hickman, S. H., C. A. Barton, et al. (1998). In situ stress and fracture permeability along the Stillwater fault zone, Dixie Valley, Nevada. 36th U. S. Rock mechanics symposium. New York, NY, Pergamon, Oxford-New York, International: 414.

Lippmann, M. J., Alfred H. Truesdell, Héctor Gutiérrez Puente (1997). Fluid Recharge at the Cerro Prieto Geothermal Field, U.S. Department of Energy Geothermal Energy Technical Site.

Lutz, S. J., Joseph N. Moore, Nigel J.F. Blamey, David I. Norman (2002). "Fluid-Inclusion Gas Chemistry of the Dixie Valley (NV) Geothermal System." PROCEEDINGS, Twenty-Seventh Workshop on Geothermal Reservoir Engineering Stanford University (in press).

Lutz, S. J., Moore, J. N., Adams, M. C., Norman, D. I., 1999, (1999). "Tracing fluid sources in the Coso geothermal system using fluid-inclusion gas chemistry." 24th Workshop on Geothermal Reservoir Engineering, Stanford University: 188-195.

Moore, J., Norman, D., Hulen, J. (1995). "Evolution of The Geysers: Data from fluid inclusion microthermometry and gas chemistry." 17th New Zealand Geothermal Workshop: 77-82.

Moore, J. N., Anderson, A. J., Adams, M. C., Aines, R. D., Norman, D. I., Walters, M. A. (1998). "The fluid inclusion and mineralogic record of the transition from liquid- to vapor-dominated conditions in The Geysers geothermal system, California." Twenty-third Workshop on Geothermal Reservoir Engineering, Stanford University: 211-218.

- Moore, J. N., D. I. Norman, et al. (2001). "Fluid inclusion gas compositions from an active magmatic hydrothermal system: A case study of The Geysers geothermal field, USA." *Chemical Geology* 173: 3-30.
- Moore, J. N., Norman, D. I., Kennedy, B. M., Adams, M. C. (1997). "Origin and chemical evolution of The Geysers, California, hydrothermal fluids: Implications from fluid inclusion gas compositions: Geothermal Resources Council Annual Meeting, 1997." 635-641.
- Moore, J. N., Norman, D. I., Kennedy, B. M., Adams, M. C. (1999). "The thermal and chemical evolution of the hydrothermal minerals in Awibengkok 1-2, Awibengkok geothermal field, Indonesia." *Geothermal Resources Council Transactions*: 25-29.
- Moore, J. N., Powell, T. S., Bruton, C. J., Norman, D. I., Heizler, M. T., 1998, (1998). "Thermal and chemical evolution of the Tiwi geothermal system, Philippines." *Proceedings of the 9th International Conference on Water-Rock Interaction, Taupo, N.Z.*: 671-674.
- Moore, J. N., Powell, T. S., Heizler, M. T., Norman, D. I (2000). "Mineralization and hydrothermal history of the Tiwi geothermal system, Philippines." *Economic Geology* 95(1001-1023).
- Moore, J. N., Powell, T. S., Norman, D.I., Johnson, G. (1997). "Hydrothermal alteration and fluid-inclusion systematics of the reservoir rocks in Matalibong-25, Tiwi, Philippines: Twenty Second Workshop on Geothermal Reservoir Engineering, Stanford University." 447-456.
- Norman, D. I., Bernhart, C (1982). *Assessment of geothermal reservoirs by analysis of gases in thermal waters*, New Mexico Energy Institute, EMI-2-68-2305.
- Norman, D. I., Chomiak, B. A., Moore, J. N., (1998). "Approaching equilibrium from the hot and cold sides in the pyrite-pyrrhotite-magnetite-H₂S-CO₂-CH₄ system in light of fluid inclusion gas analysis. *Proceedings of the 9th International Conference on Water-Rock Interaction, Taupo, N.Z., Taupo, New Zealand.*
- Norman, D. I., Moore, J. N. (1994). "Fluid source tracing via fluid inclusion gas analysis in an evolving magmatic system: The Geysers California (abs.)." *VII International Symposium on the Observation of the Continental Crust Through Drilling, Santa Fe, N.M., April 25-30, 1994.*
- Norman, D. I., Moore, J.N (1999). *Methane and Excess N₂ and Ar in geothermal fluid inclusions. Proceedings: Twenty-fourth Workshop of Geothermal Reservoir Engineering, Stanford University, Stanford, California.*
- Norman, D. I., Moore, J.N., Musgrave J. (1997). *Gaseous species as tracers in geothermal systems. Proceedings: Twenty-second Workshop of Geothermal Reservoir Engineering, Stanford University, Stanford, California.*
- Norman, D. I., Moore, J.N., Yonaka, B., Musgrave, J (1996). *Gaseous species in fluid inclusions: A tracer of fluids and an indicator of fluid processes. Proceedings: Twenty-first Workshop of Geothermal Reservoir Engineering, Stanford University, Stanford, California.*
- Norman, D. I., Musgrave, J.A. (1994). "N₂-Ar-He compositions in fluid inclusions: Indicators of fluid source." *Geochimica et Cosmochimica Acta* 58: 1119-1131.
- Norman, D. I., Nigel Blamey (2002). "New Applications of Geothermal Gas Analysis to Exploration." *Geothermal Resources Council Transactions (in press).*
- Norman, D. I., Nigel Blamey, Joseph N. Moore (2002). *Interpreting Geothermal Processes and Fluid Sources from Fluid Inclusion Organic Compounds and CO₂/N₂ Ratios. PROCEEDINGS, Twenty-Seventh Workshop on Geothermal Reservoir Engineering Stanford University, Stanford, California.*
- Norman, D. I., Nigel J.F. Blamey Joseph N. Moore (2001). *Overabundance of Gaseous Species and the Source of Organic Compounds in Geothermal Fluids. PROCEEDINGS, Twenty-Sixth Workshop on Geothermal Reservoir Engineering, Stanford University, Stanford, California.*
- Norman, D. I. and Blamey, Nigel J.F., (2001). "Quantitative Analysis of Fluid Inclusion Volatiles with a Two Mass Spectrometer System." *Proceedings of ECROFI XVI, Oporto, Portugal, April, 2001.*

Key Word Index

3D map - 43
air - 91
analysis – 3, 5, 10, 20, 21, 23, 24, 26, 30, 36, 43, 44, 6, 53, 57, 58, 59, 60, 62, 64, 65, 66, 68, 72, 77, 79, 80, 81, 82 83, 84, 85, 86, 87, 89, 90, 91, 93, 94, 112, 115, 117, 118, 119, 121, 124, 125
Awibengkok – 30, 64, 65, 66, 67, 68, 69, 70, 71, 116, 125
Basin & Range – 1, 2, 10, 11, 12, 13, 14, 17, 18, 19, 42
boiling – 12, 21, 24, 28, 29, 30, 69, 98, 101, 106, 108, 109, 117, 118, 119, 120, 121
borehole effects – 50, 51, 53, 54, 55, 57, 58, 59
breakout – 50, 54, 105, 106
breccias - 2
capillary pressure – 87, 88, 89, 91
computer models - 73
conceptual model – 1, 2, 3, 14, 27, 30, 41, 83
condensate – 29, 87, 117
condensation – 92, 118, 119
COSO – 4, 13, 43, 44, 46, 47, 48, 49, 102, 118, 119, 120, 121, 122, 124
Cove Fort-Sulphurdale Utah – 5, 19, 20, 21, 25, 26, 104
crack density – 43,, 46, 47
crack distribution – 43, 46, 48, 49
deformation – 35, 40, 81, 84, 86
Dixie Valley – 1, 2, 3, 4, 10, 11,12, 14, 16, 17, 19, 20, 23, 24, 25, 38, 40, 41, 59, 62, 83, 102, 103, 111, 113, 114, 155, 116, 124
dynamics – 32, 106, 108
electrical properties – 38, 64, 65, 67, 68, 69, 70
electromagnetics – 40, 41, 42, 51, 55
EOS – 41, 48, 49, 94, 101, 106, 109, 110
evolution – 1, 2, 5, 12, 27, 28, 29, 30, 32, 33, 35, 36, 79, 92, 93, 108, 117, 124, 125
exploration – 2, 3, 5, 10, 11, 12, 13, 14, 17, 20, 21, 24, 25, 26, 27, 28, 37, 40, 41, 43, 50, 51, 54, 63, 64, 117, 118, 119, 121, 125
extension – 2, 10, 12, 15, 35, 36, 41, 42, 79, 81
faults – 1, 11, 12, 17, 20, 21, 22, 23, 24, 48, 78, 83
finite element – 39, 81, 82, 84, 85
fluid flow – 2, 4, 11, 12, 36, 51, 52, 55, 56, 72, 73, 74, 77, 78, 81, 82, 84, 85, 86, 87, 111, 123
fluid inclusion – 27, 28, 29, 30, 31, 33, 34, 109, 117, 118, 119, 120, 121, 122, 124, 125
fluid properties – 33, 35
fluorescein – 98, 103, 111, 112, 114, 115, 116
fluorescence detection - 112

fluorinated alcohols – 100, 101, 102
fracture mechanics – 72, 73, 79, 80
fracture network – 2, 69, 72
fractures – 1, 12, 17, 30, 32, 50, 51, 54, 55, 59, 60, 68, 72, 75, 77, 78, 79, 80, 81, 82, 83, 84, 85, 89, 90, 91, 120
gas – 3, 21, 27, 30, 64, 88, 89, 91, 98, 101, 105, 106, 107, 113, 117, 118, 119, 121, 122, 123, 124, 125
geophysics – 30, 40, 41, 42, 49, 54, 84, 123
Geothermal system – 1, 2, 3, 4, 5, 10, 11, 12, 13, 14, 15, 17, 18, 20, 21, 25, 27, 28, 29, 30, 31, 36, 37, 38, 41, 79, 84, 91, 94, 100, 103, 104, 105, 108, 111, 117, 118, 119, 121, 122, 123, 124, 125
geothermal tracers – 98, 103, 111, 112, 115, 116
geysers – 1, 3, 4, 5, 15, 19, 27, 32, 33, 34, 36, 46, 48, 49, 65, 66, 67, 68, 69, 70, 71, 87, 89, 100, 103
GIS – 25, 104
Glass Mountain – 1, 2, 3, 4
granite - 80
granitoid - 5
heat content – 105, 110
heat transfer – 11, 81, 86
hydrothermal - 1, 2, 3, 4, 5, 14, 15, 20, 21, 23, 24, 27, 30, 32, 33, 34, 35, 36, 64, 93, 105, 106, 110, 111, 114, 119, 125
hydrothermal alteration – 23, 24, 28, 35, 68, 125
hydrothermal system – 1, 2, 4, 30, 32, 33, 125
Hyperspectral – 20, 21, 23, 24, 25
igneous intrusion = 2
induction logging – 50, 53, 54, 57, 58, 60, 62, 63
injection – 2, 4, 11, 14, 39, 52, 56, 72, 74, 77, 78, 80, 81, 82, 83, 87, 88, 89, 90, 92, 98, 100, 102, 103, 105, 107, 111, 115, 123
instrumentation – 37, 41, 55, 55
magmatic – 27, 29, 39, 117, 118, 119, 121, 122, 123, 124, 125
meteoric – 11, 29, 118, 119, 122, 123, 124
mineralization – 3, 5, 24, 30, 125
mineralogy – 2, 3, 20, 23, 24, 25, 30, 64, 66
monitoring – 3, 5, 39, 46, 52, 56, 64, 77, 104, 118, 121, 123
multi-physics - 85
nanocollidal silica - 93
naphthalene sulfonates – 98, 111, 112, 113, 116
numerical simulation – 37, 87
permeability – 2, 4, 12, 20, 21, 29, 38, 53, 57, 62, 70, 72, 74, 83, 85, 87, 88, 89, 90, 91, 105, 106, 108, 119, 124
phase coexistence - 108

physical models – 64, 69
 plume – 118, 119, 122, 123
 porosity – 2, 4, 52, 56, 65, 66, 67, 68, 69, 72, 92
 production chemistry - 106
 relative permeability – 87, 88, 89, 90, 91
 remote sensing – 20, 25, 26, 30, 31
 reservoirs – 1, 14, 17, 27, 32, 37, 42, 43, 48, 58, 64, 69, 72, 78, 81, 85, 87, 88, 89, 90, 104, 106, 108, 110, 111, 112, 113, 114, 115, 116, 123, 125
 rhyolite – 4, 5
 Salton Sea – 1, 3, 4, 5, 19, 25, 92, 93, 94, 109
 saturated – 45, 46, 52, 56, 65, 66, 67, 68, 71, 79, 91, 115
 scaling – 4, 51, 55, 69, 90, 105, 107, 109, 110
 shear-wave splitting – 43. 44. 47. 48. 49. 72
 silica scale – 92, 93, 94, 107
 simulations – 39, 58, 59, 60, 61, 62, 76, 84, 106, 108, 110
 solubility – 94, 98, 100, 101, 107
 steam-water flow – 87, 88
 stratigraphy – 119, 120, 121, 122
 supercritical fluids - 36
 technology transfer – 4, 14, 20, 25, 37, 39, 52, 57, 62, 69, 94, 102, 105, 110, 115
 temperature – 1, 2, 3, 4, 5, 11, 12, 13, 14, 19, 27, 28, 29, 33, 35, 36, 64, 69, 72, 73, 77, 78, 82, 83, 89, 90, 91, 98, 100, 101, 102, 103, 105, 106, 107, 108, 109, 111, 112, 113, 114, 115, 116, 118, 119, 121, 123
 The Geysers¹, 3, 4, 5, 13, 27, 28, 30, 34, 43, 44, 48, 49, 64, 67, 68, 70, 87, 89, 98, 99, 100, 102, 103, 124, 125
 thermodynamic properties - 105
 tracers – 98, 99, 100, 102, 103, 104, 111, 112, 113, 114, 115, 116, 123, 125
 two-phase tracers – 98, 99, 100, 102, 103, 104, 111, 112, 113, 114, 115, 116, 123, 125
 vapor-dominated regimes
 vapor-phase tracers
 velocities – 64, 65, 66, 67, 68, 69, 70, 71
 volcanic-hosted geothermal systems – 27, 30
 water injection – 74, 77, 87, 88, 89, 90, 102

Author Index

Adams, Michael C. – 1, 4, 30, 98, 100, 103, 104, 116, 117, 124, 125
Alumbaugh, David L. – 37, 39, 41, 58, 60, 62, 63
Blackwell, David – 10, 11, 14, 15, 17, 41
Boitnott, G.N. – 64, 66, 67, 69, 70
Brantley, Susan L. – 1, 94
Creed, Robert – i
Ghassemi, A. – 72, 73, 74, 77, 79
Harris, Joel M. – 85, 111, 116
Heaney, Peter J. – 92, 94, 95
Horne, Roland N. – 87, 88, 90, 91
Hulen, Jeffery B. – 1, 2, 3, 4, 5, 30, 33, 36, 37, 65, 67, 70, 117, 124
Kasteler, Christian – 111, 115
Kilbourn, Phaedra – 103, 104, 111, 115, 116
Li, Kewen - 88
Lutz, Susan J. – 1, 3, 4, 5, 30, 117, 124
Moller, Nancy - 105, 110
Moore, Joseph N. – 1, 4, 5, 25, 27, 28, 29, 30, 31, 33, 36, 53, 103, 104, 117, 119, 124, 125
Nash, Gregory D. – 4, 20, 25, 30, 31, 103, 104
Norman, David I. – 4, 30, 31, 117, 118, 119, 124, 125
Norton, Denis L. – 1, 3, 5, 32, 33, 36
Rial, J.A – 43, 48, 49.
Richards, Maria – 10, 15
Rose, Peter E. – 46, 47, 67, 98, 104, 111, 113, 115, 116
Stodt, John A. – 37, 42
Swenson, Daniel – 81, 82, 85, 86
Tripp, A.C. – 28, 29, 30, 31, 41, 50, 51, 52, 53, 54, 55, 56, 57
Wannamaker, Philip E. – 5, 30, 37, 38, 39, 40, 41, 42
Weare, John H. – 105, 110
Wisian, Kenneth W. – 10, 13, 14, 15